Functional and phylogenetic analysis of the endosomal-targeted proteins CML4 and CML5 in *Arabidopsis thaliana*

Dissertation

der Fakultät für Biologie

der

Ludwig-Maximilians-Universität München

Vorgelegt von

Henning Ruge

München, den 21.12.2017

Gutachter/in: 1. Prof. Dr. Ute C. Vothknecht

2. Prof. Dr. Peter Geigenberger

Datum der Einreichung: 21.12.2017

Datum der Promotion: 07.05.18

Eidesstattliche Erklärung

Ich versichere hiermit an Eides statt, dass die vorliegende Dissertation von mir selbständig und ohne unerlaubte Hilfe angefertigt wurde.

Erklärung

Diese Dissertation wurde keiner weiteren Prüfungskommission weder in Teilen noch als Ganzes vorgelegt. Ich habe nicht versucht, anderweitig eine Dissertation einzureichen oder mich einer Doktorprüfung zu unterziehen.

München, 07.08.2018

Ort, Datum *Henning Ruge*

Content

1. Introduction

1.1 Calcium ions – tight regulation of a cytotoxic second messenger

Calcium ions (Ca^{2+}) are essential ions to biological systems and serve various functions, e.g. as structural element in proteins (Drucker *et al.* 1971) and tissues (Baker *et al.* 1946, Demarty *et al.* 1984). However, Ca^{2+} also play a vital role as second messengers in eukaryotic systems. Plants are sessile life forms and therefore require mechanisms for perceiving changes in environmental conditions and for initiating responses on a cellular level, in order to maintain fitness for their habitat. Therefore, plants encode an extensive set of sensor and signal transducer proteins to decode Ca^{2+} signals, which are invoked by external and internal stimuli (reviewed in Clapham 1995, Dodd *et al.* 2010, Kudla *et al.* 2010, Perochon *et al.* 2011). Ca^{2+} signalling potentially already emerged in the last common ancestor of eukaryotes, and from there on evolution of proteins participating in Ca^{2+} signalling proceeded differently in unikonta and bikonta (Plattner *et al.* 2015, Marchadier *et al.* 2016). The variety of processes involving Ca^{2+} as second messenger in plants comprises response to abiotic and biotic stress factors, hormone signalling and growth regulation pathways, interaction with symbiotic partners and others (Zhou *et al.* 2009, Drerup *et al.* 2013, Miller *et al.* 2013, Zhang *et al.* 2016, Ligaba-Osena *et al.* 2017). Many of these processes involve elevations in cytoplasmic free calcium ion concentration ($[Ca^{2+}]_f$) that would - given a permanent establishment - be cytotoxic due to the potential of Ca^{2+} to form insoluble complexes with free phosphate, leading to energetic breakdown of the cell. This favoured the development of mechanisms to sequester Ca^{2+} in storage compartments, e.g. endoplasmic reticulum (ER), apoplast and vacuole. These processes are mediated by the activity of ATP-dependent pumps (Bonza *et al.* 2000, Schiøtt *et al.* 2004, Kamrul Huda *et al.* 2013) and Ca^{2+}/H^{+} -antiporters (Cheng *et al.* 2005, Hirschi *et al.* 1996) in the respective compartment membranes. This tight maintenance of low cytoplasmic base levels of $[Ca^{2+}]_f$ is one of the reasons for which Ca^{2+}can serve as potent second messengers. However, in order to evoke transient elevations in cytoplasmic $[Ca^{2+}]_f$, the presence of channels facilitating transport across the membranes of the internal calcium stores is essential. Whereas in *Homo sapiens* eight different types of Ca^{2+} channels are present, higher plants harbour a less diverse set of proteins mediating Ca^{2+} influx into the cytoplasm. The *Arabidopsis thaliana* (*A. thaliana*) genome encodes one two-pore channel, 20 glutamate receptors, 20 cyclic nucleotide-gated channels and ten

mechanosensitive ion channels (Verret *et al.* 2010). In addition, there is a set of osmosensing channels, termed OSCAs (Yuan *et al.* 2014). Through their opposed and tightly controlled functions Ca^{2+}-permeable channels together with Ca^{2+}/H^{+} -antiporters and Ca^{2+}-ATPases generate, modulate and terminate stimulus-specific Ca^{2+} signals in the cell. However, these signals need to be perceived and translated into a specific cellular response, which requires a toolset of Ca^{2+}-binding proteins that has evolved to a system of low diversity but high versatility in the plant kingdom.

1.2 Ca^{2+} signatures and their translation into cellular responses by Ca^{2+}-sensor proteins

Investigation of Ca^{2+} as second messenger gave rise to the question of the mechanisms establishing a sufficient degree of specificity, since a vast variety of stimuli evoke Ca^{2+} fluxes in a cell, often within the same compartment. One level of specificity has been found to be constituted by the spatiotemporal patterning of $[Ca^{2+}]_f$ alterations as well as the modulation of their amplitude (McAinsh *et al.* 2009, McAinsh *et al.* 1998), termed Ca^{2+} "signatures". A key feature of Ca^{2+} rendering it an ideal locally acting second messenger is its very low diffusion rate in an environment like the cytoplasm, due to interaction with other ions, lipids or proteins (Allbritton *et al.* 1992). This allows for large amounts of Ca^{2+} to be accumulated in a limited volume of cellular space, reducing the absolute amount of Ca^{2+} required to elevate the $[Ca^{2+}]_f$ in the defined area. Further, it represents the basis for the occurrence of Ca^{2+} microdomains providing additional signal specificity by triggering only Ca^{2+}-binding proteins present in this very sub-domain of the respective cellular compartment. Last, it enables $[Ca^{2+}]_f$ oscillations to be modulated at high frequencies and with high amplitudes, for under these conditions, channel conductance and transporter kinetics represent the major limiting factors. Additionally, it has been shown that the stimulus-specific Ca^{2+} signatures are different depending on the cell type they are invoked in, adding another layer of complexity, but also specificity to the Ca^{2+} signalling network (Martí *et al.* 2013).

Further specificity is established by a range of Ca^{2+}-binding proteins in plant cells, their defined sub-cellular localisation and expression patterns. Despite a huge variety of these proteins in plants, mainly three groups shape the Ca^{2+} signature-decoding protein landscape in the green lineage of organisms: calmodulins (CAMs) and calmodulin-like proteins (CMLs), calcium-dependent protein kinases (CDPKs) and the two-component system of calcineurin B-like proteins (CBLs) and CBL-interacting protein kinases (CIPKs) (Edel *et al.* 2017, Edel *et*

al. 2014, Bender *et al.* 2013, Kudla *et al.* 2010, Luan 2009, Batistič *et al.* 2009, McCormack *et al.* 2005, McCormack *et al.* 2003). These sensor proteins can be grouped according to whether they possess enzymatic activity (CDPKs; termed "signal responders"), or whether they modulate the activity of their interaction partners following a Ca^{2+}-dependent change in their own conformation (CAMs, CBLs, CMLs; termed "sensor relays") (Sanders *et al.* 2002).

CIPKS

Since CIPKs do not harbour motifs for Ca^{2+} binding and constitute the main downstream targets for CBLs hitherto identified (Guo *et al.* 2002, Costa *et al.* 2017, Drerup *et al.* 2013, Steinhorst *et al.* 2015, Guo *et al.* 2001, Shi *et al.* 1999), the combination of CBL-CIPKs resembles a chimera of both aforementioned groups. However, there is evidence for CBL10 in *A. thaliana* directly interacting with TOC34, thereby negatively affecting its GTPase activity (Cho *et al.* 2016). CBL proteins share major parts of their sequence with calcineurin B and neuronal Ca^{2+} sensors from the animal system (Liu *et al.* 1998), containing four EF-hands, of which the first one comprises 14 amino acids instead of the canonical twelve, and they do not harbour any intrinsic enzymatic activity (Nagae *et al.* 2003). The sub-cellular localisation and often the physiological function of CBLs are influenced by the presence of motifs for myristoylation and other lipid modifications (Ishitani *et al.* 2000, Batistič *et al.* 2008), N-terminal signal-anchors, and tonoplast targeting signals (reviewed in Mao *et al.* 2016). Multiple interactions between the ten CBLs and 26 CIPKs in *A. thaliana* increase the versatility of this two-component signalling system (Batistic *et al.* 2004, Drerup *et al.* 2013, Tang *et al.* 2012). Upon binding of Ca^{2+}, CBLs change their globular conformation and expose hydrophobic residues serving as interaction interface with the NAF-domain of CIPKs (Sanchez-Barrena *et al.* 2005, Guo *et al.* 2001), thereby releasing the autoinhibition of the kinase. Functional investigations on CBLs and CIPKs have shown their major role in ion homeostasis (Tang *et al.* 2015) and stress signalling, especially abscissic acid (ABA)-related stress responses to drought and salt (Sanyal *et al.* 2017, Tang *et al.* 2012, Guo *et al.* 2002). Several CBL-CIPK pathways include regulation of ion channels or pumps, e.g. CBL4-CIPK24 activates an Na^+/H^+ -exchanger in the plasma membrane in response to salt stress (Qiu *et al.* 2002); CBL10-CIPK24 regulates a Na^+/H^+ -exchanger in the tonoplast membrane influencing ion homeostasis (Kim *et al.* 2007); CBL4-CIPK6 alters AKT2 channel conductance and localisation (Held *et al.* 2011). Additionally, CBL-CIPK complexes have been found to provide a functional link between Ca^{2+}- and reactive oxygen species-signalling (Drerup *et al.* 2013). However, the significance of CBL-CIPK complexes is not restricted to

stress response scenarios. It has been shown that pollen tube growth in Arabidopsis is retarded in plants with altered CBL3 and CBL2 transcript abundance. This macroscopic phenotype has been linked to distorted vacuole morphology and indicates a constitutive role of both proteins in regulating vacuolar and ultimately developmental processes (Steinhorst *et al.* 2015). In general, the role of CBL-CIPKs, independent of their influence on development, response to salt stress or osmotic stress, is remarkably often related to ion redistribution or homeostasis.

CDPKs

Though CDPKs and CIPKs are similar in terms of their kinase activity being constitutively repressed by an autoinhibitory domain, CDPKs do not require proteins like CBLs for activation. C-terminal to their autoinhibitory domain, they usually harbour a CAM-domain, which undergoes sequential conformational changes resulting in the dislocation of the inhibitory domain (Chandran *et al.* 2006). Autophosphorylation is common among CDPKs and has recently been shown for AtCPK28 to lead to increased sensitisation towards Ca^{2+}, probably providing a mechanism for priming the kinase for subsequent Ca^{2+} stimuli after an initial triggering $[Ca^{2+}]_f$ elevation (Bender *et al.* 2017). Similar to CBLs, CDPKs in *A. thaliana* can be clustered according to their sub-cellular localisation, which ranges from exclusively membrane associated, e.g. AtCPK7 and AtCPK9 to mainly membrane associated, e.g. AtCPK2 and AtCPK25, or membrane localised and soluble, e.g. AtCPK5 and AtCPK3 (Boudsocq *et al.* 2012). This behaviour can be at least partially attributed to the finding that CDPKs are often myristoylated and/or palmitoylated, providing them with a membrane anchor. Although many CDPKs have been found to be plasma membrane-localised, the sub-cellular destinations of CDPKs are diverse (summarised in Simeunovic *et al.* 2016). Alterations of the acylation status of AtCPK16 affecting its sub-cellular localisation indicated a potential regulatory function of reversible acylations on CDPK activity (Stael *et al.* 2011). Additionally, CDPKs display differences in the following three parameters: i) Ca^{2+} binding affinity, ii) the extent to which their enzymatic activity is dependent on Ca^{2+} binding, iii) the extent to which their affinity towards Ca^{2+} is altered depending on the substrate they bind (Boudsocq *et al.* 2012). Differences in these characteristics probably further determine the wide range of physiological functions, served by CDPKs (Gao *et al.* 2014, Simeunovic *et al.* 2016, Ormancey *et al.* 2017). AtCPK11 and AtCPK24 have been shown to regulate the pollen tube-specific potassium channel AtSPIK by Ca^{2+}-dependent and Ca^{2+}-independent phosphorylation, respectively, which in turn affects pollen tube growth. Additionally, AtCPK11 acts in ABA-induced ethylene production by

phosphorylating AtACS6, a synthase of the ethylene precursor, which then leads to reduction of root growth (Luo *et al.* 2014). AtCPK28 is involved in developmental processes regulated by jasmonic acid (JA) and gibberellic acid (GA) involving stem elongation and vascular architecture (Matschi *et al.* 2013, Matschi *et al.* 2015).

CAMs and CMLs

In addition to phosphorylation as translation of Ca^{2+} signals into cellular response, the Ca^{2+} sensor toolkit comprises proteins, CAMs and CMLs, that modulate effector protein function directly via interaction. CAM harbours no other functional domains than EF-hands required for Ca^{2+} binding and its evolutionary origins can be traced back to the common ancestor of all eukaryotes, since it is ubiquitously present in proteomes of species from simple amoeba and algae up to mammals and angiosperms (reviewed in Plattner 2017, McCormack *et al.* 2003). A potential homologue of CAM has been identified in the genome of the prokaryote *Streptomyces erythraeus*, emphasising its long phylogenetic roots (Swan *et al.* 1987). Apo-CAM is a globular, acidic protein of 149 amino acids, which form four EF-hands that can bind Ca^{2+} in a cooperative fashion (Klevit *et al.* 1984). Ca^{2+} binding induces a conformational change of the protein, leading to exposure of hydrophobic residues (Zhang *et al.* 1995, Ikura *et al.* 1992). Together with a variety of hydrophilic amino acids these residues form an α-helical interface between the N-terminal EF-hand pair (N-lobe) and the C-terminal EF-hand pair (C-lobe) that enables holo-CAM to bind other proteins in a Ca^{2+}-dependent manner (Chattopadhyaya *et al.* 1992). The interaction establishment process involves initial electrostatic interactions followed by hydrophobic interactions, which determine affinity and specificity of the binding, and conformational changes in the flexible CAM and its target structure (Liu *et al.* 2017). The large amount of methionine residues exposed upon Ca^{2+} binding, significantly contribute to the interaction partner promiscuity of CAM due to their highly flexible side chains (Zhang *et al.* 1995, Liu *et al.* 2017). The classical CAM target motif is a short α-helical peptide characterised by the consensus sequence IQXXXRGXXXR (in which X represents any amino acid), which was first discovered as interaction interface in unconventional mysosins (Espreafico *et al.* 1992). Spacing of the hydrophobic residues rather than overall sequence is the interaction efficacy-determining feature of this peptide. Different variations of this motif, including the 1-8-14 and 1-5-10 motif (numbers indicate positions of conserved hydrophobic residues required for interaction) have been identified in various proteins (summarised in Rhoads *et al.* 1997). In accordance with the broad interaction partner specificity of CAMs, the cellular functions they are

involved in are very diverse. Among CAMs in Arabidopsis AtCAM7 is especially noteworthy, because it has been shown to directly bind Z-box DNA via its Arg_{127} residue, whereas the highly similar AtCAM2, AtCAM3 and AtCAM5 do not display DNA-binding capacity (Kumar *et al.* 2016). AtCAM7 serves as transcription factor enhancing the expression of light-induced genes, thereby actively influencing photomorphogenesis of *A. thaliana* seedlings (Kushwaha *et al.* 2008). In this respect it also interacts with AtHY5, a bZIP transcription factor involved in orchestrating photomorphogenesis and different hormone signalling pathways, in a Ca^{2+}-dependent manner, driving AtHY5 expression (Abbas *et al.* 2014). Further, AtCAM7 was found to interact with the ATP-binding cassette transporter AtPEN3, which is a mediator of non-host resistance in Arabidopsis triggered upon recognition of pathogen-associated molecular patterns (Campe *et al.* 2016). There are also indications for a role of CAMs in regulating the import machinery of mitochondria (Parvin *et al.* 2017) and peroxisomes as well as peroxisomal enzymes (Corpas *et al.* 2014, Corpas *et al.* 2017). Despite their lack of motifs/domains other than EF-hand domains, CAMs exert their function as sensor relays in a vast variety of physiological processes. Whereas CAMs have retained their invariant structure in animal and plant cells alike, a rather similar but structurally more diverse Ca^{2+} sensor protein family has evolved in the bikonta lineage, the CMLs.

McCormack and Braam analysed CAM and CAM-related proteins in the *A. thaliana* proteome, and classified proteins as CMLs if they showed at least 16 % overall amino acid identity to CAM and contained at least two EF-hands (with the exception of CML1 containing only one EF-hand). Their sequence analyses showed that the seven CAMs in *A. thaliana*, which represent three isoforms, display only little sequence diversity. However, the sequence similarities between CMLs vary to great extent, which probably even affects the Ca^{2+} binding capabilities of different EF-hands and interaction partner variety in single proteins (McCormack *et al.* 2003). Similar analyses have also been carried out in species, including *Oryza sativa* (Boonburapong *et al.* 2007), *Brassica rapa* subsp. *pekinensis* (Nie *et al.* 2017) and *Lotus japonicus* (Liao *et al.* 2017). Additionally, expression analyses in *A. thaliana* and *Oryza sativa* have revealed that whereas CAMs are ubiquitously expressed, CMLs display strong variation in their spatiotemporal expression patterns. This indicates cellular functions specific to those organs or developmental stages rather than constitutive roles of these proteins (McCormack *et al.* 2005, Boonburapong *et al.* 2007). Given the great number of CML genes in Arabidopsis, hitherto only a small fraction of CMLs have been functionally analysed and since investigations indicated single CMLs to be potentially involved in a

variety of pathways, determination of the entire set of functions for each CML is challenging. AtCML24 is expressed in pollen tubes and has been shown to affect pollen tube growth by regulating cytoplasmic Ca^{2+} and K^{+} levels and the correct establishment of the actin cytoskeleton required for pollen tube elongation (Yang *et al.* 2014). Additionally, it interacts with AtATG4b, a component of the autophagy system (Tsai *et al.* 2013b), which is also vital for pollen tube growth. A similar function has been attributed to AtCML25, which also controls inward Ca^{2+} and K^{+} fluxes and influences pollen tube growth and pollen fertility (Wang *et al.* 2015). Another CML involved in developmental process control is AtCML42, which is expressed in various cell types, e.g. support cells at the basis of trichomes, and is required for establishment of trichome architecture (Dobney *et al.* 2009). Furthermore, AtCML42 has been found to be a repressor of herbivore attack response mediated by JA (Vadassery *et al.* 2012), exemplifying the versatility of CML function in cellular processes. Expression analyses for AtCML37, AtCML38 and AtCML39 showed constitutive expression of these genes in root cortex, root tip and stipules (AtCML37), guard cells of developing leaves and lateral root buds (AtCML38) and pollen (AtCML39), indicating tissue-specific functions (Vanderbeld *et al.* 2007). Another example of a CML potentially involved in developmental and stress signalling is AtCML43, whose expression is constitutive in root tips and is triggered in more proximal parts of the root by ectopic salicylic acid (SA) application (Bender *et al.* 2014). In addition to differential expression patterns, structural differences of CMLs add further potential to functional diversification. Aside from sequence alterations within the EF-hands themselves, several CMLs harbour either N- or C-terminal sequence stretches pre- or succeeding their set of EF-hands, which might affect their target specificity and sub-cellular localisation. The sequence of AtCML3 contains a C-terminal "SNL" tripeptide targeting it to peroxisomes, where it mediates the dimerisation of the peroxisomal protease AtDEG15, thereby modulating its cleavage behaviour (Dolze *et al.* 2013). The N-terminal sequence stretch of AtCML30 targets this sensor to mitochondria (Chigri *et al.* 2012). AtCML36, which contains a 60 amino acid N-terminal stretch, has been shown to be bound to the plasma membrane and activate AtACA8 to remove Ca^{2+} from the cytoplasm following transient $[Ca^{2+}]_f$ elevation (Benschop *et al.* 2007, Astegno *et al.* 2017). Initial investigation of AtCML4 and AtCML5, two paralogous Ca^{2+} sensors in Arabidopsis, revealed them to be unique among the different CMLs, CDPKs and CBL-CIPKs investigated hitherto, for they were found to be localised at vesicle membranes, where none of the other Ca^{2+} sensor proteins had been detected before (Flosdorff 2014). These two Ca^{2+} sensors

suggest a potential link between Ca^{2+} signalling and the vesicular trafficking system, which was thus far unprecedented.

1.3 The endomembrane system

The compartmentalisation of the cytoplasm by means of membrane-enclosed domains is a key characteristic of eukaryotic cells. The major components of this system are the ER, the Golgi apparatus, the vacuole(s) and the plasma membrane, which are interconnected by a variety of tubular structures or transient vesicles mediating soluble and membrane-bound cargo transport. By definition, the plasma membrane is not an endomembrane due to its cell-delimiting nature enclosing the cytoplasm, but since it is a main destination and origin for vesicular trafficking, it is functionally connected. The correct sorting and distribution of soluble and membrane-bound cargo among the components of this system is a requirement for functionality and perturbations of the sorting processes are often related to severe phenotypes (Zhao *et al.* 2016, Laval *et al.* 2003, Hirano *et al.* 2011). Proteins synthesised at the ER enter anterograde transport towards the Golgi either in a receptor-dependent or receptor-independent (bulk flow) fashion (Malkus *et al.* 2002). Through special motifs, e.g. diacidic patches (Hanton *et al.* 2005), the cargo receptors and other transmembrane proteins are recognised by Sec24 (Pagant *et al.* 2015) in complex with Sec23 and Sar1 (Bi *et al.* 2002) on the cytoplasmic ER surface, by which they are gathered into domains. Sar1 mediates membrane curvature and fission (Hariri *et al.* 2014, Hanna *et al.* 2016) and recruits the outer coat proteins Sec13 and Sec31, which stabilise the curved membrane and complete the COPII complex required for anterograde transport (Townley *et al.* 2008). The function of these proteins has been mostly studied in yeast and functional complementation assays have proven the similar function of their plant homologues (De Craene *et al.* 2014). However, there is still ongoing debate about whether there is a tubular connection between ER and Golgi, for their physical interaction has been shown (Sparkes *et al.* 2009) and might coexist with the COPII-coated vesicle pathway. In yeast and mammals, most ER-resident proteins are transported back from the *cis*-Golgi via vesicles coated by the heptameric COPI complex, the coatomer (Letourneur *et al.* 1994). Despite lack of information on the specific function of the respective COPI components in the plant system, the localisation of the coatomer subunits to the *cis*-Golgi and their requirement for retrograde transport and cell viability has been shown. Comparable to Sar1 for COPII function, the GTPase ARF1 has been found to be required for this process (Pimpl *et al.* 2000, Ahn *et al.* 2015, Langhans *et al.* 2008). Cargo is further

transported along the Golgi cisternae towards the *trans*-Golgi network (TGN), which merges with early endosomes (EE) originating from the endocytic pathway. Soluble cargo destined for lytic vacuoles and protein storage vacuoles are bound by the vacuolar sorting proteins VPS1, VPS3 and VPS4 (Lee *et al.* 2013) and FRET-FLIM analyses have revealed that cargo binding events occur in ER and Golgi, but further transport through TGN and multivesicularbodies (MVB) towards the vacuole are VSR-independent and probably occur by default (Künzl *et al.* 2016). Whereas export of VSRs from the ER towards *cis*-Golgi is mediated receptor-independently in bulk flow, the cytosolic tail of VSRs with their YMPL motif interacts with AP1, an adaptor protein in the clathrin coat of vesicles, and thus enables transport towards the vacuole instead of the plasma membrane (Gershlick *et al.* 2014). Cargo derived from endocytosis and destined to be degraded in the lytic vacuole, progresses from the TGN/EE via MVBs and the (late) pre-vacuolar compartment (PVC) to the vacuole. This involves maturation processes including alterations in luminal pH, vesicle structure and protein composition (Shen *et al.* 2013, Martinière *et al.* 2013, Scheuring *et al.* 2011, Nodzyński *et al.* 2013). The retromer complex is required for the recycling of VSRs back to the Golgi from TGN and MVBs and retromer subunit mutants can cause severe structural abnormalities in the PVC (Oliviusson *et al.* 2006, Nodzyński *et al.* 2013, Niemes *et al.* 2010). Transmembrane proteins and soluble cargo to be secreted into the apoplast are transported towards the plasma membrane in clathrin-coated vesicles (Larson *et al.* 2017). Clathrin complexes are also required for endocytosis similar to the animal system, and additionally for recycling plasma membrane proteins back to the cell surface (Kitakura *et al.* 2011, Bandmann *et al.* 2012). Concomitantly to the described trafficking processes, pathways directly linking ER and tonoplast (Viotti *et al.* 2013) or Golgi and tonoplast exist (Hinz *et al.* 1999, Hillmer *et al.* 2001, Wen *et al.* 2015).

Implications for Ca^{2+} in endomembrane system function are represented by the role of annexins as Ca^{2+} binding proteins in the tethering of ER and plasma membrane at specific junction sites. Additionally, Ca^{2+} have been shown to serve as electrostatic bridging ions during membrane fusion (Tsai *et al.* 2013a) and their binding to phosphoinositides alters the relative orientation of head groups, thereby influencing binding of lipid-interacting proteins (Bilkova *et al.* 2017).

1.4 Aim of this work

In contrast to the animal system, in which CAM has been implicated in vesicle fusion events (Mills *et al.* 2001), evidence for Ca^{2+} sensors mediating such processes in plants is currently missing. In spite of their wide association with membranes, thus far no CBL or CDPK was shown to be associated with vesicular membranes of the endosomal system. The only exception is AtCBL10, which is anchored in the tonoplast and membranes of the PVC (Kim *et al.* 2007). This raises the question for the function and evolutionary origin of Ca^{2+} sensors on the surface of plant endosomal membranes, as presented by AtCML4 and AtCML5.

To elucidate the physiological function of AtCML4 and AtCML5, different approaches have to be followed, including i) the potential phenotypes of *atcml4* and *atcml5* loss-of-function single and *atcml4*/*atcml5* loss-of-function double mutants, ii) the spatiotemporal expression patterns of *AtCML4* and *AtCML5* and iii) the identification of potential interaction partners of AtCML4 and AtCML5. An RNA interference-approach has to be used in wild-type and *atcml5* knock-out mutant plants to generate *atcml4* and *atcml4*/*atcml5* loss-of-function mutants, respectively. Thus generated and previously available mutant plants are to be analysed regarding their phenotypes under different growth conditions, including the simulation of various stress scenarios. Furthermore, wild-type plants need to be stably transformed to express LUCIFERASE reporter constructs under the control of the *AtCML4* and the *AtCML5* promoters to analyse at which developmental time points and in which tissues *AtCML4* and *AtCML5*, respectively, are expressed. Potential interaction partners of AtCML4 and AtCML5 have to be identified in a pull-down approach, using recombinantly expressed variants of both proteins as bait. Additionally, the sub-cellular localisation of AtCML4 and AtCML5 has to be further dissected by quantitative assessment of microscopic data gained from *in planta* co-expression of compartment marker constructs with fluorescent fusion constructs of AtCML4 and AtCML5. In relation to that, the N-terminus of both proteins needs to be analysed with regard to its sequence and effect on overall protein topology. Also, the phylogenetic origin, development and distribution of CMLs targeted to the endosomal system within the green lineage of plants should be investigated.

2. Material and methods

2.1 Material

2.1.1 Chemicals, enzymes and kits

If not otherwise mentioned, all chemicals were of premium quality and have been purchased from known suppliers. Dexamethasone and (D)-luciferin were purchased from Sigma-Aldrich (Sigma-Aldrich, St. Louis, MO, USA). Restriction enzymes required for cloning were supplied by New England Biolabs (Boston, MD, USA) or Fermentas (St. Leon Roth, Germany). T4-DNA ligase was supplied by Fermentas (St. Leon Roth, Germany). DNA extraction from agarose gels and out of polymerase chain reactions (PCR) were performed with the Nucleospin Extract II Kit by Macherey-Nagel (Düren, Germany). Plasmid DNA isolation from *Escherichia coli* (*E. coli*) cells was performed using the Nucleobond PC 100 and PC 500 kits by Macherey-Nagel (Düren, Germany).

2.1.2 Seeds and bacterial strains

Propagation of plasmid DNA was performed in *E. coli* strain DH5α (NEB, Boston, MD, USA), whereas protein expression was performed in BL21-CodonPlus(DE3)-RIPL cells (Agilent technologies, Santa Clara, CA, USA). Transient transformation of *Nicotiana benthamiana* (*N. benthamiana*) plants was performed with *Agrobacterium rhizogenes* (*A. rhizogenes*) strain LBA1334 (Visser *et al.* 1989), whereas stable transformation of *A. thaliana* plants was carried out with *Agrobacterium tumefaciens* (*A. tumefaciens*) strain GV3101 (Vahala *et al.* 1989).

Seed material for the T-DNA insertion line GABI-Kat 703E02 was supplied by the GABI-Kat project (Bielefeld, Germany). Arabidopsis wild-type (WT) seed material was purchased from LEHLE SEEDS (Round Rock, TX, USA) or The European Arabidopsis Stock Centre NASC (Nottingham, UK) and *N. benthamiana* seed material was supplied by the in-house plant cultivation facility. Seed material for plants stably transformed with the pOpOff2-LUC construct, were kindly provided by Iris Finkemeier (WWU Münster, Münster, Germany).

2.1.3 Vectors, constructs and primers. GST – glutathione S-transferase.

General description of basic vectors used in this work

pBIN19-AN-YFP	Binary vector applied for stable *A. thaliana* or transient *N. benthamiana* transformation. If not indicated otherwise, restriction sites ApaI/NotI were used for the fusion gene or KpnI/ApaI for the promoter. Selection markers: Kanamycin/BASTA.	Supplied by Dr Norbert Mehlmer (Mehlmer et al. 2012)
pBIN19-ANX	Binary vector applied for stable *A. thaliana* or transient *N. benthamiana* transformation. Derived from pBIN19-AN-YFP. If not indicated otherwise, restriction sites used for cloning were ApaI/NotI and NotI/XhoI for the fusion gene or KpnI/ApaI for the promoter. Selection markers: Kanamycin/BASTA	Designed in this work
pGEX4T-3	Vector for expression fusion proteins with N-terminal GST tag in *E. coli*, restriction sites used for cloning were BamHI/NotI. Selection marker: Ampicillin	GE Healthcare Europe GmbH, Freiburg, Germany
pGREENII	Vector for transformation of *A. thaliana* leaf mesophyll protoplasts. Used for expression of fusion proteins under control of endogenous promoter regions. Restriction sites used for cloning: EcoRI/XhoI for promoter, NcoI/SpeI for fusion genes. Selection marker: Ampicillin	Kindly provided by Dr Peter Pimpl (ZMBP, University of Tübingen, Tübingen, Germany)
pSOUP	Helper plasmid for amplification of pGREENII plasmids in *A. rhizogenes*. Selection marker: Tetracyclin	Supplied by Nottingham Arabidopsis Stock Centre (Nottingham, UK)
pOpOff2	Vector for stable transformation of *A. thaliana* plants. Allows inducible expression of nucleotide sequences serving as double-stranded RNA samples for RNAi, cloning is described in 2.2.1.6. Selection marker: Spectinomycin/Hygromycin B	Kindly provided by Prof Dr Katrin Philippar (Wielopolska et al. 2005)

Table 1: Plasmids used in this work. AA – amino acid, CDS – coding sequence, NT – nucleotide, GST – glutathione S-transferase, * - construct supplied by AG Vothknecht or donor mentioned

Denotation	Vector	Description
CML5-YFP*	pBIN19-AN-YFP	At2g43290 CDS
CML4-mCherry	pBIN19-AN-YFP	At3g59440 CDS
CML4-YFP	pBIN19-AN-YFP	At3g59440 CDS
$CML5_{1-28}$-YFP*	pBIN19-AN-YFP	AAs 1-28 of At2g43290 (NTs 1-84)
AtARA6-mCherry*	pBIN19-AN-YFP	At3g54840.1 CDS
GmMAN1-mCherry*	pBIN19-AN-YFP	(Nelson *et al.* 2007)
AtWAK1-mCherry-HDEL*	pBIN19-AN-YFP	(Nelson *et al.* 2007)
mCherry-SKL	pBIN19-AN-YFP	mCherry protein followed by AA stretch "SKL"
pAtCML5::$CML5_{1-28}$-YFP-AEQ	pBIN19-AN-YFP	Promoter region and 5'UTR of At2g43290 (1123 NTs upstream of CDS), followed by NTs 1-84 of the At2g43290 CDS
pUBI::CML4	pBIN19-ANX	Ubiquitin promoter followed by At3g59440 CDS
pUBI::CML5	pBIN19-ANX	Ubiquitin promoter followed by At2g34290 CDS
pAtCML5::CML5	pBIN19-ANX	Promoter region and 5'UTR of At2g43290 (1123 NTs upstream of CDS), followed by At2g43290 CDS
pAtCML4::LUC	pBIN19-ANX	Promoter region and 5'UTR of At3g59440 (1822 NTs upstream of CDS), followed by FIREFLY LUCIFERASE CDS
pAtCML5::LUC	pBIN19-ANX	Promoter region and 5'UTR of At2g43290 (1123 NTs upstream of CDS), followed by FIREFLY LUCIFERASE CDS
GST-$CML5_{21-215}$	pGEX4T-3	NTs 61-648 of At2g43290 CDS
GST-$CML4_{21-195}$	pGEX4T-3	NTs 61-588 of At3g59440 CDS
pAtCML4::CML5-YFP	pGREENII	Promoter region and 5'UTR of At3g59440 (1822 NTs upstream of CDS), followed by At2g43290 CDS
pAtCML5::CML5-YFP	pGREENII	Promoter region and 5'UTR of At2g43290 (1123 NTs upstream of CDS), followed by At2g43290 CDS
siRNA-$CML4_{1-300}$	pOpOff2	NTs 1-300 of At3g59440 CDS

Table 2: Primers used for cloning procedures. The restriction sites utilised are denoted in every primer name. Fw – forward primer, Rv – reverse primer, CDS – coding sequence, NT – nucleotide

Primer name	Sequence (5'→3')	Amplicon
Fw_CML4_XhoI	AAGCTCGAGATGGTGAGAGTCTTTC	At3g59440 CDS
Rv_CML4_NcoI	TCGCCCTTGCTCACCATGGCTGATCTATTGCTAAAGTC	At3g59440 CDS
Fw_YFP_CML4_NcoI	GACTTTAGCAATAGATCAGCCATGGTGAGCAAGGGCGA	YFP CDS
Rv_YFP_SpeI	AATCCTCGGACTAGTCTAGCGCCCGCTCTTGTAC	YFP CDS
Fw_CML5specPromCDS5UTR_EcoRI	GCAACTTGAATTCACATTTTTTCAGTTATTTTGTG	1123 NTs upstream of At2g43290 CDS to the 3' end of the CDS
Rv_CML5_PromCDS5UTR _XhoI	AAGCTCGAGAACTGTTGAATCACAACTC	1123 NTs upstream of At2g43290 CDS to the 3' end of the CDS
Fw_CML5_XhoI	GCCAAGCTCGAGATGGTGAGAATATTCCTTCTC	At3g43290 CDS
Rv_CML5_NcoI	TCGCCCTTGCTCACCATGGCATTACTGCTGCTAAAG	At3g43290 CDS
Fw_YFP_CML5_NcoI	CTTTAGCAGCAGTAATGCCATGGTGAGCAAGGGCGA	YFP CDS
Rv_YFP_SpeI	AATCCTCGGACTAGTCTAGCGCCCGCTCTTGTAC	YFP CDS
Fw_CML4_PromCDS5UTR_EcoRI	CTTGAATTCTTTTCTGTCTGAATCTCTG	1822 NTs upstream of At3g59440 CDS to the 3' end of the CDS
Rv_CML4_PromCDS5UTR _XhoI	AAGCTCGAGAACTCTTGGCTTTG	1822 NTs upstream of At3g59440 CDS to the 3' end of the CDS
FwCML5_Promspec_KpnI	GGCGGTACCACATTTTTTCAGTTATTTTGTG	1123 NTs upstream of At2g43290 CDS to the 5' end of the CDS
Rv_CML5_Prom5UTR _ApaI	AAGGGGCCCAACTGTTGAATCACAACTC	1123 NTs upstream of At2g43290 CDS to the 5' end of the CDS
Fw_CML4_Prom_KpnI	GAAGGTACCTTTTCTGTCTGAATCTCTGAGTTTAGG	1822 NTs upstream of At3g59440 CDS to the 5' end of the CDS
Rv_CML4_Prom5UTR _ApaI	AAGGGGCCCAACTCTTGGCTTTGTTGAGAAC	1822 NTs upstream of At3g59440 CDS to the 5' end of the CDS
mCherry_ApaI_fw	TCCGGGCCCATGGTGAGCAAGGGCG	mCherry CDS
mCherry_SKL_NotI_rv	CGTTAGCGGCCGCTTACAATTTTGACTTGTACAGCTCGTC	mCherry CDS with SKL-coding NTs

At3g61760_cDNA_fw	ATGGAGAGTTTGATTGCG CTTGTGAAC	At3g61760 CDS
At3g61760_cDNA_rv	CTTGGACCAAGCAACTGC TTCAATATC	At3g61760 CDS
At3g61760_Apa_fw	TTCGGGCCCATGGAGAGT TTGATTGCGCTTG	At3g61760 CDS
At3g61760_Not_rv	AACGCGGCCGCACTTGGA CCAAGCAACTG	At3g61760 CDS
At4g11850_cDNA_fw	ATGGCGTATCATCCGGCTT ATACTGAG	At4g11850 CDS
At4g11850_cDNA_rv	TATGGTGAGGTTTTCTTGT AGTGCAAGG	At4g11850 CDS
At4g11850_Apa_fw	TTCGGGCCCATGGCGTATC ATCCGGCTTATAC	At4g11850 CDS
At4g11850_Not_rv	AGGGCGGCCGCATATGGT GAGGTTTTCTTGTAG	At4g11850 CDS
5g55050_cDNA_fw	ATGCCGACGAACAACACT CCG	At5g55050 CDS
5g55050_cDNA_rv	TCATGTAGAGACCAACTG AGTAAGAG	At5g55050 CDS
5g55050_Apa_fw	TTGGGGCCCATGCCGACG AACAACACTC	At5g55050 CDS
5g55050_Not_rv	CAAGCGGCCGCCTGTAGA GACCAACTG	At5g55050 CDS
Fw_PreCis_BamHI	CCTGGATCCTTAGAAGTGT TATTTCAGGGCC	BamHI site, and recognition site for PreScission protease
Fw_CML5$_{61\text{-}648}$_PreCis	TGTTATTTCAGGGCCCGAA GAAGCTACGAACTC	At2g43290 CDS NTs 61-588 with N-terminal PreScission recognition site
Rv_CML5stop_NotI	AGGGCGGCCGCTCAATTA CTGCTGC	At2g43290 CDS
Fw_CML4ab$_{61\text{-}588}$_Pre Cis	TGTTATTTCAGGGCCCGAA GAAGCTTAGAG	At3g59440 CDS NTs 61-588 with N-terminal PreScission recognition site
Rv_CML4stop_NotI	AGGGCGGCCGCTCATGAT CTATTGC	At3g59440 CDS
C4_TOPO_Fw	CACCATGGTGAGAGTCTT TCTTC	NTs 1-300 of At3g59440 CDS
C4_TOPO_Rw	GCATCCATCTTCTGGATCA TCTG	NTs 1-300 of At3g59440 CDS

2.1.4 Blotting membranes, protein and DNA ladders, chromatography resins

The protein ladders used for SDS-PAGE analysis were the PageRuler™ Plus Prestained Protein Ladder (Thermo Fisher Scientific, Waltham, MA, USA) and the Peqlab Marker Gold I (Peqlab, Wilmington, DE, USA). The DNA ladder applied in agarose gel nucleic acid analysis was the 1 kb plus GeneRuler™ DNA Ladder (Thermo Fisher Scientific, Waltham, MA, USA). For western blot analysis, proteins were transferred onto nitrocellulose membranes Portran BA 83, 0.2 µm (Schleicher und Schüll, Dassel, Germany); Whatman paper was supplied by GE Healthcare (GE Healthcare Europe GmbH, Freiburg, Germany). Isolation of glutathione S-transferase (GST)-tagged proteins was performed on glutathione sepharose 4B resin (GE Healthcare Europe GmbH, Freiburg, Germany). Tag-independent immobilisation of proteins was performed using CNBr-activated sepharose 4B (GE Healthcare Europe GmbH, Freiburg, Germany).

2.1.5 Antisera

Detection of YFP-tagged proteins and mCherry-tagged proteins was performed with the rat monoclonal primary antibodies α-GFP 3H9 and α-RFP 5F8 (ChromoTek, Martinsried, Germany). Horse radish peroxidase-coupled AffiniPure Goat α-rat IgG-IgM (Jackson ImmunoResearch, PA, USA) was used as secondary antibody. Antibodies against AtCML4 (clones 28C11 and 15A3-131) as well as secondary sub-class-specific mouse α-rat and rat α-mouse antibodies were supplied by the Monoclonal Antibody core facility (HelmholtzZentrum Munich, Neuherberg, Germany).

2.2 Methods

2.2.1 Molecular biological and cell biological methods

2.2.1.1 General methods

Cultivation of bacteria, DNA extraction via alkaline lysis, concentration determination of isolated DNA and standard other molecular biological methods were performed according to Sambrook and Russel (Sambrook *et al.* 2006). Chemical competence of *E. coli* cells was established as published (Hanahan 1983). *E. coli* cells were transformed with plasmids via heat-shock method as published (Pope *et al.* 1996). To prepare and transform

electro-competent *A. rhizogenes* cells, guidelines presented in the "Micropulser™ Electroporation Apparatus Operation Instructions and Application Guide" by BIO-RAD (Bio-Rad Laboratories, Inc., Hercules, CA, USA) were followed.

2.2.1.2 Cultivation of *A. thaliana* plants, seed sterilisation, stress assays

A. thaliana plants were either cultivated on soil or under sterile conditions on ½ MS (Murashige & Skoog) medium solidified by addition of 1 % plant agar (DUCHEFA BIOCHEMIE B.V., RV Haarlem, The Netherlands). Cultivation conditions were as follows: 100 µM s^{-1} m^{-2} photons (unless indicated otherwise) light intensity, 16 h light / 8 h dark period (unless indicated otherwise), light period temperature: 22°C, dark period temperature: 18°C.

A. thaliana seeds were sterilised prior to cultivation under sterile conditions. For that, seeds were submerged for 10 min in 400 µl of sterilisation solution (1:1 ratio ddH_2O and DanKlorix drain cleaning agent), followed by five washing steps, during which the seeds were rinsed with 700 µl of sterile ddH_2O to remove sterilisation solution remnants.

After the seeds were placed on either soil or sterile ½ MS medium, dormancy was overcome by cultivation at 4°C in the dark for 2 d (stratification), prior to cultivation under the conditions mentioned above. Salt stress and osmotic stress conditions were simulated under sterile conditions by addition of either 100 mM NaCl or 200 mM mannitol to the cultivation medium. Root growth analysis was carried out by cultivation of plants under sterile conditions in a vertical fashion. Growth of etiolated seedlings was achieved by cultivating the seeds under standard growth conditions for 6 h after stratification to induce germination, and subsequent cultivation for 5 d under the same conditions under exclusion of light.

After photo documentation of the cultivation plates, root or hypocotyl lengths were measured using ImageJ. The data were analysed in box plots and subjected to statistical analysis of potential differences applying Student's *t*-test.

To induce small interfering RNA (siRNA) expression in plants stably transformed with the pOpOff2 plasmid, the plants were cultivated under sterile conditions with 20 µM Dexamethasone or a comparable amount of DMSO as solvent control added to the medium.

2.2.1.3 Polymerase chain reaction

For amplification of DNA fragments from genomic or plasmid DNA either Taq polymerase (Genaxxon bioscience GmbH, Ulm, Germany) or Phusion polymerase (New England Biolabs GmbH, Frankfurt am Main, Germany) were applied according to manufacturer's instructions, using the assay compositions displayed in Table 3.

Table 3: Composition of the standard PCR mix for Taq and Phusion polymerase

	Taq polymerase	Phusion polymerase
DNA template (5-50 ng/µl)	1.00 µl	1.00 µl
Forward primer (20 pmol/µl)	0.25 µl	0.25 µl
Reverse primer (20 pmol/µl)	0.25 µl	0.25 µl
dNTPs (20 mM each)	0.25 µl	0.25 µl
$MgCl_2$ (25 mM)	1.25 µl	-
Buffer (10 x)	2.50 µl	5.00 µl
Polymerase	0.20 µl	0.20 µl
ddH_20	19.30 µl	18.75 µl
Total	25.00 µl	25.00 µl

PCR was carried out following the protocol in Table 4. Denaturation temperature was adjusted to 94°C for Taq polymerase or 98°C for phusion polymerase. Hybridisation temperature was determined empirically for each primer pair (*). Elongation time was estimated depending on expected PCR product size and polymerase applied (#).

Table 4: Standard PCR protocol. * - hybridisation temperature depended on the primer pair applied in the reaction. # - elongation temperature was chosen according to expected product size and polymerase applied in the reaction.

Initial denaturation	94 °C / 98 °C	180 s	
Denaturation	94 °C / 98 °C	30 s	
Hybridisation	*	30 s	35 cycles
Elongation	72 °C	#	
Final elongation	72 °C	600 s	
Pause	4 °C	∞	

PCR products were analysed on agarose gels (see 2.2.1.4) and purified using the PCR and gel extraction kit Nucleospin II by Macherey-Nagel (Dühren, Germany) according to manufacturer's instructions.

2.2.1.4 Agarose gel electrophoresis

DNA samples were analysed by separation on 1 % NEEO agarose ultra quality (Roth GmbH, Karlsruhe, Germany). Nucleic acids were labelled via in-gel staining with DNA stain G (SERVA Electrophoresis GmbH, Heidelberg, Germany) according to manufacturer's instructions and separation of DNA fragments was carried out at 150 V for 10-15 min. Documentation was performed on a Gerix® 1000 gel documentation system (biostep GmbH, Burkhardtsdorf, Germany).

2.2.1.5 Cut-and-paste cloning of DNA fragments into vectors

In order to clone *A. thaliana* genes into plasmids of choice for downstream application, genes were amplified from genomic DNA (gDNA) using 5'overhang primers for addition of suitable restriction sites. If genes of interest were already present in a vector system, plasmid DNA was used as template for PCR. Subsequently, PCR amplicons were purified as described in 2.2.1.3. Vector DNA and purified PCR products were treated with the respective restriction enzymes by New England Biolabs GmbH (Frankfurt am Main, Germany) or Fermentas (St. Leon Roth, Germany) according to manufacturer's instructions using the restrictions sites indicated in Table 1 and Table 2. Restriction fragments were separated on agarose gels (see 2.2.1.4), purified (see 2.2.1.3) and ligation was carried out at 22°C for a minimum of 1 h with T4 DNA ligase (New England Biolabs GmbH, Frankfurt am Main, Germany) applying a molar vector:insert ratio of 1:4 in a 20 µl reaction assay, which was subsequently used for transformation of chemically competent *E. coli* cells via heat-shock (see 2.2.1.1).

2.2.1.6 Generation of inducible knock-down lines via the pOpOff2 vector

For generation of stable transgenic *atcml4* knock-down lines, the coding sequence (CDS) of At3g59440 was screened for sections that might serve as well-suited targets for siRNA-based post-transcriptional silencing, applying the Clontech RNA interference (RNAi) target

sequence selector tool (http://bioinfo.clontech.com/rnaidesigner/sirnaSequenceDesign.do, Takara Bio USA, Mountain View, CA, USA, as accessed on 21 August 2017). Nucleotides 1-300 of the *AtCML4* CDS were chosen as target region and amplified via site-specific PCR (see 2.2.1.3) for further TOPO® cloning into vector pENTR (Thermo Fisher Scientific, Waltham, MA, USA). The resulting clones were checked via sequencing by the in-house sequencing service (Sequencing unit LMU Biocenter, Munich, Germany) and one of them was applied in an LR-cloning (Thermo Fisher Scientific, Waltham, MA, USA) reaction according to manufacturer's instructions to transfer the insert into the binary vector pOpOff2 (Wielopolska *et al.* 2005) for stable transformation of *A. thaliana* plants.

2.2.1.7 Isolation of gDNA from *A. thaliana*

In order to isolate gDNA from *A. thaliana* for amplification of genomic sequences, a single leaf was submerged in 410 µl of extraction buffer (200 mM Tris-HCl, pH 7.5, 250 mM NaCl, 0.5 % SDS (w/v)) and lysed in the TissueLyser II (Qiagen, produced by Retsch, Hilden, Germany) for 45 s at 30 Hz. Separation of DNA and cell debris was achieved by centrifugation at 17,000 x g and room temperature for 10 min. 300 µl of the supernatant were mixed with 300 µl of isopropanol to precipitate the DNA. Separation of DNA and solvent was achieved by centrifugation at 17,000 x g and room temperature for 10 min. The supernatant was discarded. After air-drying the DNA pellet, it was dissolved in 40 µl of ddH_2O.

2.2.1.8 Stable transformation and downstream selection of *A. thaliana* plants

Stable transformation of *A. thaliana* plants by floral dip method was performed according to a protocol published by Zhang and colleagues (Zhang *et al.* 2006). Plants stably transformed with the pOpOff2 were selected as described by Harrison and colleagues (Harrison *et al.* 2006). Plants stably transformed with pBIN19-NA-YFP plasmid derivatives were cultivated on soil and sprayed with a 0.25 % BASTA solution when they entered the 4-leaf developmental stage and a second time seven days later.

2.2.1.9 Transient transformation of *N. benthamiana* leaf cells

Transient transformation of *N. benthamiana* leaf cells was performed with the *A. rhizogenes* strain LBA1334. For this, bacterial cells transformed with the respective constructs for fusion protein expression, were cultivated overnight at 28°C with 150 rpm agitation. The bacteria were pelleted via centrifugation at 4,000 x g and room temperature for 10 min. The resulting pellet was resuspended in infiltration solution (10 mM MES-KOH pH 5.6, 10 mM $MgCl_2$, 100 µM acetosyringon) and adjusted to an optical density at 600 nm (OD_{600}) of 0.5 in case of single transformation with one construct or OD_{600} of 1, if the plants were to be co-infiltrated with two different constructs from two different transgenic bacterial cell lines. Subsequently, the cell suspensions were incubated at room temperature with 100 rpm agitation in the dark for at least 2 h to allow for expression of tumour inducing genes in the Agrobacterium cells. The suspensions were applied to the abaxial side of the leaves of 3–4 week-old *N. benthamiana* plants, using an Injekt®-F syringe (B. Braun Melsungen AG, Melsungen, Germany) without needle. The plants were sprayed with water and left in the dark at room temperature overnight, before they were cultivated for 2-3 d at 28°C.

2.2.1.10 Isolation of *N. benthamiana* leaf mesophyll cell protoplasts

All required buffers and their respective composition are listed in Table 5 below. 48 h after transient transformation of *N. benthamiana* leaf cells (see 2.2.1.9), leaf material was checked for expression of fluorescent fusion proteins using a fluorescence microscope DM1000 (Leica Microsystems, Wetzlar, Germany). Expressing leaves were harvested for isolation of mesophyll cell protoplasts and sliced into ribbons of approx. 5 mm width. 10 ml of F-PIN buffer were supplemented with 1 % (w/v) Cellulase R10 and 0.3 % (w/v) Macerozyme R10 and incubated at 55°C with agitation for 10 min to activate the enzymes. Ten of the previously prepared leaf slices were submerged in 10 ml of room temperature F-PIN buffer and infiltrated with the solution via repeated application of vacuum. The suspended leaf pieces were incubated on a horizontal shaker for 90 min at 80 rpm in the dark, followed by 1 min of incubation at 160 rpm to release the protoplasts from the surrounding tissue debris. The cells were filtered through a 100 µm nylon mesh and transferred to a centrifugation vessel, in which the suspension was overlaid by 2 ml of F-PCN buffer. Intact protoplasts were separated from cellular debris by centrifugation for 10 min at room temperature and 70 x g in a SIGMA 3K30 centrifuge with a 11391 swing-out rotor (SciQuip Ltd., Newtown, Wem, Shropshire,

Ireland). Intact protoplasts accumulated at the interface between the two buffer phases and were transferred into 10 ml of washing buffer, prior to centrifugation for 10 min at room temperature and 50 x g to pellet the cells. The supernatant was discarded and the cell pellet was gently resuspended in an appropriate amount of F-PCN buffer to yield a cell density suitable for subsequent microscopic analysis (see 2.2.1.12).

Table 5: Composition of solutions required for protoplast isolation from *N. benthamiana* leaf tissue. Micro MS (Murashige & Skoog micro nutrients) composition has been published (Murashige *et al.* 1962). All solutions were filtrated through a 0.45 µm filter for sterility.

Macro MS modified (10x)	KNO3 CaCl2 x 2 H2O MgSO4 x 7 H2O KH2PO4 ddH2O	1012 mg 440 mg 370 mg 170 mg ad 100 ml	
PC vitamins (500x)	Myo-inositol Thiamine-HCl Ca-panthotenate Nicotinic acid Pyridoxine-HCl Biotin ddH_2O	10 g 50 mg 100 mg 100 mg 100 mg 1 mg ad 100 ml	
F-PIN	Macro MS-modified (10x) Micro MS (1000x) PC Vitamins (500x) MES Sucrose ddH_2O	100 ml 1 ml 2 ml 1952 mg Approx. 120 g ad 1000 ml	Adjusted to 550 mOsm with sucrose pH 5.8
F-PCN	Macro MS-modified (10x) Micro MS (1000x) PC Vitamins (500x) MES Glucose ddH_2O	100 ml 1 ml 2 ml 1952 mg Approx. 80 g ad 1000 ml	Adjusted to 550 mOsm with glucose pH 5.8
Wash buffer	$MgCl_2$ x 6 H_2O MES Mannitol (0.5 M) ddH_2O	3.05 g 1 g Approx. 90 g ad 1000 ml	Adjusted to 550 mOsm with mannitol pH 5.8

2.2.1.11 Isolation and transformation of *A. thaliana* leaf mesophyll cell protoplasts

The composition of all buffers required for isolation and transformation of protoplasts from *A. thaliana* are listed in Table 6. Solutions and materials used were sterilised by filtration and the whole procedure was carried out under sterile conditions. Centrifugation steps were carried out in a SIGMA 3K30 centrifuge with an 11391 swing-out rotor (SciQuip Ltd., Newtown, Wem, Shropshire, Ireland). 14 day-old *A. thaliana* plants sterilely cultivated on ½ MS medium solidified with 0.5°% plant agar were used for protoplast isolation. The cotyledons of approx. 100 plants were suspended in 9 ml of MMC buffer, cut with a sterile razor blade and incubated in the dark at room temperature for 1 h. 500 µl of macerozyme solution and 500 µl of cellulose solution were added and the suspension was incubated overnight in the dark at 21°C. To separate the protoplasts from cell debris, the solution was gently stirred and filtered through a 100 µm nylon mesh. Concentration of the isolated cells was achieved via centrifugation for 10 min at 50 x g and room temperature. The supernatant was discarded and the cells were resuspended in 8 ml of MSC solution, which was subsequently overlaid by 2 ml of MMM solution. Separation of intact protoplasts from damaged cells was achieved by centrifugation at 70 x g and room temperature for 10 min. Intact protoplasts, which accumulated at the interface between the two buffer phases, were transferred to a new vessel and resuspended in 9 ml of MMM solution for washing. Separation of the cells from surrounding medium was accomplished by centrifugation at 50 x g and room temperature for 10 min. The supernatant was discarded, the cells were resuspended in 100 µl of MMM solution and transferred into a small Petri dish. 5 µl of a 4 µg/µl solution of the respective plasmid DNA required for transformation were added. Subsequently, 125 µl of freshly prepared PEG4000 solution were added and the mixture was incubated for 7.5 min at room temperature. Then, 125 µl of MMM solution were added, followed by 2 min of incubation at room temperature. After addition of 2.5 µl of PCA medium the Petri dish was sealed with parafilm for overnight incubation of the protoplast suspension in the dark at room temperature. The following day, microscopic analysis was performed (see 2.2.1.12).

Table 6: Buffers and solutions required for isolation and transformation of protoplasts from *A. thaliana* seedlings. All solutions were filtrated through a 0.45 µm filter for sterility. NAA – 1-Naphthaleneacetic acid, MES – 2-(N-Morpholino)ethanesulfonic acid, PEG – polyethylene glycol. * - Gamborg B5 medium (DUCHEFA BIOCHEMIE B.V., RV Haarlem, The Netherlands)

MMC	MES $CaCl_2$ Mannitol	10 mM 20 mM 0.5 M	Adjusted to 550 mOsm with mannitol pH 5.8
MSC	MES $MgCl_2$ Sucrose	10 mM 20 mM 120 g/l	Adjusted to 550 mOsm with sucrose pH 5.8
MMM	MES $MgCl_2$ $MgSO_4$ Mannitol	10 mM 10 mM 10 mM 0.5 M	Adjusted to 550 mOsm with mannitol pH 5.8
PCA medium	Gamborg B5 medium * MgSO4 CaCl Glutamin Casein hydrolysate NAA Glucose	1x 746 mg/l 450 mg/l 50 mg/l 100 mg/l 0.5 mg/l 70 g/l	Adjusted to 550 mOsm with glucose pH 5.8
PEG4000 solution	PEG4000 Mannitol (1M) $Ca(NO_3)_2$ (1M) Sterile ddH_2O	2 g 1 ml 500 µl 1.75 ml	
Macerozyme solution	Macerozyme MMM solution	1 g ad 10 ml	Supernatant separated from insoluble fraction by centrifugation for 1 min at 10,000 x g
Cellulase solution	Cellulase MMM solution	1 g ad 10 ml	Supernatant separated from insoluble fraction by centrifugation for 1 min at 10,000 x g

2.2.1.12 Microscopic analysis of *A. thaliana* and *N. benthamiana* leaf mesophyll protoplasts

Analysis of isolated protoplasts was carried out using a Leica TCS SP5 confocal laser scanning microscope (Leica Microsystems, Wetzlar, Germany). For detection of YFP, samples were excited at 488 nm using an argon laser and emission was detected between 500 nm and

550 nm with a Leica HyD™ detector (Leica Microsystems, Wetzlar, Germany). Excitation of fusion constructs containing mCherry was performed at 561 nm using a diode-pumped solid-state continuous wave laser and the detection range of the HyD™ detector was set to 595-620 nm. Chlorophyll fluorescence was captured via photomultiplier tubes (GaAsP detector) set to detect signals in the spectral range between 680 nm and 750 nm.

2.2.1.13 *In vivo* $[Ca^{2+}]_f$ measurements in *A. thaliana* seedlings

A. thaliana seedlings stably expressing either AtCML5$_{1-28}$-YFP-AEQ, AtOEP7-YFP-AEQ or AtCPK17(G2A)-YFP-AEQ have been cultivated for 14 d as described in 2.2.1.2. Plants of each genotype were pooled in one well of a 6-well cultivation plate and immersed in ddH_2O containing 2.5 µM coelenterazine for reconstitution of holo-aequorin overnight in the dark at room temperature. Afterwards, the plants were transferred to a Berthold 96-well plate for analysis in a TriStar² LB 942 Multimode reader (BERTHOLD TECHNOLOGIES GmbH & Co. KG, Bad Wildbad, Germany) loading each well with one plant and adding 100 µl of ddH_2O. Measurement took place in a well-by-well consecutive fashion. The measurement was divided into two phases. During the first 1800 s the luminescence reporting the *in vivo* $[Ca^{2+}]_f$ was detected. After induction of the discharge of the aequorin pool in the plant achieved by injection of 100 µl of a 3 µM $CaCl_2$ / 20 % ethanol solution, luminescence was detected for another 1800 s to allow for subsequent determination of total aequorin amount that had been available for reporting $[Ca^{2+}]_f$ changes in each plant. The luminescence was determined in photon counts per second at a 1 s interval. The determined values at each time point were used to calculate *in vivo* $[Ca^{2+}]_f$ at a given time by a correlation equation determined by Allen *et al.* (1977) and specifically adjusted for the aequorin variant present in the constructs used here by Brini *et al.* (1995).

2.2.1.14 Luciferase-based promoter activity reporter assay in *A. thaliana* plants

The whole assay was conducted under reduced light-conditions. *A. thaliana* plants stably expressing FIREFLY LUCIFERASE under the control of either *AtCML4* or *AtCML5* promoters were chosen for analysis after cultivation of 5, 14 or 28 d of cultivation under sterile conditions. *In vivo* supply of the enzyme with its substrate (D)-Luciferin was achieved by submerging the entire plants in an aequous solution of 20 µM (D)-luciferin (Sigma-

Aldrich, St. Louis, MO, USA) and applying a light vacuum for up to 3 min. After arranging the plants on a moisturised glass plate, photo documentation of LUCIFERASE activity was performed using an ImageQuant LAS4000 system (GE Healthcare, Freiburg, Germany).

2.2.2 Biochemical methods

2.2.2.1 SDS-PAGE analysis of protein samples

For analysis on SDS-PAGE, protein samples were mixed with the appropriate amount of 2x or 4x Laemmli buffer (Laemmli 1970) depending on overall sample volume and incubated at 96°C for 3 min for protein denaturation. Polyacrylamide gels were prepared with Tris-glycine buffer according to the expected size of the proteins of interest. For size estimation, either 7.5 µl of Peqlab Marker Gold I (Peqlab, Wilmington, DE, USA) or 5 µl of PageRuler™ protein ladder plus prestained marker (Thermo Fisher Scientific, Waltham, MA, USA) were used. Samples were separated at 20 A for 1 h and detection of proteins was achieved either via Coomassie or silver staining of the gels (see 2.2.2.2).

2.2.2.2 Coomassie and silver staining of SDS-PAGE gels

After gel electrophoresis, SDS-PAGE gels were incubated for 20 min with agitation in a Coomassie staining solution (20 % isopropanol, 20 % acetic acid, 0.3 % Coomassie R, 0.06 % Coomassie G). This was followed by incubation in a destaining solution (10 % isopropanol, 10 % acetic acid) for background staining reduction, until an optimal signal-to-noise ratio was achieved.

Silver staining was carried out following a published protocol (Blum *et al.* 1987).

2.2.2.3 Western blot protein analysis

Protein samples were separated via SDS-PAGE (see 2.2.2.1) and subsequently transferred onto 7.5 cm x 8.5 cm nitrocellulose membranes (Schleicher und Schüll, Dassel, Germany) at 64 A for 45 min according to an established protocol (Kyhse-Andersen 1984). Then, the transfer membranes were incubated in blocking buffer (1 x TBS, 0.05 % Tween 20®, 3 % milk powder) for 30 min with agitation and room temperature to saturate the binding capacity of the membrane. This was followed by incubation with the respective antibodies (see Table **7**)

diluted in TBS-T (1 x TBS, 0.05 % Tween 20®) with agitation at 4°C overnight. Afterwards, membranes were washed three times for 10 min with blocking buffer to remove excess antibody. Then, the corresponding secondary antibody diluted in TBS-T was applied for 1 h at room temperature with agitation at the dilutions indicated in Table 7. Afterwards, membranes were washed twice for 10 min with blocking buffer and once for 10 min with TBS-T without milk powder to remove excess antibody. Detection of the secondary antibody was achieved by overlaying the transfer membranes with Western Lightning *Plus* ECL solutions (PerkinElmer Inc., Waltham, MA, USA), previously mixed at a 1:1 ratio according to manufacturer's instructions. After 1 min of incubation in the dark, the result of the western blot was documented using an ImageQuant LAS4000 system (GE Healthcare Europe GmbH, Freiburg, Germany) in precision mode.

Table 7: Antibodies applied in western blot analysis. Donor species are indicated in brackets.

Antibody	Dilution factor
α-GFP (rat)	1,000
α-RFP (rat)	1,000
α-rat (goat)	10,000
28C11 α-AtCML4 (rat)	1,000
15A3-131 α-AtCML4 (mouse)	1,000
α-rat (mouse)	10,000
α-mouse (rat)	10,000

2.2.2.4 Purification of proteins on glutathione sepharose 4B resin

GST-tagged proteins were expressed in *E. coli* cells and purified directly from the cell lysate. If not indicated otherwise, all steps were carried out at 4°C. Approximately 500 ml of cell culture were used to harvest cells via centrifugation for 10 min at 6,000 x g. The supernatant was discarded and the cells were resuspended in binding buffer (140 mM NaCl, 2.7 mM KCl, 10 mM Na_2HPO_4, 2 mM DTT, adjusted to pH 7.3). Cell lysis was achieved by physical rupture in a French press device (unknown manufacturer), followed by three sonication pulses of 10 s duration at 50 % amplitude to fragment genomic DNA reducing viscosity of the suspension. Soluble proteins were separated from aggregated and membrane proteins as well as cell debris by centrifugation at 20,000 x g for 30 min. The pellet was discarded, whereas

the supernatant containing the soluble protein fraction was further processed. 500 µl of glutathione sepharose 4B resin (GE Healthcare GmbH, Freiburg, Germany) were added onto a column and washed with five bed volumes of ddH_2O to remove storage buffer ethanol, followed by rinsing with five bed volumes of binding buffer to equilibrate the resin. Subsequently, the resin was incubated with the bacterial lysate for 1 h with agitation in a 360° overhead rotator. Afterwards, the flow-through of the column was collected and the resin was washed with 200 bed volumes of binding buffer to remove unspecifically retained proteins. Elution was carried out by incubating the resin with one bed volume of elution buffer (50 mM Tris-HCl, 10 mM reduced glutathione, 10 mM DTT, adjusted to pH 8.0) at 25°C for 10 min. The flow-through was collected. This procedure was repeated five times. Samples of all steps of the purification process were analysed via SDS-PAGE (see 2.2.2.1) followed by Coomassie staining of the gels (see 2.2.2.2) to assess purification efficacy.

2.2.2.5 Dialysis of proteins

In order to change the buffer composition of previously isolated proteins, a dialysis approach was chosen. For that, isolated proteins were transferred into regenerated cellulose Spectra/Por dialysis tubes (Spectrum Laboratories Inc., Los Angeles, CA, USA) with 20 kDa size exclusion limit. The tubes were then incubated overnight with agitation at 4°C in an external buffer solution. The volume ratio of sample buffer inside the tube to dialysis buffer surrounding the tube was of ratio 1:100 to guarantee optimum buffer exchange.

2.2.2.6 Coupling of proteins to CNBr-activated sepharose 4B

Proteins previously purified on glutathione sepharose (see 2.2.2.4) were dialysed (see 2.2.2.5) to substitute the coupling buffer (0.1 M $NaHCO_3$, 0.5 M NaCl, adjusted to pH 8.3) for GST elution buffer. The required amount of CNBr-activated sepharose B (GE Healthcare, Freiburg, Germany) was estimated according to manufacturer's instructions and determined by the amount of protein to be coupled, which was approximated by comparison to a protein standard on SDS-PAGE gels. Proteins were coupled to CNBr-activated sepharose according to manufacturer's instructions. The coupling result was analysed via SDS-PAGE (see 2.2.2.1) followed by Coomassie staining (see 2.2.2.2).

2.2.2.7 Isolation of microsomal fractions from *N. benthamiana* leaf material

Tobacco leaves transiently expressing various YFP or mCherry fusion proteins were harvested for isolation of microsomal fractions and chloroplasts. To confirm expression of the fusion proteins in leaf mesophyll cells, leaves were analysed by fluorescence microscopy 48 h after Agrobacterium infiltration. The whole subsequent isolation procedure was performed at 4°C. To yield microsomal fractions, leaves were homogenised in microsome homogenisation buffer (50 mM Tris-HCl, pH 7.5, 1 mM EDTA, 0.5 M sucrose) and filtered through a 30 µm nylon mesh. Enrichment of the microsome-containing fraction was achieved by differential centrifugation for 10 min at 4,200 x g to pellet chloroplasts (pellet was discarded), followed by 10 min of centrifugation at 10,000 x g to pellet mitochondria and nuclei (pellet was discarded). Finally, cytoplasm and microsomal fraction were separated by 1 h of centrifugation at 100,000 x g. The supernatant was discarded and the pellet was resuspended in thermolysin buffer (10 mM Tris-HCl, pH 7.5, 0.25 M sucrose, 2 mM $CaCl_2$) for performance of the protease protection assay.

2.2.2.8 Thermolysin treatment of isolated microsomal fractions

To 50 µl of isolated microsomal fractions (see 2.2.2.7) resuspended in thermolysin buffer (10 mM Tris-HCl, pH 7.5, 0.25 M sucrose, 2 mM $CaCl_2$), thermolysin was added to a final concentration of 2 µg/µl. The same volume of buffer was added to a negative control sample. After 20 min of incubation at 4°C both samples were mixed with EDTA solution to a final concentration of 5 mM EDTA to stop the reaction. The samples were subjected to centrifugation for 10 min at 4°C and 289,000 x g to separate membrane fraction from soluble protein fraction. 17 µl of 4x Laemmli buffer (Laemmli 1970) were added to supernatant and resuspended membrane fraction alike and the samples were incubated for 3 min at 96°C. The samples were separated on SDS-PAGE (see 2.2.2.1) followed by western blot protein analysis with α–GFP or α–RFP antibody (see 2.2.2.3).

2.2.2.9 Pull-down of *A. thaliana* proteins from combined microsome/cytoplasm extracts on CNBr-activated sepharose coated with recombinant protein

All steps of the procedure were carried out at 4°C, if not indicated otherwise. Microsome and cytoplasmic fractions from *A. thaliana* leaf material were isolated as described in 2.2.2.7 with two alterations: The microsome homogenisation buffer had a different composition (50 mM

Tris-HCl, pH 7.5, 0.5 M sucrose) and the final centrifugation step to separate microsomal from cytoplasmic fraction was omitted. The extract was separated into two fractions of which one was adjusted to a final concentration of 1 mM $CaCl_2$, whereas the other one was adjusted to a final concentration 5 mM EDTA / 5 mM EGTA. The CNBr-sepharose samples, to which the previously purified recombinant proteins were coupled (see 2.2.2.4, 2.2.2.5, 2.2.2.6), were also separated into two fractions each. One fraction was equilibrated by addition of five bed volumes of calcium-containing extraction buffer (50 mM Tris-HCl, pH 7.5, 1 mM $CaCl_2$, 0.5 M sucrose), whereas the other one was treated with an equal amount of EDTA/EGTA-containing extraction buffer (50 mM Tris-HCl, pH 7.5, 5 mM EDTA, 5 mM EGTA, 0.5 M sucrose). The resins were incubated with the respective calcium- or EDTA/EGTA-containing plant extract fraction for 1 h on a 360° overhead rotator. The supernatant was collected via gravitational flow and the resins were washed with 200 bed volumes of the according calcium- or EDTA/EGTA-containing extraction buffers to remove unspecifically retained proteins. Elution of the proteins was carried out twice for 10 min. Therefore, half a bed volume of the opposite buffer fraction (calcium-containing buffer for EDTA/EGTA-equilibrated resin and vice versa) was added to the respective resins. Samples of all steps of the pull-down were analysed on SDS-PAGE (see 2.2.2.1) followed by silver staining of the gel (see 2.2.2.2).

2.2.3 Bioinformatical methods

Accession numbers for analysed protein sequences were obtained from the protein database of the National Center for Biotechnology Information (https://www.ncbi.nlm.nih.gov/protein, U.S. National Library of Medicine, Bethesda, MD, USA, as accessed on 21 August 2017), as well as Phytozome 12 (Joint Genome Institute, U.S. Deptartment of Energy, CA, USA, as accessed on 21 August 2017) and are listed in Appendix III. Generation of sequence alignments was performed using the online version of the MAFFT tool version 7 (http://mafft.cbrc.jp/alignment/server/index.html, as accessed on 21 August 2017) applying the L-INS-i algorithm (Katoh *et al.* 2005) and the Blosum62 substitution matrix (Henikoff *et al.* 1993). Similarity-based shading of residues in multiple sequence alignments (MSAs) was performed using the Boxshade server v3.21 (http://www.ch.embnet.org/software/BOX_form.html, as accessed on 21 August 2017, Swiss Institute of Bioinformatics, Lausanne, Switzerland). MSA processing for removal of positions

including gaps prior to reconstruction of phylogenetic trees was performed via the Gap Strip/Squeeze tool v2.1.0 (https://www.hiv.lanl.gov/content/sequence/GAPSTREEZE/gap.html, as accessed on 21 August 2017, HIV Database, www.hiv.lanl.gov, Gap Strip/Squeeze) with 0 % gap tolerance. To reconstruct maximum-likelihood phylogeny trees, RaxML Blackbox (http://embnet.vital-it.ch/raxml-bb/, as accessed on 21 August 2017, (Stamatakis *et al.* 2008)) applying the Blosum62 substitution model (Henikoff *et al.* 1993) was used. Therefore, substitution rate heterogeneity across sites was mapped with a gamma distribution. For evaluation of branch support a non-parametric rapid bootstrap approach with 100 repetitions was applied.

Overall similarity between sequences was determined using the LALIGN tool (http://www.ch.embnet.org/software/LALIGN_form.html, as accessed on 21 August 2017, (Huang *et al.* 1991)). Consensus sequence visualisation was done with the WebLogo server v. 2.8.2 (http://weblogo.berkeley.edu/, as accessed on 21 August 2017, (Schneider *et al.* 1990, Crooks *et al.* 2004)). Prediction of transmembrane domain potential in an amino acid sequence was performed using the Tmpred server (http://www.ch.embnet.org/software/TMPRED_form.html, as accessed on 21 August 2017, Swiss Institute of Bioinformatics, Lausanne, Switzerland, (Hofmann *et al.* 1993)).

Search for promoter region sequences for AT2G43290 and AT3G59440 was conducted on databases Aramemnon 8.1 (http://aramemnon.botanik.uni-koeln.de/, as accessed 21 August 2017, Flügge Lab, University of Cologne) and The Arabidopsis Gene Regulatory Information Server, AGRIS (http://arabidopsis.med.ohio-state.edu/, as accessed on 21 August 2017, The Ohio State University).

In silico analysis of expression levels and promoter *cis*-elements of AT2G43290 and AT3G59440 was performed using the Transcriptome Variation Analysis Database (http://travadb.org, as accessed on 21 August 2017) (Klepikova *et al.* 2015, Klepikova *et al.* 2016, Kasianov *et al.* 2017), the AtGenExpress Visualization Tool (http://jsp.weigelworld.org/expviz/, as accessed on 21 August 2017, Max-Planck-Institute for developmental biology, Tübingen, Germany), the Arabidopsis *cis*-regulatory element database (http://arabidopsis.med.ohio-state.edu/AtcisDB/, as accessed on 21 August 2017, The Ohio State University, OH, USA) and the e-FP browser (http://bar.utoronto.ca/efp_arabidopsis/cgi-bin/efpWeb.cgi, as accessed on 21 August 2017, University of Toronto, Toronto, Canada).

3. Results

3.1 In-depth characterisation of AtCML4 and AtCML5 sub-cellular localisation and topology

3.1.1 Sequence analysis of the N-terminus of AtCML4- and AtCML5-like proteins in Brassicaceae species

The *A. thaliana* genome encodes over 50 CML proteins (McCormack *et al.* 2003) and three CAM isoforms in six different genes. Whereas CAMs are highly conserved in their sequence and consist of four EF-hand motifs for Ca^{2+} binding, CMLs are rather diverse. Most of these proteins contain four EF-hands similar to classical CAMs, but there is a group of CMLs in which the EF-hand number varies from one, e.g. AtCML1 to six, e.g. AtCML12. In addition to that, many CMLs have a much longer amino acid sequence compared to canonical CAMs, and often comprise N-terminal sequences potentially serving as sub-cellular targeting signals. AtCML4 and AtCML5 are characterised by the presence of a CAM-domain consisting of four EF-hands. Further, they possess an N-terminal sequence stretch of 50 and 64 amino acids, respectively, which precedes an (E/D)LKR sequence pattern marking the beginning of the first of the four EF-hand motifs. This N-terminus is divided into an N-proximal region of very high conservation between AtCML4 and AtCML5 comprising amino acids 1-32, whereas the rest of the N-terminal stretch shows strong dissimilarity.

BLAST search analysis for proteins with similar sequence in the proteome of other Brassicaceae species, namely *Arabidopsis lyrata* (*A. lyrata*), *Brassica rapa* subsp. *pekinensis* (*B. Rapa*), *Brassica napus* (*B. Napus*), *Brassica oleracea* var. *oleracea* (*B. Oleracea*), *Capsella rubella* (*C. rubella*), *Eutrema salsugineum* (*E. salsugineum*), and *Raphanus sativus* (*R. Sativus*) revealed the presence of highly similar, potentially orthologous proteins for both AtCML4 and AtCML5. As shown in Figure 1 each of these proteins contains a similar N-terminal region with the same overall structure.

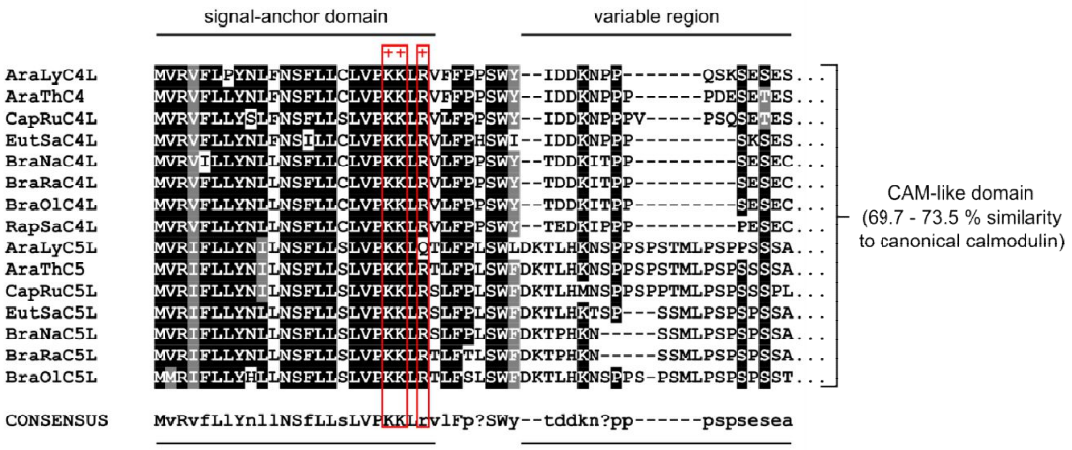

Figure 1: Identity-shaded multiple sequence alignment of the N-terminal region of AtCML4- and AtCML5-like proteins in Brassicaceae species. The N-terminal region of all sequences is divided into a conserved sequence stretch and a variable part. The highly conserved region between M_1 and R_{24} (Q_{24}) displays the common features indicative of a signal-anchor domain consisting of a hydrophobic transmembrane domain between residues M_1 and V_{19}, followed by a positive net charge originating from K_{21}, K_{22} and in most sequences R_{24} (red box, only exception is AraLyC5L with a Q_{24}), relative to the flanking region on the N-terminal end of the transmembrane domain. Downstream of residue Y_{32} the N-proximal sequence stretch is significantly less conserved between the two groups of AtCML4-like proteins and AtCML5-like proteins. Black shading – identical residue present in at least 85 % of all sequences at the respective position. Grey shading – identical chemical property present in at least 85 % of all sequences at the respective position. For species list see Appendix I.

Analysis of this N-terminal region with prediction tools recognising the propensity for transmembrane domain formation in an amino acid sequence, revealed a potential α-helical domain between amino acid M_1 and V_{19} that could serve as membrane anchor. This stretch is followed by two lysine residues and an arginine residue, K_{21}, K_{22} and R_{24}. The only exception from that is the CML5-like from *A. lyrata* (AraLyC5L), in which an aspartate is found in position 24. This causes an electrostatic gradient of increasing positive charge along the transmembrane region from the N-terminal towards the C-terminal flanking region, which – among other criteria like hydrophobicity and hydrophobicity distribution within the transmembrane region – is considered to be a typical structural element of a signal-anchor domain in a type-III single-pass transmembrane protein (Harley *et al.* 1998). Following the so-called "positive-inside-rule", this structure is known to result in a topology, in which the C-terminal part of the protein is located in the cytoplasm, whereas the N-terminus protrudes into the lumen of a membrane-enclosed compartment or the extracellular space (Harley *et al.* 1998, Heijne 1994).

3.1.2 Analysis of AtCML4 and AtCML5 co-localisation in *N. benthamiana* protoplasts and endogenous promoter-driven expression in *A. thaliana* protoplasts

Previous analyses regarding the sub-cellular localisation of AtCML5-GFP constructs in *A. thaliana* protoplasts revealed that the protein is localised in circular structures that are part of the endomembrane system of the cells, indicating a membrane association. However, there was no experimental evidence, whether AtCML4 and AtCML5 co-localised, although this was an obvious assumption due to the high degree of sequence conservation within the N-terminal region, which had been proven to determine its sub-cellular localisation in previous studies (Flosdorff 2014).

In order to determine, whether AtCML4 and AtCML5 do indeed co-localise *in vivo*, protoplasts of *N. benthamiana* plants transiently co-expressing AtCML4-mCherry and AtCML5-YFP were analysed via confocal laser scanning microscopy (see Figure 2A). Fluorescence signals emanating from both proteins clearly originated from the same sub-cellular localisation indicating co-localisation of the analysed constructs, thereby underlining the speculative conclusions drawn from bioinformatic analysis (see 3.1.1). This was also analysed quantitatively (see 3.1.3).

The unusual shape of the fluorescence signals detected for both fusion constructs, displaying a circular geometry indicative of enlarged vesicles, gave rise to the question as to whether this might be an artefact of the 35S-promoter-driven expression of the constructs. To exclude this as potential cause, genomic regions upstream of *AtCML4* (*pATCML4*) and *AtCML5* (*pATCML5*) (see 2.1.3), predicted to include promoter elements of the respective genes, were cloned to control the expression of AtCML4-YFP (*pAtCML4*::AtCML4-YFP) and AtCML5-YFP (*pAtCML5*::AtCML5-YFP), respectively, in transiently transformed *A. thaliana* protoplasts, replacing the 35S-promoter (see Figure 2B).

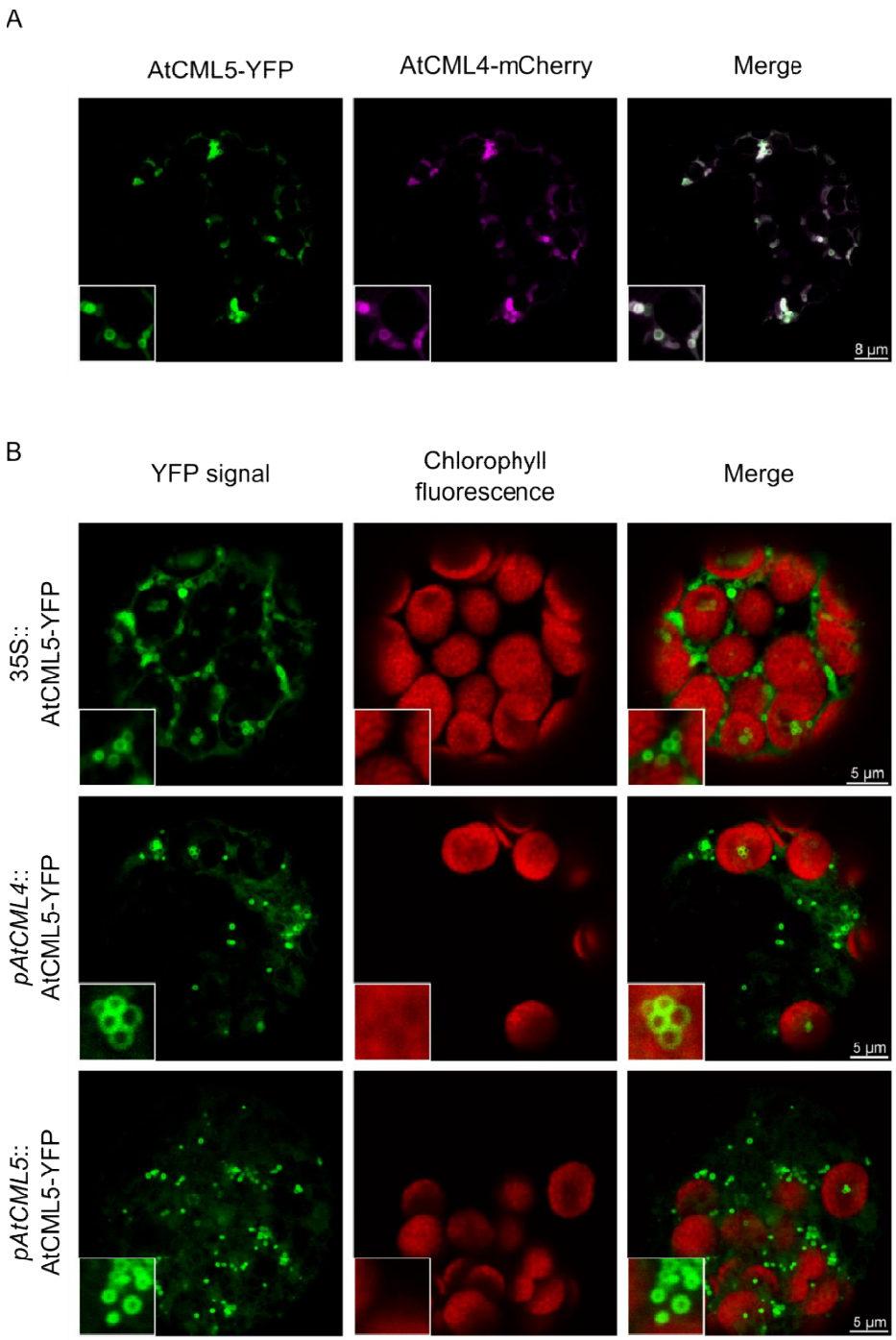

Figure 2: **Microscopic localisation analysis of AtCML4-mCherry and AtCML5-YFP.** (**A**) Protoplasts isolated from *N. benthamiana* plants transiently co-expressing AtCML4-mCherry and AtCML5-YFP showed significant overlap of fluorescence signals, indicating their co-localisation within the same compartment. (**B**) Comparison of AtCML5-YFP transiently expressed in tobacco leaf cells under the control of a 35S-promoter (row 1) with AtCML4-YFP and AtCML5-YFP expressed under control of *AtCML4* and *AtCML5* promoter region, respectively, (rows 2 and 3). *pAtCML4*::AtCML4-YFP and *pAtCML5*::AtCML5-YFP displayed circular fluorescence patterns similar to the structures detected upon 35S-promoter-driven expression in *N. benthamiana* cells. Analyses were carried out applying confocal laser scanning microscopy (single images, layer density 40 nm). White bars represent the scale of indicated size.

Analysis of *A. thaliana* protoplasts transiently expressing AtCML4-YFP and AtCML5-YFP, under control of *AtCML4* or *AtCML5* promoter region, respectively, revealed that the circular structures with unusually large diameters, previously observed under 35S-promoter driven expression, were not a result of strong overexpression of the fusion proteins. All three samples were analysed under the same conditions with identical microscope parameters except for the gain of the detector for the YFP channel. To receive comparable signal intensity, this parameter was set to 235.3 % and 71.8 % for samples under endogenous and 35S-promoter control, respectively. This indicated the substantially higher abundance of YFP-fusion construct in overexpressing protoplasts compared to cells, in which expression was driven by the endogenous promoters of both genes.

3.1.3 Detailed analysis of AtCML5-YFP sub-cellular localisation

Previously performed co-localisation experiments with AtCML5-YFP and AtARA6-mCherry, a RabGTPase labelling late endosomes (Ueda *et al.* 2004), had revealed a partial overlap between their fluorescence signals. However, a similar partial overlap had been observed, when AtCML5-YFP was expressed with the *cis*-Golgi marker GmMANI-mCherry, which is an α-1,2-MANNOSIDASE I from *Glycine max* (Saint-Jore-Dupas *et al.* 2006). Therefore, it was difficult to determine, which compartment AtCML5 ultimately resides in.

To elucidate the localisation of AtCML5, a more detailed analysis was conducted in protoplasts of *N. benthamiana* plants co-expressing AtCML5-YFP with marker proteins for peroxisomes (mCherry-SKL), *cis*-Golgi vesicles (GmMAN1-mCherry), late PVC (AtARA6-mCherry), as well as with AtCML4-mCherry. Co-localisation with GmMAN1-mCherry and AtARA6-mCherry had not been analysed in a quantitative fashion before. Additionally, fluorescence signal overlap between AtARA6-mCherry and AtCML5-YFP in *N. benthamiana* protoplasts had not been shown in previous analyses.

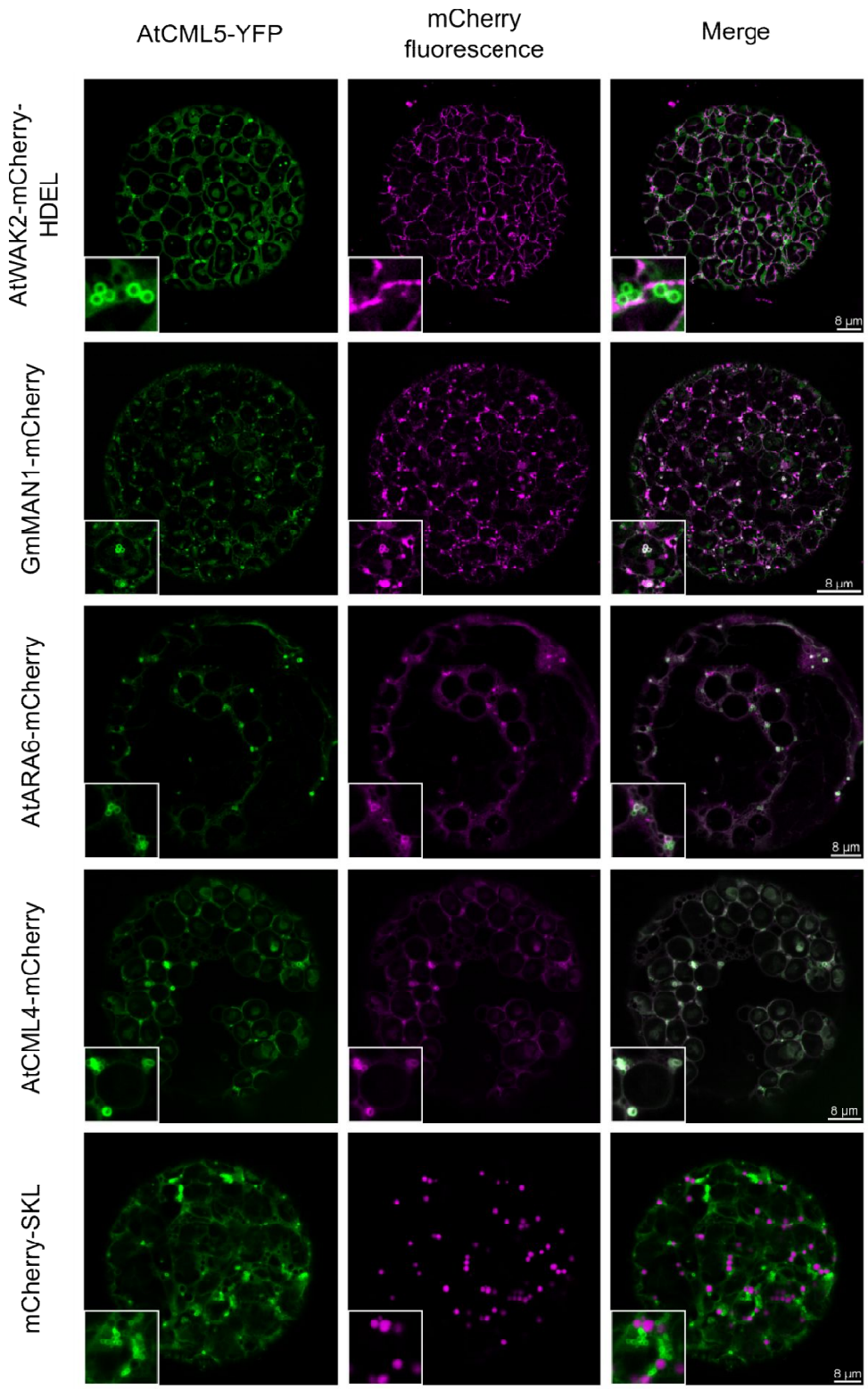

Figure 3: Co-expression analysis of AtCML5-YFP and different mCherry-fused marker constructs. Co-expression of AtCML5-YFP and several marker constructs in tobacco leaf cells was performed to subsequently gain quantitative data on the extent of overlap between the fluorescence signals in the different samples. Signal overlaps (indicated by white signal colour in the merge) with mCherry-tagged AtARA6 and GmMAN1 were observed in circular structures. Co-expression with AtCML4-mCherry served as positive control displaying complete signal overlap, whereas signals from mCherry-SKL in peroxisomes did not occur in the same positions with AtCML5-YFP, rendering it a suitable negative control. Data displayed here are examples of the microscopic data used for quantitative analysis shown below. White bars represent the scale of indicated size.

Microscopic analysis of tobacco cells expressing AtCML5-YFP and GmMAN1-mCherry or AtARA6-mCherry, respectively, showed overlaps of the different fluorescent signals in both cases (see Figure 3, rows 2 and 3). Overlaps primarily occurred at positions, where the signals were circular, indicating the co-localisation in vesicular structures. Signal geometries retrieved for these marker constructs, which usually appear as punctae upon single expression (Ueda *et al.* 2004, Saint-Jore-Dupas *et al.* 2006), were observed to be of circular character when co-expressed with AtCML5-YFP. Co-localisation never occurred at positions, at which the marker construct signals showed punctae. Protoplasts co-expressing AtCML5-YFP and the ER marker AtWAK2-mCherry-HDEL only showed signal overlaps where the YFP signal did not occur in circular structures. However, in these positions the geometry of the signals differed, whereas ER marker signals were filamentous with defined edges, YFP signals were of diffuse character indicative of a cytoplasmic localisation. Therefore, an alleged co-localisation of the two protein populations at these positions might be false-positive due to insufficient resolution. In contrast to that, AtCML4-mCherry and AtCML5-YFP signals overlapped independent of signal geometry. No overlap at all was observed for the signals in cells co-expressing AtCML5-YFP and mCherry-SKL, as had previously already been shown (Flosdorff 2014) and was repeated here to serve as example for spatially non-correlated signals in the quantitative analysis of the microscopic co-expression data described below.

Quantitative analysis of the co-expression of AtCML5-YFP with different marker constructs in *N. benthamiana* protoplasts was performed to unambiguously determine the final localisation of AtCML5 *in vivo*. For quantification of the spatial correlation between signals emanating from AtCML5-YFP and the respective mCherry-fused marker constructs, microscopic data (examples shown in Figure 3) were analysed employing the “Coloc2” plugin of the Fiji Software (ImageJ 1.51n, Wayne Rasband, National Institute of Health, Bethesda, MD, USA) with Costes threshold regression. The software calculates Pearson’s correlation coefficient as a numerical measure for spatial correlation of the signals detected in two separate channels of a microscopic image. The correlation coefficients derived from five different cells per construct combination were calculated and are depicted as box plot (see Figure 4).

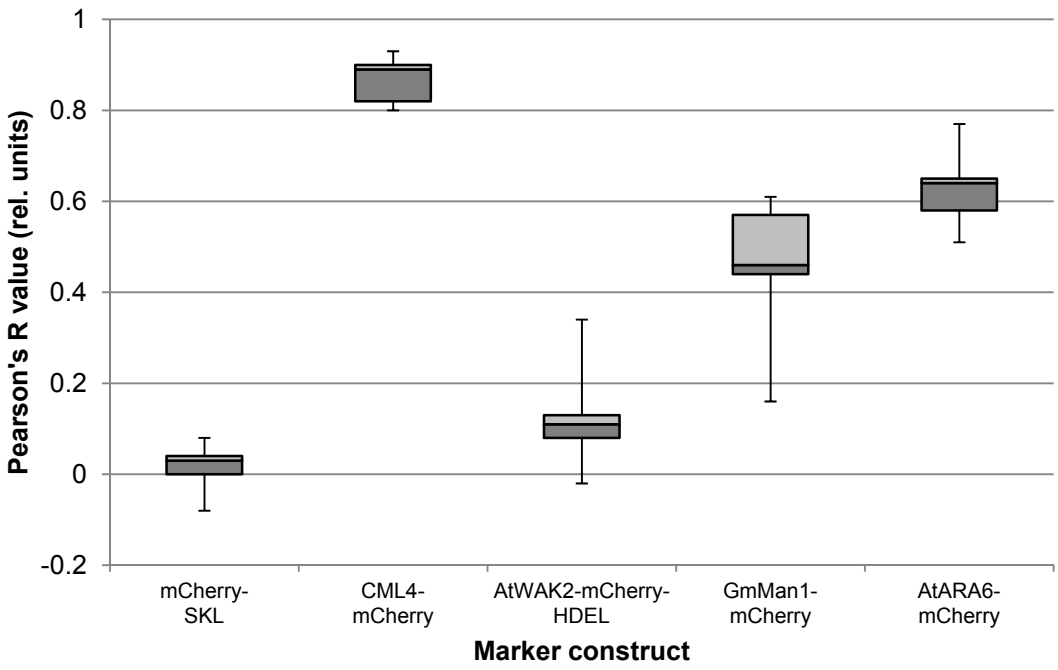

Figure 4: Spatial correlation of signals from AtCML5-YFP and different marker constructs co-expressed in *N. benthamiana* protoplasts. Microscopic data of *N. benthamiana* protoplasts co-expressing AtCML5-YFP and mCherry-fused markers were analysed employing the Fiji Software plugin "Coloc 2" with Costes threshold regression. Pearson's R values were determined for each cell, describing the extent of spatial correlation between fluorescence signals from AtCML5-YFP and the respective co-expressed construct. Person's R values depicted as box plot are derived from five different cells per fusion construct combination. R = +/- 1 indicates absolute spatial co-occurrence of two signals. With R values between 0.45 and 0.65 AtCML5-YFP shows a significant but partial co-localisation with markers for *cis*-Golgi and the late PVC.

Correlation values of 0.8-0.9 for signals between AtCML5-YFP and AtCML5-mCherry served as a measure for near-absolute co-localisation, whereas correlation values of 0-0.05 between mCherry-SKL and AtCML5-YFP signal occurrence defined the example for spatially unrelated signals. Most of the analysed cells co-expressing AtCML5-YFP and the ER marker AtWAK2-mCherry-HDEL showed a spatial correlation that was in a range comparable to the negative control, however stronger variation occurred. The median of signal correlation of AtCML5-YFP with the markers for *cis*-Golgi and the PVC was at 0.46 (*cis*-Golgi, marked by GmMAN1-mCherry) and 0.64 (late PVC, marked by AtARA6-mCherry), respectively. So the fraction of AtCML5-YFP co-localising with AtARA6-mCherry was slightly larger.

3.1.4 Topology elucidation for AtCML5-YFP and AtCML5$_{1-28}$-YFP via protease protection assay

The alleged localisation of AtCML5 (and AtCML4) on vesicular structures of the endomembrane system raised the further question, whether the catalytical CAM-domain

resides in the vesicular lumen or the cytoplasm.

A common procedure to analyse the topology of a membrane-bound protein is to perform a protease protection assay on isolated membrane fractions containing the protein of interest. The protease thermolysin is often applied in this assay, but others e.g. proteinase K or trypsin can also be utilised (Bendz *et al.* 2013). Thermolysin is incapable of entering the isolated membrane vesicles, leaving luminal proteins and transmembrane sections of integral membrane proteins unaffected, whereas protein domains protruding from the cytoplasmic surface of the isolated membranous compartments are proteolytically degraded. To perform this assay, microsomes from *N. benthamiana* plants transiently expressing AtCML5-YFP, AtCML5$_{1-28}$-YFP or AtWAK2-mCherry-HDEL were isolated (see 2.2.2.7) and treated with 2 µg/µl thermolysin (see 2.2.2.8) to degrade proteins outside of or on the cytoplasmic surface of the membranous compartments. Treatment of microsomes with an equivalent amount of protease-free assay buffer served as control. The result of the procedure was determined by SDS-PAGE separation followed by western blot analysis using α-GFP and α-mCherry antibodies (see Figure 5). AtCML5$_{1-28}$-YFP, a fusion protein containing the first 28 amino acids of AtCML5 fused to YFP, had previously been shown to be sufficient for anchoring the protein in the membrane (Flosdorff 2014). It was included in this assay in addition to the full-length AtCML5 protein, because it resembles the *in vivo* conditions more closely with the fusion protein being of comparable size as the endogenous full-length AtCML5.

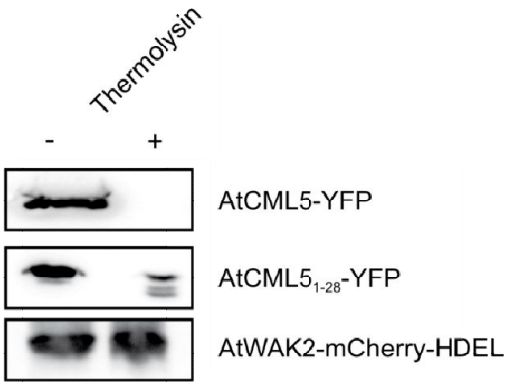

Figure 5: Thermolysin treatment of microsomes isolated from *N. benthamiana* leaves. Isolated membrane fractions from tobacco expressing either AtCML5-YFP, AtCML5$_{1-28}$-YFP or AtWAK2-mCherry-HDEL were treated with 2 µg/µl thermolysin (+) or the respective amount of buffer (-) to shave membrane proteins exposed to the cytoplasm. The assay was analysed via SDS-PAGE followed by western blot analysis using α-GFP and α-mCherry antibodies. Whereas the signals for AtCML5-YFP and AtCML5$_{1-28}$-YFP either vanished or significantly decreased upon thermolysin treatment, indicating their exposure on the cytoplasmic surface of the vesicles, the signal for AtWAK2-mCherry-HDEL remained unaltered, because the marker is an ER resident luminal protein protected from the protease by the surrounding membranes. Modified from (Ruge *et al.* 2016).

In the control samples, which were treated with buffer instead of thermolysin, signals for all protein constructs could be detected by western blot analysis (see Figure 5, left lanes). In thermolysin-treated samples, no signal was observed for microsomes containing AtCML5-YFP and the signal for AtCML5$_{1-28}$-YFP was significantly reduced in intensity (see Figure 5, right lanes). By contrast, the luminal ER control protein AtWAK2-Cherry-HDEL was not affected by the treatment, visualised by the unaltered signal intensity in both treated and untreated microsomal fractions (see Figure 5 , bottom right lane). This result indicates that the full-length protein AtCML5, as well as its first 28 amino acids have a topology with their carboxy termini being exposed on the cytoplasmic surface of the vesicles. Therefore, AtCML5 and probably also AtCML4, have their CAM-domains protruding into the cytoplasm, rendering them capable of detecting $[Ca^{2+}]_f$ fluctuations in the cytoplasm in close proximity to endosomal membranes.

This raised the question as to whether the two proteins detect changes in cytoplasmic $[Ca^{2+}]_f$ similar to cytosolic, non-membrane-attached Ca^{2+} sensors or whether they might be exposed to a microdomain around the vesicles characterised by $[Ca^{2+}]_f$ different to those in the remaining cytoplasm. In the latter case, the proteins would selectively react to $[Ca^{2+}]_f$ fluctuations in close vicinity to the vesicular membranes, e.g. caused by Ca^{2+} efflux from the vesicular lumen.

3.2 Functional analysis of AtCML4 and AtCML5

3.2.1 *In vivo* measurement of $[Ca^{2+}]_f$ fluctuations in close proximity to membranes in *A. thaliana*

To analyse the $[Ca^{2+}]_f$ in the vicinity of AtCML4 and AtCML5 *in vivo*, *A. thaliana* plants were stably transformed to express AtCML5$_{1-28}$-YFP-AEQ, a protein containing the membrane anchor of AtCML5 fused to the yellow fluorescent protein (YFP) and the Ca^{2+} sensor apo-aequorin (AEQ). This allowed the direct comparison to plants expressing the same YFP-AEQ fusion protein in the cytosol that were previously described (Mehlmer *et al.* 2012). AEQUORIN was originally isolated from the jellyfish family Aequorea (Shimomura *et al.* 1962) and requires the presence of coelenterazine, a prosthetic group, in order to be fully functional as a Ca^{2+} sensor. The protein is capable of reporting changes in cellular Ca^{2+} at physiological concentrations, by catalysing the decarboxylation of coelenterazine, which

emits luminescence light with an intensity peak at 469 nm. Ca^{2+} are required as cofactors for the reaction. Under physiological $[Ca^{2+}]_f$, there is a double logarithmic correlation between detected luminescence light and the $[Ca^{2+}]_f$ (Allen *et al.* 1977). The expression of the sensor construct was driven by the *AtCML5* promoter region to minimise the population of fusion proteins being mistargeted to the cytoplasm due to overexpression conditions. Plants expressing either a cytoplasmic Ca^{2+} sensor, AtCPK17(G2A)-YFP-AEQ, or a sensor attached to the cytoplasmic surface of the chloroplast outer envelope, AtOEP7-YFP-AEQ , served as controls for detection of $[Ca^{2+}]_f$ fluctuations in the entire cytoplasm or in close proximity to membranes. Their expression was driven by a 35S-promoter. Both of these sensor constructs had previously been analysed and published to be functional (Mehlmer *et al.* 2012). A schematic view of the applied sensor constructs, their relative size and sub-cellular localisation, as well as the result of basal $[Ca^{2+}]_f$ levels reported by these fusion proteins are shown in Figure 6.

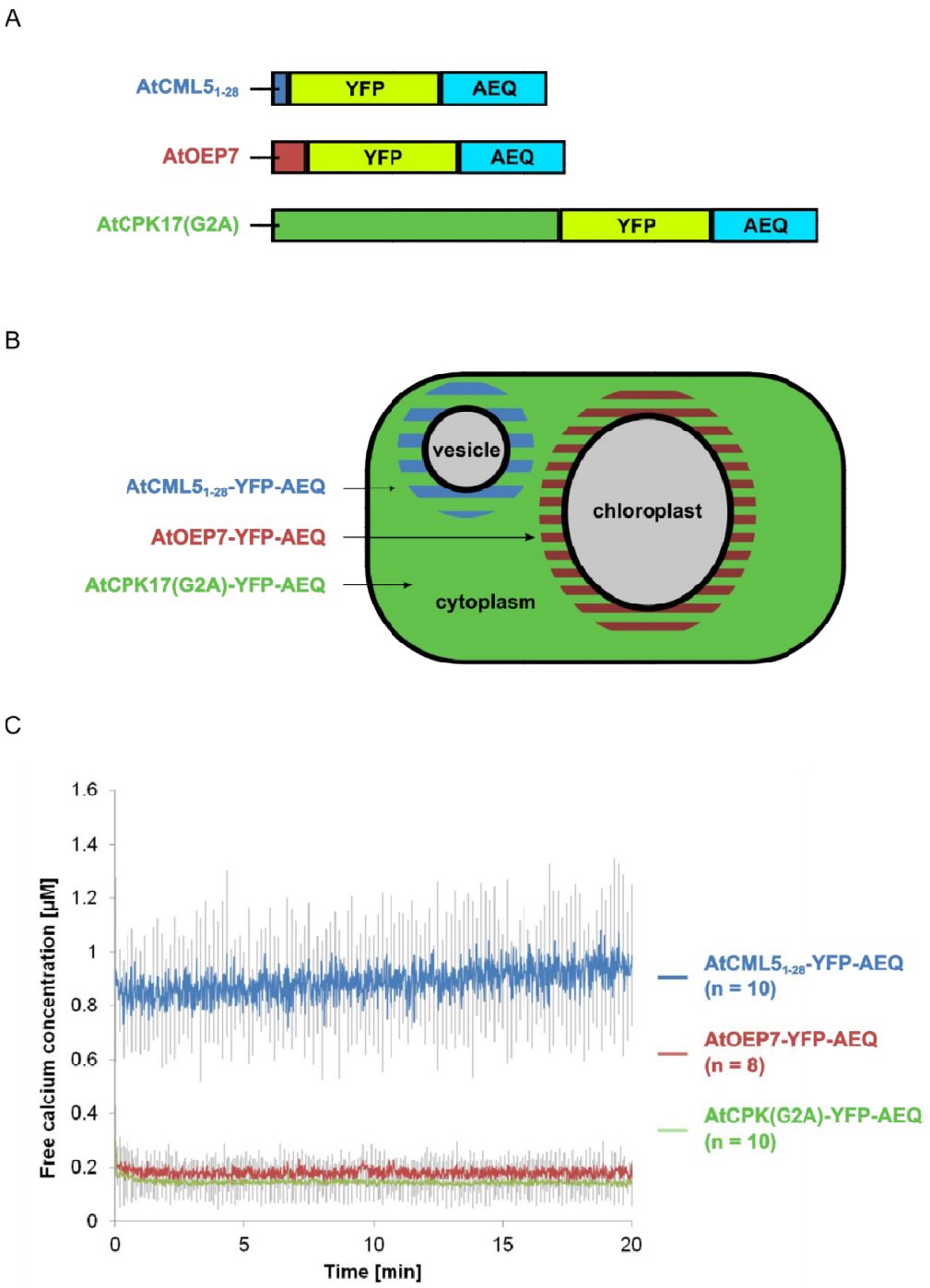

Figure 6: *In vivo* $[Ca^{2+}]_f$ fluctuation measurement. (**A**) Schematic drawing of the applied sensor constructs AtCML5$_{1-28}$-YFP-AEQ, AtOEP7-YFP-AEQ and AtCPK17(G2A)-YFP-AEQ with their relative size and (**B**) their sub-cellular localisation. Whereas AtCPK17(G2A)-YFP-AEQ senses $[Ca^{2+}]_f$ changes in the whole cytoplasm, as well as in vicinity to all membranes facing it, AtCML5$_{1-28}$-YFP-AEQ and AtOEP7-YFP-AEQ only sense cytoplasmic $[Ca^{2+}]_f$ fluctuations in close proximity to endosomal membranes and chloroplast outer envelope, respectively. The relative size of the displayed schematic cell and its compartments do not resemble the *in vivo* relations. (**C**) Basal $[Ca^{2+}]_f$ levels in 5 day-old *A. thaliana* seedlings detected by the respective stably expressed sensor construct differed significantly, with $[Ca^{2+}]_i$ having been highest close to endosomal membranes (approx. 0.9-1 µM), exceeding the $[Ca^{2+}]_f$ around chloroplasts (approx. 0.2 µM) and the $[Ca^{2+}]_f$ detected in the whole cytoplasm (approx. 0.18 µM) by a factor of five. The normalised levels of $[Ca^{2+}]_f$ in the microdomain surrounding the vesicles also are less steady and vary more strongly between the different plants analysed. $[Ca^{2+}]_f$ for each plant line shown in the graph are mean values of the $[Ca^{2+}]_f$ measured in ten (eight) different plants. Error bars indicate the standard error.

Instead of using the full-length AtCML5 for targeting the sensor construct to the respective endosomal vesicles, only the first 28 amino acids of AtCML5 comprising the signal-anchor were chosen. This reduced the distance of the sensor protein AEQ to the membrane, thereby allowing for a higher probability of detecting differences in the local $[Ca^{2+}]_f$ within the microdomain surrounding the vesicles compared to $[Ca^{2+}]_f$ in the remaining cytoplasm. The sensor protein AtOEP7-YFP-AEQ is of comparable size and topology as AtCML5$_{1-28}$-YFP-AEQ, but anchored in the outer envelope of chloroplasts, which defined it as ideal control for the detection of $[Ca^{2+}]_f$ levels in the cytoplasmic environment surrounding a membrane-enclosed compartment. Additionally, it granted the possibility of distinguishing between stimuli that selectively evoked $[Ca^{2+}]_f$ fluctuations around either endosomes (see Figure 6 B, blue halo around vesicle) or chloroplasts (see Figure 6 B, red halo around chloroplast). In order to separate this from $[Ca^{2+}]_f$ changes in the whole cytoplasm (see Figure 6 B, regions coloured green), the sensor construct AtCPK17(G2A)-YFP-AEQ was included in the analysis.

Prior to consecutive analysis of the plants stably expressing the respective sensor constructs, the AEQ moiety of the sensors had to be reconstituted with its prosthetic group coelenterazine. Since the binding of coelenterazine by AEQ is the rate-limiting step in the decarboxylation reaction catalysed by holo-AEQUORIN, the reconstitution was performed by immersing the plants in de-ionised water including 2.5 µM coelenterazine and incubating them overnight in the dark. The measured luminescence intensity values were translated into $[Ca^{2+}]_f$, applying an algorithm specifically designed for the AEQUORIN isoform present in the constructs (2.2.1.13). In comparison to the $[Ca^{2+}]_f$ reported by AtCPK17(G2A)-YFP-AEQ ($[Ca^{2+}]_{Cyt}$) to be approx. 0.18 µM, the $[Ca^{2+}]_f$ around the chloroplasts ($[Ca^{2+}]_{Chl}$) as detected by AtOEP7-YFP-AEQ was slightly elevated to 0.2 µM. This showed that there is only a minor difference in the basal levels of $[Ca^{2+}]_{Cyt}$ in the whole cytoplasm and the region in close vicinity to the chloroplast membrane. In strong contrast to that was the basal $[Ca^{2+}]_f$ level detected around the endosomes, marked by AtCML5$_{1-28}$-YFP-AEQ, $[Ca^{2+}]_{End}$. In this region the $[Ca^{2+}]_f$ was less steady and fluctuated around a value of 0.9 µM, indicating the existence of a potential Ca^{2+} microdomain around certain populations of endosomal vesicles. Due to a lack of time, initial analyses involving the application of different stimuli, e.g. salt stress, cold stress, osmotic stress, triggering Ca^{2+} fluxes have been performed, but more experiments are required for valid results.

3.2.2 Interaction partner identification via Ca^{2+}-dependent pull-down assay from microsome/cytoplasm extracts from *A. thaliana* leaf tissue

The topology of AtCML5 with its CAM-domain protruding into the cytoplasm enables it to bind potential interaction partners localised either in the cytoplasm or attached to the membranes of the vesicles AtCML5 is anchored in or even attached to other vesicles in sufficient proximity. Therefore, pull-down assays to find interaction partners of AtCML5 in combined microsome and cytoplasm extracts were performed.

To isolate potential interaction partners from combined microsome and cytoplasm extracts from *A. thaliana* leaf tissue, AtCML5 was heterologously expressed in *E. coli* with an N-terminal GST tag for purification. Heterologous expression of the tagged full-length AtCML5 yielded only small amounts of soluble recombinant protein, probably due to enhanced aggregation of the overexpressed protein, stimulated by the hydrophobicity of its membrane anchor, which ultimately resulted in degradation of the protein. Therefore, a GST-tagged, truncated version of AtCML5 lacking the first 20 amino acids comprising its signal-anchor domain was used (GST-AtCML5$_{21-215}$). Recombinant GST was chosen to serve as negative control in the pull-down assay and was expressed, purified and subsequently processed equally to GST-AtCML5$_{21-215}$.

Isolation of the soluble recombinant protein from *E. coli* lysates was performed on a Glutathione sepharose 4B resin (GE Healthcare Europe GmbH, Freiburg, Germany) yielding large amounts of sufficiently pure recombinant protein (see 2.2.2.4). Due to the abundance of glutathione S-transferases and other glutathione-binding proteins in extracts from *A. thaliana*, the pull-down could not be performed on GST-AtCML5$_{21-215}$-coated glutathione sepharose. Hence, the fusion protein had to be eluted and subsequently transferred into a new buffer environment via overnight dialysis at 4°C (see 2.2.2.5) to prepare it for coupling to a CNBr-activated sepharose 4B resin (GE Healthcare Europe GmbH, Freiburg, Germany). This pre-activated resin is designed for coupling proteins in a tag-independent manner, requiring only free amino groups being available as active coupling moiety in the respective protein. After covalently linking the purified protein to the resin material (see 2.2.2.6), microsome/cytoplasm extracts previously adjusted to contain either 1 mM $CaCl_2$ (+ Ca^{2+}) or 5 mM EDTA / 5 mM EGTA (- Ca^{2+}) were added to the resin (see 2.2.2.9 for details). The goal was to transfer AtCML5$_{21-215}$ from its apo- to its holo-state by supplying it with Ca^{2+}, thus enabling it to bind potential interaction partners in the extract. Elution was accomplished by removing the Ca^{2+} via addition of an EDTA/EGTA-containing buffer, transferring

$AtCML5_{21-215}$ to its apo-state again, thereby causing the release of the previously bound interacting proteins. The eluted fractions were analysed via SDS-PAGE followed by silver staining (see Figure 7). Protein bands occurring exclusively in the elution of the "+ Ca^{2+}" sample, but not in the "– Ca^{2+}" sample or the GST controls were considered potential interaction partners. The assay was repeated three times, the results were compared and bands that re-occurred at least in two of the assays were isolated and sent for mass spectrometric analysis by the *Zentrallabor für Proteinanalytik* at the BMC, LMU Munich. A schematic overview of the experimental procedure and representative elutions analysed via SDS-PAGE are shown in Figure 7.

A

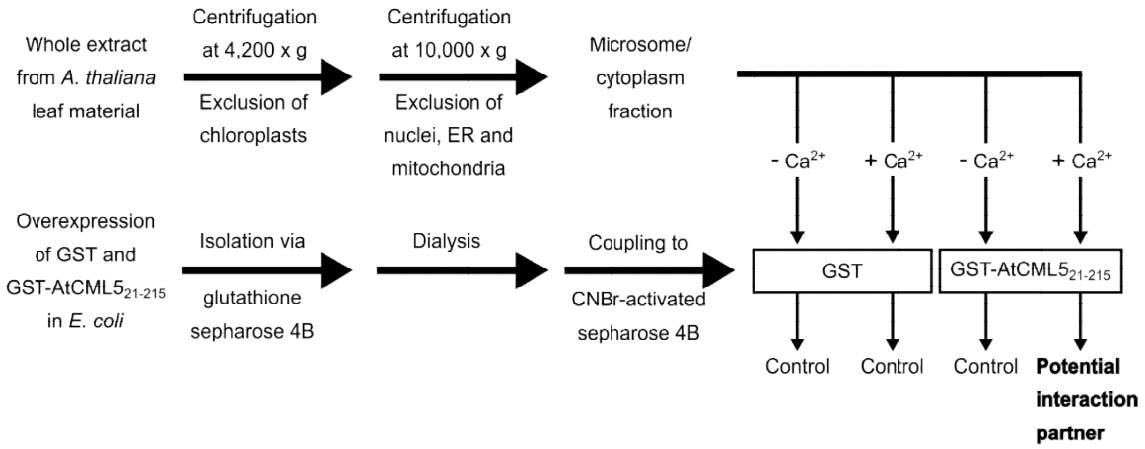

B

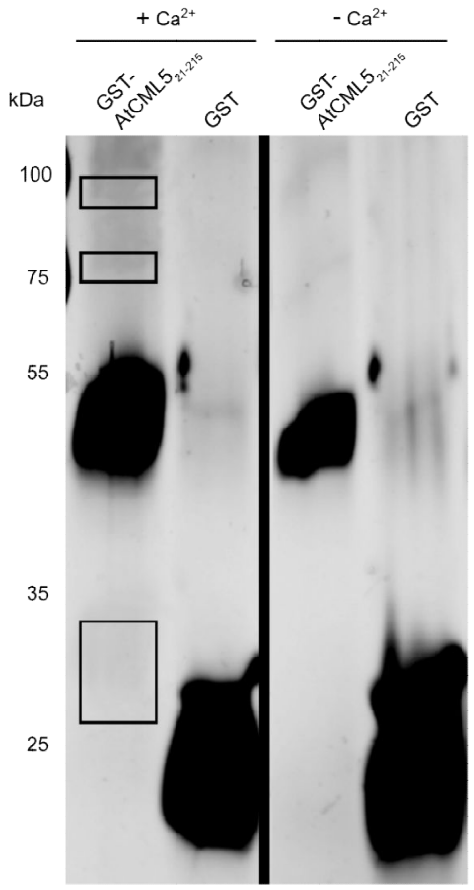

Figure 7: Ca^{2+}-dependent pull-down assay of potential binding partners from *A. thaliana* microsome/cytoplasm extracts from leaf tissue. (**A**) Schematic overview of the workflow to isolate potential interaction partners from an *A. thaliana* leaf tissue extract in a Ca^{2+}-dependent manner, applying the recombinant construct GST-AtCML5$_{21-215}$ as bait and GST as bait control. (**B**) SDS-PAGE analysis of the different elution fractions from GST-AtCML5$_{21-215}$- or GST-coated CNBr resins in the presence or absence of Ca^{2+}. Potential interaction partners represented by bands present in lane 1, but none of the other lanes, are marked by boxes. These bands were isolated from the gel and analysed by mass spectrometry for identification.

Unfortunately, the elutions also contained large amounts of GST-AtCML5$_{21-215}$ or GST, which should have been retained on the column. Due to the design of the assay and its conduction, it

is possible that small fractions of the matrix material contaminated the elutions. However, this was unlikely to have affected the overall result of the assay, since it was still possible to detect bands, exclusively present in the elution of interest (see Figure 7, GST-AtCML5$_{21-215}$, + Ca^{2+}).

The isolated bands detected via SDS-PAGE followed by silver staining were submitted to the protein analysis core facility (*Zentrallabor für Proteinanalytik*, BMC, LMU Munich), where peptides were generated via tryptic digest, followed by separation via short gradient nano-liquid chromatography and subsequent analysis via quadrupol/ion-trap mass spectrometry. The identities of the proteins from which the analysed peptides were derived, were determined by comparison of the mass spectrometry analysis results with the MASCOT database.

Out of the list of detected proteins, two candidates were selected as potential interactors: DYNAMIN-RELATED PROTEIN 1B (AT3G61760, further referred to as "AtDRP1B"), identified with 100 % probability based on two detected peptides and PHOSPHOLIPASE D GAMMA 1 (AT4G11850, further referred to as "AtPLDGAMMA1"), identified with 100 % probability based on six detected peptides (see Appendix II for detailed mass spectrometry analysis data). Dynamin-related GTPases are involved in various processes, such as endocytosis (Collings *et al.* 2008) and cytokinesis (Miyagishima *et al.* 2008) and AtDRP1A was reported to be localised in the *trans*-Golgi network (Sawa *et al.* 2005).

As presented in 3.1.2, AtCML5-YFP-labelled structures indicative of vesicles with enlarged lumina, which suggested a potential role of AtCML5 in vesicular fusion processes. This had also been previously shown and hypothesised (Flosdorff 2014). Since dynamin-related proteins had been shown to play a role in vesicular trafficking (Kang *et al.* 2003), AtDRP1B was considered to be a promising candidate for interaction with AtCML5. AtPLDGAMMA1 had been shown to influence coatomer assembly by producing phosphatidic acid through hydrolytic cleavage (Ktistakis *et al.* 1996). AtARF1 had been found to regulate AtPLDGAMMA1 activity, but an additional Ca^{2+}-dependent regulation could not be excluded.

Apart from these two proteins, a third candidate was selected for further analysis as potential interaction partner: a GDSL-motif esterase/acyltransferase/lipase (AT5g55050, further referred to as "AtGML"). Proteins belonging to this family of enzymes have broad substrate specificity due to their highly flexible active site, but only for a few members their molecular function has been elucidated, yet. The protein was included in further analyses, because it was

identified as potential interaction partner of AtCML5 by mass spectrometric analysis following a pull-down assay of different setup in a previous study (Flosdorff 2014), but had not been investigated in detail.

3.2.3 Microscopic co-localisation analysis of potential interaction partners of AtCML4 and AtCML5

Concomitant to biochemical interaction studies between the potential interaction partners (see 3.2.2) and AtCML4 or AtCML5, their sub-cellular localisation relative to AtCML4 and AtCML5 was analysed. To that end, *N. benthamiana* plants co-expressing either AtDRP1B or AtPLDGAMMA1 (both as mCherry fusion constructs) together with AtCML5-YFP were used for protoplast isolation and subsequent microscopic analysis (see Figure 8 B). Since expression of the AtGML fused to mCherry failed and an AtCML5-mCherry construct was not reliably expressed either, a YFP fusion construct of the lipase was chosen to be co-expressed with AtCML4-mCherry (see Figure 8 A), which has previously been shown to co-localise with AtCML5-YFP (see 3.1.2).

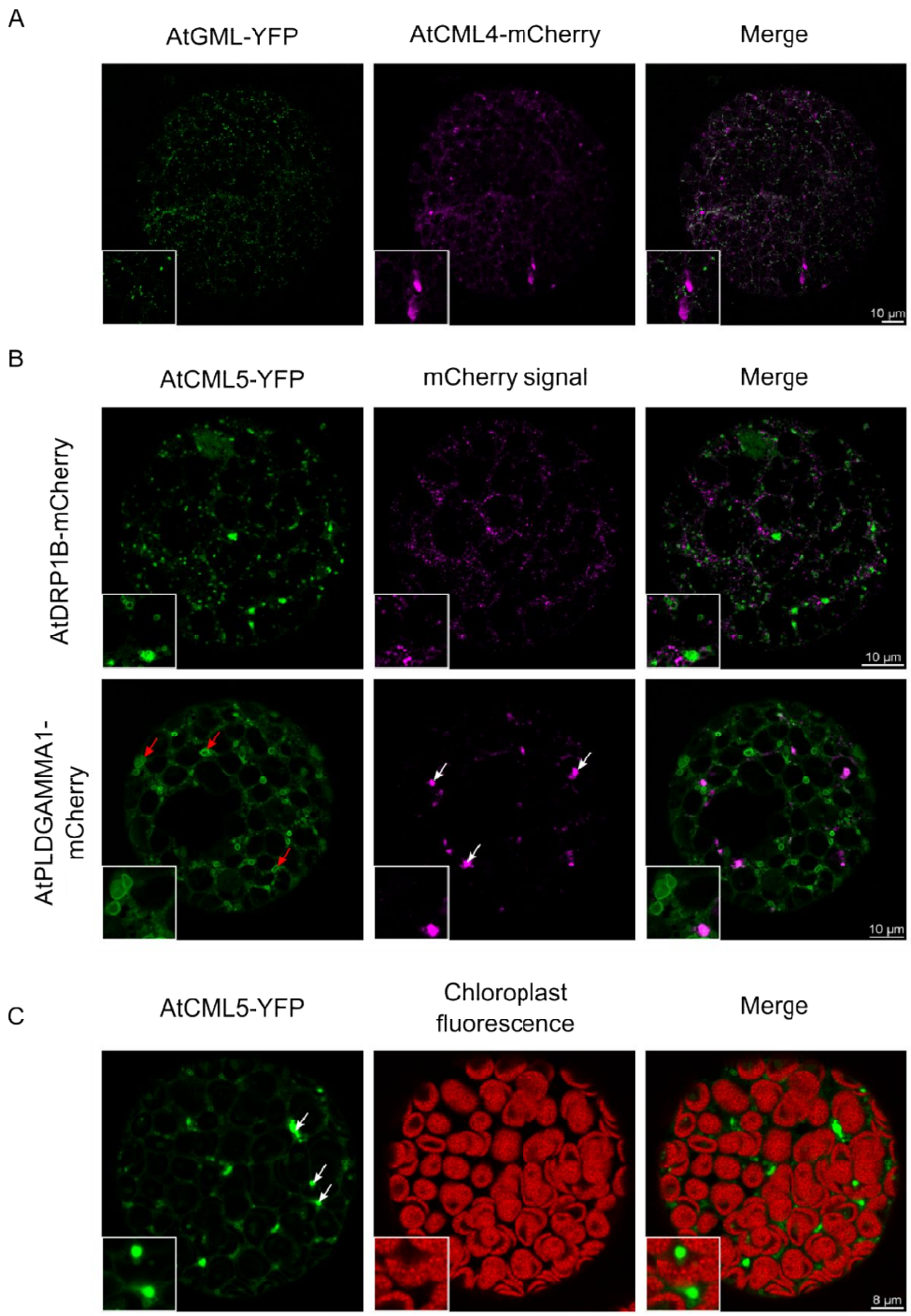

Figure 8: Analysis of AtCML4-mCherry and AtCML5-YFP co-expressed with different interaction partner candidates. (**A**) Analysis of *N. benthamiana* leaf protoplasts co-expressing AtGML-YFP and AtCML4-mCherry suggested that the lipase localises to vesicular structures, indicated by its punctuate fluorescence patterns, but there was no co-localisation with AtCML4-mCherry detectable. (**B**) Protoplasts co-expressing AtCML5-YFP together with AtDRP1B–mCherry or AtPLDGAMMA1-mCherry showed no co-localisation of either construct with AtCML5-YFP. Still, both potential interacting partners might be localised in vesicles, since their fluorescence signals occurred in punctae. It is noteworthy that in protoplasts expressing AtCML5-YFP and AtPLDGAMMA1-mCherry, AtCML5-YFP-labelled vesicles were unusually enlarged and often displayed a distorted structure (red arrows) not resembling the isodiametric, circular shape that had been observed in other samples before. AtPLDGAMMA1-mCherry signals occurred as small and also large punctae (white arrows), which resembled (**C**) the signals of AtCML5-YFP when detected in accumulations of a large number of vesicles. However, AtPLDGAMMA1-mCherry signals also appeared as ring-shaped structures with large luminal volumes (data not shown). White bar represents scale of indicated size.

Microscopic analysis of fluorophore-tagged versions of all three potential interaction partners expressed in *N. benthamiana* leaf tissue, showed their localisation in vesicular structures, indicated by the punctuate signal character. However, there was no visible overlap with the signals originating from AtCML5-YFP or AtCML4-mCherry, respectively, suggesting that they are localised in different vesicles of the endomembrane system. In contrast to AtGML-YFP and AtDRP1B-mCherry, AtPLDGAMMA1-mCherry signals sometimes also occurred in foci of high fluorescence intensity and spatial spread (compare Figure 8 B and C, white arrows) as often observed for AtCML5-YFP signals in cells with very high levels of expression (see Figure 8 C, white arrows). In addition to that, signals originating from AtCML5-YFP and AtPLDGAMMA1-mCherry both appeared in circular structures with unusually large diameter albeit not overlapping (see Figure 8B, red arrows). Very often, these structures were not isodiametric as observed for AtCML5-YFP upon single expression or co-expression with other fusion proteins (see Figure 2 and Figure 3). Whether this peculiar behaviour of the structures indicated a potential interaction of AtCML5 and AtPLDGAMMA1 *in planta*, or whether this was merely an effect caused by AtPLDGAMMA1-mCherry overexpression, could not be deduced from the microscopic data.

In general, the lack of co-localisation of two proteins does not equal functional independence. Especially in a compartment like the vesicular trafficking system, in which vesicle populations interchange and maturation processes coincide with retrograde transport pathways, interaction between proteins in different compartment populations occurs frequently (Moyer *et al.* 2001). Therefore, biochemical studies were attempted to elucidate, whether the identified proteins were indeed interaction partners of AtCML4 or AtCML5. In order to perform such assays, heterologous expression of the proteins and purification was required. However, the potential interactors proved difficult to express in *E. coli* and different approaches for expression conditions, fusion tags and bacterial strains were tested, but the proteins were either not expressed at all, or only at minor amounts which complicated downstream analyses. All three proteins were predicted to contain transmembrane domains, which often cause difficulties upon expression in *E. coli*, due to their tendency to lead to aggregation of the recombinant proteins in the bacterial cytoplasm. In order to circumvent this problem, expression with an N-terminal maltose-binding protein tag was tested. Unfortunately, even this expression system, although specifically designed for heterologous membrane protein expression, did not result in a significant improvement of the expression. Since these experiments were carried out in the late phase of this work, biochemical evidence

for potential interaction could not be provided.

Information about the function of a protein can also be deduced from phenotypic analysis of mutant plants. Hence, such analyses were carried out in parallel to biochemical and microscopic approaches.

3.2.4 Phenotypic analysis of an *atcml5* knock-out mutant line

For many genes in *A. thaliana* mutant lines have been generated by random insertion of T-DNAs, interrupting genes in either their exons, introns or regulating regions like the promoter, 5'UTR or 3'UTR (untranslated region) (Koncz *et al.* 1992). These DNA fragments randomly inserted into the plant cell genome usually comprise several thousand base pairs, interfering with gene expression. The most reliable T-DNA insertion lines in terms of preventing a functional protein from being expressed from such genes are those, in which the insertion occurs inside an exon, which is present in all splicing variants of the gene. In case of *AtCML5*, the GABI-Kat 703E02 line is commercially available and was generated by infecting WT *A. thaliana* plants of ecotype Columbia with an Agrobacterium strain carrying the inserted T-DNA on a pGABI1 plasmid. The T-DNA is located within the only exon of *AtCML5* and it had previously been shown via reverse transcription PCR that this mutant line does not produce a functional *AtCML5* mRNA, thus rendering it a homozygous knock-out mutant (*atcml5-ko*) (Flosdorff 2014). Phenotypic analysis under standard growth conditions (100 µM s^{-1} m^{-2} photons, 16 h light/8 h dark, 22°C day/18°C night temperature) had been performed, but no phenotypic differences could be detected in comparison to WT plants grown under identical conditions. However, *AtCML5* might be i) required in processes like certain stress-induced pathways that have not been triggered under artificial climate chamber and greenhouse cultivation conditions; or ii) *AtCML4* being highly similar in sequence might complement for the function of *AtCML5*, or iii) the phenotypic abnormalities were not detectable by the applied means of analysis.

In order to analyse this further, *atcml5-ko* mutant and WT plants were subjected to different kinds of treatment (see 2.2.1.2). Plants were cultivated under sterile conditions on ½ MS medium solidified with 1 % plant agar to apply various kinds of stresses, e.g. salt stress by addition of 100 mM NaCl to the medium, osmotic stress by addition of 200 mM mannitol to the medium, growth under high light conditions (150 µM s^{-1} m^{-2} photons). Root growth was analysed by vertical cultivation of plants under sterile conditions with and without addition of

3-indol acetic acid (IAA, 15 nM). Hypocotyl growth analyses were conducted by stratification of seeds for 2 d in the dark at 4°C, followed by 6 h of exposure to light (100 µM s^{-1} m^{-2} photons, 22°C) to induce germination, followed by 5 d of growth in the dark at 22°C to trigger etiolated growth of hypocotyls. Under none of the cultivation conditions significant differences between WT and mutant plant phenotype could be detected.

The only experiment, in which some minor differences between WT and mutant plants could be observed, was the analysis of the shoot length at different time points under standard growth conditions. During the development of Arabidopsis plants there is a shift from a vegetative to a generative growth phase, which is characterised by the production of a primary inflorescence, whose growth is controlled by the shoot apical meristem. This process is followed by the development of flower buds and secondary inflorescences that diverge laterally from the primary inflorescence. A variety of regulatory mechanisms control this and other developmental transition processes in plants (reviewed in Huijser *et al.* 2011, Poethig 1990). The development of the shoot of WT and *atcml5-ko* was monitored daily by measuring the distance from the rosette centre to the tip of the shoot, from which the pedicels of the apical flowers develop. Since not all plants cultivated together also entered the generative growth phase at the same time, only plants showing beginning shoot growth on the same day, were compared with one another. The values of the measured shoot length for plants of each group were analysed in a box plot and are displayed in Figure 9 for every second day of measurement. The day on which the first plants entered the generative growth phase was marked as day 1.

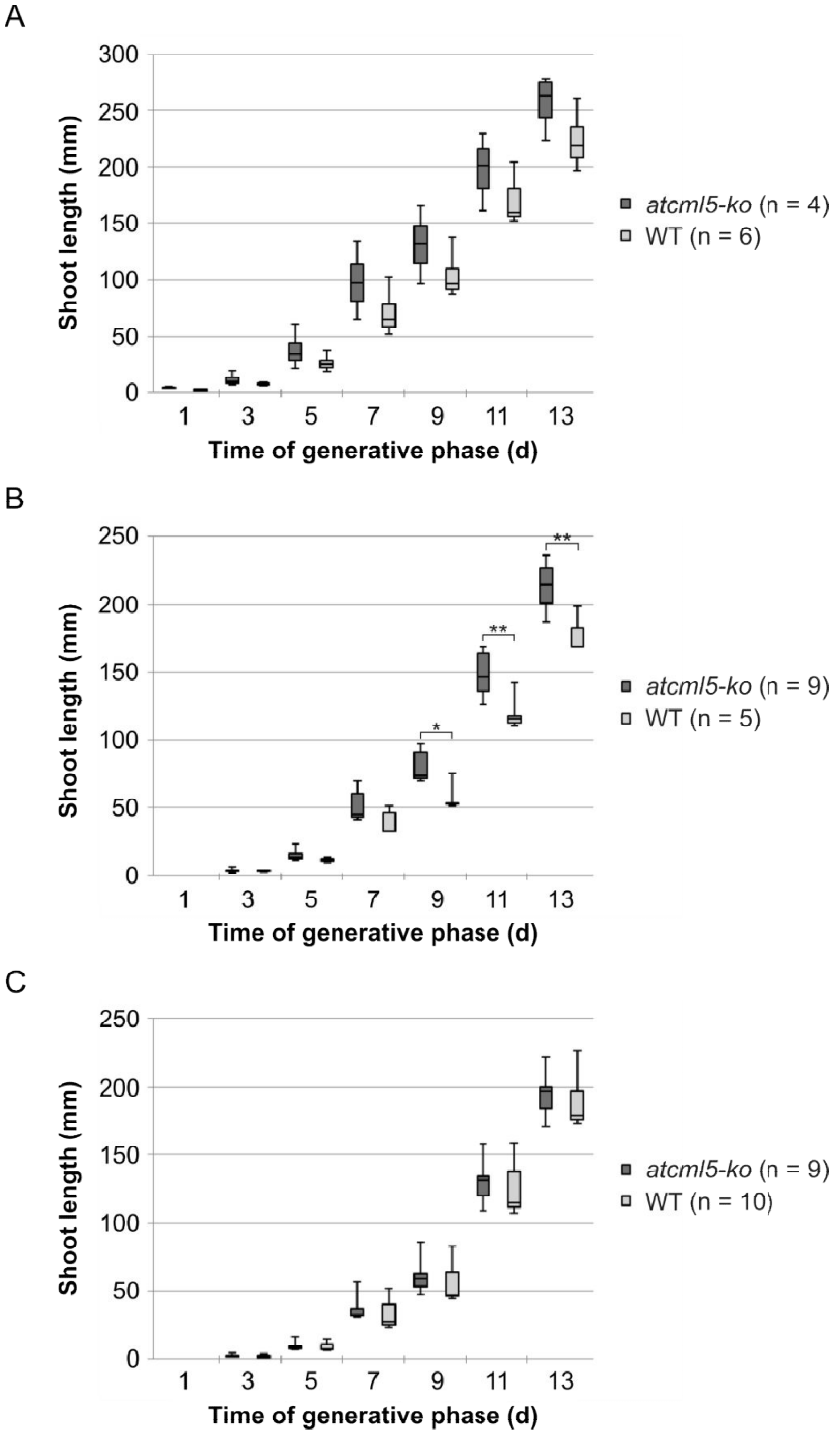

Figure 9: Analysis of the shoot length in *A. thaliana* WT and *atcml5-ko* plants. Comparison of the shoot length in mm of WT and *atcml5-ko* plants entering generative growth phase on (**A**) day 1, (**B**) day 2 or (**C**) day 3. The values of the measured shoot length development for the plants of the respective genotype on each day are shown as box plot. The day the first plants showed shoot growth was defined as day 1. There were minor differences in the development of the shoot between WT and *atcml5-ko* plants. *Atcml5-ko* plants that started generative growth on day 2, had significantly longer shoots than the WT after day 8 and a similar tendency was observed in *atcml5-ko* plants analysed since day 1. However, no such effect was detected in plants that entered the generative growth phase on the third day of analysis. Significance values were determined by Student's *t*-test (* = $p<0.05$, ** = $p<0.01$). The amount of plants of each genotype compared in the assay is indicated in brackets in the legends of the graphs.

Analysis of the plants was carried out at the same time every day. Three groups of plants, defined by the day they entered the generative growth phase and started producing a visible shoot, were analysed and compared. Only the group starting generative growth on day 2 showed differences in shoot length between the two genotypes that were statistically significant on the last days of analysis (see Figure 9B, days 9 to 13). In this group *atcml5-ko* plants had longer shoots than the compared WT plants. A similar tendency, though not statistically significant, could be observed in the group of plants entering generative growth phase on day 1 (see Figure 9A). Group three, in which shoot development began on day 3 of the analysis did not show any differences at all (see Figure 9 C). Other experiments of equal setup returned similar results, rendering any deduction about an involvement of AtCML5 in developmental processes affecting shoot growth poorly supported. A potential phenotype caused by the lack of functional AtCML5 could be attenuated by functional complementation via AtCML4. In order to exclude this possibility, *atcml4/atcml5* double knock-out plants had to be analysed.

One option to generate a double mutant was to use a plant line, in which the *AtCML4* gene was disrupted by a T-DNA insertion, and to cross it with *atcml5-ko* plants. Several T-DNA insertion lines of *A. thaliana* are available, but unfortunately, for none of these lines, the disruption of the *AtCML4* gene by a T-DNA insertion could be confirmed via site-specific PCR. Hence, other methods had to be chosen to reduce or completely abolish expression of *AtCML4 in planta.* A small interfering RNA (siRNA)-based approach was selected to down-regulate *AtCML4* gene expression on a post-transcriptional level.

3.2.5 Stable siRNA-based reduction of *AtCML4* transcript abundance *in planta* for phenotype analysis

In order to knock-down *AtCML4 in planta* with only minor or no effects on *AtCML5* transcript abundance, a region in the *AtCML4* gene serving as guide RNA source to ensure mRNA degradation had to be determined. This region had to be specific to the *AtCML4* transcript, so that the *AtCML5* mRNA would remain unaffected. Figure 10 shows an excerpt of a sequence alignment of the CDSs of *AtCML4* and *AtCML5* to highlight the sequence stretches identified as described in 2.2.1.6 to serve as potential guide RNAs.

```
AtCML4       1 ATGGTGAGAGTCTTTCTTCTCTACAACCTCTTTAACTCCTTTCTTCTTTGTTTAGTTCCC
AtCML5       1 ATGGTGAGAATATTCCTTCTCTACAATATACTAAATTCGTTTCTTCTCTCTTTAGTACCA
consensus    1 ********* * ** ***********  *  * ** ** ******** * ****** **

AtCML4      61 AAGAAGCTTAGAGTTTTCTTCCCTCCTTCTTGGTACATCGA------CGACAAGAACCCA
AtCML5      61 AAGAAGCTACGAACTCTTTTCCCTCTTTCTTGGTTCGACAAAACTCTCCACAAGAACTCA
consensus   61 ********  **  * * ******* ******** *  * *      * ******** **

AtCML4     115 CCACCGCCT-----------------------------------GATGAATCGGAAACT
AtCML5     121 CCACCGTCTCCGTCAACGATGTTACCTTCTCCATCATCTTCTTCAGCGCCGACGAAAAGA
consensus  121 ****** **                                  *      ** ***

AtCML4     139 GAATCTCCGGTAGATCTAAAACGAGTGTTTCAGATGTTCGACAAGAACGGAGATGGACGC
AtCML5     181 ATAGATCCGTCCGAGCTCAAACGCGTTTTCCAGATGTTCGACAAGAACGGTGACGGTCGA
consensus  181   *  ****   ** ** ***** ** ** ******************** ** ** **

AtCML4     199 ATCACAAAGGAAGAGCTGAACGATTCTCTAGAGAATCTAGGAATCTTTATGCCTGACAAA
AtCML5     241 ATCACAAAGGAAGAGCTCAACGACTCGCTTGAGAATCTTGGAATCTACATACCAGACAAA
consensus  241 ***************** ***** ** ** ******** *******  ** ** ******

AtCML4     259 GATCTGATCCAGATGATCCAGAAGATGGATGCAAATGGAGA...]  Remaining
AtCML5     301 GATCTGACTCAAATGATCCACAAGATCGATGCTAACGGTGA...]     MSA
consensus  301 *******  ** ******** ***** ***** ** ** **
```

Figure 10: Partial sequence alignment of *AtCML4* and *AtCML5* CDSs. The alignment of the CDSs of *AtCML4* and *AtCML5* focused on the first 300 NTs and 342 NTs, respectively. In this region, all positions in the *AtCML4* CDS serving as potential targets for guide RNAs (red markups), were found in positions, which display at least one mismatch to the *AtCML5* CDS. Hence, they were expected to allow for a maximum degree of specificity given the high similarity between the CDSs of the two genes. Only the relevant part of the entire sequence alignment is shown, which is indicated by the bracket at the end of the alignment. Asterisks in the consensus line mark positions at which both CDSs are identical.

The partial sequence stretch of *AtCML4* comprising NTs 1-300 as displayed in Figure 10 was introduced into the pOpOff2 vector designed by Wielopolska and colleagues (2005) for stable transformation of *A. thaliana* WT and *atcml5-ko* plants to generate single knock-down (a*tcml4-kd*) and double knock-down / knock-out (*atcml4-kd* / *atcml5-ko*) plants, respectively. This vector allows for expression of a hairpin RNA of desired sequence under the control of a dexamethasone-inducible pOp promoter (Craft *et al.* 2005). This hairpin RNA is the basis for the post-transcriptional silencing of gene expression by RNAi, which is an important defence mechanism in plants as reaction to virus infection (reviewed in Susi *et al.* 2004). The RNAi-based reduction of transcript abundance can result in a significant decrease in the concentration of the protein encoded by the respective mRNA.

After transformation of the plants and several rounds of selection via growth on Hygromycin B-containing medium, two lines of each genotype were chosen for further analyses. A plant line stably transformed with the pOpOff2 vector harbouring the CDS of

firefly luciferase (pOpOff2-LUC) was used as vector control in all assays. In order to exclude the possibility of DMSO, the solvent for dexamethasone, having any impact on plant cultivation, all assays were concomitantly performed on medium containing dexamethasone and on medium containing an equal amount of DMSO.

The plants were analysed under standard growth conditions to determine, whether the mutant lines displayed defects in development. For that, plants were cultivated in a horizontal and a vertical fashion for 21 days each. Since no differences between either *atcml4*-k*d* or *atcml4-kd*/*atcml5-ko* lines and the control plants could be detected, growth under different stress conditions was examined. In order to analyse hypocotyl elongation, seedlings were cultivated in the dark as described in 2.2.1.2. Additionally, phenotypic differences upon cultivation under salt stress (100 mM NaCl), osmotic stress (200 mM mannitol) or hormone influence (15 nM IAA) were analysed. However, no significant differences between the mutant lines and the control lines could be detected under any cultivation condition. Shoot growth under prolonged cultivation conditions could not be analysed, because RNAi induction by dexamethasone is not feasible in a soil-based plant cultivation system.

A potential function-related phenotype can also be caused by overexpression of genes. For this reason, *A. thaliana* WT plants were stably transformed with pBIN19-ANX constructs to express either *AtCML4* or *AtCML5* under the control of the endogenous promoter of the *UBIQUITIN* gene (see 2.1.3). This promoter is active throughout the whole plant and since it is an endogenous promoter, silencing effects on transcriptional level as observed for the viral 35S-promoter can be avoided. In addition, *atcml5-ko* and WT plants were transformed with a pBIN19-ANX construct to express *AtCML5* under control of its endogenous promoter in order to generate a rescue line as control and a mild overexpressor line for further phenotypic analyses. Though the plants have already been subjected to two rounds of selection, phenotypic analyses could not be carried out due to a lack of time.

3.2.6 Detection of endogenous AtCML4 protein levels with monoclonal antibodies

While a lack of transcript should guarantee the absence of protein, complete confirmation can only be obtained by analyses of protein levels. This is especially important in case of inducible RNAi lines. However, for both AtCML4 and AtCML5 no sufficiently selective antibody was available. The only polyclonal antibody that would detect purified, recombinant $AtCML5_{29\text{-}215}$ did not have sufficient specificity towards AtCML5 and western blots on

concentrated leaf extracts would yield signals from several bands that did not correspond to the expected size of AtCML5. Therefore, monoclonal peptide antibodies against regions specific to either AtCML4 or AtCML5 were raised (Monoclonal Antibody core facility HelmholtzZentrum Munich, Neuherberg, Germany).

A

```
AtCML4   1 MVRVFLLYNLFNSFLLCLVPKKLRVFFPPSWYID--DKNPPP------PDESETES----  48
AtCML5   1 MVRIFLLYNILNSFLLSLVPKKLRTLFPLSWFDKTLHKNSPPSPSTMLPSPSSSSAPTKR  60
           *** *****  ***** *******  ** **      ** **      *  *

AtCML4  49 --PVDLKRVFQMFDKNGDGRITKEELNDSLENLGIFMPDKDLIQMIQKMDANGDGCVDIN 106
AtCML5  61 IDPSELKRVFQMFDKNGDGRITKEELNDSLENLGIYIPDKDLTQMIHKIDANGDGCVDID 120
             *  ******************************  ***** *** * **********

AtCML4 107 EFESLYGSIVEEK------EEGDMRDAFNVFDQDGDGFITVEELNSVMTSLGLKQGKTLE 160
AtCML5 121 EFESLYSSIVDEHHNDGETEEEDMKDAFNVFDQDGDGFITVEELKSVMASLGLKQGKTLD 180
           ****** *** *       ** ** ******************** *** **********

AtCML4 161 CCKEMIMQVDEDGDGRVNYKEFLQMMKSGDFSNRS 195
AtCML5 181 GCKKMIMQVDADGDGRVNYKEFLQMMKGGGFSSSN 215
           ** ****** **************** * **
```

B

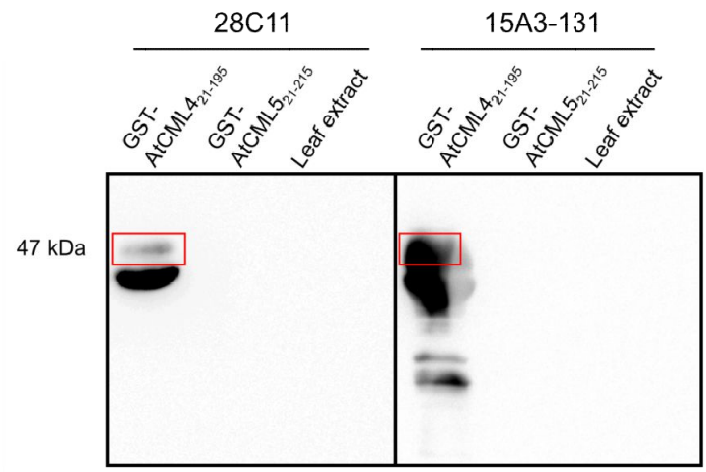

Figure 11: Testing of monoclonal anti-AtCML4 antibodies. (**A**) Sequence alignment of AtCML4 and AtCML5 amino acid sequences with markups for the sequence stretches within each protein, which monoclonal peptide antibodies have been raised against. (**B**) Western blot analysis to test specificity and sensitivity of two anti-AtCML4 antibody clones, 28C11 and 15A3-131. Both antibodies detected recombinant GST-tagged $AtCML4_{21-195}$ protein purified on glutathione sepharose 4B, but did not show cross-reactivity for similarily purified GST-$AtCML5_{21-215}$. In WT *A. thaliana* crude leaf extracts, endogenous AtCML4 could not be detected. Compared to clone 28C11, the signals derived from antibody clone 15A3-131 marked more protein bands at lower molecular range than the 47 kDa of full-length fusion construct, which correspond to degradation products that have been observed to occur during purification of the fusion proteins. It also showed a higher intensity at the position the full-length fusion protein is expected to migrate (red box).

The two peptides identified as suitable targets for antibody production were chosen according to their antigenicity and whether they would allow for sufficient specificity of the

corresponding antibodies to reduce off-target recognition. In accordance, the target peptides for both proteins were located in regions, characterised by low similarity between AtCML4 and AtCML5 (see grey boxes, Figure 11 A). Due to difficulties with the hybridoma cell lines used for production of the anti-AtCML5 antibodies, only final anti-AtCML4 antibodies from two different cell lines could be obtained (see Figure 11 B).

After initial screenings of preliminary antibody clones with regard to their specificity and cross-reactivity, two clones, 28C11 from rat and 15A3-131 from mouse, were established and tested further. Both antibodies detected GST-AtCML4$_{21-195}$, resulting in a signal at about 47 kDa and showed a sufficient degree of specificity, since no signal could be detected for the lanes loaded with comparable amounts of purified GST-AtCML5$_{21-215}$. Unfortunately, detection of endogenous amounts of AtCML4 in crude leaf extracts of WT *A. thaliana* was not possible. A potential reason could be the very low expression levels of AtCML4 as predicted by different Arabidopsis gene expression databases relying on microarray bulk data (see Table 8).

3.2.7 Promoter activity analysis for AtCML4 and AtCML5

Dissection of promoter activity of a gene can provide valuable information that might help elucidate the potential function of the corresponding protein based on tissue- and/or developmental stage-specific expression of the gene.

Several databases (see 2.2.3) were screened for information regarding the spatial and temporal patterning of gene expression, promoter activity in response to biotic and abiotic stimuli and the *cis*-elements identified in the promoter sequence of *AtCML4* and *AtCML5*. The most relevant are listed in Table 8.

Table 8: *In silico* analysis of *AtCML4* and *AtCML5* expression levels and promoter sequence. Microarray data for organ-specific expression were supplied by the Transcriptome Variation Analysis Database, whereas information on promoter *cis*-elements is derived from the Arabidopsis *cis*-regulatory element database (see 2.2.3).

	Organ	Absolute normalised expression counts	
		AtCML4	*AtCML5*
Organ-specific expression	Flowers	3-12	1013-1881
	Sepals (flower 3)	1	3580
	Petals (flower 3)	1	6288
	Anthers (flower 1)	2	5235
	Siliques (without seeds)	0-16	2385-9493
	Hypocotyl (1-day seedling)	12	2407
	Apical meristem with adjacent tissues (1-day seedling)	48	1280
	Senescent petiole	0	4962
	Senescent vein	1	5586
	First elongated internode	10	2638
	Root apex	66	1344
	Root (without apex)	71	2927
	Dry seeds	0	54
	Leaf petiole	16-22	229-336

	AtCML4	*AtCML5*
Promoter *cis*-elements	ATB2/AtbZIP53/AtbZIP44/GBF5 BS in ProDH	Bellringer/replumless/pennywise BS1 IN AG
	ARF1 binding site motif	GATA promoter motif [LRE]
	RAV1-A binding site motif	RAV1-A binding site motif
	W-box promoter motif	MYB4 binding site motif
		SOULREP3 binding motif

High expression levels of *AtCML5* were found in a variety of organs with the exception of dry seeds (54) and leaf petioles (229-336), in which expression was significantly lower. Peak values of normalised expression were found in petals (6288), siliques (up to 9493) and senescent veins (5586). By contrast, *AtCML4* is generally expressed to a much lower extent than *AtCML5*, showing highest expression in the apical meristem (48) and in root tissue (66-71).

The promoters for *AtCML4* and *AtCML5* as listed in the Arabidopsis *cis*-regulatory element database (see 2.2.3) comprise 478 and 2910 base pairs, respectively. Hence, the amount of

detected *cis*-elements is correspondingly smaller for *AtCML4*. The identified motifs indicated *AtCML4* to be regulated by auxin (ARF1 binding site motif), abscisic acid (RAV1-A binding site motif, W-box promoter motif), as well as transcription factors of the bZIP family under hypoosmolarity conditions (ATB2/AtbZIP53/AtbZIP44/GBF5 BS in ProDH). The potential promoter sequence of *AtCML5* contains a variety of *cis*-elements, of which the most abundant ones indicated that the gene might also be regulated by abscisic acid (RAV1-A binding site motif) and could be involved in light-dependent processes (GATA promoter motif, SOULREP3 binding motif, MYB4 binding site motif). Additionally, a sequence stretch known to be bound by the proteins BELLRINGER, REPLUMLESS and PENNYWISE had been identified, which would link *AtCML5* expression to patterning processes in fruit, shoot and flower. Judging from the *cis*-elements, *AtCML4* seems to be controlled mainly by phytohormones, whereas the *AtCML5* promoter region is characterised by several binding motifs involved in light-dependent regulation. Hence, databases were screened for potential up- or down-regulation of *AtCML4* and *AtCML5* in response to abiotic stresses and hormones (Table 9).

Table 9: Response of *AtCML4* and *AtCML5* promoter activity to hormone influence and abiotic stress stimuli. The listed changes in expression level compared to untreated control samples were provided by the AtGen Express Visualization Tool (see 2.2.3).

	Hormone	**Expression level compared to control samples**	
		AtCML4	***AtCML5***
Hormone response	Abscisic acid (10 µM)	Unaffected	Elevated
	1-aminocyclopropane-1-carboxylic acid (10 µM)	Unaffected	Decreased
	Brassinolide (10 nM)	Unaffected	Elevated
	3-indol acetic acid (1 µM)	Unaffected	Elevated
	Methyl-jasmonate (1 µM)	Unaffected	Decreased
Stress stimulus response	**Stress stimulus**	**Expression level compared to control samples**	
		AtCML4	***AtCML5***
	Cold	Unaffected	Elevated (root tissue)
	Osmotic	Unaffected	Elevated (root tissue)
	Drought	Unaffected	Elevated (root tissue)
	Heat	Unaffected	Decreased (aerial tissue)

According to the AtGen Express Visualization Tool (see 2.2.3), *AtCML4* expression is unaffected by treatments with different hormones or by influence of abiotic stress stimuli. Considering the presence of auxin- and abscisic acid-responsive *cis*-elements in the *AtCML4* promoter region, the lack of response to treatment with these hormones is surprising. By contrast, *AtCML5* expression was found to be elevated, when abscisic acid (ABA), brassinolide or auxins (AUX, 3-indol acetic acid) were applied. ABA is often involved in abiotic stress response, but also plays a role in root architecture development (reviewed in Harris 2015). Brassinolide and AUX are key hormones in the regulation of growth processes, especially in mediating growth by cell elongation (reviewed in Vaughan-Hirsch *et al.* 2017, Clouse 1996). In this respect, the fact that *AtCML5* expression is elevated upon treatment with ABA corresponds to its enhanced expression upon cold, osmotic and drought stress conditions. Down-regulation of *AtCML5* expression under influence of either 1-aminocyclopropane-1-carboxylic acid (ACC) (reviewed in Bleecker *et al.* 1997) or methyl-jasmonate (Chen *et al.* 2017), which are both directly or indirectly (ACC is a biosynthetic precursor of ethylene) involved in senescence promoting processes (reviewed in Bleecker *et al.* 1997, Chen *et al.* 2017), further indicated a role of *AtCML5* in growth-promoting processes.

Overall, whereas *AtCML5* seemed to be almost ubiquitously expressed and controlled by many different factors of abiotic and biotic character, *AtCML4* expression levels are very low and the lack of response to stimuli of any kind raised the question as to whether it is actively involved in any cellular processes at all. In order to compare the *in silico* data to *in vivo* information on the expression of both genes, a promoter activity reporter assay was conducted.

One possible approach to analyse promoter activity of a gene *in vivo* is to express a reporter protein under the control of the respective promoter. Different reporter genes, e.g. GLUCORONIDASE (GUS), FIREFLY LUCIFERASE (LUC) or fluorescent proteins can be chosen with different advantages and disadvantages. To analyse the promoter activity of *AtCML4* and *AtCML5*, 1822 nucleotides (for *AtCML4*) and 1123 nucleotides (for *AtCML5*) upstream of the respective CDS were cloned into a pBIN19-ANX plasmid to drive the expression of a LUC gene (*pAtCML4*::LUC, *pAtCML5*::LUC) (see 2.1.3). *A. thaliana* WT plants were transformed using these plasmids and selected to yield several independent lines for each genotype via their plasmid-encoded BASTA resistance. The cloned regions were chosen according to promoter sequence predictions in the Aramemnon and AGRIS

databases (see 2.2.3) and comprise putative promoter regions and 5'UTRs as well as the *cis*-elements listed in Table 8. Differences in the promoter region length as displayed in the databases result from the application of different prediction methods for promoter sequences.

Plants sterilely cultivated for either 5, 14 or 28 d were infiltrated with a 20 µM aqueous (D)-luciferin (LUCIFERASE substrate) solution under vacuum application, arranged on a moisturised glass plate and subsequently analysed with an LAS4000 ImageQuant system (see 2.2.1.14).

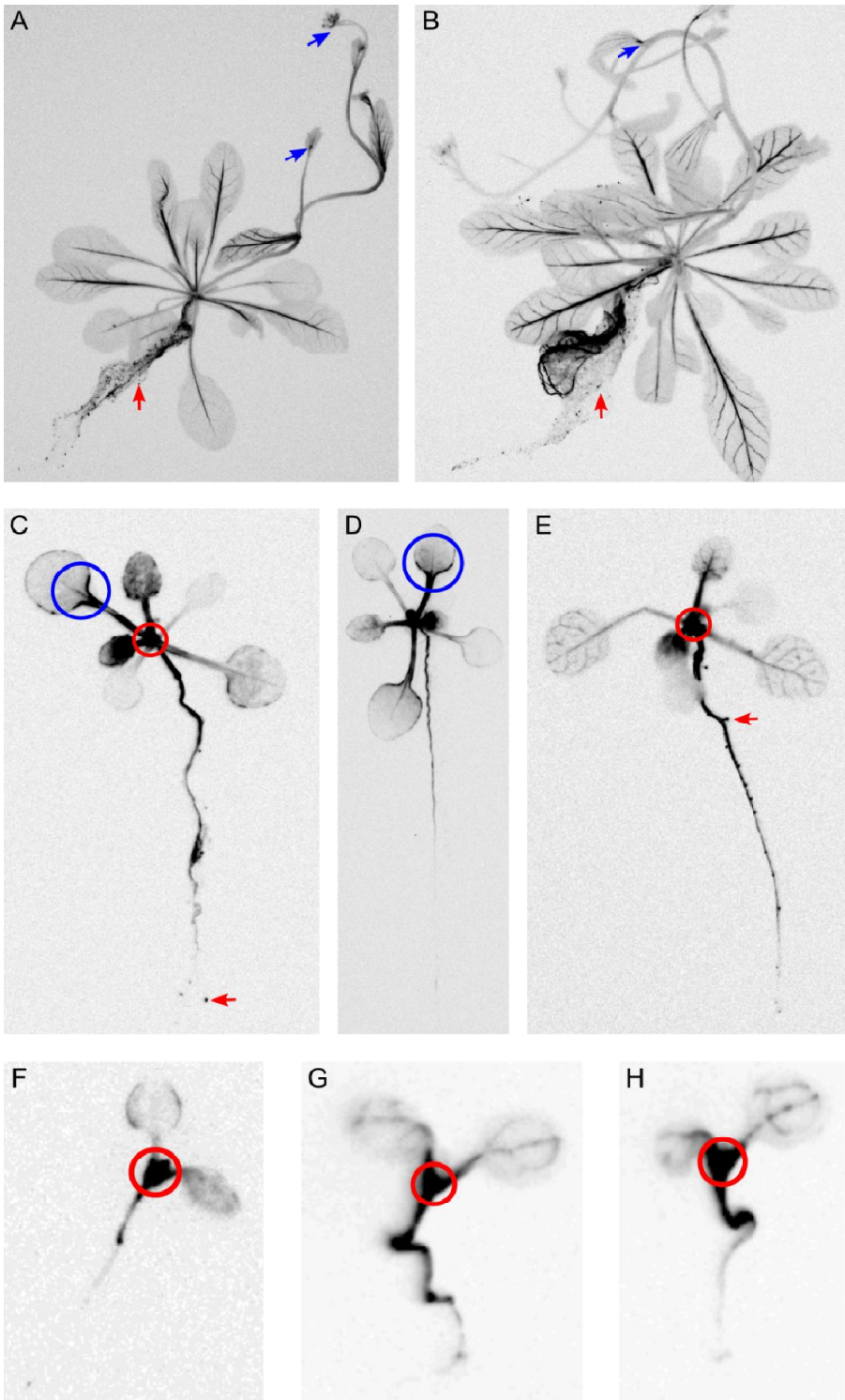

Figure 12: LUCIFERASE activity in *pAtCML4*::LUC *A. thaliana* plants. Analysis of (**A**, **B**) 28 d-old, (**C**-**E**) 14 d-old and (**F**-**H**) 5 d-old plants expressing *LUC* under control of the *AtCML4* promoter. Both plants in (**A**) and (**B**) showed a strong LUC activity in the leaf veins, the pedicel (blue arrows) and distinct parts of the root including the primary root and lateral roots of larger diameter than the majority of lateral roots. In addition, foci of luminescence could be detected at different positions along the lateral roots (**A**, **B**, red arrows). 14 d-old seedlings also showed high LUC activity in root and hypocotyl (**C**-**E**) accompanied by luminescence foci all along the primary root (**C**, **E**, red arrow). Luminescence also emanated from the centre of the rosette, along the petioles and also from the veins (**E**), as well as along the margins of some leaves at the transition zone between petiole and leaf blade (**C**, **D**, blue circle). In accordance, 5 d-old seedlings showed strong luminescence in the upper primary root, the hypocotyl, the hypocotyl apex (**F**-**H**, red circle) as well as the cotyledon veins (**G**, **H**).

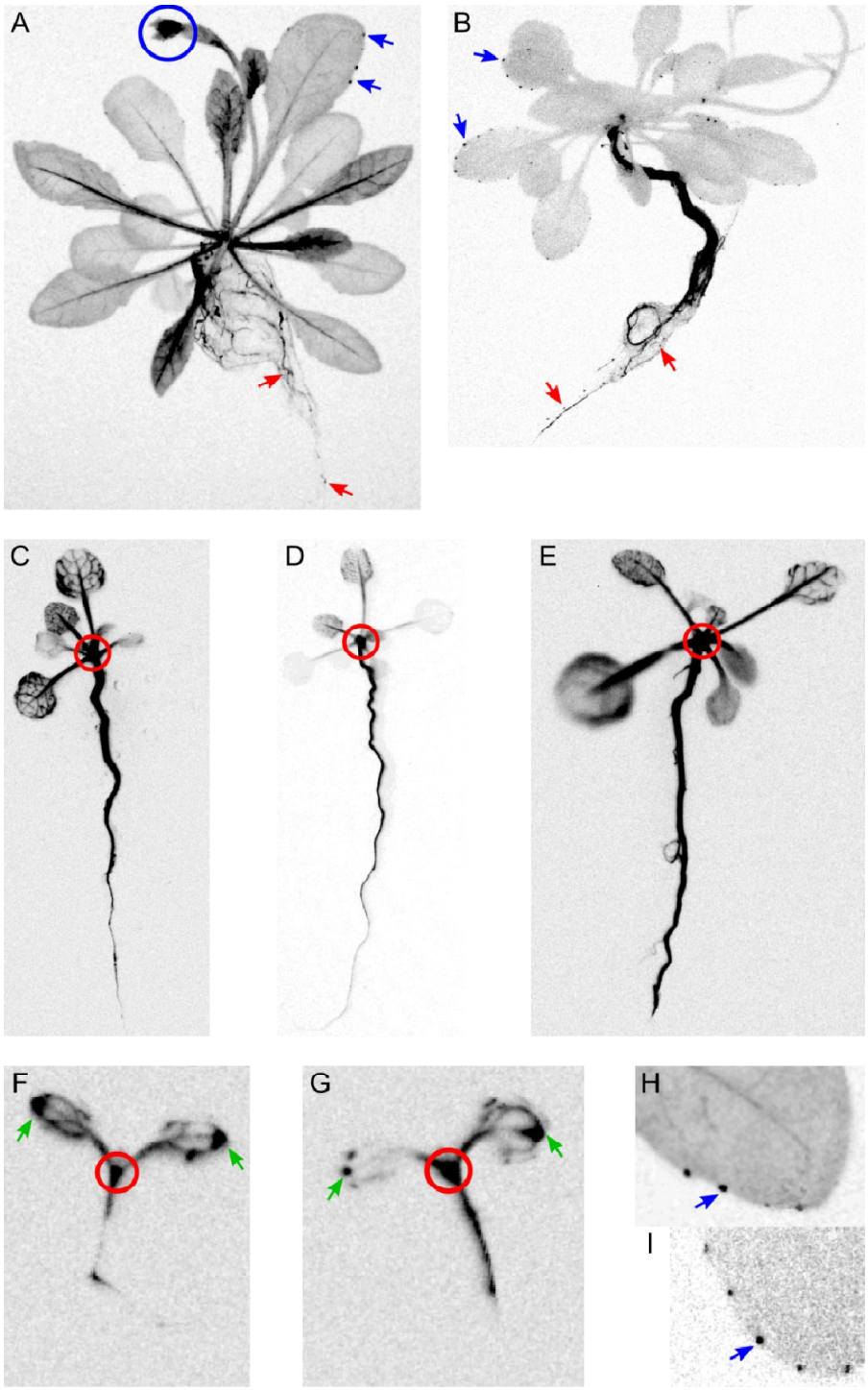

Figure 13: LUCIFERASE activity in *pAtCML5*::LUC *A. thaliana* plants. Analysis of (**A**, **B**, **H**, **I**) 28 d-old, (**C**-**E**) 14 d-old and (**F**, **G**) 5 d-old plants expressing *LUC* under control of the *AtCML5* promoter. Adult *pAtcml5::*LUC plants displayed strong LUC activity in the sink organs, which was restricted to the primary root and some lateral roots. The petioles and veins as well as the area of petals and sepals (**A**, blue circle) were also marked by LUC activity. Additionally, luminescence foci occurred at the leaf margins labelling positions at which hydathodes are located (**A**, **B**, blue arrows, magnified in **H**, **I**). 14 d-old plants showed strong LUC activity along the whole length of the root, the hypocotyl, the rosette centre (**C**-**E**, red circle), as well as the petioles and veins. In addition to LUC activity in the primordial root, hypocotyl, petioles and leaf veins, 5 d-old plants showed strong LUC expression at the leaf apex (**F**, **G**, green arrows).

*pAtCML4::*LUC and *pAtCML5::*LUC seedlings after 5 d of cultivation showed a similar LUC activity distribution in primordial root, hypocotyl, petioles and veins. In both cases LUC activity was high at the hypocotyl apex, where the petioles diverge and which later forms the rosette centre (see Figure 12 F-H, Figure 13 F, G, red circle). This observation already indicated that the promoters of *AtCML4* and *AtCML5* are active in the vascular tissue or adjacent cells. The major difference between the two was a strong expression in *pAtCML5*::LUC at the leaf apex (see Figure 13 F, G, green arrows).

A similar distribution of promoter activity could be observed in 14 day-old seedlings, but *AtCML4* promoter activity seemed less pronounced within the leaf veins and the roots compared to the *AtCML5* promoter (compare Figure 12 D and Figure 12 E). However, direct comparison of expression levels is difficult, due to the non-quantitative character of the assay. At this developmental stage, *pAtCML4*::LUC seedlings also showed LUC activity at the basal leaf margins close to the transition zone to the petiole (see Figure 12 C, D, blue circle).

*pAtCML4::*LUC adult plants displayed LUC activity in roots and the vascular system extending from petioles to leaf veins and through the inflorescence stem to the pedicels and petals (see Figure 12 A, blue arrows). The plant displayed in Figure 12 B also showed expression at the basis of cauline leaves, and flowers (blue arrows), but expression in the shoot could not be detected. This might be due to an increased shoot diameter compared to the plant shown in Figure 12 A, resulting in reduced signal intensity in tissues localised in a proximal part of the organ, e.g. the vascular system. *pAtCML5::*LUC plants also showed expression in cauline leaves and sepals (see Figure 13 A, blue circle), as well as the shoot (data not shown). LUC expression in root tissue was similar for *pAtCML4::*LUC and *pAtCML5::*LUC plants, characterised by expression in the primary root and several lateral roots, whereas the majority of lateral roots showed no expression at all or only localised in foci at distinct positions along the root length (see Figure 12 B, Figure 13 A, B, red arrows). One feature only observed in plants expressing *LUC* under *AtCML5* promoter control, was the occurrence of luminescence signals in distinct foci along the leaf margins (see Figure 13 A, B, magnified in H, I, blue arrows), which correspond to hydathodes. Hydathodes are a special type of opening in the terminal leaf tissue or at trichome tips (trichome hydathodes), which is characterised by the involvement in active or passive secretion of water in liquid form, termed guttation (Sitte *et al.* 2002).

3.3 Phylogenetic analysis of CMLs harbouring a signal-anchor sequence similar to AtCML4 and AtCML5 in the green lineage

Closely connected to the function of AtCML4 and AtCML5 is the question as to when in the evolutionary history of the green lineage, these Ca^{2+} sensors at endosomal membranes emerged. The high degree of sequence conservation in the N-terminal region of both proteins as depicted in Figure 1 allowed further analysis, how far the existence of CMLs with such a targeting sequence could be traced back in the plant kingdom.

In an initial analysis (Ruge *et al.* 2016), protein sequences of AtCML4 and AtCML5 were applied in a screening for sequentially similar protein sequences in the species of the green lineage, by using a reverse best-hit BLAST approach. This led to the identification of three populations of protein sequences across different plant families that were distinguished by the sequence of the N-terminal extension rather than the sequence of the CAM-domain. All these proteins share strong similarities in the most N-proximal part of the sequence, the signal-anchor domain. However, they differ in the variable region. Due to their significant sequence similarity in this sequence part to either AtCML4 or AtCML5, two of these groups could be unequivocally termed “AtCML4-like” and “AtCML5-like” proteins, respectively. These proteins were only detected in members of the Brassicaceae family. The third group was termed “AtCML4_5-like” proteins, because the variable sequences in this group shared overall much less similarity and could not be closely correlated to either AtCML4 or AtCML5.

During a further analysis, proteins were found in the databases, which also contained a highly similar N-terminal signal-anchor, but displayed a high degree of similarity to either AtCML3 or AtCML7 in the CAM-domain. CML3 and CML7 in *A. thaliana* are highly similar in their CAM-domain and lack the N-proximal region present in AtCML4 or AtCML5. Therefore, the analysis was extended to include the sequence of AtCML3 to find AtCML3-like proteins harbouring an AtCML4_5-like N-terminus, with the specific characteristics outlined in Figure 1. This led to the identification of AtCML3-like and AtCML7-like proteins with a signal-anchor domain. Furthermore, the collected sequences were analysed in an MSA to identify a consensus for the conserved sequence stretch in the N-terminus of all the protein sequences retrieved by this approach. This consensus was then used as query in a similar search, in order to identify potential CMLs that do not share sufficient similarity in the region of their CAM-domain to be identified by submitting the sequences of AtCML3, AtCML4 or AtCML5 as query in a BLAST search, but still harbour an AtCML4_5-like N-terminus.

Appendix III provides a list of all sequences retrieved in this approach with their sequence, corresponding plant species, family and order, as well as their name as depicted in the phylogenetic tree (see Figure 14). After analysing the sequences in an MSA (see Appendix IV) and removal of gap-containing positions for reconstruction of the phylogenetic tree, identical sequences were removed from the data set prior to tree reconstruction. The remaining sequence was given a special name, by which all species also possessing the respective protein can be identified using the list in Appendix III (e.g. Bna1Bol2, representing BraNaC5L1 and BraOlC5L2). AtCML24 (AraThC24) was chosen as outgroup, because it does not belong to sub-group VII within the CMLs of *A. thaliana*, and is therefore sufficiently phylogenetically different to serve as outgroup allowing to root the tree. Applying the method of maximum-likelihood, phylogenetic relations between the protein sequences from the data set were inferred (Figure 14).

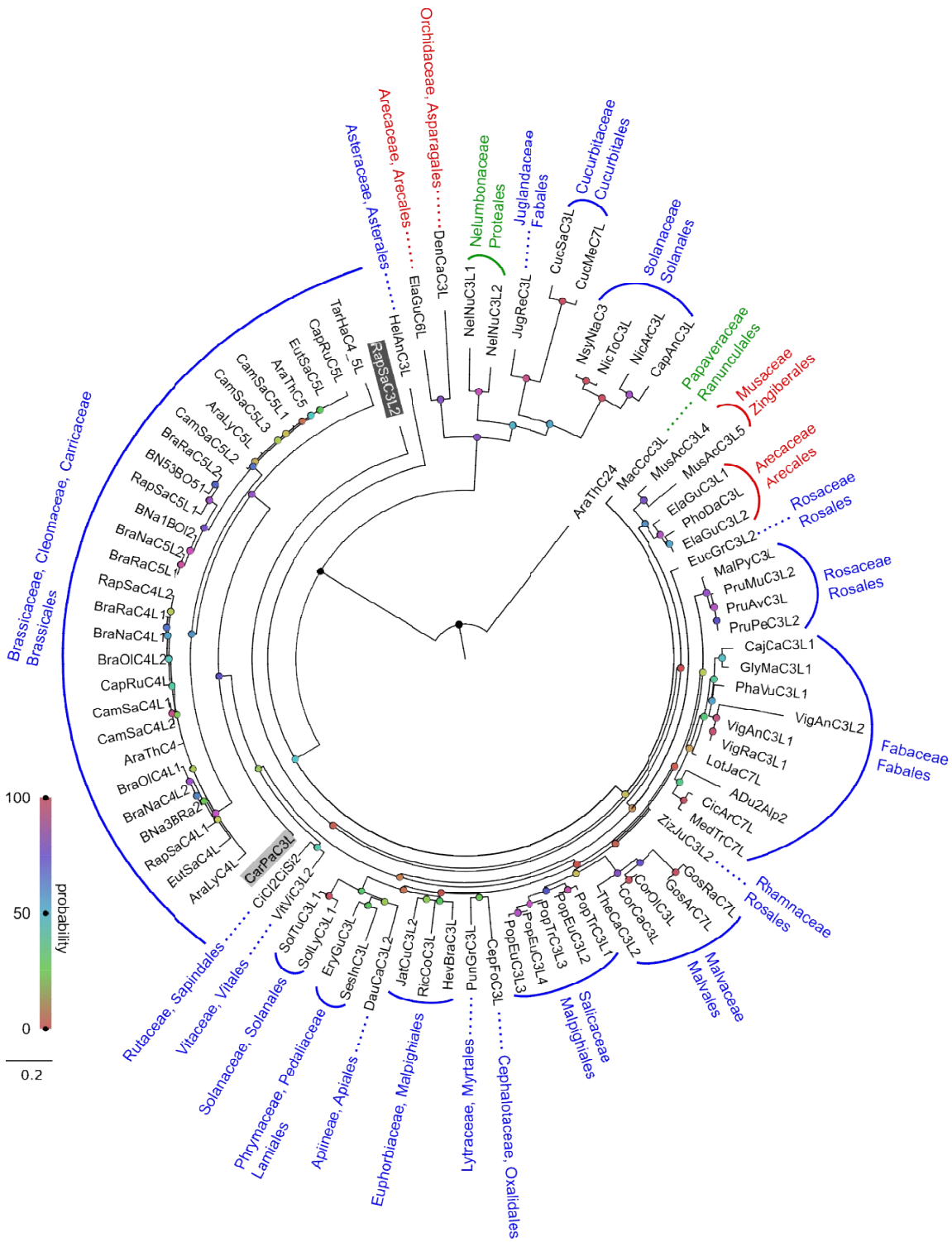

Figure 14: Maximum-likelihood tree depicting the relative similarity between AtCML3-, AtCML4-, AtCML5-, AtCML6- and AtCML7-like proteins with an AtCML4_5-like signal-anchor sequence in different plant species. The proteins in the tree could be grouped according to their similarity to AtCML4 and AtCML5 (restricted to Brassicaceae and Cleomaceae) or AtCML3 and AtCML7 with respect to their CAM-domain. Only one protein with similarity to AtCML6 was identified (ElaGuC6L). With the exception of RapSaC3L2 (dark grey box), no AtCML3- or AtCML7-like proteins harbouring an AtCML4_5-like signal-anchor sequence could be identified in species of the Brassicaceae family. The corresponding plant families and orders for the represented species are depicted in blue (dicots), green (early-diverging dicots) and red (monocots). AtCML24 (AraThC24) served as outgroup to root the tree. Probability values for the nodes were retrieved by rapid bootstrap analysis with 100 repetitions and are depicted colour-coded.

Dotted or continuous blue lines in the tree group proteins according to the different plant families and plant orders. CMLs harbouring a conserved AtCML4_5-like N-terminal domain could be identified in many different dicot plant species as well as some monocots, namely *Musa accuminata* subsp. *malaccensis*, *Elaeis guineensis*, *Phoenix dactylifera* and *Dendrobium catenatum* (see Figure 14, red labels). In all of them the N-proximal region preceding the CAM-domain includes the highly conserved N-terminal signal-anchor followed by a less conserved variable region. The preservation of this sequence among distantly related angiosperm orders supports its biological relevance. Interestingly, only in species of the Brassicaceae family orthologues for both AtCML4 and AtCML5 were identified. Species belonging to other plant families were found to only harbour AtCML3-like, AtCML7-like or, in one case, AtCML6-like (ElaGu6L) proteins with a similar N-terminal signal-anchor. These families range from Carricaceae (CarPaC3L, Figure 14, light grey box), a Brassicales family, over the phylogenetically distant Nelumbonaceae and Papaveraceae, early-diverging eudicots (see Figure 14, green labels), to some monocot families (see Figure 14, red labels). The only exception is *Tarenaya hassleriana*, which was found to contain one protein similar to AtCML4 and AtCML5 (TarHaC4_5L). However, since it shares a comparable overall similarity with AtCML4 (88.7 % similarity) and AtCML5 (86.1 % similarity) alike, it could not be unambiguously correlated with one of them and was thus termed to be AtCML4_5-like. The majority of angiosperm families contain AtCML3-like and AtCML7-like proteins with this specific signal-anchor, instead of AtCML4, AtCML5 and their orthologues. Divergence of the Brassicaceae and Cleomaceae gave rise to AtCML4-, AtCML5- and AtCML4_5-likes, whereas AtCML3- and AtCML7-likes lost the N-terminal sequence extension. Among the analysed angiosperm species the preservation of the paralogous pair of AtCML4 and AtCML5 and their homologues is unique among the members of the Brassicaceae family. Some of these species even contain several copies of both paralogues, e.g. *Brassica napa* or *Camelina sativa*. For both AtCML4- and AtCML5-likes, sequence features within the variable part of the N-terminal extension (see Figure 1) and the CAM-domain (see Appendix IV), which are specific to the respective orthologue group, can be found.

Sequence analysis of the conserved part of the N-terminus in the proteins depicted in Figure 14 led to the generation of a consensus sequence, which unravelled a difference between the AtCML4-like and AtCML5-likes in the Brassicaceae species compared to most of the proteins from other organisms. The sequences of ElaGuC3L2, CajCa3L1, CamSaC4L1, CamSaC4L2 and MusAcC3L5 were excluded from the analysis, for they contained additional residues

marking them as outliers, and RapSaC3L2 was omitted, due to its lack of the residues forming the TMD. The resulting sequence logo is shown in Figure 15.

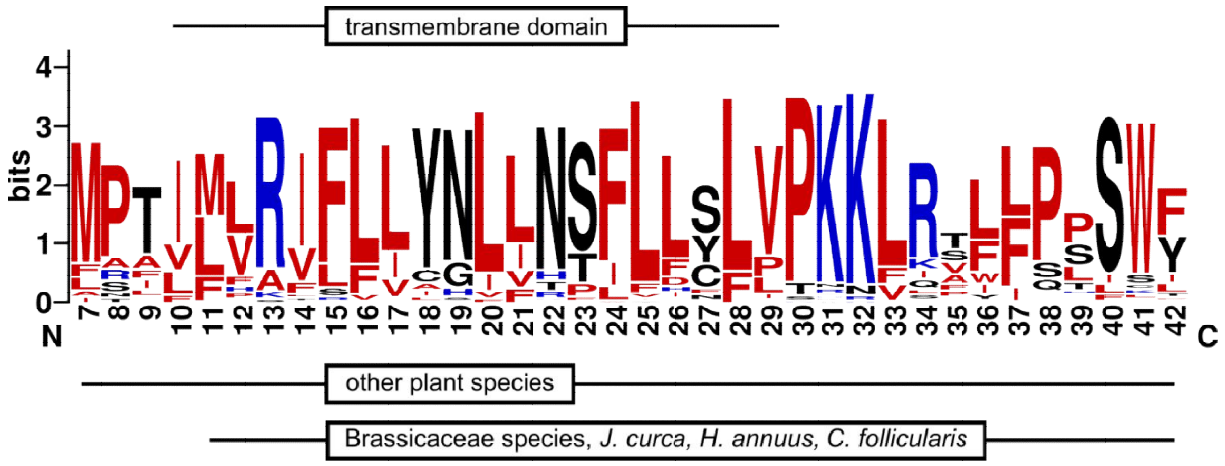

Figure 15: Sequence logo of the conserved AtCML4_5-like N-terminus in the analysed proteins. With the exception of RapSaC3L2, CajCa3L1, CamSaC4L1, CamSaC4L2, MusAcC3L5, ElaGuC3L2 and AraThC24 all proteins depicted in the phylogenetic tree (see Figure 14) were analysed in an MSA and a sequence logo covering the highly conserved region ranging from position 7 to 42 was generated with the WebLogo server tool (see 2.2.3). The residues constituting the TMD were determined by Tmpred server (see 2.2.3). Except for proteins found in *J. Curca*, *H. Annuus* and *C. follicularis*, all analysed proteins from non-Brassicaceae families were found to share the presence of four residues, preceding the highly conserved N-terminus found in the Brassicaceae species. The sequence logo also outlines the high degree of conservation for basic residues at positions 31, 32 and 34, which determine the topology of the proteins within the membrane.

The sequence logo showed that the highly conserved N-terminus characterising all the analysed proteins starts with residue 7 of 42 and exists in two different variants. In case of all proteins of the Brassicaceae species, as well as *Jatrophus curca*, *Helianthus annuus* and *Cephalotus follicularis* the conserved part starts with position 11, whereas the other variant is preceded by four additional residues and is the dominant form detected in proteins of species outside of the Brassicaceae family. Some of these proteins also contain more additional N-terminal residues, but they are not widely conserved. Since residues 11 to 30 are sufficient to serve as functional signal-anchor, the function of these four additional residues remains unclear, even though position 10 is predicted to also be part of the membrane-spanning section of the signal-anchor in the respective proteins.

In some species that fall within the phylogenetic distribution indicated by the tree, no CML with an AtCML4_5-like N-terminus could be identified in the database: *Asparagus officinalis*, *Beta vulgaris subs. vulgaris*, *Citrullus lanatus*, *Morus notabilis*, *Phalaenopsis equestris*.

4. Discussion

Ca^{2+} serve as second messengers in animal and plant cells and although both systems have developed various and, in case of CAM, conserved sets of Ca^{2+}-sensing proteins, the enormous diversity of CMLs is a plant-specific trait (Zhu *et al.* 2015, Plattner *et al.* 2015). Sequence diversity of CMLs is high and many harbour sequence stretches in addition to their CAM-domain, potentially affecting their sub-cellular localisation. Members of this protein family have been detected at the plasma membrane, the nucleus and for certain CMLs; direct correlations between their sequence and their sub-cellular localisation in mitochondria or peroxisomes have been made (Benschop *et al.* 2007, Chigri *et al.* 2012, Flosdorff 2014). The relevance of the N-terminal sequence extension of AtCML5 for its localisation in vesicles labelled by GmMAN1 and AtARA6 had previously been shown (Flosdorff 2014). However, it was hitherto unknown that the first 24 amino acids of AtCML4 and AtCML5 harbour features characteristic of a signal-anchor domain, comprising a TMD (amino acids 1-20) with an electrostatic charge gradient with a positive net charge on its C-proximal end (see Figure 1). Further, this sequence stretch is highly conserved among orthologues of AtCML4 and AtCML5 in other species belonging to the Brassicaceae family. According to analyses by Harley, Heijne and colleagues, the features of this conserved N-terminus suggested a topology for AtCML4 and AtCML5, in which the CAM-domain of both proteins protrudes into the cytoplasm (Heijne 1994, Harley *et al.* 1998). The signal-anchor sequence serves as translocation signal for the ER recognised by the SRP-complex and as membrane anchor at the same time (High *et al.* 1991). The topology hypothesis was experimentally proven in a protease protection assay on isolated membrane fractions, in which the YFP tag of a C-terminally labelled AtCML5 fusion protein was not protected from the protease activity (compare left with right lane in Figure 5). The similar behaviour of a comparable fusion construct with only the signal-anchor domain of AtCML5 instead of the full-length protein showed that it is indeed the N-terminus causing this topology.

It is obvious to assume a similar topology for AtCML4, since it shares substantially high sequence similarity with AtCML5 within its 28 N-terminal amino acids and was found to be localised in the same compartment (see Figure 2 A). Quantitative analysis of AtCML5-YFP localisation in tobacco protoplasts revealed that it partially co-localises with the *cis*-Golgi marker GmMAN1-mCherry and that a slightly bigger fraction showed overlap with the late PVC marker AtARA6-mCherry (see Figure 4). Initial analyses of the sub-cellular localisation

of GmMAN1 have revealed that there is a major population of the protein labelling the *cis*-Golgi, whereas smaller fractions also occurred in medial and *trans*-Golgi as well as the TGN/EE (Saint-Jore-Dupas *et al.* 2006). Further, it has been found that under overexpression conditions, AtARA6 also labels TGN structures (Bottanelli *et al.* 2012), potentially rendering its co-localisation with AtCML5 artificial. Probably, the main localisation for AtCML5 is in Golgi cisternae membranes. This would be corroborated by the unusually large diameter of the structures observed by YFP-fusion expressions of AtCML4 and AtCML5 in Arabidopsis (see Figure 2) and tobacco cells (data not shown) under 35S- and endogenous promoter-driven expression conditions. Similar observations in Arabidopsis had previously been made for structures labelled by the Golgi cisternae proteins AtGNOM (Naramoto *et al.* 2014) and AtERD2 (Boevink *et al.* 1998) as well as a constitutive GTP-binding form of the MVB protein Rab5-GTPase AtARA7 (Jia *et al.* 2013). However, the latter example was characterised by enhanced homotypic fusion and therefore does not resemble the native state of the system; AtARA7-labelled structures usually appear as punctae in microscopic analyses (Ueda *et al.* 2004, Haas *et al.* 2007). It has been shown that Ca^{2+} and pH are critical determinants for the binding of soluble cargo by VSRs; however, Ca^{2+} seem to be the major component in this system (Watanabe *et al.* 2002, Kirsch *et al.* 1994). The ER in plants is assumed to serve as a major Ca^{2+} storage compartment, probably with $[Ca^{2+}]_f$ within the high micro molar range in its lumen (Stael *et al.* 2012). This is emphasised by the presence of several Ca^{2+}-ATPases in the ER membrane (Hong *et al.* 1999, Liang *et al.* 1997). Analyses with a Ca^{2+} sensor construct anchored in the membranes of the Golgi stack have revealed the resting concentration in the lumen to be approx. 700 nM, which is several times lower than the assumed $[Ca^{2+}]_f$ in the ER lumen (Ordenes *et al.* 2012). Considering the observation that cargo binding by VSRs occurs in ER and *cis*-Golgi and that cargo is released in the TGN (Künzl *et al.* 2016), it is likely to assume that the $[Ca^{2+}]_f$ in the TGN lumen is even lower than in the Golgi. Concomitantly, the luminal pH in ER, Golgi and TGN has been shown to follow a gradient beginning at 7.1-7.5 in the ER and ranging from 6.8-6.9 in the Golgi to 6.1-6.5 in the TGN (Shen *et al.* 2013, Martinière *et al.* 2013). Whereas the influx of protons from the cytoplasm mediated by the vacuolar H^+-ATPase in the TGN membranes explains the low pH in the TGN (Dettmer *et al.* 2006), decrease in luminal Ca^{2+} probably occurs via yet unidentified channels in Golgi and TGN membranes. Since this influences cargo trafficking, it can be considered a constitutive process and would explain the 4-5 times higher resting $[Ca^{2+}]_f$ in the vicinity of AtCML5-positive compartments compared to the $[Ca^{2+}]_f$ measured

around chloroplasts or in the entire cytoplasm (see Figure 6). Measurements of luminal Golgi $[Ca^{2+}]_f$ resulted in similarly unsteady graphs in comparison to measurements of cytosolic $[Ca^{2+}]_f$ (Ordenes *et al.* 2012) as retrieved by the AtCML5$_{1-28}$-YFP-AEQ sensor in this work (see Figure 6, blue and green graphs), indicating a compartment-specific behaviour of the $[Ca^{2+}]_f$.

Although Ca^{2+} channels have not yet been identified in Golgi, TGN or MVB membranes, the Ca^{2+}/Mn^{2+}-selective cation pump AtECA3 has been found to be localised in Golgi stacks (Mills *et al.* 2008) and also MVBs (Li *et al.* 2008), hence showing a similar sub-cellular distribution as AtCML4 and AtCML5. Li and colleagues have proven that *eca3* mutants are characterised by increased protein secretion (Li *et al.* 2008), which can probably be explained by reduced luminal $[Ca^{2+}]_f$ in the Golgi lumen. This might lead to premature dissociation of VSRs from their vacuole-destined cargo, which then travels to the plasma membrane by default. Since similar phenotypes were observed in *vsr* mutant plants, this indicates that VSR function is abolished or reduced when Ca^{2+} homeostasis in the Golgi is perturbed. This is further supported by the observation that activity of the Ca^{2+}-ATPase SPCA1 was found to be required for Ca^{2+}-dependent cargo binding and membrane association of the cargo receptor Cab45 in the TGN lumen of HeLa cells (von Blume *et al.* 2012).

Taking into account the sub-cellular localisation of AtCML4 and AtCML5, the measured $[Ca^{2+}]_f$ in the vicinity of AtCML5-labelled structures and the fact that AtPLDγ1 and AtDRP1B were identified as potential interaction partners of AtCML5 in a pull-down assay (see 3.2.2), the following working model could be envisioned describing the function of AtCML5 and potentially AtCML4 *in vivo*. AtCML4 and AtCML5 are located at the interface of maturation of *trans*-Golgi cisternae into tubulovesicular TGN structures. Here, they serve as sensors for the maturation process characterised by the efflux of Ca^{2+} from the Golgi/early stage-TGN lumen, which is required for cargo release from VSRs concomitantly to luminal acidification (Watanabe *et al.* 2002, Dettmer *et al.* 2006). Along with cargo release, processes involving recycling of VSRs by the retromer complex (Niemes *et al.* 2010), formation of clathrin-coated (Teh *et al.* 2013) secretory vesicles and MVB maturation (Scheuring *et al.* 2011) coincide. AtCML5 could activate AtPLDγ1 and AtDRP1B to facilitate membrane curvature by generation of phosphatidic acid from more complex lipids and fission of the thus forming membrane bottleneck, respectively, to separate the nascent vesicles from the donor membrane. Hence, AtCML5 would coordinate the luminal cargo release from VSRs with the formation of the transport vesicles, in order to avoid premature vesicle detachment. In yeast, it

has been shown that Ca^{2+}/CAM is required for late stages in fusion of vesicles with vacuoles and the authors speculated on a role of CAM in triggering membrane mixing proteins (Peters *et al.* 1998). Ca^{2+}/CAM has also been found to stabilise the interaction between early endosome antigen 1, a protein essential for homotypic early endosome fusion in animal cells, and membranes in COS-7 cells (Lawe *et al.* 2003). Therefore, an involvement of AtCML5 in vesicular trafficking processes is not unlikely. As previously described, AtCML4 and AtCML5 might not localise to the late PVC, because the observed partial overlap with AtARA6 was probably the result of artificial AtARA6 mislocalisation. Further, since TGN structures usually appear as punctae in confocal microscopic analyses (Bottanelli *et al.* 2012, Künzl *et al.* 2016, Robinson *et al.* 2011), it is also possible that AtCML4 and AtCML5 are exclusively localised at Golgi stacks. Similar to AtGNOM, which co-localises with the TMD of sialyl transferase from rat, a *trans*-Golgi marker (Naramoto *et al.* 2014, Boevink *et al.* 1998), but also influences AtPIN1 recycling to the plasma membrane (Geldner *et al.* 2003), AtCML5 could still interact with AtPLDγ1 and AtDRP1B on the TGN membrane. This would explain the lack of co-localisation of both AtPLD1γ and AtDRP1B with AtCML5-YFP as displayed in Figure 8, since both potential interacting proteins showed a fluorescence pattern typical of post-Golgi compartments. However, in this scenario the partial co-localisation with AtARA6 cannot be explained. Nevertheless, the hypothesis explained above is still suited to connect the indications retrieved from the experimental data and is further supported by other aspects. AtDRP1B is very weakly expressed several parts of the plant, including hypocotyl, cotyledon and juvenile leaves (Collings *et al.* 2008), which were found to be characterised by a high activity of the *AtCML5* promoter (see Figure 13). Hence, the identification of AtDRP1B in the pull-down assay (see 3.2.2) is likely not a false-positive hit. Further, the related protein AtDRP1A has been shown to be involved in trafficking processes and plants lacking functional AtDRP1A have defects in cell expansion and vascular continuity in leaves (Collings *et al.* 2008, Sawa *et al.* 2005). Therefore, a role of AtDRP1B in vesicular trafficking processes seems likely. AtPLDγ1 was found to be expressed in different tissues with the highest levels in roots (Qin *et al.* 2006), which also showed high activity of the *AtCML5* promoter region (see Figure 13). Further, PLDs were demonstrated to promote separation of nascent secretory vesicles from the TGN in the animal GH3 cell line (Chen *et al.* 1997).

The results of the *in vivo* analysis of promoter activity for *AtCML5* (see Figure 13) were partially in line with the data retrieved by *in silico* analysis of *AtCML5* expression (see Table

1 and Table 9). The high expression levels of *AtCML5* in the different organs shown in Table 8 were in accordance with *AtCML5* promoter activity in the area of the central cylinder in the root, as well as the vascular and adjacent tissues. Indication for an involvement of *AtCML5* in growth-affecting processes as provided by the stimulating effect of growth-promoting hormones (AUX, brassinolide) and the down-regulation of *AtCML5* expression in response to negative regulators of growth (jasmonate, ACC), would not be contradicted by the results of the LUC-based promoter activity assay, showing its expression throughout almost all parts of the plant. Additionally, the presence of promoter *cis*-elements involved in light-response (GATA, MYB4, SOULREP3-binding motifs) and meristem function (Bellringer/replumless/pennywise BS1 IN AG) further support the indication for *AtCML5* being involved in long-term growth-regulation, rather than triggering short-term responses to external or internal stimuli. However, the response to ABA in combination with the *AtCML5* promoter activity detected in hydathodes (see Figure 13 H, I) renders a potential role in water homeostasis possible as well.

Comparison of *AtCML4* promoter activity data as obtained by the *in vivo* LUC-based assay revealed a significant difference to the information received by *in silico* analysis in terms of tissue expression levels (compare Figure 12 to Table 8). Although expression levels could not be quantitatively assessed in the assay, *AtCML4* promoter activity was sufficiently high to result in LUC levels in the analysed plants that would allow signal detection with the same detector setting parameters as for *pAtCML5*::LUC plants. Hence, the signal intensities between the two different reporter plant populations did not differ severely. This is in contradiction to the organ-specific expression values determined by microarray analysis as displayed in Table 8. It is possible that the promoter activity is repressed at the original *AtCML4* locus and this repression is lacking at the sites of T-DNA insertion of the *pAtCML4*::LUC construct. Despite the differences between *AtCML4* and *AtCML5* expression patterns retained from *in silico* analysis, *in vivo* analysis showed that – with minor differences – both genes are expressed in the same parts of the plant, e.g. roots, leaf veins, petioles, in the developmental stages analysed. Whereas for *AtCML5* speculations about potential functions supported by *in vivo* and *in silico* data can be made, the potential role of *AtCML4* remains difficult to evaluate.

Unfortunately, phenotypic analysis of the single and double mutant plants analysed did not yield any conclusive results, thereby not providing any information on potential pathways AtCML4 and AtCML5 might be involved in. However, phylogenetic analysis of both proteins

revealed valuable details about the evolutionary background of these Ca^{2+} sensors and allow for speculation about their potential impact on plant development. The main characteristic of AtCML4 and AtCML5, separating them from the other CMLs in clade VII of Arabidopsis CMLs, is the presence of signal-anchor preceding the CAM-domain (see Figure 1). The relevance of the N-terminal signal-anchor for sub-cellular targeting had previously been proven (Flosdorff 2014, Ruge *et al.* 2016) and in this work it was found to place AtCML4 and AtCML5 in an endomembrane-associated microdomain with a $[Ca^{2+}]_f$ environment distinct of that in the cytoplasm (see 3.2.1). Hence, it was interesting to analyse whether the Ca^{2+}-sensing function at this sub-cellular localisation was phylogenetically conserved in plants, that is, whether CMLs with a similar signal-anchor sequence could also be found in other species of the green lineage. The phylogenetic analysis (see 3.3) revealed that the occurrence of a paralogous pair of AtCML4-like and AtCML5-like proteins as found in *A. thaliana* was restricted to species of the Brassicaceae family (see Figure 14, on the left). The most closely related family of Brassicaceae within the Brassicales order is the Cleomaceae family, which is represented in this analysis by *Tarenaya hassleriana*. This species encodes only one CML with a comparable signal-anchor sequence and about equal sequence similarity to both AtCML4 and AtCML5. Hence, the gene duplication event that gave rise to the paralogous AtCML4-like and AtCML5-like proteins in the Brassicaceae probably occurred after their divergence from the other Brassicales species, but before the divergence of Brassicaceae members. The split of Brassicaceae from Cleomaceae is supposed to have occurred approx. 20 million years ago (Wikström *et al.* 2001) and a whole-genome duplication event that might have given rise to AtCML4 and AtCML5 occurred after the split (Schranz *et al.* 2006). *Carica papaya*, a Carricaceae species belonging to the Brassicales, also contains a CML with a homologous signal-sequence (CarPa3L, Figure 14, light grey box), but it displays more sequence similarity to AtCML3 than to AtCML4 or AtCML5. Further, CMLs with an AtCML4/5-like signal-anchor sequence were detected in plant species outside the Brassicales. However, all of them shared highest sequence similarity to either AtCML3 or AtCML7. Significantly more of these species contain an AtCML3-like rather than an AtCML7-like protein with a signal-anchor sequence, therefore an AtCML3-like protein has to be considered the phylogenetic origin of AtCML4 and AtCML5 in Brassicaceae. In addition, it is likely to assume that there was a gene duplication event within the Brassicales, leading to the emergence of two AtCML3-like proteins with a signal-anchor sequence. Then, one of the two was subject to deletions and lost the whole N-terminal sequence extension,

whereas the other was altered within the CAM-domain leading to the AtCML4/5-like protein as found in *Tarenaya hassleriana*. An indication for the loss of the formerly present signal-anchor within one of the original AtCML3-like genes is provided by the presence of an AtCML3-like protein with a degenerate N-terminal extension in *Raphanus sativus* (RapSaC3L2, Figure 14, dark grey box). Its N-terminus lacks a considerable amount of residues of the TMD region (TMD displayed in Figure 15) required for membrane interaction. It might be a remnant of the described process. Analysis of the signal-anchor sequence of most proteins displayed in Figure 14 revealed that *Jatrophus curca*, *Helianthus annuus*, *Cephalotus follicularis* and the Brassicaceae species contain a signal-anchor domain that is four residues shorter on the N-terminal end than the one in the CMLs of all other analysed species (Figure 15). However, it is unclear why these residues were lost in the CMLs of these particular species, but only the residue at position -1 respective to the shorter signal-anchor sequence is supposed to contribute to the TMD as predicted by Tmpred (see 2.2.3). Further, none of the species other than *Raphanus sativus* contain an AtCML4- or AtCML5-like protein together with a signal-anchor-harbouring AtCML3- or AtCML7-like protein. Additionally, only in Brassicaceae, some species contain AtCML3-like proteins with a C-terminal peroxisomal targeting sequence similar to AtCML3 in *A. thaliana* (Chigri *et al.* 2012). This shows that the emergence of AtCML4- and AtCML5-like proteins coincided not only with a loss of the whole N-terminal sequence in AtCML3, but also with a potential change in its localisation to peroxisomes or maybe the cytoplasm (for AtCML3-like proteins without a targeting signal). Together, these findings underline the complex phylogenetic history of CML clade VII in *A. thaliana*, which is characterised by duplication and deletion events affecting certain protein domains or entire genes. This exacerbates the elucidation of a clear phylogenetic relationship with deductions regarding origin, localisation and function of the respective proteins.

In order to illustrate the complicated phylogenetic relationship for better understanding, Figure 16 provides an overview of the conservation of a CML with an AtCML4/5-like signal-anchor sequence across a huge variety of dicot species (blue), some early-diverging dicots (green) and even a few monocot species (red), which emphasises the evolutionary pressure on and physiological relevance of this protein.

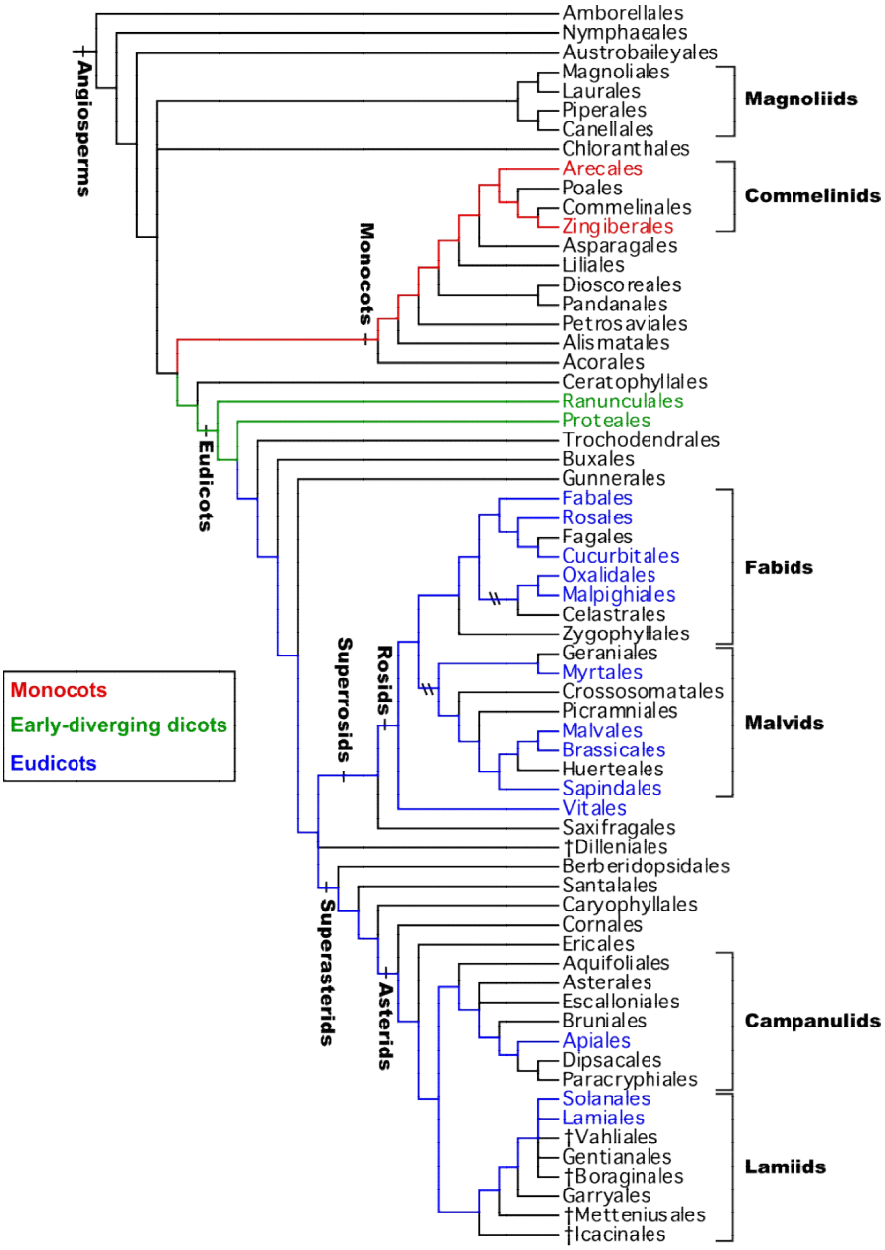

Figure 16: Phylogenetic tree of angiosperm orders. The tree depicts the phylogenetic relations between the known angiosperm orders with coloured markups for those orders, in which a CML with an AtCML4/5-like signal-anchor sequence was detected. Red – monocots, green – early-diverging dicots, blue – eudicots. This tree was originally published in "An update of the Angiosperm Phylogeny Group classification for the orders and families of flowering plants: APG IV" (The Angiosperm Phylogeny 2016) and was slightly altered and incorporated here by permission of Oxford University Press (see Appendix V).

The wide distribution over many dicot and some monocot species, together with the fact that no comparable homologue could be identified in earlier stages of plant evolution, indicates that the Golgi-targeted CMLs are required for an angiosperm-specific trait, potentially predominant in dicot species. Taking into account the expression patterns of AtCML4 and AtCML5 as found in the LUCIFERASE-based promoter activity assay (see Figure 12 and Figure 13, leaf veins and hypocotyl apex) a role for both proteins in the development of

vascular tissue, especially leaf venation could be envisioned. The complexity of vein architecture, represented by the vein density per leaf area, has been shown to have risen significantly from ferns and early seed plants to angiosperms (Boyce *et al.* 2009). Furthermore, whereas most leaves of most monocots are characterised by several parallel primary veins with few interconnections, dicot leaves display a more hierarchical, ramified structure with several higher orders of veins and extensive interconnections and tapering towards the leaf margin also occurring in secondary veins (reviewed in Sack *et al.* 2013). Photosynthetic mesophyll delimits water transport and a more complex venation system improves water transport towards stomata whilst maintaining optimum water supply to the surrounding mesophyll. This leads to higher photosynthetic rates, due to improved transpiration activity (Brodribb *et al.* 2007). Sack and Scoffoni further mention that certain monocot families, e.g. banana family, to which *Musa accuminata* subsp. *malaccensis* belongs, have developed vein architectures similar to eudicots (Sack *et al.* 2013). *Musa accuminata* subsp. *malaccensis* was found to contain two AtCML3-like proteins with an AtCML4/5 signal-anchor sequence (see Figure 14, MusAcC3L4, MusAcC3L5). Whether the other species shown to contain signal-anchor-carrying AtCML3-like proteins also have eudicot-like vein systems should be further investigated. Several species falling within the phylogenetic distribution displayed in Figure 15 were found not to contain a CML with an AtCML4/5-like signal-anchor sequence (see 3.3). However, all of these species are currently in a very early annotation state, rendering sequence information retrieved from the databases less reliable as for organisms in an advanced state of genome annotation, e.g. *A. thaliana*, for which also experimental evidence for bioinformatically inferred annotations exists. Thus, the fact that these species seem entirely devoid of CMLs with a comparable pre-sequence, has to be considered only tentative.

The results presented here provide a basis for further analyses to determine the physiological function of AtCML4 and AtCML5 in the future. However, the lack of a visible phenotype in the mutant plants analysed under the described conditions impedes the determination of their function. In addition to the mutant lines generated in this work, a double knock-out line lacking functional *AtCML4* and *AtCML5* should be generated to avoid potential complementation effects. To assess the mutants regarding their protein levels, the monoclonal antibodies raised in this work (see 3.2.6) could be utilised. However, enriched membrane fractions should be used for analysis, since whole-plant extracts do not contain enough protein to be detected by western blot analysis with the given antibodies, at least in case of

AtCML4 (see Figure 11, leaf extract). Further, the antibodies could be used for co-immunoprecipitation experiments to either identify more potential interaction partners, or to verify AtPLDγ1 and AtDPR1B as binding partners in an approach different to the pull-down presented here (see 3.2.2). Also, future analyses performed with the *pAtCML5*::AtCML5$_{1-28}$-YFP-AEQ sensor should be conducted in comparison to control constructs, whose expression is driven by the same promoter, to measure Ca^{2+} signals only in those cells *pAtCML5*::AtCML5$_{1-28}$-YFP-AEQ is expressed in. Additionally, prior to utilising plants expressing sensor constructs under endogenous promoter control, a calibration curve correlating relative luminescence counts and $[Ca^{2+}]_f$ should be established for these constructs to provide precision across the whole range of physiological $[Ca^{2+}]_f$.

5. Abbreviations

ACA	Autoinhibited Ca^{2+}-ATPase
CAM	Calmodulin
cAMP	Cyclic adenosine monophosphate
CAX	Ca^{2+}/H^{+} -antiporter
CBL	Calcineurin B-like protein
CDS	Coding sequence
cGMP	Cyclic guanosine monophosphate
CML	Calmodulin-like protein
CNBr	Cyanide bromide
CNGC	Cyclic nucleotide-gated channel
CPK	Calcium-dependent protein kinase
ddH_2O	Double de-ionised water
DMSO	Dimethylsulfoxide
DNA	Deoxyribonucleic acid
DTT	Dithiotreitol
ECA	ER-type Ca^{2+}-ATPase
EEs	Early endosomes
GFP	Green fluorescent protein
gDNA	Genomic DNA
GLR	Glutamate receptor
GST	Glutathione S-transferase
LEs	Late endosomes
McsS	Mechanosensitive channel
MVBs	Multivesicular bodies
PAGE	Poly acrylamide gel electrophoresis
PCR	Polymerase chain reaction
PMCA	Plasma membrane Ca^{2+}-ATPase
PVC	Pre-vacuolar compartment
PVDF	Poly vinyleden fluoride
RFP	Red fluorescent protein
RNA	Ribonucleic acid
RNAi	RNA interference
SDS	Sodium dodecylsulfate
SERCA	(Sarco)endoplasmic reticulum Ca^{2+}-ATPase
siRNA	Small interfering RNA
TBS	Tris-buffered saline
UTR	Untranslated region
VGCC	Voltage-gated Ca^{2+} channel
YFP	Yellow fluorescent protein

6. References

Abbas, N., J. P. Maurya, D. Senapati, S. N. Gangappa & S. Chattopadhyay (2014) Arabidopsis CAM7 and HY5 Physically Interact and Directly Bind to the HY5 Promoter to Regulate Its Expression and Thereby Promote Photomorphogenesis. *The Plant Cell,* 26**,** 1036-1052.

Ahn, H.-K., Y. W. Kang, H. M. Lim, I. Hwang & H.-S. Pai (2015) Physiological Functions of the COPI Complex in Higher Plants. *Molecules and Cells,* 38**,** 866-875.

Allbritton, N. L., T. Meyer & L. Stryer (1992) Range of Messenger Action of Calcium Ion and Inositol 1,4,5-Trisphosphate. *Science,* 258**,** 1812-1815.

Allen, D., Blinks & F. Prendergast (1977) Aequorin luminescence: relation of light emission to calcium concentration--a calcium-independent component. *Science,* 195**,** 996-998.

Astegno, A., M. C. Bonza, R. Vallone, V. La Verde, M. D'Onofrio, L. Luoni, B. Molesini & P. Dominici (2017) Arabidopsis calmodulin-like protein CML36 is a calcium (Ca2+) sensor that interacts with the plasma membrane Ca2+-ATPase isoform ACA8 and stimulates its activity. *Journal of Biological Chemistry,* 292**,** 15049-15061.

Baker, S. L., E. C. Butterworth & F. A. Langley (1946) The calcium and nitrogen content of human bone tissue cleaned by micro-dissection. *Biochemical Journal,* 40**,** 391-396.

Bandmann, V., J. D. Müller, T. Köhler & U. Homann (2012) Uptake of fluorescent nano beads into BY2-cells involves clathrin-dependent and clathrin-independent endocytosis. *FEBS Letters,* 586**,** 3626-3632.

Batistic, O. & J. Kudla (2004) Integration and channeling of calcium signaling through the CBL calcium sensor/CIPK protein kinase network. *Planta,* 219**,** 915-924.

Batistič, O. & J. Kudla (2009) Plant calcineurin B-like proteins and their interacting protein kinases. *Biochimica et Biophysica Acta (BBA) - Molecular Cell Research,* 1793**,** 985-992.

Batistič, O., N. Sorek, S. Schültke, S. Yalovsky & J. Kudla (2008) Dual Fatty Acyl Modification Determines the Localization and Plasma Membrane Targeting of CBL/CIPK Ca(2+) Signaling Complexes in Arabidopsis. *The Plant Cell,* 20**,** 1346-1362.

Bender, K. W., R. K. Blackburn, J. Monaghan, P. Derbyshire, F. L. H. Menke, C. Zipfel, M. B. Goshe, R. E. Zielinski & S. C. Huber (2017) Autophosphorylation-based Calcium Ca2+Sensitivity Priming and Ca2+/Calmodulin Inhibition of Arabidopsis thaliana Ca2+-dependent Protein Kinase 28 (CPK28). *The Journal of Biological Chemistry,* 292**,** 3988-4002.

Bender, Kyle W., S. Dobney, A. Ogunrinde, D. Chiasson, Robert T. Mullen, Howard J. Teresinski, P. Singh, K. Munro, Steven P. Smith & Wayne A. Snedden (2014) The calmodulin-like protein CML43 functions as a salicylic-acid-inducible root-specific Ca2+ sensor in Arabidopsis. *Biochemical Journal,* 457**,** 127-136.

Bender, K. W. & W. A. Snedden (2013) Calmodulin-related proteins step out from the shadow of their namesake. *Plant Physiology,* 163**,** 486-495.

Bendz, M., M. Skwark, D. Nilsson, V. Granholm, S. Cristobal, L. Käll & A. Elofsson (2013) Membrane protein shaving with thermolysin can be used to evaluate topology predictors. *Proteomics,* 13**,** 1467-1480.

Benschop, J. J., S. Mohammed, M. O'Flaherty, A. J. R. Heck, M. Slijper & F. L. H. Menke

(2007) Quantitative Phosphoproteomics of Early Elicitor Signaling in Arabidopsis. *Molecular & Cellular Proteomics,* 6**,** 1198-1214.

Bi, X., R. A. Corpina & J. Goldberg (2002) Structure of the Sec23/24-Sar1 pre-budding complex of the COPII vesicle coat. *Nature,* 419**,** 271-277.

Bilkova, E., R. Pleskot, S. Rissanen, S. Sun, A. Czogalla, L. Cwiklik, T. Róg, I. Vattulainen, P. S. Cremer, P. Jungwirth & Ü. Coskun (2017) Calcium Directly Regulates Phosphatidylinositol 4,5-Bisphosphate Headgroup Conformation and Recognition. *Journal of the American Chemical Society,* 139**,** 4019-4024.

Bleecker, A. B. & S. E. Patterson (1997) Last exit: senescence, abscission, and meristem arrest in Arabidopsis. *The Plant Cell,* 9**,** 1169-1179.

Blum, H., H. Beier & H. J. Gross (1987) Improved silver staining of plant proteins, RNA and DNA in polyacrylamide gels. *Electrophoresis,* 8**,** 93-99.

Boevink, P., K. Oparka, S. S. Cruz, B. Martin, A. Betteridge & C. Hawes (1998) Stacks on tracks: the plant Golgi apparatus traffics on an actin/ER network. *The Plant Journal,* 15**,** 441-447.

Bonza, M. C., P. Morandini, L. Luoni, M. Geisler, M. G. Palmgren & M. I. De Michelis (2000) At-ACA8 Encodes a Plasma Membrane-Localized Calcium-ATPase of Arabidopsis with a Calmodulin-Binding Domain at the N Terminus. *Plant Physiology,* 123**,** 1495-1506.

Boonburapong, B. & T. Buaboocha (2007) Genome-wide identification and analyses of the rice calmodulin and related potential calcium sensor proteins. *BMC Plant Biology,* 7**,** 1-17.

Bottanelli, F., D. C. Gershlick & J. Denecke (2012) Evidence for Sequential Action of Rab5 and Rab7 GTPases in Prevacuolar Organelle Partitioning. *Traffic,* 13**,** 338-354.

Boudsocq, M., M.-J. Droillard, L. Regad & C. Laurière (2012) Characterization of Arabidopsis calcium-dependent protein kinases: activated or not by calcium? *Biochemical Journal,* 447**,** 291-299.

Boyce, C. K., T. J. Brodribb, T. S. Feild & M. A. Zwieniecki (2009) Angiosperm leaf vein evolution was physiologically and environmentally transformative. *Proceedings of the Royal Society B: Biological Sciences,* 276**,** 1771-1776.

Brini, M., R. Marsault, C. Bastianutto, J. Alvarez, T. Pozzan & R. Rizzuto (1995) Transfected Aequorin in the Measurement of Cytosolic Ca2+ Concentration ([Ca2+]c): A CRITICAL EVALUATION. *Journal of Biological Chemistry,* 270**,** 9896-9903.

Brodribb, T. J., T. S. Feild & G. J. Jordan (2007) Leaf Maximum Photosynthetic Rate and Venation Are Linked by Hydraulics. *Plant Physiology,* 144**,** 1890-1898.

Campe, R., C. Langenbach, F. Leissing, G. V. Popescu, S. C. Popescu, K. Goellner, G. J. M. Beckers & U. Conrath (2016) ABC transporter PEN3/PDR8/ABCG36 interacts with calmodulin that, like PEN3, is required for Arabidopsis nonhost resistance. *New Phytologist,* 209**,** 294-306.

Chandran, V., E. J. Stollar, K. Lindorff-Larsen, J. F. Harper, W. J. Chazin, C. M. Dobson, B. F. Luisi & J. Christodoulou (2006) Structure of the regulatory apparatus of a calcium-dependent protein kinase (CDPK): a novel mode of calmodulin-target recognition. *Journal of Molecular Biology,* 357**,** 400-410.

Chattopadhyaya, R., W. E. Meador, A. R. Means & F. A. Quiocho (1992) Calmodulin structure refined at 1.7 A resolution. *Journal of Molecular Biology,* 228**,** 1177-1192.

Chen, Y.-G., A. Siddhanta, C. D. Austin, S. M. Hammond, T.-C. Sung, M. A. Frohman, A. J. Morris & D. Shields (1997) Phospholipase D Stimulates Release of Nascent Secretory Vesicles from the *trans*-Golgi Network. *The Journal of Cell Biology,* 138**,** 495-504.

Chen, Y., Y. Wang, J. Huang, C. Zheng, C. Cai, Q. Wang & C.-A. Wu (2017) Salt and methyl jasmonate aggravate growth inhibition and senescence in Arabidopsis seedlings via the JA signaling pathway. *Plant Science,* 261**,** 1-9.

Cheng, N.-H., J. K. Pittman, T. Shigaki, J. Lachmansingh, S. LeClere, B. Lahner, D. E. Salt & K. D. Hirschi (2005) Functional Association of Arabidopsis CAX1 and CAX3 Is Required for Normal Growth and Ion Homeostasis. *Plant Physiology,* 138**,** 2048-2060.

Chigri, F., S. Flosdorff, S. Pilz, E. Kolle, E. Dolze, C. Gietl & U. C. Vothknecht (2012) The Arabidopsis calmodulin-like proteins AtCML30 and AtCML3 are targeted to mitochondria and peroxisomes, respectively. *Plant Molecular Biology,* 78**,** 211-222.

Cho, J. H., J. H. Lee, Y. K. Park, M. N. Choi & K.-N. Kim (2016) Calcineurin B-like Protein CBL10 Directly Interacts with TOC34 (Translocon of the Outer Membrane of the Chloroplasts) and Decreases Its GTPase Activity in Arabidopsis. *Frontiers in Plant Science,* 7**,** 1911.

Clapham, D. E. (1995) Calcium signaling. *Cell,* 80**,** 259-268.

Clouse, S. D. (1996) Plant Chromosomes: Brassinosteroids in the spotlight. *Current Biology,* 6**,** 658-661.

Collings, D. A., L. K. Gebbie, P. A. Howles, U. A. Hurley, R. J. Birch, A. H. Cork, C. H. Hocart, T. Arioli & R. E. Williamson (2008) Arabidopsis dynamin-like protein DRP1A: a null mutant with widespread defects in endocytosis, cellulose synthesis, cytokinesis, and cell expansion. *Journal of Experimental Botany,* 59**,** 361-376.

Corpas, F. J. & J. B. Barroso (2014) Peroxisomal plant nitric oxide synthase (NOS) protein is imported by peroxisomal targeting signal type 2 (PTS2) in a process that depends on the cytosolic receptor PEX7 and calmodulin. *FEBS Letters,* 588**,** 2049-2054.

Corpas, F. J. & J. B. Barroso (2017) Calmodulin antagonist affects peroxisomal functionality by disrupting both peroxisomal Ca2+ and protein import. *Journal of Cell Science***,** E1-E14.

Costa, A., L. Luoni, C. A. Marrano, K. Hashimoto, P. Köster, S. Giacometti, M. I. De Michelis, J. Kudla & M. C. Bonza (2017) Ca2+-dependent phosphoregulation of the plasma membrane Ca2+-ATPase ACA8 modulates stimulus-induced calcium signatures. *Journal of Experimental Botany,* 68**,** 3215-3230.

Craft, J., M. Samalova, C. Baroux, H. Townley, A. Martinez, I. Jepson, M. Tsiantis & I. Moore (2005) New pOp/LhG4 vectors for stringent glucocorticoid-dependent transgene expression in Arabidopsis. *The Plant Journal,* 41**,** 899-918.

Crooks, G. E., G. Hon, J.-M. Chandonia & S. E. Brenner (2004) WebLogo: A Sequence Logo Generator. *Genome Research,* 14**,** 1188-1190.

De Craene, J.-O., F. Courte, B. Rinaldi, C. Fitterer, M. C. Herranz, C. Schmitt-Keichinger, C. Ritzenthaler & S. Friant (2014) Study of the Plant COPII Vesicle Coat Subunits by Functional Complementation of Yeast Saccharomyces cerevisiae Mutants. *PLoS ONE,* 9**,** e90072.

Demarty, M., C. Morvan & M. Thellier (1984) Calcium and the cell wall. *Plant, Cell & Environment,* 7**,** 441-448.

Dettmer, J., A. Hong-Hermesdorf, Y.-D. Stierhof & K. Schumacher (2006) Vacuolar H+-ATPase Activity Is Required for Endocytic and Secretory Trafficking in Arabidopsis. *The Plant Cell,* 18**,** 715-730.

Dobney, S., D. Chiasson, P. Lam, S. P. Smith & W. A. Snedden (2009) The Calmodulin-related Calcium Sensor CML42 Plays a Role in Trichome Branching. *The Journal of Biological Chemistry,* 284**,** 31647-31657.

Dodd, A. N., J. Kudla & D. Sanders (2010) The language of calcium signaling. *Annual Review of Plant Biology,* 61**,** 593-620.

Dolze, E., F. Chigri, T. Howing, G. Hierl, E. Isono, U. C. Vothknecht & C. Gietl (2013) Calmodulin-like protein AtCML3 mediates dimerization of peroxisomal processing protease AtDEG15 and contributes to normal peroxisome metabolism. *Plant Molecular Biology,* 83**,** 607-624.

Drerup, M. M., K. Schlücking, K. Hashimoto, P. Manishankar, L. Steinhorst, K. Kuchitsu & J. Kudla (2013) The Calcineurin B-Like Calcium Sensors CBL1 and CBL9 Together with Their Interacting Protein Kinase CIPK26 Regulate the Arabidopsis NADPH Oxidase RBOHF. *Molecular Plant,* 6**,** 559-569.

Drucker, H. & S. L. Borchers (1971) The role of calcium in thermolysin: Effect on kinetic properties and autodigestion. *Archives of Biochemistry and Biophysics,* 147**,** 242-248.

Edel, K. H. & J. Kudla (2014) Increasing complexity and versatility: How the calcium signaling toolkit was shaped during plant land colonization. *Cell Calcium,* 57**,** 231-246.

Edel, K. H., E. Marchadier, C. Brownlee, J. Kudla & A. M. Hetherington (2017) The Evolution of Calcium-Based Signalling in Plants. *Current Biology,* 27**,** R667-R679.

Espreafico, E. M., R. E. Cheney, M. Matteoli, A. A. Nascimento, P. V. De Camilli, R. E. Larson & M. S. Mooseker (1992) Primary structure and cellular localization of chicken brain myosin-V (p190), an unconventional myosin with calmodulin light chains. *The Journal of Cell Biology,* 119**,** 1541-1557.

Flosdorff, S. 2014. Lokalisierung und Charakterisierung Calmodulin-ähnlicher Proteine aus Arabidopsis thaliana. In *LMU Biocentre Biology Dep. I*, 99. Ludwig-Maximilians-University.

Gao, X., K. Cox Jr. & P. He (2014) Functions of Calcium-Dependent Protein Kinases in Plant Innate Immunity. *Plants,* 3**,** 160.

Geldner, N., N. Anders, H. Wolters, J. Keicher, W. Kornberger, P. Muller, A. Delbarre, T. Ueda, A. Nakano & G. Jürgens (2003) The Arabidopsis GNOM ARF-GEF Mediates Endosomal Recycling, Auxin Transport, and Auxin-Dependent Plant Growth. *Cell,* 112**,** 219-230.

Gershlick, D. C., C. de Marcos Lousa, O. Foresti, A. J. Lee, E. A. Pereira, L. L. P. daSilva, F. Bottanelli & J. Denecke (2014) Golgi-Dependent Transport of Vacuolar Sorting Receptors Is Regulated by COPII, AP1, and AP4 Protein Complexes in Tobacco. *The Plant Cell,* 26**,** 1308-1329.

Guo, Y., U. Halfter, M. Ishitani & J.-K. Zhu (2001) Molecular Characterization of Functional Domains in the Protein Kinase SOS2 That Is Required for Plant Salt Tolerance. *The Plant Cell,* 13**,** 1383-1400.

Guo, Y., L. Xiong, C. P. Song, D. Gong, U. Halfter & J. K. Zhu (2002) A calcium sensor and its interacting protein kinase are global regulators of abscisic acid signaling in Arabidopsis.

Developmental Cell, 3**,** 233-244.

Haas, T. J., M. K. Sliwinski, D. E. Martínez, M. Preuss, K. Ebine, T. Ueda, E. Nielsen, G. Odorizzi & M. S. Otegui (2007) The Arabidopsis AAA ATPase SKD1 Is Involved in Multivesicular Endosome Function and Interacts with Its Positive Regulator LYST-INTERACTING PROTEIN5. *The Plant Cell,* 19**,** 1295-1312.

Hanahan, D. (1983) Studies on transformation of Escherichia coli with plasmids. *Journal of Molecular Biology,* 166**,** 557-580.

Hanna, M. G., I. Mela, L. Wang, R. M. Henderson, E. R. Chapman, J. M. Edwardson & A. Audhya (2016) Sar1 GTPase Activity Is Regulated by Membrane Curvature. *The Journal of Biological Chemistry,* 291**,** 1014-1027.

Hanton, S. L., L. Renna, L. E. Bortolotti, L. Chatre, G. Stefano & F. Brandizzi (2005) Diacidic Motifs Influence the Export of Transmembrane Proteins from the Endoplasmic Reticulum in Plant Cells. *The Plant Cell,* 17**,** 3081-3093.

Hariri, H., N. Bhattacharya, K. Johnson, A. J. Noble & S. M. Stagg (2014) Insights into the Mechanisms of Membrane Curvature and Vesicle Scission by the Small GTPase Sar1 in the Early Secretory Pathway. *Journal of Molecular Biology,* 426**,** 3811-3826.

Harley, C. A., J. A. Holt, R. Turner & D. J. Tipper (1998) Transmembrane Protein Insertion Orientation in Yeast Depends on the Charge Difference across Transmembrane Segments, Their Total Hydrophobicity, and Its Distribution. *Journal of Biological Chemistry,* 273**,** 24963-24971.

Harris, J. M. (2015) Abscisic Acid: Hidden Architect of Root System Structure. *Plants,* 4**,** 548-572.

Harrison, S. J., E. K. Mott, K. Parsley, S. Aspinall, J. C. Gray & A. Cottage (2006) A rapid and robust method of identifying transformed Arabidopsis thaliana seedlings following floral dip transformation. *Plant Methods,* 2**,** 1-7.

Heijne, G. V. (1994) Membrane Proteins: From Sequence to Structure. *Annual Review of Biophysics and Biomolecular Structure,* 23**,** 167-192.

Held, K., F. Pascaud, C. Eckert, P. Gajdanowicz, K. Hashimoto, C. Corratgé-Faillie, J. N. Offenborn, B. Lacombe, I. Dreyer, J.-B. Thibaud & J. Kudla (2011) Calcium-dependent modulation and plasma membrane targeting of the AKT2 potassium channel by the CBL4/CIPK6 calcium sensor/protein kinase complex. *Cell Research,* 21**,** 1116-1130.

Henikoff, S. & J. G. Henikoff (1993) Performance evaluation of amino acid substitution matrices. *Proteins: Structure, Function, and Bioinformatics,* 17**,** 49-61.

High, S., N. Flint & B. Dobberstein (1991) Requirements for the membrane insertion of signal-anchor type proteins. *The Journal of Cell Biology,* 113**,** 25-34.

Hillmer, S., A. Movafeghi, D. G. Robinson & G. Hinz (2001) Vacuolar Storage Proteins Are Sorted in the *Cis*-Cisternae of the Pea Cotyledon Golgi Apparatus. *The Journal of Cell Biology,* 152**,** 41-50.

Hinz, G., S. Hillmer, M. Bäumer & I. Hohl (1999) Vacuolar Storage Proteins and the Putative Vacuolar Sorting Receptor BP-80 Exit the Golgi Apparatus of Developing Pea Cotyledons in Different Transport Vesicles. *The Plant Cell,* 11**,** 1509-1524.

Hirano, T., T. Matsuzawa, K. Takegawa & M. H. Sato (2011) Loss-of-Function and Gain-of-Function Mutations in FAB1AB Impair Endomembrane Homeostasis, Conferring

Pleiotropic Developmental Abnormalities in Arabidopsis. *Plant Physiology,* 155**,** 797-807.

Hirschi, K. D., R. G. Zhen, K. W. Cunningham, P. A. Rea & G. R. Fink (1996) CAX1, an H+/Ca2+ antiporter from Arabidopsis. *Proceedings of the National Academy of Sciences,* 93**,** 8782-8786.

Hofmann, K. & W. Stoffel (1993) TMBASE - A database of membrane spanning protein segments. *Biological Chemistry Hoppe-Seyler,* 374.

Hong, B., A. Ichida, Y. Wang, J. Scott Gens, B. G. Pickard & J. F. Harper (1999) Identification of a Calmodulin-Regulated Ca2+-ATPase in the Endoplasmic Reticulum. *Plant Physiology,* 119**,** 1165-1176.

Huang, X. & W. Miller (1991) A time-efficient, linear-space local similarity algorithm. *Advances in Applied Mathematics,* 12**,** 337-357.

Huijser, P. & M. Schmid (2011) The control of developmental phase transitions in plants. *Development,* 138**,** 4117-4129.

Ikura, M., G. M. Clore, A. M. Gronenborn, G. Zhu, C. B. Klee & A. Bax (1992) Solution Structure of a Calmodulin-Target Peptide Complex by Multidimensional NMR. *Science,* 256**,** 632-638.

Ishitani, M., J. Liu, U. Halfter, C.-S. Kim, W. Shi & J.-K. Zhu (2000) SOS3 Function in Plant Salt Tolerance Requires N-Myristoylation and Calcium Binding. *The Plant Cell,* 12**,** 1667-1677.

Jia, T., C. Gao, Y. Cui, J. Wang, Y. Ding, Y. Cai, T. Ueda, A. Nakano & L. Jiang (2013) ARA7(Q69L) expression in transgenic Arabidopsis cells induces the formation of enlarged multivesicular bodies. *Journal of Experimental Botany,* 64**,** 2817-2829.

Kamrul Huda, K. M., S. Yadav, M. S. Akhter Banu, D. K. Trivedi & N. Tuteja (2013) Genome-wide analysis of plant-type II Ca2+ATPases gene family from rice and Arabidopsis: Potential role in abiotic stresses. *Plant Physiology and Biochemistry,* 65**,** 32-47.

Kang, B.-H., J. S. Busse & S. Y. Bednarek (2003) Members of the Arabidopsis Dynamin-Like Gene Family, ADL1, Are Essential for Plant Cytokinesis and Polarized Cell Growth. *The Plant Cell,* 15**,** 899-913.

Kasianov, A. S., A. V. Klepikova, I. V. Kulakovskiy, E. S. Gerasimov, A. V. Fedotova, E. G. Besedina, A. S. Kondrashov, M. D. Logacheva & A. A. Penin (2017) High-quality genome assembly of Capsella bursa-pastoris reveals asymmetry of regulatory elements at early stages of polyploid genome evolution. *The Plant Journal,* 91**,** 278-291.

Katoh, K., K.-i. Kuma, H. Toh & T. Miyata (2005) MAFFT version 5: improvement in accuracy of multiple sequence alignment. *Nucleic Acids Research,* 33**,** 511-518.

Kim, B.-G., R. Waadt, Y. H. Cheong, G. K. Pandey, J. R. Dominguez-Solis, S. Schültke, S. C. Lee, J. Kudla & S. Luan (2007) The calcium sensor CBL10 mediates salt tolerance by regulating ion homeostasis in Arabidopsis. *The Plant Journal,* 52**,** 473-484.

Kirsch, T., N. Paris, J. M. Butler, L. Beevers & J. C. Rogers (1994) Purification and initial characterization of a potential plant vacuolar targeting receptor. *Proceedings of the National Academy of Sciences,* 91**,** 3403-3407.

Kitakura, S., S. Vanneste, S. Robert, C. Löfke, T. Teichmann, H. Tanaka & J. Friml (2011) Clathrin Mediates Endocytosis and Polar Distribution of PIN Auxin Transporters in

Arabidopsis. *The Plant Cell,* 23**,** 1920-1931.

Klepikova, A. V., A. S. Kasianov, E. S. Gerasimov, M. D. Logacheva & A. A. Penin (2016) A high resolution map of the Arabidopsis thaliana developmental transcriptome based on RNA-seq profiling. *The Plant Journal,* 88**,** 1058-1070.

Klepikova, A. V., M. D. Logacheva, S. E. Dmitriev & A. A. Penin (2015) RNA-seq analysis of an apical meristem time series reveals a critical point in Arabidopsis thaliana flower initiation. *BMC Genomics,* 16**,** 466.

Klevit, R. E., D. C. Dalgarno, B. A. Levine & R. J. P. Williams (1984) 1H-NMR studies of calmodulin. *European Journal of Biochemistry,* 139**,** 109-114.

Koncz, C., K. Nemeth, G. P. Redei & J. Schell (1992) T-DNA insertional mutagenesis in Arabidopsis. *Plant Molecular Biology,* 20**,** 963-976.

Ktistakis, N. T., H. A. Brown, M. G. Waters, P. C. Sternweis & M. G. Roth (1996) Evidence that phospholipase D mediates ADP ribosylation factor-dependent formation of Golgi coated vesicles. *The Journal of Cell Biology,* 134**,** 295-306.

Kudla, J., O. Batistic & K. Hashimoto (2010) Calcium signals: the lead currency of plant information processing. *The Plant Cell,* 22**,** 541-563.

Kumar, S., M. Mazumder, N. Gupta, S. Chattopadhyay & S. Gourinath (2016) Crystal structure of Arabidopsis thaliana calmodulin7 and insight into its mode of DNA binding. *FEBS Letters,* 590**,** 3029-3039.

Künzl, F., S. Früholz, F. Fäßler, B. Li & P. Pimpl (2016) Receptor-mediated sorting of soluble vacuolar proteins ends at the *trans*-Golgi network/early endosome. *Nature Plants,* 2**,** 1-10.

Kushwaha, R., A. Singh & S. Chattopadhyay (2008) Calmodulin7 Plays an Important Role as Transcriptional Regulator in Arabidopsis Seedling Development. *The Plant Cell,* 20**,** 1747-1759.

Kyhse-Andersen, J. (1984) Electroblotting of multiple gels: a simple apparatus without buffer tank for rapid transfer of proteins from polyacrylamide to nitrocellulose. *Journal of Biochemical and Biophysical Methods,* 10**,** 203-209.

Laemmli, U. K. (1970) Cleavage of Structural Proteins during the Assembly of the Head of Bacteriophage T4. *Nature,* 227**,** 680-685.

Langhans, M., M. J. Marcote, P. Pimpl, G. Virgili-López, D. G. Robinson & F. Aniento (2008) In vivo Trafficking and Localization of p24 Proteins in Plant Cells. *Traffic,* 9**,** 770-785.

Larson, E. R., E. Van Zelm, C. Roux, A. Marion-Poll & M. R. Blatt (2017) Clathrin Heavy Chain Subunits Coordinate Endo- and Exocytic Traffic and Affect Stomatal Movement. *Plant Physiology,* 175**,** 708-720.

Laval, V., F. Masclaux, A. Serin, M. Carrière, C. Roldan, M. Devic, R. F. Pont-Lezica & J. P. Galaud (2003) Seed germination is blocked in Arabidopsis putative vacuolar sorting receptor (atbp80) antisense transformants. *Journal of Experimental Botany,* 54**,** 213-221.

Lawe, D. C., N. Sitouah, S. Hayes, A. Chawla, J. V. Virbasius, R. Tuft, K. Fogarty, L. Lifshitz, D. Lambright & S. Corvera (2003) Essential role of Ca2+/Calmodulin in Early Endosome Antigen-1 Localization. *Molecular Biology of the Cell,* 14**,** 2935-2945.

Lee, Y., M. Jang, K. Song, H. Kang, M. H. Lee, D. W. Lee, J. Zouhar, E. Rojo, E. J. Sohn & I. Hwang (2013) Functional Identification of Sorting Receptors Involved in Trafficking of Soluble Lytic Vacuolar Proteins in Vegetative Cells of Arabidopsis. *Plant Physiology,* 161**,**

121-133.

Letourneur, F., E. C. Gaynor, S. Hennecke, C. Démollière, R. Duden, S. D. Emr, H. Riezman & P. Cosson (1994) Coatomer is essential for retrieval of dilysine-tagged proteins to the endoplasmic reticulum. *Cell,* 79**,** 1199-1207.

Li, X., S. Chanroj, Z. Wu, S. M. Romanowsky, J. F. Harper & H. Sze (2008) A Distinct Endosomal Ca(2+)/Mn(2+) Pump Affects Root Growth through the Secretory Process. *Plant Physiology,* 147**,** 1675-1689.

Liang, F., K. W. Cunningham, J. F. Harper & H. Sze (1997) ECA1 complements yeast mutants defective in Ca2+ pumps and encodes an endoplasmic reticulum-type Ca2+-ATPase in Arabidopsis thaliana. *Proceedings of the National Academy of Sciences,* 94**,** 8579-8584.

Liao, J., J. Deng, Z. Qin, J. Tang, M. Shu, C. Ding, J. Liu, C. Hu, M. Yuan, Y. Huang, R. Yang & Y. Zhou (2017) Genome-Wide Identification and Analyses of Calmodulins and Calmodulin-like Proteins in Lotus japonicas. *Frontiers in Plant Science,* 8**,** 482.

Ligaba-Osena, A., Z. Fei, J. Liu, Y. Xu, J. Shaff, S.-C. Lee, S. Luan, J. Kudla, L. Kochian & M. Piñeros (2017) Loss-of-function mutation of the calcium sensor CBL1 increases aluminum sensitivity in Arabidopsis. *New Phytologist,* 214**,** 830-841.

Liu, F., X. Chu, H. P. Lu & J. Wang (2017) Molecular mechanism of multispecific recognition of Calmodulin through conformational changes. *Proceedings of the National Academy of Sciences,* 114**,** E3927-E3934.

Liu, J. & J.-K. Zhu (1998) A Calcium Sensor Homolog Required for Plant Salt Tolerance. *Science,* 280**,** 1943-1945.

Luan, S. (2009) The CBL-CIPK network in plant calcium signaling. *Trends in Plant Science,* 14**,** 37-42.

Luo, X., Z. Chen, J. Gao & Z. Gong (2014) Abscisic acid inhibits root growth in Arabidopsis through ethylene biosynthesis. *The Plant Journal,* 79**,** 44-55.

Malkus, P., F. Jiang & R. Schekman (2002) Concentrative sorting of secretory cargo proteins into COPII-coated vesicles. *The Journal of Cell Biology,* 159**,** 915-921.

Mao, J., S. M. Manik, S. Shi, J. Chao, Y. Jin, Q. Wang & H. Liu (2016) Mechanisms and Physiological Roles of the CBL-CIPK Networking System in Arabidopsis thaliana. *Genes (Basel),* 7**,** 1-15.

Marchadier, E., M. E. Oates, H. Fang, P. C. J. Donoghue, A. M. Hetherington & J. Gough (2016) Evolution of the Calcium-Based Intracellular Signaling System. *Genome Biology and Evolution,* 8**,** 2118-2132.

Martí, M. C., M. A. Stancombe & A. A. R. Webb (2013) Cell- and Stimulus Type-Specific Intracellular Free Ca(2+) Signals in Arabidopsis. *Plant Physiology,* 163**,** 625-634.

Martinière, A., E. Bassil, E. Jublanc, C. Alcon, M. Reguera, H. Sentenac, E. Blumwald & N. Paris (2013) In Vivo Intracellular pH Measurements in Tobacco and Arabidopsis Reveal an Unexpected pH Gradient in the Endomembrane System. *The Plant Cell,* 25**,** 4028-4043.

Matschi, S., K. Hake, M. Herde, B. Hause & T. Romeis (2015) The Calcium-Dependent Protein Kinase CPK28 Regulates Development by Inducing Growth Phase-Specific, Spatially Restricted Alterations in Jasmonic Acid Levels Independent of Defense Responses in Arabidopsis. *The Plant Cell,* 27**,** 591-606.

Matschi, S., S. Werner, W. X. Schulze, J. Legen, H. H. Hilger & T. Romeis (2013) Function of calcium-dependent protein kinase CPK28 of Arabidopsis thaliana in plant stem elongation and vascular development. *The Plant Journal: For Cell and Molecular Biology,* 73**,** 883-896.

McAinsh, M. R. & A. M. Hetherington (1998) Encoding specificity in Ca2+ signalling systems. *Trends in Plant Science,* 3**,** 32-36.

McAinsh, M. R. & J. K. Pittman (2009) Shaping the calcium signature. *New Phytologist,* 181**,** 275-294.

McCormack, E. & J. Braam (2003) Calmodulins and related potential calcium sensors of Arabidopsis. *New Phytologist,* 159**,** 585-598.

McCormack, E., Y. C. Tsai & J. Braam (2005) Handling calcium signaling: Arabidopsis CaMs and CMLs. *Trends in Plant Science,* 10**,** 383-389.

Mehlmer, N., N. Parvin, C. H. Hurst, M. R. Knight, M. Teige & U. C. Vothknecht (2012) A toolset of aequorin expression vectors for in planta studies of subcellular calcium concentrations in Arabidopsis thaliana. *Journal of Experimental Botany,* 63**,** 1751-1761.

Miller, J. B., A. Pratap, A. Miyahara, L. Zhou, S. Bornemann, R. J. Morris & G. E. D. Oldroyd (2013) Calcium/Calmodulin-Dependent Protein Kinase Is Negatively and Positively Regulated by Calcium, Providing a Mechanism for Decoding Calcium Responses during Symbiosis Signaling. *The Plant Cell,* 25**,** 5053-5066.

Mills, I. G., S. Urbe & M. J. Clague (2001) Relationships between EEA1 binding partners and their role in endosome fusion. *Journal of Cell Science,* 114**,** 1959-1965.

Mills, R. F., M. L. Doherty, R. L. López-Marqués, T. Weimar, P. Dupree, M. G. Palmgren, J. K. Pittman & L. E. Williams (2008) ECA3, a Golgi-Localized P(2A)-Type ATPase, Plays a Crucial Role in Manganese Nutrition in Arabidopsis. *Plant Physiology,* 146**,** 116-128.

Miyagishima, S.-y., H. Kuwayama, H. Urushihara & H. Nakanishi (2008) Evolutionary linkage between eukaryotic cytokinesis and chloroplast division by dynamin proteins. *Proceedings of the National Academy of Sciences,* 105**,** 15202-15207.

Moyer, Bryan D., Bernard B. Allan & William E. Balch (2001) Rab1 Interaction with a GM130 Effector Complex Regulates COPII Vesicle *cis*-Golgi Tethering. *Traffic,* 2**,** 268-276.

Murashige, T. & F. Skoog (1962) A Revised Medium for Rapid Growth and Bio Assays with Tobacco Tissue Cultures. *Physiologia Plantarum,* 15**,** 473-497.

Nagae, M., A. Nozawa, N. Koizumi, H. Sano, H. Hashimoto, M. Sato & T. Shimizu (2003) The Crystal Structure of the Novel Calcium-binding Protein AtCBL2 from Arabidopsis thaliana. *Journal of Biological Chemistry,* 278**,** 42240-42246.

Naramoto, S., M. S. Otegui, N. Kutsuna, R. de Rycke, T. Dainobu, M. Karampelias, M. Fujimoto, E. Feraru, D. Miki, H. Fukuda, A. Nakano & J. Friml (2014) Insights into the localization and function of the membrane trafficking regulator GNOM ARF-GEF at the Golgi apparatus in Arabidopsis. *The Plant Cell,* 26**,** 3062-3076.

Nelson, B. K., X. Cai & A. Nebenführ (2007) A multicolored set of in vivo organelle markers for co-localization studies in Arabidopsis and other plants. *The Plant Journal,* 51**,** 1126-1136.

Nie, S., M. Zhang & L. Zhang (2017) Genome-wide identification and expression analysis of

calmodulin-like (CML) genes in Chinese cabbage (Brassica rapa L. ssp. pekinensis). *BMC Genomics,* 18**,** 1-12.

Niemes, S., M. Langhans, C. Viotti, D. Scheuring, M. San Wan Yan, L. Jiang, S. Hillmer, D. G. Robinson & P. Pimpl (2010) Retromer recycles vacuolar sorting receptors from the *trans*-Golgi network. *The Plant Journal,* 61**,** 107-121.

Nodzyński, T., M. I. Feraru, S. Hirsch, R. De Rycke, C. Niculaes, W. Boerjan, J. Van Leene, G. De Jaeger, S. Vanneste & J. Friml (2013) Retromer Subunits VPS35A and VPS29 Mediate Prevacuolar Compartment (PVC) Function in Arabidopsis. *Molecular Plant,* 6**,** 1849-1862.

Oliviusson, P., O. Heinzerling, S. Hillmer, G. Hinz, Y. C. Tse, L. Jiang & D. G. Robinson (2006) Plant Retromer, Localized to the Prevacuolar Compartment and Microvesicles in Arabidopsis, May Interact with Vacuolar Sorting Receptors. *The Plant Cell,* 18**,** 1239-1252.

Ordenes, V. R., I. Moreno, D. Maturana, L. Norambuena, A. J. Trewavas & A. Orellana (2012) In vivo analysis of the calcium signature in the plant Golgi apparatus reveals unique dynamics. *Cell Calcium,* 52**,** 397-404.

Ormancey, M., P. Thuleau, C. Mazars & V. Cotelle (2017) CDPKs and 14-3-3 Proteins: Emerging Duo in Signaling. *Trends in Plant Science,* 22**,** 263-272.

Pagant, S., A. Wu, S. Edwards, F. Diehl & Elizabeth A. Miller (2015) Sec24 Is a Coincidence Detector that Simultaneously Binds Two Signals to Drive ER Export. *Current Biology,* 25**,** 403-412.

Parvin, N., C. Carrie, I. Pabst, A. Lasser, D. Laha, M. V. Paul, P. Geigenberger, R. Heermann, K. Jung, U. C. Vothknecht & F. Chigri (2017) TOM9.2 Is a Calmodulin-Binding Protein Critical for TOM Complex Assembly but Not for Mitochondrial Protein Import in Arabidopsis thaliana. *Molecular Plant,* 10**,** 575-589.

Perochon, A., D. Aldon, J. P. Galaud & B. Ranty (2011) Calmodulin and calmodulin-like proteins in plant calcium signaling. *Biochimie,* 93**,** 2048-2053.

Peters, C. & A. Mayer (1998) Ca2+/calmodulin signals the completion of docking and triggers a late step of vacuole fusion. *Nature,* 396**,** 575-580.

Pimpl, P., A. Movafeghi, S. Coughlan, J. Denecke, S. Hillmer & D. G. Robinson (2000) In Situ Localization and in Vitro Induction of Plant COPI-Coated Vesicles. *The Plant Cell,* 12**,** 2219-2235.

Plattner, H. (2017) Evolutionary Cell Biology of Proteins from Protists to Humans and Plants. *Journal of Eukaryotic Microbiology***,** 1-60.

Plattner, H. & A. Verkhratsky (2015) The ancient roots of calcium signalling evolutionary tree. *Cell Calcium,* 57**,** 123-132.

Poethig, R. S. (1990) Phase Change and the Regulation of Shoot Morphogenesis in Plants. *Science,* 250**,** 923-930.

Pope, B. & H. M. Kent (1996) High efficiency 5 min transformation of Escherichia coli. *Nucleic Acids Research,* 24**,** 536-537.

Qin, C., M. Li, W. Qin, S. C. Bahn, C. Wang & X. Wang (2006) Expression and characterization of Arabidopsis phospholipase Dγ2. *Biochimica et Biophysica Acta (BBA) - Molecular and Cell Biology of Lipids,* 1761**,** 1450-1458.

Qiu, Q.-S., Y. Guo, M. A. Dietrich, K. S. Schumaker & J.-K. Zhu (2002) Regulation of SOS1, a plasma membrane Na+/H+ exchanger in Arabidopsis thaliana, by SOS2 and SOS3. *Proceedings of the National Academy of Sciences,* 99**,** 8436-8441.

Rhoads, A. R. & F. Friedberg (1997) Sequence motifs for calmodulin recognition. *The FASEB Journal,* 11**,** 331-340.

Robinson, D. G., D. Scheuring, S. Naramoto & J. Friml (2011) ARF1 Localizes to the Golgi and the *Trans*-Golgi Network. *The Plant Cell,* 23**,** 846-849.

Ruge, H., S. Flosdorff, I. Ebersberger, F. Chigri & U. C. Vothknecht (2016) The calmodulin-like proteins AtCML4 and AtCML5 are single-pass membrane proteins targeted to the endomembrane system by an N-terminal signal anchor sequence. *Journal of Experimental Botany,* 67**,** 3985-3996.

Sack, L. & C. Scoffoni (2013) Leaf venation: structure, function, development, evolution, ecology and applications in the past, present and future. *New Phytologist,* 198**,** 983-1000.

Saint-Jore-Dupas, C., A. Nebenfuhr, A. Boulaflous, M. L. Follet-Gueye, C. Plasson, C. Hawes, A. Driouich, L. Faye & V. Gomord (2006) Plant N-glycan processing enzymes employ different targeting mechanisms for their spatial arrangement along the secretory pathway. *The Plant Cell,* 18**,** 3182-3200.

Sambrook, J. & D. W. Russell (2006) A Laboratory Manual. *Cold Spring Harbor Protocols,* 2006.

Sanchez-Barrena, M. J., M. Martinez-Ripoll, J. K. Zhu & A. Albert (2005) The structure of the Arabidopsis thaliana SOS3: molecular mechanism of sensing calcium for salt stress response. *Journal of Molecular Biology,* 345**,** 1253-1264.

Sanders, D., J. Pelloux, C. Brownlee & J. F. Harper (2002) Calcium at the Crossroads of Signaling. *The Plant Cell,* 14**,** S401-S417.

Sanyal, S. K., P. Kanwar, A. K. Yadav, C. Sharma, A. Kumar & G. K. Pandey (2017) Arabidopsis CBL interacting protein kinase 3 interacts with ABR1, an APETALA2 domain transcription factor, to regulate ABA responses. *Plant Science,* 254**,** 48-59.

Sawa, S., K. Koizumi, S. Naramoto, T. Demura, T. Ueda, A. Nakano & H. Fukuda (2005) DRP1A Is Responsible for Vascular Continuity Synergistically Working with VAN3 in Arabidopsis. *Plant Physiology,* 138**,** 819-826.

Scheuring, D., C. Viotti, F. Krüger, F. Künzl, S. Sturm, J. Bubeck, S. Hillmer, L. Frigerio, D. G. Robinson, P. Pimpl & K. Schumacher (2011) Multivesicular Bodies Mature from the *Trans*-Golgi Network/Early Endosome in Arabidopsis. *The Plant Cell,* 23**,** 3463-3481.

Schiøtt, M., S. M. Romanowsky, L. Bækgaard, M. K. Jakobsen, M. G. Palmgren & J. F. Harper (2004) A plant plasma membrane Ca2+ pump is required for normal pollen tube growth and fertilization. *Proceedings of the National Academy of Sciences of the United States of America,* 101**,** 9502-9507.

Schneider, T. D. & R. M. Stephens (1990) Sequence logos: a new way to display consensus sequences. *Nucleic Acids Research,* 18**,** 6097-6100.

Schranz, M. E. & T. Mitchell-Olds (2006) Independent Ancient Polyploidy Events in the Sister Families Brassicaceae and Cleomaceae. *The Plant Cell,* 18**,** 1152-1165.

Shen, J., Y. Zeng, X. Zhuang, L. Sun, X. Yao, P. Pimpl & L. Jiang (2013) Organelle pH in the Arabidopsis Endomembrane System. *Molecular Plant,* 6**,** 1419-1437.

Shi, J., K.-N. Kim, O. Ritz, V. Albrecht, R. Gupta, K. Harter, S. Luan & J. Kudla (1999) Novel Protein Kinases Associated with Calcineurin B–like Calcium Sensors in Arabidopsis. *The Plant Cell,* 11**,** 2393-2405.

Shimomura, O., F. H. Johnson & Y. Saiga (1962) Extraction, Purification and Properties of Aequorin, a Bioluminescent Protein from the Luminous Hydromedusan, Aequorea. *Journal of Cellular and Comparative Physiology,* 59**,** 223-239.

Simeunovic, A., A. Mair, B. Wurzinger & M. Teige (2016) Know where your clients are: subcellular localization and targets of calcium-dependent protein kinases. *Journal of Experimental Botany,* 67**,** 3855-3872.

Sitte, P., W. E. W., J. W. Kadereit, A. Bresinsky & C. Körner. 2002. *Strasburger - Lehrbuch der Botanik*. Berlin: Spektrum Akademischer Verlag GmbH Heidelberg.

Sparkes, I. A., T. Ketelaar, N. C. A. De Ruijter & C. Hawes (2009) Grab a Golgi: Laser Trapping of Golgi Bodies Reveals in vivo Interactions with the Endoplasmic Reticulum. *Traffic,* 10**,** 567-571.

Stael, S., R. G. Bayer, N. Mehlmer & M. Teige (2011) Protein N-acylation overrides differing targeting signals. *FEBS Letters,* 585**,** 517-522.

Stael, S., B. Wurzinger, A. Mair, N. Mehlmer, U. C. Vothknecht & M. Teige (2012) Plant organellar calcium signalling: an emerging field. *Journal of Experimental Botany,* 63**,** 1525-1542.

Stamatakis, A., P. Hoover, J. Rougemont & S. Renner (2008) A Rapid Bootstrap Algorithm for the RAxML Web Servers. *Systematic Biology,* 57**,** 758-771.

Steinhorst, L., A. Mahs, T. Ischebeck, C. Zhang, X. Zhang, S. Arendt, S. Schultke, I. Heilmann & J. Kudla (2015) Vacuolar CBL-CIPK12 Ca(2+)-sensor-kinase complexes are required for polarized pollen tube growth. *Current Biology,* 25**,** 1475-1482.

Susi, P., M. Hohkuri, T. Wahlroos & N. J. Kilby (2004) Characteristics of RNA Silencing in Plants: Similarities and Differences Across Kingdoms. *Plant Molecular Biology,* 54**,** 157-174.

Swan, D. G., R. S. Hale, N. Dhillon & P. F. Leadlay (1987) A bacterial calcium-binding protein homologous to calmodulin. *Nature,* 329**,** 84-85.

Tang, R.-J., H. Liu, Y. Yang, L. Yang, X.-S. Gao, V. J. Garcia, S. Luan & H.-X. Zhang (2012) Tonoplast calcium sensors CBL2 and CBL3 control plant growth and ion homeostasis through regulating V-ATPase activity in Arabidopsis. *Cell Research,* 22**,** 1650-1665.

Tang, R.-J., F.-G. Zhao, V. J. Garcia, T. J. Kleist, L. Yang, H.-X. Zhang & S. Luan (2015) Tonoplast CBL–CIPK calcium signaling network regulates magnesium homeostasis in Arabidopsis. *Proceedings of the National Academy of Sciences,* 112**,** 3134-3139.

Teh, O.-K., Y. Shimono, M. Shirakawa, Y. Fukao, K. Tamura, T. Shimada & I. Hara-Nishimura (2013) The AP-1 μ Adaptin is Required for KNOLLE Localization at the Cell Plate to Mediate Cytokinesis in Arabidopsis. *Plant and Cell Physiology,* 54**,** 838-847.

The Angiosperm Phylogeny, G. (2016) An update of the Angiosperm Phylogeny Group classification for the orders and families of flowering plants: APG IV. *Botanical Journal of the Linnean Society,* 181**,** 1-20.

Townley, A. K., Y. Feng, K. Schmidt, D. A. Carter, R. Porter, P. Verkade & D. J. Stephens (2008) Efficient coupling of Sec23-Sec24 to Sec13-Sec31 drives COPII-dependent

collagen secretion and is essential for normal craniofacial development. *Journal of Cell Science,* 121**,** 3025-3034.

Tsai, H.-H. G., W.-F. Juang, C.-M. Chang, T.-Y. Hou & J.-B. Lee (2013a) Molecular mechanism of Ca2+ -catalyzed fusion of phospholipid micelles. *Biochimica et Biophysica Acta (BBA) - Biomembranes,* 1828**,** 2729-2738.

Tsai, Y.-C., Y. Koo, N. A. Delk, B. Gehl & J. Braam (2013b) Calmodulin-related CML24 interacts with ATG4b and affects autophagy progression in Arabidopsis. *The Plant Journal,* 73**,** 325-335.

Ueda, T., T. Uemura, M. H. Sato & A. Nakano (2004) Functional differentiation of endosomes in Arabidopsis cells. *The Plant Journal,* 40**,** 783-789.

Vadassery, J., M. Reichelt, B. Hause, J. Gershenzon, W. Boland & A. Mithöfer (2012) CML42-Mediated Calcium Signaling Coordinates Responses to Spodoptera Herbivory and Abiotic Stresses in Arabidopsis. *Plant Physiology,* 159**,** 1159-1175.

Vahala, T., P. Stabel & T. Eriksson (1989) Genetic transformation of willows (Salix spp.) byAgrobacterium tumefaciens. *Plant Cell Reports,* 8**,** 55-58.

Vanderbeld, B. & W. A. Snedden (2007) Developmental and stimulus-induced expression patterns of Arabidopsis calmodulin-like genes CML37, CML38 and CML39. *Plant Molecular Biology,* 64**,** 683-697.

Vaughan-Hirsch, J., B. Goodall & A. Bishopp (2017) North, East, South, West: mapping vascular tissues onto the Arabidopsis root. *Current Opinion in Plant Biology,* 41**,** 16-22.

Verret, F., G. Wheeler, A. R. Taylor, G. Farnham & C. Brownlee (2010) Calcium channels in photosynthetic eukaryotes: implications for evolution of calcium-based signalling. *New Phytologist,* 187**,** 23-43.

Viotti, C., F. Krüger, M. Krebs, C. Neubert, F. Fink, U. Lupanga, D. Scheuring, Y. Boutté, M. Frescatada-Rosa, S. Wolfenstetter, N. Sauer, S. Hillmer, M. Grebe & K. Schumacher (2013) The Endoplasmic Reticulum Is the Main Membrane Source for Biogenesis of the Lytic Vacuole in Arabidopsis. *The Plant Cell,* 25**,** 3434-3449.

Visser, R. G. F., E. Jacobsen, B. Witholt & W. J. Feenstra (1989) Efficient transformation of potato (Solanum tuberosum L.) using a binary vector in Agrobacterium rhizogenes. *Theoretical and Applied Genetics,* 78**,** 594-600.

von Blume, J., A.-M. Alleaume, C. Kienzle, A. Carreras-Sureda, M. Valverde & V. Malhotra (2012) Cab45 is required for Ca2+-dependent secretory cargo sorting at the *trans*-Golgi network. *The Journal of Cell Biology,* 199**,** 1057-1066.

Wang, S.-S., W.-Z. Diao, X. Yang, Z. Qiao, M. Wang, B. R. Acharya & W. Zhang (2015) Arabidopsis thaliana CML25 mediates the Ca2+ regulation of K+ transmembrane trafficking during pollen germination and tube elongation. *Plant, Cell & Environment,* 38**,** 2372-2386.

Watanabe, E., T. Shimada, M. Kuroyanagi, M. Nishimura & I. Hara-Nishimura (2002) Calcium-mediated Association of a Putative Vacuolar Sorting Receptor PV72 with a Propeptide of 2S Albumin. *Journal of Biological Chemistry,* 277**,** 8708-8715.

Wen, L., M. Fukuda, M. Sunada, S. Ishino, Y. Ishino, T. W. Okita, M. Ogawa, T. Ueda & T. Kumamaru (2015) Guanine nucleotide exchange factor 2 for Rab5 proteins coordinated with GLUP6/GEF regulates the intracellular transport of the proglutelin from the Golgi apparatus to the protein storage vacuole in rice endosperm. *Journal of Experimental*

Botany, 66**,** 6137-6147.

Wielopolska, A., H. Townley, I. Moore, P. Waterhouse & C. Helliwell (2005) A high-throughput inducible RNAi vector for plants. *Plant Biotechnology Journal,* 3**,** 583-590.

Wikström, N., V. Savolainen & M. W. Chase (2001) Evolution of the angiosperms: calibrating the family tree. *Proceedings of the Royal Society of London. Series B: Biological Sciences,* 268**,** 2211-2220.

Yang, X., S.-S. Wang, M. Wang, Z. Qiao, C.-C. Bao & W. Zhang (2014) Arabidopsis thaliana calmodulin-like protein CML24 regulates pollen tube growth by modulating the actin cytoskeleton and controlling the cytosolic Ca2+ concentration. *Plant Molecular Biology,* 86**,** 225-236.

Yuan, F., H. Yang, Y. Xue, D. Kong, R. Ye, C. Li, J. Zhang, L. Theprungsirikul, T. Shrift, B. Krichilsky, D. M. Johnson, G. B. Swift, Y. He, J. N. Siedow & Z.-M. Pei (2014) OSCA1 mediates osmotic-stress-evoked Ca2+ increases vital for osmosensing in Arabidopsis. *Nature,* 514**,** 367-371.

Zhang, F., L. Li, Z. Jiao, Y. Chen, H. Liu, X. Chen, J. Fu, G. Wang & J. Zheng (2016) Characterization of the calcineurin B-Like (CBL) gene family in maize and functional analysis of ZmCBL9 under abscisic acid and abiotic stress treatments. *Plant Science,* 253**,** 118-129.

Zhang, M., T. Tanaka & M. Ikura (1995) Calcium-induced conformational transition revealed by the solution structure of apo calmodulin. *Nature Structural Biology,* 2**,** 758-767.

Zhang, X., R. Henriques, S.-S. Lin, Q.-W. Niu & N.-H. Chua (2006) Agrobacterium-mediated transformation of Arabidopsis thaliana using the floral dip method. *Nature Protocols,* 1**,** 641-646.

Zhao, B., H. Shi, W. Wang, X. Liu, H. Gao, X. Wang, Y. Zhang, M. Yang, R. Li & Y. Guo (2016) Secretory COPII Protein SEC31B Is Required for Pollen Wall Development. *Plant Physiology,* 172**,** 1625-1642.

Zhou, L., Y. Fu & Z. Yang (2009) A Genome-wide Functional Characterization of Arabidopsis Regulatory Calcium Sensors in Pollen Tubes. *Journal of Integrative Plant Biology,* 51**,** 751-761.

Zhu, X., C. Dunand, W. Snedden & J. P. Galaud (2015) CaM and CML emergence in the green lineage. *Trends in Plant Science,* 20**,** 483-489.

Summary

In this work, the two Ca^{2+} sensors AtCML4 and AtCML5 from *A. thaliana* were analysed regarding their topology, sub-cellular localisation, potential cellular function and phylogenetic origin. The proteins were found to be co-localised and quantitative assessment of co-localisation experiments revealed further that AtCML5 co-localises with GmMAN1, a Golgi stack marker and AtARA6, a marker for the late PVC, to almost similar extent. However, the circular geometry of the structures observed for AtCML4 and AtCML5 under overexpression conditions, as well as under control of their native promoter, led to the conclusion that these proteins predominantly reside in Golgi cisternae membranes. Sequence analyses showed that AtCML4 and AtCML5 harbour an N-terminal signal-anchor sequence typical of type-III single-pass transmembrane proteins. Protease protection assays on isolated membrane fractions confirmed that the N-terminal domain of AtCML5 anchors the protein in the membrane with its CAM-domain protruding into the cytoplasm. Transgenic *A. thaliana* plant lines stably expressing a Ca^{2+} sensor fusion construct with the signal-anchor sequence of AtCML5 (*pAtCML5*::AtCML5$_{1-28}$-YFP-AEQ) revealed that the protein is targeted to a microdomain with a basal $[Ca^{2+}]_f$ 4-5 times higher compared to the remaining cytoplasm. Together with the identification of AtPLDγ1 and AtDRP1B as potential interaction partners, it can be hypothesised that AtCML5 senses Ca^{2+} efflux from the Golgi lumen, and promotes vesicle budding processes via its interaction partners, thereby coupling the Golgi-internal cargo sorting processes to the formation of vesicles for further trafficking to the vacuole or the plasma membrane. Phylogenetic analysis of AtCML4 and AtCML5 with a special focus on their N-terminal signal-anchor sequence unravelled that the proteins probably originated from an AtCML3-like protein with a similar signal-anchor, which was found to be conserved among a huge variety of dicot species and some monocots. This indicated an angiosperm-specific, predominantly dicot-typical function of these proteins. I*n vivo* expression patterns analysed in a LUCIFERASE-based promoter activity assay revealed *AtCML4* and *AtCML5* to be expressed in roots, hypocotyls, stem, petioles and leaf vascular tissue. Expression in secondary leaves and petals could also be detected and the *AtCML5* promoter was further active in hydathodes. A potential function of AtCML4 and AtCML5 could be connected to the formation of the vascular tissue network architecture, whose complexity has been found to be unprecedentedly high in angiosperms and specifically in dicots.

Zusammenfassung

In dieser Arbeit wurden die zwei Calciumsensoren AtCML4 und AtCML5 aus *A. thaliana* bezüglich ihrer Topologie, sub-zellulären Lokalisierung, potentiellen zellulären Funktion und ihres phylogenetischen Ursprungs untersucht. Es wurde festgestellt, dass beide Proteine identisch lokalisiert sind und quantitative Analysen zeigten weiterhin, dass AtCML5 zu nahezu gleichen Teilen mit dem Golgi-Zisternen Marker GmMAN1 und AtARA6 - einem Marker für das späte prävakuoläre Kompartiment - kolokalisiert. Allerdings markierte AtCML5-YFP unabhängig von seinem Expressionslevel große zirkuläre Strukturen, was deutlich auf eine Lokalisation im Golgi-Apparat hinwies. Sequenzanalysen zeigten, dass AtCML4 und AtCML5 über eine N-terminale Signal-Anker Sequenz verfügen, welche die Proteine als Typ-III *Singlepass*-Transmembranproteine kennzeichnet. Proteasebehandlungen isolierter Membranfraktionen bestätigten, dass die N-terminale Domäne von AtCML5 das Protein in der Membran verankert, sodass seine CAM-Domäne ins Zytoplasma weist. In transgenen *A. thaliana* Linien, die stabil ein Fusionskonstrukt aus diesem N-terminus und einem Calciumreporter (*pAtCML5*::AtCML5$_{1-28}$-YFP-AEQ) exprimierten, war die basale $[Ca^{2+}]_f$ 4-5 mal höher als im Gesamtzytoplasma in Kontrollpflanzen. Da zugleich AtPLDγ1 und AtDRP1B als potentielle AtCML5 Interaktionspartner identifiziert wurden, wäre es möglich, dass AtCML5 von Ca^{2+} Strömen aus dem Golgi aktiviert wird und mittels seiner Interaktionspartner Vesikelabschnürung an Proteinsortierungsprozesse koppelt. Phylogenetische Analysen deuten darauf hin, dass AtCML4 und AtCML5 von einem AtCML3-ähnlichen Protein mit einem homologen Signal-Anker abstammen. Dieser Vorgänger ist in diversen Dikotyledonenspezies und einigen Monokotyledonenarten konserviert, was auf eine Angiosperm-spezifische Funktion hindeutet, die möglicherweise primär in dikotyledonen Pflanzen relevant ist. In LUCIFERASE-basierten Promoteraktivitätsstudien wurde festgestellt, dass *AtCML4* und *AtCML5* stark in Wurzeln, Spross, Hypokotyl und Blattgefäßen exprimiert sind. Auch in Kelchblättern und Sekundärblättern waren die Promotoren der beiden Gene aktiv. Überdies wird *AtCML5* in Hydathoden exprimiert. Eine potentielle Funktion von AtCML4 und AtCML5 könnte im Zusammenhang mit der Ausbildung des Blattgefäßnetzwerks stehen. Dies würde dazu passen, dass die Komplexität dieses Netzwerks in Angiospermen und besonders in Dikotyledonen deutlich ausgeprägter ist als in anderen Tracheophyten.

Acknowledgements

I am profoundly grateful to Prof Dr Ute C. Vothknecht for offering me the opportunity to working on this project. During the time in her laboratory, I learned a lot from her example, especially – but not only – with regard to scientific thinking, and grew significantly as a scientist and a person. Her way of providing constructive criticism and constant support, together with being a highly skilled, always objective and responsible group leader will always serve as reference for excellent leadership to me.

I am also very grateful to Dr Fatima Chigri and Dr Norbert Mehlmer, who always let me share in their extensive scientific experience and knowledge to help me find alternative solutions to persistent problems without becoming tired of answering all my questions.

I would also like to cordially thank Julia Faltermeier and Edoardo Cutolo, who were one of the reasons for my good times in the lab, even in case of depression over failed experiments or confusing results. Julia was exceptionally proficient in establishing order in a laboratory with two chaotic young men and her cheerful character made the bad days bearable and the good days great. I also truly miss the long evenings spent with Edoardo, discussing our recent scientific problems or pondering about life in general, whilst switching from the lab with pipette and samples to the kitchen with beer and “Brezn”, and back again.

To all my friends I am incredibly grateful for their patience and their understanding attitude, when I was complaining about experiments not working or plants not growing, which often made me come late to our gatherings. They always brought me back on track, when I felt like all my efforts were leading to no fruitful end and even helped me out with valuable advice on scientific matters. On top of that, they always managed to make me feel at home – priceless.

Finally, I would like to express my deepest gratitude to my family and foremost to my parents, who spent so much of their time helping me get to where I am now and always made it seem as if it was no effort at all. Their constant support and interest in my work are as invaluable to me as their opinion and advice. Such a family is not to just be taken for granted.

Appendices

Appendix I. Species list for sequence alignment in Figure 1

Abbreviation in MSA	Species
AraLy	*Arabidopsis lyrata* subsp. *lyrata*
AraTh	*Arabidopsis thaliana*
CapRu	*Capsella rubella*
EutSa	*Eutrema salsugineum*
BraNa	*Brassica napa*
BraRa	*Brassica rapa* subsp. *pekinensis*
BraOl	*Brassica oleracea* var. *oleracea*
RapSa	*Raphanus sativus*

Appendix II. MASCOT analysis of peptides identified in mass spectrometric analysis

Phospholipase D gamma 1 (PLDGAMMA1), OS=Arabidopsis thaliana

Peptide	Protein identification probability	Mascot ion score	Actual peptide mass (AMU)	Peptide start index	Peptide stop index
TVIVDAEAAQNR	99,7%	67,0	1.285,66	372	383
EVPVGTVSVYNSPR	100,0%	40,0	1.502,77	669	682
KKVEGEK	100,0%	34,9	816,47	74	80
KPPQPNANANAAQVQALK	100,0%	34,9	1.859,00	683	700
LGGMLSGLGR	100,0%	21,1	975,52	64	73
SSSDDSLLR	100,0%	38,5	978,46	473	481

PLDG1_ARATH (100%), 95.589,0 Da
Phospholipase D gamma 1 OS=Arabidopsis thaliana GN=PLDGAMMA1 PE=1 SV=1
6 exclusive unique peptides, 6 exclusive unique spectra, 6 total spectra, 70/858 amino acids (8% coverage)

```
M A Y H P A Y T E T   M S M G G G S S H G   G G Q Q Y V P F A T   S S G S L R V E L L   H G N L D I W V K E
A K H L P N M D G F   H N R L G G M L S G   L G R K K V E G E K   S S K I T S D P Y V   T V S I S G A V I G
R T F V I S N S E N   P V W M Q H F D V P   V A H S A A E V H F   V V K D S D I I G S   Q I M G A V G I P T
E Q L C S G N R I E   G L F P I L N S S G   K P C K Q G A V L G   L S I Q Y T P M E R   M R L Y Q M G V G S
G N E C V G V P G T   Y F P L R K G G R V   T L Y Q D A H V D D   G T L P S V H L D G   G I Q Y R H G K C W
E D M A D A I R Q A   R R L I Y I T G W S   V F H P V R L V R R   T N D P T E G T L G   E L L K V K S Q E G
V R V L V L V W D D   P T S R S L L G F K   T Q G V M N T S D E   E T R R F F K H S S   V Q V L L C P R S G
G K G H S F I K K S   E V G T I Y T H H Q   K T V I V D A E A A   Q N R R K I V A F V   G G L D L C N G R F
D T P K H P L F R T   L K T L H K D D F H   N P N F V T T A D D   G P R E P W H D L H   S K I D G P A A Y D
V L A N F E E R W M   K A S K P R G I G K   L K S S S D D S L L   R I D R I P D I V G   L S E A S S A N D N
D P E S W H V Q V F   R S I D S S S V K G   F P K D P K E A T G   R N L L C G K N I L   I D M S I H A A Y V
K A I R S A Q H F I   Y I E N Q Y F L G S   S F N W D S N K D L   G A N N L I P M E I   A L K I A N K I R A
R E K F A A Y I V I   P M W P E G A P T S   N P I Q R I L Y W Q   H K T M Q M M Y Q T   I Y K A L V E V G L
D S Q F E P Q D F L   N F F C L G T R E V   P V G T V S V Y N S   P R K P P Q P N A N   A N A A Q V Q A L K
S R R F M I Y V H S   K G M V V D D E F V   L I G S A N I N Q R   S L E G T R D T E I   A M G G Y Q P H Y S
W A M K G S R P H G   Q I F G Y R M S L W   A E H L G F L E Q G   F E E P E N M E C V   R R V R Q L S E L N
W R Q Y A A E E V T   E M S G H L L K Y P   V Q V D R T G K V S   S L P G C E T F P D   L G G K I I G S F L
A L Q E N L T I
```

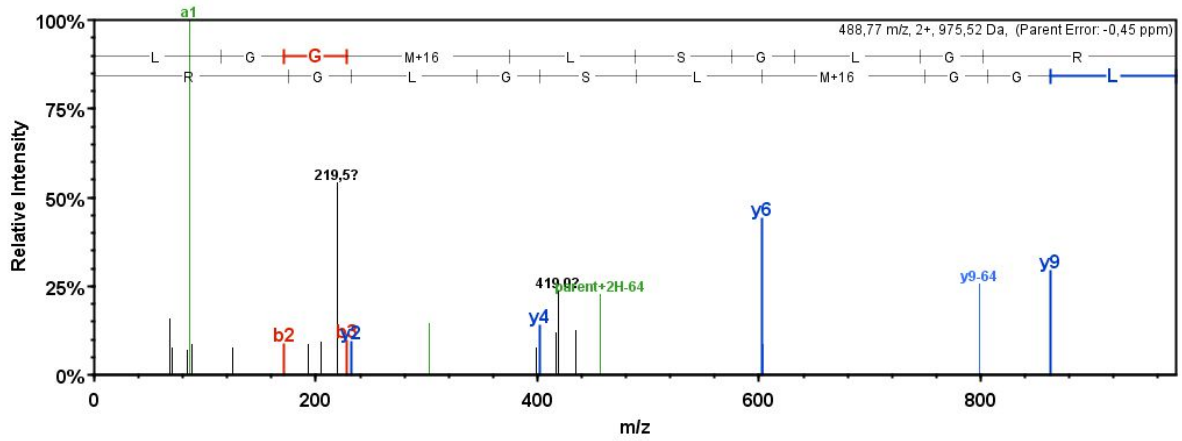

Dynamin-related protein 1B (DRP1B), OS=Arabidopsis thaliana

Peptide	Protein identification probability	Mascot ion score	Actual peptide mass (AMU)	Peptide start index	Peptide stop index
IPGLQSLITK	99,5%	0,220	1.068,66	372	383
LYMIMEICR	99,7%	1,61	1.227,57	669	682

DRP1B_ARATH (100%), 68.086,1 Da
Dynamin-related protein 1B OS=Arabidopsis thaliana GN=DRP1B PE=2 SV=1
2 exclusive unique peptides, 2 exclusive unique spectra, 2 total spectra, 19/610 amino acids (3% coverage)

```
M E S L I A L V N K   I Q R A C T A L G D   H G E G S S L P T L   W D S L P A I A V V   G G Q S S G K S S V
L E S V V G K D F L   P R G A G I V T R R   P L V L Q L H R I D   E G K E Y A E F M H   L P K K K F T D F A
A V R Q E I S D E T   D R E T G R S S K V   I S T V P I H L S I   F S P N V V N L T L   V D L P G L T K V A
V D G Q P E S I V Q   D I E N M V R S F I   E K P N C I I L A I   S P A N Q D L A T S   D A I K I S R E V D
P K G D R T F G V L   T K I D L M D Q G T   N A V D I L E G R G   Y K L R Y P W V G V   V N R S Q A D I N K
S V D M I A A R R R   E R D Y F Q T S P E   Y R H L T E R M G S   E Y L G K M L S K H   L E V V I K S R I P
G L Q S L I T K T I   S E L E T E L S R L   G K P V A A D A G G   K L Y M I M E I C R   A F D Q T F K E H L
D G T R S G G E K I   N S V F D N Q F P A   A I K R L Q F D K H   L S M D N V R K L I   T E A D G Y Q P H L
I A P E Q G Y R R L   I E S C L V S I R G   P A E A A V D A V H   S I L K D L I H K S   M G E T S E L K Q Y
P T L R V E V S G A   A V D S L D R M R D   E S R K A T L L L V   D M E S G Y L T V E   F F R K L P Q D S E
K G G N P T H S I F   D R Y N D A Y L R R   I G S N V L S Y V N   M V C A G L R N S I   P K S I V Y C Q V R
E A K R S L L D I F   F T E L G Q K E M S   K L S K L L D E D P   A V Q Q R R T S I A   K R L E L Y R S A Q
T D I E A V A W S K
```

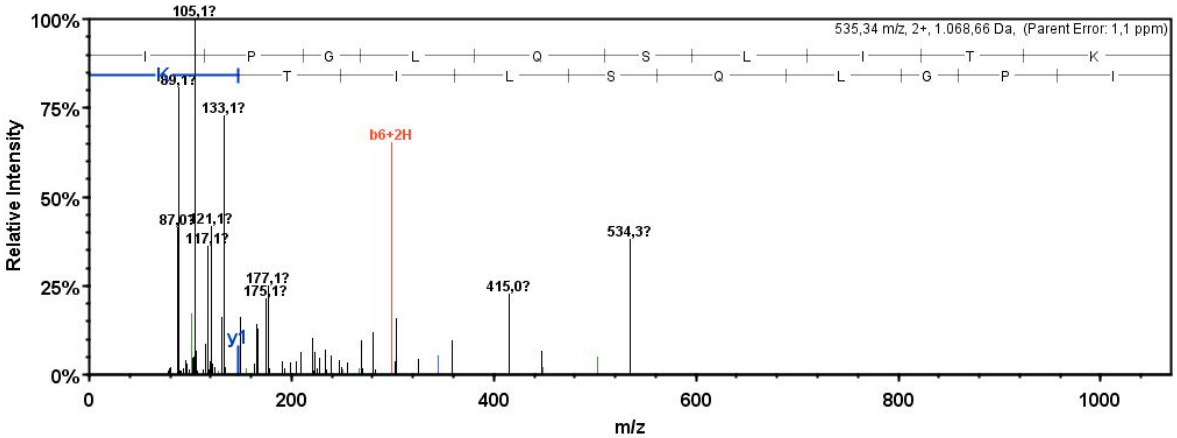

Appendix III. Protein sequences subjected to phylogenetic analysis

Label in MSA and phylogenetic tree	Sequence	Species	Family	Order	Names of combined sequences in tree
RapSaC3L2	>XP_018490833.1 PREDICTED: calmodulin-like protein 3 [Raphanus sativus] MATNLLKLSSQIRRLSPITRSLTIRT SATSTTSSGSKKMDQAELSRIFQMFD RNGDGKITKQELSDSLENLGIYIPDK DLVQMIEKIDLNGDGYVDIEEFGGLY QSIMEDRDEEEDIREAFNVFDQNRDG FITVEELRSVLSSLGLKQGRTLEDCK RMISKVDVDGDGMVNFKEFKQMMKGG GFAALESSL	Raphanus sativus	Brassicaceae	Brassicales	
EucGrC3L2	>XP_010069294.1 PREDICTED: calmodulin-like protein 3 [Eucalyptus grandis] MPAIITRIFLLYHLLHTWFHYLVPKK LRVYLPPSWSPLRLDPTPPPLPRSLS LVKAPMDAAELKRVFQMFDRNGDGRI TKKELSDSLENLGIYIPDKELAEMIE KIDVNGDGCVDIDEFGALYRSIMEER DEEEDMREAFNVFDQNGDGFITVDEL RSVLASLGLKQGRTLEDCKRMIMKVD VDGDGMVDFKEFKQMMKGGGFSALS	Eucalyptus grandis	Myrtaceae	Myrtales	
ZizJuC3L2	>XP_015886996.1 PREDICTED: calmodulin-like protein 3 [Ziziphus jujuba] MPTIFLRIFLIYNLFNSLLLSLVPKK IRHFFPPSWFPLQAPPLPSPPSPPSS SCSFLAQKRMDPTELKRVFQMFDRNG DGRITKKELNDSLENLGIFIPDKELT QMIEKIDVNGDGCVDMDEFGELYQSI MDEKDEEEDMREAFNVFDQNGDGFIT VDELRSVLASLGLKQGRTVEDCKRMI MKVDVDGDGMVNYKEFKQMMKGGGFS ALS	Ziziphus jujuba	Rhamnaceae	Rosales	

LotJaC7L	>CAB63264.3 calcium-binding protein [Lotus japonicus] MPTILHRIFLLYNLLNSFLLSLVPKK VIAFLPQSWFPHQTPSFSSSSSSSSS RGNLVIQKTTDDCDPCQLLPLDTSLI PKMDPTELKRVFQMFDRNGDGRITKK ELNDSLENLGIFIPDKELTQMIERID VNGDGCVDIDEFGELYQSIMDERDEE EDMREAFNVFDQNGDGFITVEELRTV LASLGIKQGRTVEDCKKMIMKVDVDG DGMVDYKEFKQMMKGGGFSALT	Lotus japonicus	Fabaceae	Fabales	
VigAnC3L1	>XP_017425433.1 PREDICTED: calmodulin-like protein 7 [Vigna angularis] MPTIMLRFFLLYNLLRPFLLCLVPKK VRAILSPSWFRSSSTTAPTPTQPSSS SSSSSAFTRISLSMDPNELKRVFQMF DRNGDGRITKKELSDSLDNLGIFIPD KELTVMIERIDVNGDGCVDIDEFGEL YQTIMDERDEEDDMREAFNVFDQNGD GFITVEELRTVLSSLGLKQGRTVEDC KKMIMKVDVDGDGMVDYKEFKQMMKG GGFSALT	Vigna angularis	Fabaceae	Fabales	
VigRaC3L1	>XP_014521900.1 PREDICTED: calmodulin-like protein 7 [Vigna radiata var. radiata] MPTIMLRFFLLYNLLRPFLLCLVPKK VRAILSPSWFRSSTTTTAPTPTQPSS SSSSSSSSAITRISLSMDPNELKRVF QMFDRNGDGRITKKELSDSLDNLGIF IPDKELTVMIERIDVNGDGCVDIDEF GELYQTIMDERDEEDDMREAFNVFDQ NGDGFITVEELRTVLSSLGLKQGRTV EDCKKMIMKVDVDGDGMVDYKEFKQM MKGGGFSALT	Vigna radiata var. radiata	Fabaceae	Fabales	

PhaVuC3L1	>XP_007150430.1 hypothetical protein PHAVU_005G152900g [Phaseolus vulgaris] MPTILHRFFLLYNLLHPFLLFLVPKK VRAILSPSWFRSTTTPPPPSSSSSRL ITTISPPMDPHELKRVFQMFDRNGDG RITKKELNDSLENLGIFIPDKELTLM IERIDVNGDGCVDIDEFGELYQHIMD DRDEDEDMREAFNVFDQNGDGFITVE ELRTVLSSLGLKQGRTVEDCKKMIMK VDVDGDGMVDYKEFKQMMKGGGFSAL T	Phaseolus vulgaris	Fabaceae	Fabales	
GlyMaC3L1	>NP_001236739.2 EF-hand, calcium binding motif-containing protein precursor [Glycine max] MPTILHRIFLLYNLVHSFLLCLVPKK VRPFLPPSWFQTKTITAPSSSSSSSS SARIIKRTTMDPNELKRVFQMFDRNG DGRITKKELNDSLENLGIFIPDKELG QMIERIDVNGDGCVDIDEFGELYQTI MDERDEEEDMREAFNVFDQNADGFIT VDELRTVLSSLGLKQGRTVQDCKNMI SKVDVDGDGMVDFKEFKQMMKGGGFS ALT	Glycine max	Fabaceae	Fabales	
CajCaC3L1	>XP_020223613.1 calmodulin-like protein 7 [Cajanus cajan] MPTIFHRIVVVYEVLYPFLVRLIPKK VRAFFPSAGGSWSSQKSRRTSMDPQE LRRVFQMFDRNGDGRITKKELSDSLE NLGIFIPDKELSLMIEKIDVNGDGCV DIDEFGELYQTIMDERDEEEDMREAF NVFDQNGDGFITVDELRTVLSSLGLK QGRTVEDCKNMIMKVDVDGDGMVDFK EFKHMMKGGGFNALT	Cajanus cajan	Fabaceae	Fabales	
PruMuC3L2	>XP_008237262.1 PREDICTED: calmodulin-like protein 3 [Prunus mume] MPTIFPRIFLIYNLLNTFLLSLVPKN LRPLLPSSWFPCQTNLVATNTPLPHF PPSSSSSSLPCGAPKVIR MDPNELKRVFQMFDRNGDGRITKQEL NDSLENLGIFIPDKELFNMIQKIDVD GDGCVDIDEFGELYQSIMDERDEDED MKEAFNVFDQNGDGFITVDELRSVLS SLGLKQGRTIEDCKRMIMKVDVDGDG RVNYKEFKQMMKGGGFSALS	Prunus mume	Rosaceae	Rosales	

PruPeC3L2	>XP_020411008.1 calmodulin-like protein 3 [Prunus persica] MPTIFPRIFLIYNLLNTFLLSLVPKN LRPLLPSSWFPCQTNLVATNTSLPHF PPSSSSSSLPLPLPLPCG APKVIRMDPNELKRVFQMFDRNGDGR ITKQELNDSLENLGIFIPDKELFNMI QKIDVNGDGCVDIDEFGELYQSIMDE RDEDEDMKEAFNVFDQNGDGFITVDE LRSVLSSLGLKQGRTIEDCKRMIMKV DVDGDGRVNYKEFKQMMKGGGFSALS	Prunus persica	Rosaceae	Rosales	
PruAvC3L	>XP_021808428.1 calmodulin-like protein 3 [Prunus avium] MPTIFPRIFLIYNLLNTFLLSLVPKN LRPLLPSSWFPCQTNLVATSTPLPHF PPSSSSSSSCGAHKVIRMDPNELKRV FQMFDRNGDGRITKQELNDSLENLGI FIPDKELFNMIQKIDVNGDGCVDIDE FGELYQSIMDERDEDEDMKEAFNVFD QNGDGFITVDELRSVLSSLGLKQGRT IEDCKRMIMKVDVDGDGRVNYKEFKQ MMKGGGFSALS	Prunus avium	Rosaceae	Rosales	MalPyC3L
MalDoC3L4	>XP_008369144.1 PREDICTED: calmodulin-like protein 3 [Malus domestica] MPTIFPRIFLIYNLLNTFLLSLVPKH LRHLLPSSWFPHHTTLLDTKTPSPQP PPPSSLSLPLPLPSGGAC HVRMDPNELKRVFQMFDRNGDGRITK QELNDSLENLGIYIPDKELFNMIEKI DVNGDGCVDIDEFGELYQSIMDERDE EEDMKEAFNVFDQNGDGFITVDELRS VLSSLGLKQGRTIEDCKRMIMKVDVD GDGRVNFKEFRQMMKGGGFSALS	Malus domestica	Rosaceae	Rosales	MalPyC3L
PyrBrC3_7L	>XP_009347665.1 PREDICTED: calmodulin-like protein 7 [Pyrus x bretschneideri] MPTIFRRIFLIYNLLNTFLLSLVPKH LRPLLPSSWFPHHTTLLDTKTPSPQP PPPSLLSLPLPLPLPSGG ACHVRMDPNELKRVFQMFDRNGDGRI TKQELNDSLENLGIYIPDKELFNMIE KIDVNGDGCVDIDEFGELYQSIMDER DEEEDMKEAFNVFDQNGDGFITVDEL RSVLSSLGLKQGRTIEDCKRMIMKVD VDGDGRVNYKEFRQMMKGGGFSALS	Pyrus x bretschneideri	Rosaceae	Rosales	

PopEuC3L2	>XP_011037098.1 PREDICTED: calmodulin-like protein 3 [Populus euphratica] MPTILLRIFLLYNLLNSFLLSLVPKK LRFLLPTSWYHHHQANTNTSWCHPHQ ANTNTKKPSSLLPSPSFVLTRMDQAE LKRVFQMFDRNGDGKITKKELNDSLE NLGIFIPDKELTQMIETIDVNGDGCV DIDEFGELYQSLMDEKDEEEDMREAF KVFDQNGDGFITVDELRSVLASLGLK QGRTLEDCKRMIMKVDVDGDGMVDYK EFKKMMKGGGFSALG	Populus euphratica	Salicaceae	Malpighiales	
PopTrC3L1	>XP_006372871.1 hypothetical protein POPTR_0017s05860g [Populus trichocarpa] MPTILLRIFLLYNLLNSFLLSLVPKK LRFLLPTSWYHPHQANTNTSWCHPHQ ANTNTKKPSSLLPSPSFVLARMDQAE LKRVFQMFDRNGDGKITKKELNDSLE NLGIFIPDKELTQMIETIDVDGDGCV DIDEFGELYQSLMDDKDEEEDMREAF KVFDQNGDGFITVDELRSVLASLGLK QGRTLEDCKRMIMKVDVDGDGMVDYK EFKKMMKGGGFSALG	Populus trichocarpa	Salicaceae	Malpighiales	
PopEuC3L3	>XP_011012929.1 PREDICTED: calmodulin-like protein 3 [Populus euphratica] MRTILLRIFLLYNLLNSFLLSLVPKK LRFLLPTSWYHHPHQAITNTRKPSSL LPSSSNFVVKRMDQAELKRVFQMFDR NGDGRITQKELNDSLENIGIFIPDKE LTQMIENIDANGDGCVDIDEFGELYR SLMDEKDEEEDMREAFNVFDQNGDGF ITVEELRSVLASLGLKQGRTFEDCKR MIMKVDVDGDGMVDYREFQKMMKGGG FSAVG	Populus trichocarpa	Salicaceae	Malpighiales	
PopEuC3L4	>XP_011026425.1 PREDICTED: calmodulin-like protein 3 [Populus euphratica] MRTILLRIFLLYNLLNSFLLSLVPKK LRFLLPTSWYHHPHQAITNTRKPSSL LPSSSNFAVKRMDQAELKRVFQMFDR NGDGRITQKELNDSLENIGIFIPDKE LTQMIENIDANGDGCVDIDEFGELYR SLMDEKDEEEDMREAFNVFDQNGDGF ITVDELRSVLASLGLKQGRTFEDCKR MIMKVDVDGDGMVDYREFQKMMKGGG FSAVG	Populus trichocarpa	Salicaceae	Malpighiales	

PopTrC3L3	>XP_002310432.2 hypothetical protein POPTR_0007s01960g [Populus trichocarpa] MRTILLRIFLLYNLLNSFLLSLVPKK LRFLLPTSWYHHPHQAITNTKKPSSL LPSSSNFVLKRMDQAELKRVFQMFDR NGDGRITQKELNDSLENIGIFIPDKE LTQMIEKIDVNGDGCVDIDEFGELYQ SLMDEKDEEEDMREAFNVFDQNGDGF ITVDELRSVLASLGLKQGRTFEDCKR MIMKVDVDGDGMVDYREFKKMMKGGG FSAVG	Populus trichocarpa	Salicaceae	Malpighiales	
CarPaC3L	>XP_021906924.1 calmodulin-like protein 7 [Carica papaya] MPTILLRIFLVYNLLNSILLYLIPKK LRGFLPPSWYPHPHPHHHHQQQQQP NLVLDSSSKSPSPSPSSVSGLKRMDS AELKRVFQMFDKNGDGRITKKELNDS LENLGIFIPDKELAQMIEKIDVNGDG CVDIDEFGSLYKSIMDEHDEEEDMRE AFNVFDQNGDGFITVDELKSVLASLG LKQGKTVEDCKKMIMQVDEDGDGMVN YKEFRQMMKGGGFSALS	Carica papaya	Carricaceae	Brassicales	
JatCuC3L2	>XP_012065170.1 calmodulin-like protein 3 [Jatropha curcas] MLKIFLLYHLLHSLLVYLLPKKLRFL LPSSWLPHQANFPPNKKPPSSSSNTS SSSSSSVVHKRMDTTELRRVFQMFDR NGDGRITRKELSDSLENLGIFIPDSE LTQMIDNIDVNGDGCVDIEEFGVLYQ SIMDERDEEEDMREAFNVFDRNGDGY ITVDELRSVLASLGLKQGKAVEDCKR MIMRVDVDGDGMVNFMEFKQMMKGGG FSALS	Jatropha curcas	Euphorbiaceae	Malpighiales	
HevBraC3L	>XP_021652705.1 calmodulin-like protein 3 [Hevea brasiliensis] MPTILLTIFLLYNLLNSFLLYLIPKK LRTFFLPSSWCSHQANSLFKQQTLPP SSSSSAAAVVRKRMDSVELARVFQMF DRNGDGRITKKELNDSLENLGIFIPD LELTQMIQNIDVNGDGCVDIDEFGAL YQSIMDERDEEEDMKEAFNVFDQNGD GYITVDELRSVLAALGLKQGRTLEDC KTMIMKVDVDGDGMVNFKEFKQMMKG GGFSALG	Hevea brasiliensis	Euphorbiaceae	Malpighiales	

VitViC3L2	>XP_002266359.1 PREDICTED: calmodulin-like protein 3 [Vitis vinifera] MPTFLHRIFLLYNLLNSLVLFLVPKK LRIFLPTSWFHPHQTQEANLVDSKTS KTPGRSLVSRKRMESAEMKRVFQMFD RNGDGRITKTELNDSLENLGIYIPDK DLAQMIEKIDVNGDGCVDIDEFRALY ESIMEEKDEDEDMKEAFNVFDQNGDG FITVDELKSVLGSLGLRHGRTVEDCK RMIMKVDEDGDGKVDLKEFKQMMRGG GFSALS	Vitis vinifera	Vitaceae	Vitales	
CicArC7L	>XP_012570335.1 PREDICTED: calmodulin-like protein 7 [Cicer arietinum] MPTILLRIFLLYNVVNSFLISLVPKK LRTFFPHSWFSHQTLKTNLNTTTLSS SKKGFVVITKSITMDPNELKRVFQMF DRNDDGRITKKELNDSLENLGIFIPD KELSQMIEKIDVNRDGCVDIEEFREL YESIMNGREEEEEEDMREAFNVFDQN GDGFISVEELRSVLVTLGLKQGRTVE DCKKMIGKVDVDGDGLVDYKEFVQMM KGGGFTALS	Cicer arietinum	Fabaceae	Fabales	
MedTrC7L	>XP_003597517.1 EF hand calcium-binding family protein [Medicago truncatula] MPTILLRIFLLYNVVNSFLISLVPKK LITFFPHSWFTHQTLTTPSSTSKRGL VFTKTITMDPNELKRVFQMFDRNDDG RITKKELNDSLENLGIFIPDKELSQM IEKIDVNRDGCVDIEEFRELYESIMS ERDEEEEEDMREAFNVFDQNGDGFIS VDELRSVLVSLGLKQGRTVEDCKKMI GTVDVDGNGLVDYKEFKQMMKGGGFT ALS	Medicago truncatula	Fabaceae	Fabales	
CitClC3L2	>XP_006443024.1 hypothetical protein CICLE_v10022299mg [Citrus clementina] MRFILLRIFLLYTFILHLLPKKLRRF LPRSWFPAPALGPSLSSQSNTNPTRS TMDQAELDRVFQMFDHNGDGRISKKE LNDSLENLGIYIPDVELTQMIERIDV NGDGCVDIDEFGALYKSIMEEKDEEE DMKEAFNVFDQNGDGFITFDELKSVL GSLGLKQGRTVEDCKRMIMKVDVDGD GMVDYKEFKQMMKGGGFSALT	Citrus clementina	Rutaceae	Sapindales	CiCl2CiSi2

CitSiC3L2	>XP_006478702.1 PREDICTED: calmodulin-like protein 3 [Citrus sinensis] MRFILLRIFLLYTFILHLLPKKLRRF LPRSWFPAPALGPSLSSQSNTNPTRS TMDQAELDRVFQMFDHNGDGRISKKE LNDSLENLGIYIPDVELTQMIERIDV NGDGCVDIDEFGALYKSIMEEKDEEE DMKEAFNVFDQNGDGFITFDELKSVL GSLGLKQGRTVEDCKRMIMKVDVDGD GMVDYKEFKQMMKGGGFSALT	Citrus sinensis	Rutaceae	Sapindales	CiCl2CiSi2
ElaGuC3L1	>XP_019708251.1 PREDICTED: calmodulin-like protein 3 [Elaeis guineensis] MPTVLLRISLICHLLKTLLHYFLPKK LSFLRTAKVSAPRVFILATPPGMDPS ELKRVFQMFDRNGDGRITKKELSDSL ENLGIYIPEGDLEAMIEKIDANGDGC VDVEEFGALYQNIMDERDEEEDMREA FNVFDQNGDGFITVEELRSVLASLGL KQGRTVEDCRRMISKVDADGDGMVNF KEFKQMMRGGGFAALS	Elaeis guineensis	Arecaceae	Arecales	
ElaGuC3L2	>XP_010912790.2 PREDICTED: calmodulin-like protein 3 [Elaeis guineensis] MALKPPFLQPFSPPIPPHHSLHWQSP PPPLNSPMPTVFLRISLICHLLNSLL HYFLPHKLISLLLPSSRSSSGRPRVL ILATPPEMDPSELKRVFQMFDRNGDG RITKKELSDSLENLGIYIPEGDLESM IGKIDVNGDGCVDIEEFGALYQTIMD ERDEEEDMREAFNVFDQNGDGFITVE ELRSVLASLGLKQGRTVEDCRRMISK VDVDGDGMVNFKEFKQMMRGGGFAAL G	Elaeis guineensis	Arecaceae	Arecales	
PhoDaC3L	>XP_008791779.1 PREDICTED: calmodulin-like protein 3 [Phoenix dactylifera] MPPVLLRISLVCHLLNSLLHYFLPHK LSSLLPSSWLPRACLQEPAPDAAKAP SHCPSPRSSPCPRVSILATPPGMEPS ELKRVFQMFDRNGDGRITKKELGDSL ENLGIHIPEGDLESMIGKIDANGDGC VDIEEFGALYQTIMDERDEEEDMREA FNVFDQNGDGFITVEELRSVLASLGL KQGRTVEDCRKMITKVDVDGDGMVDF KEFKQMMRGGGFAALS	Phoenix dactylifera	Arecaceae	Arecales	

MacCoC3L	>OVA04582.1 EF-hand domain [Macleaya cordata] MPTVFLRISLLINLLNSILFYFFPNK LKSILPPSWFPNSHQSFSTNSTTSIP NTTIIPSTFSSSSSSSLPSSSSLIQQ EVMDPAELKRVFQMFDRNGDGRITKK ELSDSLDNLGIFIPDKDLTQMIEKID VNGDGCVDIDEFGALYQTIMDEKDEE EDMREAFNVFDQNGDGFITVEELRSV LSSLGLKQGRTVEDCRRMIRKVDVDG DGMVNFKEFKQMMRGGGFAALS	Macleaya cordata	Papaveraceae	Ranunculales	
EryGuC3L	>XP_012851006.1 PREDICTED: calmodulin-like protein 3 [Erythranthe guttata] MPTILLRIFLLYKLLNTIFLYLVPKK LRTFLPPSWYPYLHQQEQQKQQKHNN TNTINEPASPSSSPVISPLHKFPRRM DADELRRVFQMFDRNGDGRITQKELS DSLENMGIFIPDKELSQMIDKIDVNG DGCVDIEEFGNLYQNIMDERDEEEDM REAFNVFDQNGDGFITVDELKAVLAS LGLKQGRAVEDCKKMIMRVDADGDGM VNFTEFKQMMRGGGFAALGN	Erythranthe guttata	Phrymaceae	Lamiales	
SesInC3L	>XP_011084127.1 calmodulin-like protein 3 [Sesamum indicum] MPTILLRIFLVYNLILSYLVPKKLRA YLPSSWYPYQQQQQQQQQVKKEPTVA LSSSIVPSSRIVIHRRMDPNELKRVF QMFDRNGDGRITKQELSDSLHNMGIS IPDEELTQMIDKVDINGDGCVDIDEF GTLYQTIMDERDEEEDMKEAFNVFDQ NGDGFISVDELKSVLVSLGLKQGKAA EDCRQMIMRVDVDGDGMVNFSEFKQM MRGGGFAALTN	Sesamum indicum	Pedaliaceae	Lamiales	
RicCoC3L	>XP_015583372.1 PREDICTED: calmodulin-like protein 3 [Ricinus communis] MPTILLRIFLLYNLLNSFLLSLVPKK LVRFFVPSSWYNSNTHQANLLINQEL QQQEEEEETLVVPSAARKRMDSTELK KVFQMFDTNGDGRITKEELNGSLENL GIFIPDKELSQMMETIDVNGDGGVDI EEFGALYQSIMDEKDEDEDMREAFNV FDQNGDGYITGDELRSVLASLGLKQG RTAEDCKKIIMKVDVDGDGMVDFKEF KQMMKGGVFTALSSCN	Ricinus communis	Euphorbiaceae	Malpighiales	

GosArC7L	>XP_017647023.1 PREDICTED: calmodulin-like protein 7 [Gossypium arboreum] MPSLLFRIFLLYNLLLDYLVPRKLKS FLSPSCTITTPFVSVGGETEKNPSPA VALASVSPRCPLKRMDAAELKRVFQL FDKNGDGSISKKELNDSLENMGICIP DPELTQMIEKIDVNGDKCIDIDEFSE LYRSIMDNKDEEEDMKEAFNVFDQNG DGYISVEELRSVLESLGLKQGKGIED CKRMITKVDVDGDGRVNFMEFKQMMK GGGFTAMA	Gossypium arboreum	Malvaceae	Malvales	
TheCaC3L2	>XP_007033950.2 PREDICTED: calmodulin-like protein 7 [Theobroma cacao] MPTVLLRIFLVYNLVLDYLVPKKLKT FLPSSWIPTRTLVSTGSESKTHTSTS PAPESASAPASSACCPQRMDGAELKR VFQMFDKNGDGRITKKELNDSLENLG IFIPDGELTHMIEKIDVNGDNCVDID EFGELYHSIMDDKDEEEDMKEAFNVF DQNGDGYISVDELRSVLVSLGLKQGK TIEDCKRMIMKVDVDGDGRVNFKEFK QMMKGGGFSALT	Theobroma cacao	Malvaceae	Malvales	
CorOlC3L	>OMP07050.1 Calcium-binding EF-hand [Corchorus olitorius] MPTVLLRIFLLYNLVLDYLVPKKLKT FLPSSWIPPPPTHTLVSTATESKSSS SPEPAPAPASPSCRRQSQRMDAAELK RVFQLFDKNGDGRISKQELNDSLENL GIFIPDGELTQMIEKIDVNGDNCVDI DEFGELYQSIMDGKDEEEDMKDAFNV FDQNGDGFISVDELRSVLVSLGLKQG KTIEDCKRMIMKVDADGDGRVNFKEF KQMMKGGGFSALT	Corchorus olitorius	Malvaceae	Malvales	
CorCaC3L	>OMO52915.1 Calcium-binding EF-hand [Corchorus capsularis] MPTVLLRIFLLYNLVLDYLVPKKLKT FLPSSWIPPPTHTFVSTVTESKSSSS PEPAAAPPASPSCRRQSQRMDAAELK RVFQLFDKNGDGRISKQELNDSLENL GIFIPDGELTQMIEKIDVNGDNCVDI DEFGELYQSIMDGKDEEEDMKDAFNV FDQNGDGFISVDELRSVLISLGLKQG KTIEDCKRMIMKVDADGDGRVNFKEF KQMMKGGGFSALT	Corchorus capsularis	Malvaceae	Malvales	

PunGrC3L	>OWM87900.1 hypothetical protein CDL15_Pgr000317 [Punica granatum] MLMPTILKRIFLIYNLLLYFVPKKLR PFLPSPSWFCSAVSGTANGNVVLLPS PSLRARKATVMDPTELRRVFQMFDRN GDGSISKKELADSLENLGIFIPDKEL EDMIRRIDANGDGCVDIEEFEALYRS IMDERDEEEDMKEAFNVFDQNGDGFI TVDELRSVLASLGLKQGRTIEDCKRM IMKVDVDGDGRVNYKEFKQMMKGGGF SALS	Punica granatum	Lythraceae	Myrtales	
SolLyC3L1	>Solyc06g073245.1 MQFPAIFFKTRCIFNLFNPILLSLLP KKLISFLPPSWFHQKRIHSRSPAPPQ QSPVSVSDAVESHQKRMDSDELRRIF QIFDRNGDGRITKNELNSSLENMGIF IPDPELIQMIEKIDVNGDGCVDIDEF GSLYQTIMDERDEEEDMREAFNVFDQ NGDGFICVEELKSVLASLGLKQGRTV EDCKQMINKVDIDGDGMVNYDEFKQM MRGGGDM	Solanum lycopersicum	Solanaceae	Solanales	
SolTuC3L1	>XP_006347296.1 PREDICTED: calmodulin-like protein 3 [Solanum tuberosum] MQFPAIFFKTRFIYNLFNPILLSLLP KKLISFLPPSWFHQKHLHSRSPAPPQ QSPVSVSDAVQSHIQKRMDSDELRRI FQIFDRNGDGRITKNELNDSLENMGI FIPDPELIEMIEKIDVNGDGCVDIDE FGSLYQTIMDERDEEEDMREAFNVFD QNGDGFICVDELKSVLASLGLKQGRT VEDCKQMINKVDIDGDGMVNFAEFKQ MMRGGGFAALS	Solanum tuberosum	Solanaceae	Solanales	
AraDuC3L2	>XP_015935524.1 calmodulin-like protein 3 [Arachis duranensis] MPAILLLYNILNSFLISLIPKKLRPF FPFSWFPHQTNNTSSSSSSSSSPRR ASRAIIITKTRIMDPNEL RRVFQMFDRNGDGRISRSELTVSLEN LGIFIPDKELAQMIDKIDANGDGFVD VEEFGELYESIMVERGDEEEDMKEAF NVFDQNGDGFISVEELRAVLSSLGLK QGRTDEDCKKMIMKVDADGDGMVNYG EFKQMMKGGGFSALS	Arachis duranensis	Fabaceae	Fabales	ADu2AIp2

AraIpC3L2	>XP_016171630.1 calmodulin-like protein 3 [Arachis ipaensis] MPAILLLYNILNSFLISLIPKKLRPF FPFSWFPHQTNNTSSSSSSSSSPRR ASRAIIITKTRIMDPNEL RRVFQMFDRNGDGRISRSELTVSLEN LGIFIPDKELAQMIDKIDANGDGFVD VEEFGELYESIMVERGDEEEDMKEAF NVFDQNGDGFISVEELRAVLSSLGLK QGRTDEDCKKMIMKVDADGDGMVNYG EFKQMMKGGGFSALS	Arachis ipaensis	Fabaceae	Fabales	ADu2AIp2
MusAcC3L4	>XP_009417008.1 PREDICTED: calmodulin-like protein 3 [Musa acuminata subsp. malaccensis] MELTPMPAIFVGIFLICHHLNSRLLR FLPEKLISLLLPFSWHPPTSKDGLSP PATALSSIASFRSPSFGPKASARVMD PSELKRVFQMFDRNGDGRITKTELSD SLENLGIYIPEAELASMIEKIDVNGD GCVDMDEFGALYRSIMDERDEEEDMR EAFNVFDQNGDGYISVEELRSVLVSL GVKQGRTAEDCRMMINKVDVDGDGRV DFKEFKQMMKGGGFAALS	Musa acuminata subsp. malaccensis	Musaceae	Zingiberales	
AraLyC4L	>XP_020881472.1 calmodulin-like protein 4 [Arabidopsis lyrata subsp. lyrata] MVRVFLPYNLFNSFLLCLVPKKLRVF FPPSWYIDDKNPPQSKSESESPGRRD PVDLKRVFQMFDKNGDGRITKEELND SLENLGIFMPDKDLVQMIQKMDANGD GIVDIKEFESLYGSIVEEKEEEDMRD AFNVFDQDGDGFITVEELKSVMASLG LKQGKTLECCKEMIKQVDEDGDGRVN YMEFLQMMKSGDFSNRS	Arabidopsis lyrata subsp. lyrata	Brassicaceae	Brassicales	
AraThC4	>NP_191503.1 Calcium-binding EF-hand family protein [Arabidopsis thaliana] MVRVFLLYNLFNSFLLCLVPKKLRVF FPPSWYIDDKNPPPPDESETESPVDL KRVFQMFDKNGDGRITKEELNDSLEN LGIFMPDKDLIQMIQKMDANGDGCVD INEFESLYGSIVEEKEEGDMRDAFNV FDQDGDGFITVEELNSVMTSLGLKQG KTLECCKEMIMQVDEDGDGRVNYKEF LQMMKSGDFSNRS	Arabidopsis thaliana	Brassicaceae	Brassicales	

CamSaC4L1	>XP_010512205.1 PREDICTED: calmodulin-like protein 4 [Camelina sativa] MVKSVFLLYNLFHSFLLCLVPKKLRV LFPPSWYIDDKNPPPPSQVETESPGR TDLVDLKRVFQMFDKNGDGRITKEEL NDSLENLGIFMPDKDLIQMIQKMDAN GDGCVDINEFESLYGSIVEEKEEEDM RDAFNVFDQDGDGFITVKELKSVMAS LGLKQGRTLKCCKEMIMQVDEDGDGR VNYKEFLQMMKSVGFSNRS	Camelina sativa	Brassicaceae	Brassicales	
CamSaC4L2	>XP_010469361.1 PREDICTED: calmodulin-like protein 4 [Camelina sativa] MVRSVFLLYNLFHSFLLCLVPKKLRV LFPPSWYIDDKNPPPPSQLETESPGR TDLVDLKRVFQMFDKNGDGRITKEEL NDSLENLGIFMPDKDLIQMIQKMDAN GDGCVDINEFESLYGSIVEEKEEEDM RDAFNVFDQDGDGFITVKELKSVMAS LGLKQGRTLKCCKEMIMQVDEDGDGR VNYKEFLQMMKSVGFSNRS	Camelina sativa	Brassicaceae	Brassicales	
CapRuC4L	>XP_006291828.1 hypothetical protein CARUB_v10018003mg, partial [Capsella rubella] MVRVFLLYSLFNSFLLSLVPKKLRVL FPPSWYIDDKNPPPVPSQSETESPGR TDPVDLKRVFQMFDKNGDGRITKEEL NDSLENLGIFMPDKDLIQMIQKMDAN GDGCVDINEFESLYGSIVEEKEEEDM RDAFNVFDQDGDGFISVEELKSVMAS LGLKQGKTLKCCKEMIMQVDEDGDGR VDYKEFLQMMKSGGFSNRA	Capsella rubella	Brassicaceae	Brassicales	
BraNaC4L1	>XP_013663730.1 PREDICTED: calmodulin-like protein 4 isoform X3 [Brassica napus] MVRVILLYNLLNSFLLCLVPKKLRVL FPPSWYTDDKITPPSESECSLRTDPV DLKRVFQMFDKNGDGRITKEELNDSL ENLGIFMPDKDLIQMIRKMDANGDGC VDINEFESLYGSIVEEKEEEDMRDAF NVFDQDGDGFISVEELKSVMASLGLK QGKTLKCCKEMITQVDEDGDGRVNYK EFLQMMKSGGFSNRSS	Brassica napus	Brassicaceae	Brassicales	

BraRaC4L1	>XP_009116605.1 PREDICTED: calmodulin-like protein 4 [Brassica rapa] MVRVFLLYNLLNSFLLCLVPKKLRVL FPPSWYTDDKITPPSESECSLRTDPV DLKRVFQMFDKNGDGRITKEELNDSL ENLGIFMPDKDLIQMIRKMDANGDGC VDINEFESLYGSIVEEKEEEDMRDAF NVFDQDGDGFISVEELKSVMASLGLK QGKTLKCCKAMITQVDEDGDGRVNYK EFLQMMKSGGFSNRSS	Brassica rapa	Brassicaceae	Brassicales	
BraOlC4L2	>XP_013603279.1 PREDICTED: calmodulin-like protein 4 [Brassica oleracea var. oleracea] MVRVFLLYNLLNSFLLCLVPKKLRVL FPPSWYTDDKITPPSESECSLRTDPV DLKRVFQMFDKNGDGRITKEELNDSL ENLGIFMPDKDLIQMIQKMDANGDGC VDINEFESLYGSIVEEKEEEDMRDAF NVFDQDGDGFISVEELKSVMASLGLK QGKTLKCCKEMITQVDEDGDGRVNYK EFLQMMKSGGFSNSSSSD	Brassica oleracea var. oleracea	Brassicaceae	Brassicales	
RapSaC4L2	>XP_018489165.1 PREDICTED: calmodulin-like protein 4 [Raphanus sativus] MVRVFLLYNLLNSFLLCLVPKKLRVL FPPSWYTEDKIPPPPESECSLRTEPV DLKRVFQMFDKNGDGRITKEELNDSL ENLGIFMPDKDLIQMIQKMDANGDGC VDINEFESLYGSIVEEKEEEDMRDAF NVFDQDGDGFISVEELKSVMASLGLK QGKTLKCCKEMITQVDEDGDGRVNYN EFLQMMKSGGFSNRS	Raphanus sativus	Brassicaceae	Brassicales	
BraNaC4L2	>XP_013699103.1 PREDICTED: calmodulin-like protein 4 [Brassica napus] MVRVFLLYNLINSFLLYLVPKKLRVL FPPSWYIDDNIPPPLSEPEPKSQTRT DPVDLKQVFQMFDKNGDGRITKEELN DSLENLGIFMPDKDLIQMIHKMDANG DGCVDIHEFESLYGSIVEEKEEEDMR DAFNVFDQDGDGFISVEELKSVMASL GLKQGKTLECCKEMIMQVDEDGDGRV NYKEFLQMMKTGGFNNRSSSSN	Brassica napus	Brassicaceae	Brassicales	

BraOlC4L1	>XP_013588571.1 PREDICTED: calmodulin-like protein 4 [Brassica oleracea var. oleracea] MVRVFLLYNLINSFLLCLVPKKLRVL FPPSWYIDDNIPPPLSEPEPKSQTRT DPVDLKQVFQMFDKNGDGRITKEELN DSLENLGIFMPDKDLIQMIHKMDANG DGCVDIHEFESLYGSIVEEKEEEDMR DAFHVFDQDGDGFISVEELKSVMASL GLKQGKTLECCKEMIMQVDEDGDGRV NYKEFLQMMKTGGFNNRSSSSN	Brassica oleracea var. oleracea	Brassicaceae	Brassicales	
BraNaC4L3	>XP_013648300.1 PREDICTED: calmodulin-like protein 4 [Brassica napus] MVRVFLLYNLINSFLLCLVPKKLRVL FPPSWYIDDNIPPPLSEPEPKSQTRT DPVDLKQVFQMFDKNGDGRITKEELN DSLENLGIFMPDKDLIQMIHKMDANG DGCVDIHEFESLYGSIVVEKEEEDMR DAFNVFDQDGDGFISVEELKSVMASL GLKQGKTLECCKEMIMQVDEDGDGRV NYKEFLQMMKTGGFSNTSSSN	Brassica napus	Brassicaceae	Brassicales	BNa3BRa2
BraRaC4L2	>XP_009104207.1 PREDICTED: calmodulin-like protein 4 [Brassica rapa] MVRVFLLYNLINSFLLCLVPKKLRVL FPPSWYIDDNIPPPLSEPEPKSQTRT DPVDLKQVFQMFDKNGDGRITKEELN DSLENLGIFMPDKDLIQMIHKMDANG DGCVDIHEFESLYGSIVVEKEEEDMR DAFNVFDQDGDGFISVEELKSVMASL GLKQGKTLECCKEMIMQVDEDGDGRV NYKEFLQMMKTGGFSNTSSSN	Brassica rapa	Brassicaceae	Brassicales	BNa3BRa2
RapSaC4L1	>XP_018442929.1 PREDICTED: calmodulin-like protein 4 [Raphanus sativus] MVRVFLLYNLINSFLLCLIPKKLRVL FPPSWYMDDNIPPPLSEPEPESREAR TDPVDLKRVFQMFDKNGDGRITKEEL NDSLENLGIFMPDKDLIQMIKNIDAN GDGCVDIQEFESLYGSIVQEKEEEDM RDAFNVFDQDGDGFISVEELKSVMSS LGLKQVKTLECCKEMIMQVDEDGDGR VNYKEFLQMMKTGGVSNTSSSS	Raphanus sativus	Brassicaceae	Brassicales	

EutSaC4L	>XP_006402687.1 hypothetical protein EUTSA_v10006367mg [Eutrema salsugineum] MVRVFLLYNLFNSILLCLVPKKLRVL FPHSWIIDDKNPPPSKSESPARTDPV DLKRVFQMFDKNGDGRITKEELNDSL ENLGIFMPEKDLIQMIQKMDANGDGC VDIHEFESLYSSIVEEKVDEDMRDAF NVFDQDGDGYITVEELKSVMASLGLK QGKTLECCKDMITQVDEDGDGRVNYK EFLQMMKSGGFSNNRSSSN	Eutrema salsugineum	Brassicaceae	Brassicales	
TarHaC4_5L	>XP_010526084.1 PREDICTED: calmodulin-like protein 4 [Tarenaya hassleriana] MPAVMVRIFLLYNLFNSFLLCLVPKK LRGIFPPSWYPHHVDDDNPKNPPPSS SPSPSPPPARVDPVELKRVFQMFDKN GDGRITKEELNDSLENLGLFLPDREL AQMIQKIDANGDGCVDMDEFESLYKS IVDQSDKDDDMRDAFDVFDQDGDGFI TVEELKSVMGSLGLKQGKTLEDCKKM IMQVDVDGDGRVNYKEFLQMMKSGDL	Tarenaya hassleriana	Cleomaceae	Brassicales	
AraLyC5L	>XP_002881895.1 calmodulin-like protein 5 [Arabidopsis lyrata subsp. lyrata] MVRIFLLYNILNSFLLSLVPKKLQTL FPLSWLDKTLHKNSPPSPSTMLPSPP SSSAPTKRIDPSELKRVFQMFDKNGD GRITKEELNDSLENLGIYIPDKDLTQ MIHKIDANGDGCVDIDEFESLYSSIV DEHHNDGETEEEDMKDAFNVFDQDGD GFITVDELKSVMASLGLKQGKTLDGC KKMIMQVDADGDGRVNYKEFLQMMKG GG FSSSN	Arabidopsis lyrata subsp. lyrata	Brassicaceae	Brassicales	
AraThC5	>NP_565996.1 Calcium-binding EF-hand family protein [Arabidopsis thaliana] MVRIFLLYNILNSFLLSLVPKKLRTL FPLSWFDKTLHKNSPPSPSTMLPSPS SSSAPTKRIDPSELKRVFQMFDKNGD GRITKEELNDSLENLGIYIPDKDLTQ MIHKIDANGDGCVDIDEFESLYSSIV DEHHNDGETEEEDMKDAFNVFDQDGD GFITVEELKSVMASLGLKQGKTLDGC KKMIMQVDADGDGRVNYKEFLQMMKG GGFSSSN	Arabidopsis thaliana	Brassicaceae	Brassicales	

CamSaC5L1	>XP_010508448.1 PREDICTED: calmodulin-like protein 5 [Camelina sativa] MVRIFVLYNILNSFLLSLVPKKLRTL FPLSWFDKTLHKNSPPSPPTMLPSPS SSSSSSVPTKRIDPSDLKRVFQMFDK NGDGRITKEELNDSLENLGIYIPDKD LTQMIHKIDANGDGCVDIDEFESLYS SIVDEHQNDGETEEEDMKDAFNVFDQ DGDGFITVEELKSVMASLGLKQGKTL DGCKKMIMQVDADGDGRVNYKEFLQM MKGGGFSSSN	Camelina sativa	Brassicaceae	Brassicales	
CamSaC5L3	>XP_010517888.1 PREDICTED: calmodulin-like protein 5 [Camelina sativa] MVRIFVLYNILNSFLLSLVPKKLRTL FPLSWFDKTLHKNSPPSPSTMLPSPS SSSSSSVPTKRIDPSELKRVFQMFDK NGDGRITKEELNDSLENLGIYIPDKD LTQMIHKIDANGDGCVDKDEFESLYS SIVDEHQKDGETEEEDMKDAFNVFDQ DGDGFITVEELKSVMASLGLKQGKTL DGCKKMIMQVDADGDGRVNYKEFLQM MKGGGFSSSN	Camelina sativa	Brassicaceae	Brassicales	
CamSaC5L2	>XP_010506196.1 PREDICTED: calmodulin-like protein 5 [Camelina sativa] MVRIFVLYNILNSFLLSLVPKKLRSL FPLSWFDKTLHKNSPPSPPTMLPSPS SSSSSVPTKRIDPSELKRVFQMFDKN GDGRITKEELNDSLENLGIYIPDKDL TQMIHKIDANGDGCVDIDEFESLYSS IVDEHQNDGETEEENMKDAFNVFDQD GDGFITVEELKSVMASLGLKQGKTLD GCKKMIMQVDADGDGRVNYKEFLQMM KGGGFSSSN	Camelina sativa	Brassicaceae	Brassicales	
EutSaC5L	>XP_006397493.1 hypothetical protein EUTSA_v10001753mg [Eutrema salsugineum] MVRIFLLYNLLNSFL LSLVPKKLRSLFPLSWFDKTLHKTSP SSMLPSPSPSSAPTKRTDPSELKRVF QMFDKNGDGRITKEELNDSLENLGIY IPDKDLTQMIHKIDANGDGCVDIDEF ESLYSSIVDEHHNDGETEEEDMKDAF NVFDQDGDGFITVEELKSVMASLGLK QGKTLDGCKKMIMQVDADGDGRVNYK EFLQMMKGGGFSSSN	Eutrema salsugineum	Brassicaceae	Brassicales	

CapRuC5L	>XP_006296176.1 hypothetical protein CARUB_v10025336mg [Capsella rubella] MVRIFLLYNILNSFLLSLVPKKLRSL FPLSWFDKTLHMNSPPSPPTMLPSPS SSPLPTKKIDPSELKRVFQMFDKNGD GRITKEELNDSLENLGIYIPDQDLTQ MIHKIDANGDGCVDIDEFESLYGSIV DEHHNDGGTEEEDMKDAFNVFDQDGD GFITVEELKSVMASLGLKQGKTLDGC KKMIMQVDADGDGRVNYKEFLQMMKG GGFSSSSN	Capsella rubella	Brassicaceae	Brassicales	
BraNaC5L1	>XP_013688028.1 PREDICTED: calmodulin-like protein 5 [Brassica napus] MVRIFLLYNLLNSFLLSLVPKKLRSL FPLSWFDKTPHKNSSMLPSPSPSSAP TRKTDPSELKRVFQTFDKNGDGRITK TELNDSLENLGIYIPDKDLTQMIHNI DANGDGCVDIDEFESLYSSIVDEHRK DGETEEDDMKDAFNVFDQDGDGFITV EELKSVMGSLGLKQGKTLEGCKKMIM QVDGDGDGRVNYKEFLQMMRGGGFSC SNN	Brassica napus	Brassicaceae	Brassicales	BNa1BO12
BraOlC5L2	>XP_013631723.1 PREDICTED: calmodulin-like protein 5 [Brassica oleracea var. oleracea] MVRIFLLYNLLNSFLLSLVPKKLRSL FPLSWFDKTPHKNSSMLPSPSPSSAP TRKTDPSELKRVFQTFDKNGDGRITK TELNDSLENLGIYIPDKDLTQMIHNI DANGDGCVDIDEFESLYSSIVDEHRK DGETEEDDMKDAFNVFDQDGDGFITV EELKSVMGSLGLKQGKTLEGCKKMIM QVDGDGDGRVNYKEFLQMMRGGGFSC SNN	Brassica oleracea var. oleracea	Brassicaceae	Brassicales	BNa1BO12

BraNaC5L2	>XP_013664170.1 PREDICTED: calmodulin-like protein 5 [Brassica napus] MVRIFLLYNLLNSFLLSLVPKKLRTL FPLSWFDKTPHKNSSMLLSPSPSSAP SIKTDPTELKRVFQTFDKNGDGRITK TELNDSLENLGIYIPDQELTQMIHNI DANGDGCVDIDEFESLYSSIVDEHRK DGETEEEDMKDAFNVFDQDGDGFITV EELKSVMGSLGLKQGKTLEGCKKMIM QVDGDGDGRVNYKEFLQMMKGGGFSC SN	Brassica napus	Brassicaceae	Brassicales	
BraRaC5L1	>XP_009150184.1 PREDICTED: calmodulin-like protein 5 [Brassica rapa] MVRIFLLYNLLNSFLLSLVPKKLRTL FTLSWFDKTPHKNSSMLPSPSPSSAP SIKTDPTELKRVFQTFDKNGDGRITK TELNDSLENLGIYIPDKELTQMIHNI DANGDGCVDIDEFESLYSSIVDEHRK DGETEEEDMKDAFNVFDQDGDGFITV EELKSVMGSLGLKQGKTLEGCKKMIM QVDGDGDGRVNYKEFLQMMKGGGFSC SN	Brassica rapa	Brassicaceae	Brassicales	
BraNaC5L3	>XP_013683810.1 PREDICTED: calmodulin-like protein 5 [Brassica napus] MMRIFLLYNLLNSFLLSLVPKKLRTL FSLSWFDKTLHKNSPPSPSMLPSPSP SSTPTTKIDPSELKRVFQTFDKNGDG RITKQELKDSLENLGIYIPDKDLTQM IHNIDTNHDGCVDIDEFESLYKSIVD EHHNDGETEEEDMKEAFNVFDQDGDG FITVEELKSVMGSLGLKQGKTQEGCK KMIMQVDVDGDGRVNYKEFLQMMKGD GFSSRS	Brassica napus	Brassicaceae	Brassicales	BN53BO51
BraOlC5L1	>XP_013625660.1 PREDICTED: calmodulin-like protein 5 [Brassica oleracea var. oleracea] MMRIFLLYHLLNSFLLSLVPKKLRTL FSLSWFDKTLHKNSPPSPSMLPSPSP SSTPTTKIDPSELKRVFQTFDKNGDG RITKQELKDSLENLGIYIPDKDLTQM IHNIDTNHDGCVDIDEFESLYKSIVD EHHNDGETEEEDMKEAFNVFDQDGDG FITVEELKSVMGSLGLKQGKTQEGCK KMIMQVDVDGDGRVNYKEFLQMMKGD GFSSSS	Brassica oleracea var. oleracea	Brassicaceae	Brassicales	BN53BO51

BraRaC5L2	>XP_009133590.1 PREDICTED: calmodulin-like protein 5 [Brassica rapa] MVRIFLLYNLLNSFLLSLVPKKLRTL FSLSWFDKTLHKNSPPSPSMLPSPSP SSTPTTKIDPSELKRVFQTFDKNGDG RITKQELKDSLENLGIYIPDKDLTQM IHNIDTNHDGCVDIDEFESLYRSIVN EHHNDGETKEEDMKEAFNVFDQDGDG FITVEELKSVMSSLGLKQGKTLEGCK KMIMQVDVDGDGRVNYKEFLQMMKGD GFSRSS	Brassica rapa	Brassicaceae	Brassicales	
RapSaC5L1	>XP_018472925.1 PREDICTED: calmodulin-like protein 5 [Raphanus sativus] MVRIFLLYSLLNSFLLSLLPKKLRTL FPLSWFDKTLHKNSPPSASMLPSPSP SPSSASTRKIDPSELKRVFQTFDKNG DGRITKQELNNSLENLGIYIPDKDLT QMIHNIDKNHDGCVDIDEFESLYRSI VDEHHNDGETEEEDMKEAFNVFDQDG DGFITVEELKSVLASLGLKQGKTLEG CKKMIMQVDSDGDGRVNYKEFLQMMK GGGFSSSG	Raphanus sativus	Brassicaceae	Brassicales	
MusAcC3L5	>XP_009392598.1 PREDICTED: calmodulin-like protein 3 [Musa acuminata subsp. malaccensis] MELTPLPIVLVRLSLLCLRLISRLLY FLPKKLTSLLLSPSSSSSSSSSPSHE NPAASFTSTVAARPASSAPSMDPSEL KPVFHMFDRNGDGRITKEELSDSLRN LGMRVPEAELASMIERIDANGDGYVD SDEFATLYRSIMEERDEEEEDMREAF NVFDRNGDGFITVEELRSVLASLGLK QGRTAEDCKTMINTVDVDGDGMVDFK EFRQMMNGGGFAASS	Musa acuminata subsp. malaccensis	Musaceae	Zingiberales	

DauCaC3L2	>XP_017250190.1 PREDICTED: calmodulin-like protein 3 [Daucus carota subsp. sativus] MLKHKAISAILLRAFLFYNVLNSILA YLVPKKLRNYVPTFWYSREAGIDRNH TNLTSSNTELTLHFPRMEADELRKVF EMFDHNGDGRITKQELNESLEKMGIF IPDQELTQMIEKIDVNNDGCVDIDEF GDLYQNIMNTREEEEDMKEAFSVFDQ NGDGFITVDELKSVLASLGLKQGRTE EDCKTMIMKVDVDGDGRVNFNEFKAM MRGGGFAALN	Daucus carota subsp. sativus	Apiineae	Apiales	
CepFoC3L	>GAV85659.1 EF_hand_5 domain-containing protein [Cephalotus follicularis] MLRISLVYNLLNTFLLSLVPKKLIPA SWYHHQNNHIVDTKTLPPPLPPLARA QKRMDPTELDRVFQMFDRNGDGRITK MELNESLEKLGMFIPDKELTRMIEKI DVDGDGCVDIDEFGALYRSLMDHEVD DDEEEEEDMMKEAFNVFDSNGDGFIS VDELRSVFVSLGVKQGRTIEDCKKMI MKVDVDGDGKVDYEEFKQMMKGGGGG FSSLS	Cephalotus follicularis	Cephalotaceae	Oxalidales	
HelAnC3L	>OTG32667.1 putative calcium-binding EF-hand family protein [Helianthus annuus] MPRIFLLYNLIYSIFLSFLPKNLRHY LPKSHTQQQQQQIQNDTVSQPSQPPQ TPRTSRMNPDQLQRIFQMFDKNNDGT ITKHELNESLENMKIFISDEDLVRMI DKVDINNDGCVDLDEFGVLYKEIMDN QENEEDMMEAFNVFDQNRDGFIAVEE LRSVLESLGLKQGKVVDDCRRMIMKV DVDGDGRVSFNEFKEMMKSGGFVNLA QS	Helianthus annuus	Asteraceae	Asterales	
VigAnC3L2	>XP_017407196.1 PREDICTED: calmodulin-like protein 5 [Vigna angularis] MPTIMLRFFLLYNLLRPFLLCLVPKK VRAILSPSWFRSSSTTAPTPTQPSSS SSSSSAFTRISLSMDPNELKRVFQMF DRNGDGRITKKELSDSLDNLGIFIPD KELTVMIERIDVNGDGCVDIDEFGEL YQTIMDERDEEDDMREAFNDIYIYIL YLDILITKIYKIYSPLHSFKKHFIKV WSLY	Vigna angularis	Fabaceae	Fabales	

AraThC24	>NP_198593.1 EF hand calcium-binding protein family [Arabidopsis thaliana] MSSKNGVVRSCLGSMDDIKKVFQRFD KNGDGKISVDELKEVIRALSPTASPE ETVTMMKQFDLDGNGFIDLDEFVALF QIGIGGGGNNRNDVSDLKEAFELYDL DGNGRISAKELHSVMKNLGEKCSVQD CKKMISKVDIDGDGCVNFDEFKKMMS NGGGA	Arabidopsis thaliana	Brassicaceae	Brassicales	
ElaGuC6L	>XP_010927373.1 PREDICTED: calmodulin-like protein 6 [Elaeis guineensis] MAALLFFAILFTCGLINSYFFLHPPK LLTRLASFLYVTSTPKPIVKTPSKDG KEVVVSEIVTDKAGIETVFATFDKDG DGFITTEELEESFKRLGLFSTRNEIV SMMKRVDANGDGLIDLEEFGELYDSL GRGRGGGDGDERGERGKEEEEEGEVE LREAFDVFDENGDGLITVEELGLVLA SLGLKRGATVEDCRDMIRKVDLDGDG MVDFGEFKKMMVEGVKLF	Elaeis guineensis	Acecaceae	Arecales	
CapAnC3L	>XP_016541129.1 PREDICTED: calmodulin-like protein 3 [Capsicum annuum] MFTLLTILFLAFLFIIGLITTFFNF PTNKFQSLIQKISLKSPSLQEKTII TPSPSITMVDKKVMNRSNNY NKVELRSIFATFDKNNDGYITKQEL KLSLKNIGIFMEDKDIVEMVEKVDS NKDGLIDLDEFCDLCHTYLG IEEVSNESEMNEEEVANREKDLKDA FDVFDHDKDGLISKEELSKILSTLG MKEGKKLDYCKEMIKKVDVD GDGMVNFDEFKKMMKACGTLIPFS	Capsicum annuum	Solanaceae	Solanales	

CucMeC7L	>XP_008457058.1 PREDICTED: calmodulin-like protein 7 [Cucumis melo] MEPIFNFLLLSVLFVAGFVNFLLYFP TKRFTAWFQSIKPSSQIPHFKSTPLQ PPPPPPPPPPPPPPSAME LKKVFGTFDKNDDGFITKKELMESLK SMRMMITEKDAEEMLKEVDENGDGLI DFEEFCVLGEKLLMGFEE NKKTSVGDDEEGLKDAFGVFDKDSDG LISVEELSLVLCSLGMNEGKIVENCK EMIRKVDLDGDGMVNFDE FKKMMRNGVSILTSS	Cucumis melo	Cucurbitaceae	Cucurbitales	
CucSaC3L	>XP_004139293.1 PREDICTED: calmodulin-like protein 3 [Cucumis sativus] MEPIFNFLLLSVLFVAGFINFLLYFP SKRFSAWFQSIKPSSQITHFKSTPLQ PPPPPSPSPSPSPPPPSA MEMKKVFGTFDKNDDGFITKKELMES LKSMRMMITEKDAEEMLKGVDENGDG LIDFEEFCVLGGKLMMGF EENKKTSVEDEEDELKDAFGVFDKDS DGLISVEELSLVLCSLGMNEGKIVEN CKEMIRKVDLDGDGMVNF DEFKKMMRNGVTILTSS	Cucumis sativus	Cucurbitaceae	Cucurbitales	
DenCaC3L	>XP_020688260.1 calmodulin-like protein 3 [Dendrobium catenatum] MAALILFALLFLCGLLNSLFFPSSKL LPWFHSLLLSAISPPKPKPNPPPKPD LTKERRANRSESLADSLN LKTLFSTFDADGDGYISTAELNDSLR RLGLHATGDDLTNMMERVDANGDGLI DLNEFKELCASLGSEGEG EADEDRELREAFEVFDDNGDGLITVE ELSLVLKSLGLRQGDRAEACRDMINR VDLDGDGMVNFEEFKRMM VVDGGGSFF	Dendrobium catenatum	Orchidaceae	Asparagales	

GosRaC7L	>XP_012455812.1 PREDICTED: calmodulin-like protein 7 [Gossypium raimondii] MPTFLFRIFLLYNLLLDYLVPRKLKS FLSPSCTTTTPFVSVGGETEKNPSPA VALASVSPRCPLKRMDAA ELKRVFQLFDKNGDGTISKKELNDSL ENMGICIPDPELTQMIEKIDVNGDKC IDIDEFSELYRSIMDNKD EEEDMKEAFNVFDQNGDGYISVEELR SVLESLGIKQGKGIEDCKRMITKVDV DGDGRVNFMEFKQMMKGG GFTAMA	Gossypium raimondii	Malvaceae	Malvales	
JugReC3L	>XP_018836651.1 PREDICTED: calmodulin-like protein 3 [Juglans regia] MAIITVLLLAVLFIAGLVNILFRFPT KKFYASLKYVPANKSSSNISTTSPPT SHKERSPHNKAELKKIFA TFDKNGDGFITKQEMRESLKNIKMVV TDKEVEEMVVKVDANGDGLIEFDEFC VLCESMVSEERAAGNYDE GDGAKGVESSEGTGDEEDDLKEAFDV FDKDRDGLITVEELGLVLCSLGLKEG KKKEDCKEMIRNVDMDGD GMVNFDEFKKMMKGGGRLLLAS	Juglans regia	Juglandaceae	Fagales	
NelNuC3L1	>XP_010241567.1 PREDICTED: calmodulin-like protein 3 [Nelumbo nucifera] MMALVLLAVLFVCGLINSVFFLPPKK VITWIQSFPPISRSCTSITPPASVTV MASDKKKESAHDRAELRN IFATFDKNSDGFINKEELTESLKNIG ISTTDAEVKDMIERLDANKDGLIDLD EFCKLYDSVGKPQDRGRK DGEEGSTEEEDGGVDQEMELKEAFDV FDGNKDGLITVEELSLVLESLGLKQG WKSEDCKEMIRSVDMDGD GMVNFEEFKKMMMKAGGCLVSLS	Nelumbo nucifera	Nelumbonaceae	Proteales	

NelNuC3L2	>XP_010250191.1 PREDICTED: calmodulin-like protein 3 [Nelumbo nucifera] MVMAFVLLAVFFVCGLVNSLFYLPPK KLLAWIQALIPIAKPSLITSPATTTT TTSSDKAELRNVFATFDK NSDGIITEEELRESLKNIGFSITDTD LVHMVEKLDSNRDGLIDLEEFSKLYE SVGISRSKQRGGRDGELL DCREEEEVDEERDLKEAFDVFDGNRD GLITVEELSLVLSSLGLKQGLRSEDC REMIKSVDMDGDGMVNFE EFKKMMMKAGGSCVGIS	Nelumbo nucifera	Nelumbonaceae	Proteales	
NicAtC3L	>XP_019255618.1 PREDICTED: calmodulin-like protein 3 [Nicotiana attenuata] MSTVLSIFFLAILFIIGLITTLLNFP KEKFQTLIQSISLKSPPLHENRISTT CSSSRSMDEKKVKNSSIK STSSNNYNKLELRSIFATFDKNNDGY ITKQELKLSLKNIGIFIEDKDIIDMV EKVDSNKDGLIDIDEFYQ LCHTFLGIEAVNEEEESNREKDLKDA FDVFDYDKDGLISVEELSKILSSLGL RQGKKLDYCKEMISKVDV DGDGMVNFDEFKKMIKGCGTLVPIS	Nicotiana attenuata	Solanaceae	Solanales	
NicSyC3L	>XP_009778097.1 PREDICTED: calmodulin-like protein 3 [Nicotiana sylvestris] MLTLSILFLAFLFILGLITTLFNFPT KKFQSWIFSLSIKAQTPSSSPLFKNS TSTSPPLVEQKIMKRSTS NSHNKVELRSIFATFDKNNDGYITKQ ELKQSLNNIGIYMEDRDIVEMVEKVD SNKDGLIDLDEFYELCHS FLGIQGVIGSQENSGEMNQEEEANRE RDLKDAFDVFDYDKDGLISEEELSKV LSSLGLNQGKKLEDCKEM IRKIDVDGDGMVNFDEFKKMMKLGGR LIPIS	Nicotiana sylvestris	Solanaceae	Solanales	

NicTaC3L	>XP_016440228.1 PREDICTED: calmodulin-like protein 3 [Nicotiana tabacum] MLTLSILFLAFLFILGLITTLFNFPT KKFQSWIFSLSIKAQTPSSSPLFKNS TSTSPPLVEQKIMKRSTS NSHNKVELRSIFATFDKNNDGYITKQ ELKQSLNNIGIYMEDRDIVEMVEKVD SNKDGLIDLDEFYELCHS FLGIQGVIGSQENSGEMNQEEEANRE RDLKDAFDVFDYDKDGLISEEELSKV LSSLGLNQGKKLEDCKEM IRKIDVDGDGMVNFDEFKKMMKLGGR LIPIS	Nicotiana tabacum	Solanaceae	Solanales	
NicToC3L	>XP_009608019.1 PREDICTED: calmodulin-like protein 3 [Nicotiana tomentosiformis] MLTLSILFLALLFILGLITTLFNFPT KKFQSWIYSLSIKAQTPTPSPLVKNS TLSSPPMAEQKIMRRSTS NSHNKVELRSIFATFDKNNDGYITKQ ELKQSLKNIGIYMEDIDIVEMVEKVD SNKDGLIDLDEFYELCHS FLGIEGIIGSQENSGEMNQEEEANRE RDLKDAFDVFDYDKDGLISEEELSKV LSSLGLNQGKKLEDCKEM IRKIDVDGDGMVNFDEFKKMMKVGGR LIPIS	Nicotiana tomentosiformis	Solanaceae	Solanales	

Appendix IV. MSA of CMLs with AtCML4_5-like N-terminus

```
RapSaC3L2  ---------------------------------MATNLLK----------------LSS
EucGrC3L2  ---------------------------------MPAIITR-IFLLYHLLHTWFHYLVPK
ZizJuC3L2  ---------------------------------MPTIFLR-IFLIYNLFNSLLLSLVPK
LotJaC7L   ---------------------------------MPTILHR-IFLLYNLLNSFLLSLVPK
VigAnC3L1  ---------------------------------MPTIMLR-FFLLYNLLRPFLLCLVPK
VigRaC3L1  ---------------------------------MPTIMLR-FFLLYNLLRPFLLCLVPK
PhaVuC3L1  ---------------------------------MPTILHR-FFLLYNLLHPFLLFLVPK
GlyMaC3L1  ---------------------------------MPTILHR-IFLLYNLVHSFLLCLVPK
CajCaC3L1  ---------------------------------MPTIFHR-IVVVYEVLYPFLVRLIPK
PruMuC3L2  ---------------------------------MPTIFPR-IFLIYNLLNTFLLSLVPK
PruPeC3L2  ---------------------------------MPTIFPR-IFLIYNLLNTFLLSLVPK
PruAvC3L   ---------------------------------MPTIFPR-IFLIYNLLNTFLLSLVPK
MalPyC3L   ---------------------------------MPTIFRR-IFLIYNLLNTFLLSLVPK
PopEuC3L2  ---------------------------------MPTILLR-IFLLYNLLNSFLLSLVPK
PopTrC3L1  ---------------------------------MPTILLR-IFLLYNLLNSFLLSLVPK
PopEuC3L3  ---------------------------------MRTILLR-IFLLYNLLNSFLLSLVPK
PopEuC3L4  ---------------------------------MRTILLR-IFLLYNLLNSFLLSLVPK
PopTrC3L3  ---------------------------------MRTILLR-IFLLYNLLNSFLLSLVPK
CarPaC3L   ---------------------------------MPTILLR-IFLVYNLLNSILLYLIPK
JatCuC3L2  --------------------------------------MLK-IFLLYHLLHSLLVYLLPK
HevBraC3L  ---------------------------------MPTILLT-IFLLYNLLNSFLLYLIPK
VitViC3L2  ---------------------------------MPTFLHR-IFLLYNLLNSLVLFLVPK
CicArC7L   ---------------------------------MPTILLR-IFLLYNVVNSFLISLVPK
MedTrC7L   ---------------------------------MPTILLR-IFLLYNVVNSFLISLVPK
CiCl2CiSi2 ---------------------------------MRFILLR-IFLLY----TFILHLLPK
ElaGuC3L1  ---------------------------------MPTVLLR-ISLICHLLKTLLHYFLPK
ElaGuC3L2  -MALKPPFLQPFSPPIPPHHSLHWQSPPPPLNSPMPTVFLR-ISLICHLLNSLLHYFLPH
PhoDaC3L   ---------------------------------MPPVLLR-ISLVCHLLNSLLHYFLPH
MacCoC3L   ---------------------------------MPTVFLR-ISLLINLLNSILFYFFPN
EryGuC3L   ---------------------------------MPTILLR-IFLLYKLLNTIFLYLVPK
SesInC3L   ---------------------------------MPTILLR-IFLVYNLI---LSYLVPK
RicCoC3L   ---------------------------------MPTILLR-IFLLYNLLNSFLLSLVPK
GosArC7L   ---------------------------------MPSLLFR-IFLLYNLL---LDYLVPR
GosRaC7L   ---------------------------------MPTFLFR-IFLLYNLL---LDYLVPR
TheCaC3L2  ---------------------------------MPTVLLR-IFLVYNLV---LDYLVPK
CorOlC3L   ---------------------------------MPTVLLR-IFLLYNLV---LDYLVPK
CorCaC3L   ---------------------------------MPTVLLR-IFLLYNLV---LDYLVPK
PunGrC3L   -ML------------------------------MPTILKR-IFLIYNL----LLYFVPK
SolLyC3L1  -MQ------------------------------FPAIFFK-TRCIFNLFNPILLSLLPK
```

```
SolTuC3L1  -MQ------------------------------FPAIFFK-TRFIYNLFNPILLSLLPK
ADu2AIp2   ----------------------------------MPAIL-----LLYNILNSFLISLIPK
MusAcC3L4  -MEL---------------------------TPMPAIFVG-IFLICHHLNSRLLRFLPE
AraLyC4L   -------------------------------------MVR-VFLPYNLFNSFLLCLVPK
AraThC4    -------------------------------------MVR-VFLLYNLFNSFLLCLVPK
CamSaC4L1  -------------------------------------MVKSVFLLYNLFHSFLLCLVPK
CamSaC4L2  -------------------------------------MVRSVFLLYNLFHSFLLCLVPK
CapRuC4L   -------------------------------------MVR-VFLLYSLFNSFLLSLVPK
BraNaC4L1  -------------------------------------MVR-VILLYNLLNSFLLCLVPK
BraRaC4L1  -------------------------------------MVR-VFLLYNLLNSFLLCLVPK
BraOlC4L2  -------------------------------------MVR-VFLLYNLLNSFLLCLVPK
RapSaC4L2  -------------------------------------MVR-VFLLYNLLNSFLLCLVPK
BraNaC4L2  -------------------------------------MVR-VFLLYNLINSFLLYLVPK
BraOlC4L1  -------------------------------------MVR-VFLLYNLINSFLLCLVPK
BNa3BRa2   -------------------------------------MVR-VFLLYNLINSFLLCLVPK
RapSaC4L1  -------------------------------------MVR-VFLLYNLINSFLLCLIPK
EutSaC4L   -------------------------------------MVR-VFLLYNLFNSILLCLVPK
TarHaC4_5L ----------------------------------MPAVMVR-IFLLYNLFNSFLLCLVPK
AraLyC5L   -------------------------------------MVR-IFLLYNILNSFLLSLVPK
AraThC5    -------------------------------------MVR-IFLLYNILNSFLLSLVPK
CamSaC5L1  -------------------------------------MVR-IFVLYNILNSFLLSLVPK
CamSaC5L3  -------------------------------------MVR-IFVLYNILNSFLLSLVPK
CamSaC5L2  -------------------------------------MVR-IFVLYNILNSFLLSLVPK
EutSaC5L   -------------------------------------MVR-IFLLYNLLNSFLLSLVPK
CapRuC5L   -------------------------------------MVR-IFLLYNILNSFLLSLVPK
BNa1BOl2   -------------------------------------MVR-IFLLYNLLNSFLLSLVPK
BraNaC5L2  -------------------------------------MVR-IFLLYNLLNSFLLSLVPK
BraRaC5L1  -------------------------------------MVR-IFLLYNLLNSFLLSLVPK
BN53BO51   -------------------------------------MMR-IFLLYNLLNSFLLSLVPK
BraRaC5L2  -------------------------------------MVR-IFLLYNLLNSFLLSLVPK
RapSaC5L1  -------------------------------------MVR-IFLLYSLLNSFLLSLLPK
MusAcC3L5  -MEL---------------------------TPLPIVLVR-LSLLCLRLISRLLYFLPK
DauCaC3L2  MLKH---------------------------KAISAILLR-AFLFYNVLNSILAYLVPK
CepFoC3L   -------------------------------------MLR-ISLVYNLLNTFLLSLVPK
HelAnC3L   -------------------------------------MPR-IFLLYNLIYSIFLSFLPK
VigAnC3L2  ----------------------------------MPTIMLR-FFLLYNLLRPFLLCLVPK
ElaGuC6L   ---M-----------------------------AALLFFA-ILFTCGLINS-YFFLHPP
CapAnC3L   MFTL-----------------------------LTILFLA-FLFIIGLITT-FFNFPTN
NicAtC3L   MSTV-----------------------------LSIFFLA-ILFIIGLITT-LLNFPKE
NsyNtaC3   -MLT-----------------------------LSILFLA-FLFILGLITT-LFNFPTK
NicToC3L   -MLT-----------------------------LSILFLA-LLFILGLITT-LFNFPTK
```

```
JugReC3L    -MAI-----------------------------ITVLLLA-VLFIAGLVNI-LFRFPTK
NelNuC3L1   ---M-----------------------------MALVLLA-VLFVCGLINS-VFFLPPK
NelNuC3L2   --MV----------------------------MAFVLLA-VFFVCGLVNS-LFYLPPK
CucMeC7L    MEPI----------------------------FNFLLLS-VLFVAGFVNF-LLYFPTK
CucSaC3L    MEPI----------------------------FNFLLLS-VLFVAGFINF-LLYFPSK
DenCaC3L    ---M-----------------------------AALILFA-LLFLCGLLNS-LF-FPSS
AraThC24    ---M-------------------------------------------------------


RapSaC3L2   QI-RR-LSPI-----------------------------------TRSLTIRT---SA-
EucGrC3L2   KL-RV-YLPP---SWS---PLR-----------LD---------------PTPP---PL-
ZizJuC3L2   KI-RH-FFPP---SWF---PLQ-----------APPLPS-----------PPSP---PS-
LotJaC7L    KV-IA-FLPQ---SWF---PHQ-----------TPSFSS-----------SSSS---SS-
VigAnC3L1   KV-RA-ILSP---SWF---RSS-----------STTAPTPTQ-----P--SSSS---SS-
VigRaC3L1   KV-RA-ILSP---SWF---RSST----------TTTAPTPTQ-----PSSSSSS---SS-
PhaVuC3L1   KV-RA-ILSP---SWF---RST-----------TTPP-------------PPSS---SS-
GlyMaC3L1   KV-RP-FLPP---SWF---QTK-----------TITAPS-----------SSSS---SS-
CajCaC3L1   KV-RA-FFPSAGGSWS-----------------------------------------
PruMuC3L2   NL-RP-LLPS---SWF---PCQ-----------TNLVATNTP----LPHFPPSS---SS-
PruPeC3L2   NL-RP-LLPS---SWF---PCQ-----------TNLVATNTS----LPHFPPSS---SS-
PruAvC3L    NL-RP-LLPS---SWF---PCQ-----------TNLVATSTP----LPHFPPSS---SS-
MalPyC3L    HL-RP-LLPS---SWF---PHH-----------TTLLDTKTP----SPQPPPPS---LL-
PopEuC3L2   KL-RF-LLPT---SWY---HHHQANTNTSWCHPHQANTNTK---------KPSS---LL-
PopTrC3L1   KL-RF-LLPT---SWY---HPHQANTNTSWCHPHQANTNTK---------KPSS---LL-
PopEuC3L3   KL-RF-LLPT---SWY---HHP-----------HQAITNTR---------KPSS---LL-
PopEuC3L4   KL-RF-LLPT---SWY---HHP-----------HQAITNTR---------KPSS---LL-
PopTrC3L3   KL-RF-LLPT---SWY---HHP-----------HQAITNTK---------KPSS---LL-
CarPaC3L    KL-RG-FLPP---SWY---PHPHPHHHH---HQQQQQPNLVL-----DSSSKSP---SP-
JatCuC3L2   KL-RF-LLPS---SWL---PHQ-----------ANFPPNKKP-----PSSSSNT---SS-
HevBraC3L   KL-RTFFLPS---SWC---SHQ-----------ANSLFKQQ--------TLPPS---SS-
VitViC3L2   KL-RI-FLPT---SWF---HPH-----------QTQEANLV--------DSKTS---KT-
CicArC7L    KL-RT-FFPH---SWF---SHQ-----------TLKTNLNT-------TTLSSS---KK-
MedTrC7L    KL-IT-FFPH---SWF---THQ-----------TL-------------TTPSST---SK-
CiCl2CiSi2  KL-RR-FLPR---SWF---PAP-----------AL---------------GPSL---SS-
ElaGuC3L1   KL--S-FLRT---AKV-----------------------------------SA------P-
ElaGuC3L2   KL-IS-LLLP---SSR-----------------------------------SSSG---RP-
PhoDaC3L    KL-SS-LLPS---SWL---PRACLQEPA---PDAAKAPSHC------PSPRSSP---CP-
MacCoC3L    KL-KS-ILPP---SWF---PNSHQSFST---NSTTSIPNTTIIPSTFSSSSSSS---LP-
EryGuC3L    KL-RT-FLPP---SWY---PYLHQQEQQ---KQQKHNNTNTI-NE--PASPSSS---PV-
SesInC3L    KL-RA-YLPS---SWY---PYQQQQQQQ---QQVKKEPTVA---------LSSS---IV-
RicCoC3L    KLVRF-FVPS---SWY---NSNTHQ--------ANLLINQEL-----QQQEEEE---ET-
```

```
GosArC7L   KL-KS-FLSP---SCT---ITTPFVSVG---GETEKNPS-----------PAVA---LA-
GosRaC7L   KL-KS-FLSP---SCT---TTTPFVSVG---GETEKNPS-----------PAVA---LA-
TheCaC3L2  KL-KT-FLPS---SWI---PTRTLVSTG---SESKTHTSTS-------PAPESA---SA-
CorOlC3L   KL-KT-FLPS---SWIPPPPTHTLVSTA---TESKSSSS-----------PEPA---PA-
CorCaC3L   KL-KT-FLPS---SWI-PPPTHTFVSTV---TESKSSSS-----------PEPA---AAP
PunGrC3L   KL-RP-FLPSP--SWF---CSA-----------VSGTANGN---------VVLL---PS-
SolLyC3L1  KL-IS-FLPP---SWF---HQKRIHS-------RSPAPPQQ---------SPVS---VS-
SolTuC3L1  KL-IS-FLPP---SWF---HQKHLHS-------RSPAPPQQ---------SPVS---VS-
ADu2AIp2   KL-RP-FFPF---SWF---PHQ-----------TNNTSSSS-------SSSSSSPRRAS-
MusAcC3L4  KL-ISLLLPF---SWH---PPTSKD--------GLSPPATAL--------SSIASF-RS-
AraLyC4L   KL-RV-FFPP---SWY---IDD-----------KNPP--------------------QS-
AraThC4    KL-RV-FFPP---SWY---IDD-----------KNPPP-------------------PD-
CamSaC4L1  KL-RV-LFPP---SWY---IDD-----------KNPPP-------------------PS-
CamSaC4L2  KL-RV-LFPP---SWY---IDD-----------KNPPP-------------------PS-
CapRuC4L   KL-RV-LFPP---SWY---IDD-----------KNPPPV------------------PS-
BraNaC4L1  KL-RV-LFPP---SWY---TDD-----------KITPP----------------------
BraRaC4L1  KL-RV-LFPP---SWY---TDD-----------KITPP----------------------
BraOlC4L2  KL-RV-LFPP---SWY---TDD-----------KITPP----------------------
RapSaC4L2  KL-RV-LFPP---SWY---TED-----------KIPPP----------------------
BraNaC4L2  KL-RV-LFPP---SWY---IDD-----------NIPPP-------------------LS-
BraOlC4L1  KL-RV-LFPP---SWY---IDD-----------NIPPP-------------------LS-
BNa3BRa2   KL-RV-LFPP---SWY---IDD-----------NIPPP-------------------LS-
RapSaC4L1  KL-RV-LFPP---SWY---MDD-----------NIPPP-------------------LS-
EutSaC4L   KL-RV-LFPH---SWI---IDD-----------KNPPP----------------------
TarHaC4_5L KL-RG-IFPP---SWY---PHHVDDDNP-----KNPPP-------------------SS-
AraLyC5L   KL-QT-LFPL---SWL---DKTLH---------KNSPPSP----------STML---PS-
AraThC5    KL-RT-LFPL---SWF---DKTLH---------KNSPPSP----------STML---PS-
CamSaC5L1  KL-RT-LFPL---SWF---DKTLH---------KNSPPSP----------PTML---PS-
CamSaC5L3  KL-RT-LFPL---SWF---DKTLH---------KNSPPSP----------STML---PS-
CamSaC5L2  KL-RS-LFPL---SWF---DKTLH---------KNSPPSP----------PTML---PS-
EutSaC5L   KL-RS-LFPL---SWF---DKTLH---------KTSP-------------SSML---PS-
CapRuC5L   KL-RS-LFPL---SWF---DKTLH---------MNSPPSP----------PTML---PS-
BNa1BOl2   KL-RS-LFPL---SWF---DKTPH---------KN---------------SSML---PS-
BraNaC5L2  KL-RT-LFPL---SWF---DKTPH---------KN---------------SSML---LS-
BraRaC5L1  KL-RT-LFTL---SWF---DKTPH---------KN---------------SSML---PS-
BN53BO51   KL-RT-LFSL---SWF---DKTLH---------KNSPPS-----------PSML---PS-
BraRaC5L2  KL-RT-LFSL---SWF---DKTLH---------KNSPPS-----------PSML---PS-
RapSaC5L1  KL-RT-LFPL---SWF---DKTLH---------KNSPPS-----------ASMLPS-PS-
MusAcC3L5  KL-TS-LLLSP--SSS---SS------------SSSSPSHEN-----PAASFTS---TV-
DauCaC3L2  KL-RN-YVPT---FWY---SRE-----------AGIDRNH----------TNLT---SS-
CepFoC3L   KL-----IPA---SWY---HHQ-----------NNHIVDT----------KTLP---PP-
```

```
HelAnC3L   NL-RH-YLPK---SHT---QQQ-----------QQQIQND----------TVSQ---PS-
VigAnC3L2  KV-RA-ILSP---SWF---RSS-----------STTAPTPT---QP----SSSS---SS-
ElaGuC6L   KL-LT-RLAS---FLY---VTST------------PKPIVK---------TPSK---DG-
CapAnC3L   KF-QS-LIQK---ISL---KSPSL-----------QEKTI----------ITPS---PS-
NicAtC3L   KF-QT-LIQS---ISL---KSPPL-----------HENRIS---------TTCS---SS-
NsyNtaC3   KF-QS-WIFS---LSI---KAQTP----------SSSPLFK---------NSTS---TS-
NicToC3L   KF-QS-WIYS---LSI---KAQTP----------TPSPLVK---------NSTL---SS-
JugReC3L   KF-YA-SLKY---VPA---NKSSS-------------------------NIST---TS-
NelNuC3L1  KV-IT-WIQS---FPP---ISR----------------------------SCTS---IT-
NelNuC3L2  KL-LA-WIQA---LIP---IAK----------------------------PSLI---TS-
CucMeC7L   RF-TA-WFQS---IKP---SSQIPH--------FKSTPLQ----------PPPP------
CucSaC3L   RF-SA-WFQS---IKP---SSQITH--------FKSTPLQ----------PPPP---PS-
DenCaC3L   KL-LP-WFHS---LLL---SAISP-----------PKPKPN---------PPPK------
AraThC24   ------------------------------------------------------------SS-


RapSaC3L2  TS--------------------TTSS---G-SKKMDQAELSRIFQMFDRNGDGKITKQEL
EucGrC3L2  PR--------------------SLSL---V-KAPMDAAELKRVFQMFDRNGDGRITKKEL
ZizJuC3L2  SS--------------------CSFL---A-QKRMDPTELKRVFQMFDRNGDGRITKKEL
LotJaC7L   SRGNLVIQKTTDDCDPCQL-LPLDTS---L-IPKMDPTELKRVFQMFDRNGDGRITKKEL
VigAnC3L1  SS--------------------AFTR---I-SLSMDPNELKRVFQMFDRNGDGRITKKEL
VigRaC3L1  SS--------------------AITR---I-SLSMDPNELKRVFQMFDRNGDGRITKKEL
PhaVuC3L1  SR--------------------LITT---I-SPPMDPHELKRVFQMFDRNGDGRITKKEL
GlyMaC3L1  SS--------------------ARII---K-RTTMDPNELKRVFQMFDRNGDGRITKKEL
CajCaC3L1  ----------------------SQKS---R-RTSMDPQELRRVFQMFDRNGDGRITKKEL
PruMuC3L2  SS------------------LPCGAP---K-VIRMDPNELKRVFQMFDRNGDGRITKQEL
PruPeC3L2  SS------------LPLPLPLPCGAP---K-VIRMDPNELKRVFQMFDRNGDGRITKQEL
PruAvC3L   SS--------------------SCGAH---K-VIRMDPNELKRVFQMFDRNGDGRITKQEL
MalPyC3L   SL-------------PLPLPLPSGGA---C-HVRMDPNELKRVFQMFDRNGDGRITKQEL
PopEuC3L2  PS----------------------PSF---V-LTRMDQAELKRVFQMFDRNGDGKITKKEL
PopTrC3L1  PS----------------------PSF---V-LARMDQAELKRVFQMFDRNGDGKITKKEL
PopEuC3L3  PS--------------------SSNF---V-VKRMDQAELKRVFQMFDRNGDGRITQKEL
PopEuC3L4  PS--------------------SSNF---A-VKRMDQAELKRVFQMFDRNGDGRITQKEL
PopTrC3L3  PS--------------------SSNF---V-LKRMDQAELKRVFQMFDRNGDGRITQKEL
CarPaC3L   SP--------------------SSVS---G-LKRMDSAELKRVFQMFDKNGDGRITKKEL
JatCuC3L2  SS--------------------SSSV---V-HKRMDTTELRRVFQMFDRNGDGRITRKEL
HevBraC3L  SS--------------------AAAV---V-RKRMDSVELARVFQMFDRNGDGRITKKEL
VitViC3L2  PG--------------------RSLV---S-RKRMESAEMKRVFQMFDRNGDGRITKTEL
CicArC7L   GF--------------------VVIT---K-SITMDPNELKRVFQMFDRNDDGRITKKEL
MedTrC7L   RG--------------------LVFT---K-TITMDPNELKRVFQMFDRNDDGRITKKEL
CiCl2CiSi2 QS--------------------NTNP---T-RSTMDQAELDRVFQMFDHNGDGRISKKEL
```

```
ElaGuC3L1  RV--------------------FILA---T-PPGMDPSELKRVFQMFDRNGDGRITKKEL
ElaGuC3L2  RV--------------------LILA---T-PPEMDPSELKRVFQMFDRNGDGRITKKEL
PhoDaC3L   RV--------------------SILA---T-PPGMEPSELKRVFQMFDRNGDGRITKKEL
MacCoC3L   SS--------------------SSLI---Q-QEVMDPAELKRVFQMFDRNGDGRITKKEL
EryGuC3L   IS--------------------PLHK---F-PRRMDADELRRVFQMFDRNGDGRITQKEL
SesInC3L   PS--------------------SRIV---I-HRRMDPNELKRVFQMFDRNGDGRITKQEL
RicCoC3L   LV--------------------VPSA---A-RKRMDSTELKKVFQMFDTNGDGRITKEEL
GosArC7L   SV--------------------SPRC---P-LKRMDAAELKRVFQLFDKNGDGSISKKEL
GosRaC7L   SV--------------------SPRC---P-LKRMDAAELKRVFQLFDKNGDGTISKKEL
TheCaC3L2  PA--------------------SSAC---C-PQRMDGAELKRVFQMFDKNGDGRITKKEL
CorOlC3L   PA--------------------SPSC-RRQ-SQRMDAAELKRVFQLFDKNGDGRISKQEL
CorCaC3L   PA--------------------SPSC-RRQ-SQRMDAAELKRVFQLFDKNGDGRISKQEL
PunGrC3L   PS--------------------LRAR---K-ATVMDPTELRRVFQMFDRNGDGSISKKEL
SolLyC3L1  DA--------------------VESH-----QKRMDSDELRRIFQIFDRNGDGRITKNEL
SolTuC3L1  DA--------------------VQSH---I-QKRMDSDELRRIFQIFDRNGDGRITKNEL
ADu2AIp2   RA--------------------IIIT---K-TRIMDPNELRRVFQMFDRNGDGRISRSEL
MusAcC3L4  PSF-------------------GPKA---S-ARVMDPSELKRVFQMFDRNGDGRITKTEL
AraLyC4L   KS----------------------ESE---S-PGRRDPVDLKRVFQMFDKNGDGRITKEEL
AraThC4    ES----------------------ETE---S------PVDLKRVFQMFDKNGDGRITKEEL
CamSaC4L1  QV----------------------ETE---S-PGRTDLVDLKRVFQMFDKNGDGRITKEEL
CamSaC4L2  QL----------------------ETE---S-PGRTDLVDLKRVFQMFDKNGDGRITKEEL
CapRuC4L   QS----------------------ETE---S-PGRTDPVDLKRVFQMFDKNGDGRITKEEL
BraNaC4L1  -S----------------------ESE---C-SLRTDPVDLKRVFQMFDKNGDGRITKEEL
BraRaC4L1  -S----------------------ESE---C-SLRTDPVDLKRVFQMFDKNGDGRITKEEL
BraOlC4L2  -S----------------------ESE---C-SLRTDPVDLKRVFQMFDKNGDGRITKEEL
RapSaC4L2  -P----------------------ESE---C-SLRTEPVDLKRVFQMFDKNGDGRITKEEL
BraNaC4L2  EP----------------------EPK---S-QTRTDPVDLKQVFQMFDKNGDGRITKEEL
BraOlC4L1  EP----------------------EPK---S-QTRTDPVDLKQVFQMFDKNGDGRITKEEL
BNa3BRa2   EP----------------------EPK---S-QTRTDPVDLKQVFQMFDKNGDGRITKEEL
RapSaC4L1  EP----------------------EPE---SREARTDPVDLKRVFQMFDKNGDGRITKEEL
EutSaC4L   -S----------------------KSE---S-PARTDPVDLKRVFQMFDKNGDGRITKEEL
TarHaC4_5L SP--------------------SPSP---P-PARVDPVELKRVFQMFDKNGDGRITKEEL
AraLyC5L   PP--------------------SSSA---P-TKRIDPSELKRVFQMFDKNGDGRITKEEL
AraThC5    PS--------------------SSSA---P-TKRIDPSELKRVFQMFDKNGDGRITKEEL
CamSaC5L1  PS--------------------SSSSSSVP-TKRIDPSDLKRVFQMFDKNGDGRITKEEL
CamSaC5L3  PS--------------------SSSSSSVP-TKRIDPSELKRVFQMFDKNGDGRITKEEL
CamSaC5L2  PS--------------------SSSS-SVP-TKRIDPSELKRVFQMFDKNGDGRITKEEL
EutSaC5L   PS--------------------PSSA---P-TKRTDPSELKRVFQMFDKNGDGRITKEEL
CapRuC5L   PS--------------------SSPL---P-TKKIDPSELKRVFQMFDKNGDGRITKEEL
BNa1BOl2   PS--------------------PSSA---P-TRKTDPSELKRVFQTFDKNGDGRITKTEL
BraNaC5L2  PS--------------------PSSA---P-SIKTDPTELKRVFQTFDKNGDGRITKTEL
```

```
BraRaC5L1  PS--------------------PSSA---P-SIKTDPTELKRVFQTFDKNGDGRITKTEL
BN53BO51   PS--------------------PSST---P-TTKIDPSELKRVFQTFDKNGDGRITKQEL
BraRaC5L2  PS--------------------PSST---P-TTKIDPSELKRVFQTFDKNGDGRITKQEL
RapSaC5L1  PS--------------------PSSA---S-TRKIDPSELKRVFQTFDKNGDGRITKQEL
MusAcC3L5  AA--------------------RPAS---S-APSMDPSELKPVFHMFDRNGDGRITKEEL
DauCaC3L2  NT--------------------ELTL---H-FPRMEADELRKVFEMFDHNGDGRITKQEL
CepFoC3L   LP--------------------PLAR---A-QKRMDPTELDRVFQMFDRNGDGRITKMEL
HelAnC3L   QP--------------------PQTP---R-TSRMNPDQLQRIFQMFDKNNDGTITKHEL
VigAnC3L2  SS--------------------AFTR---I-SLSMDPNELKRVFQMFDRNGDGRITKKEL
ElaGuC6L   KE---------------------VVV---S-EIVTDKAGIETVFATFDKDGDGFITTEEL
CapAnC3L   IT--MVDKKVMN-----------------R-SNNYNKVELRSIFATFDKNNDGYITKQEL
NicAtC3L   RS--MDEKKVKN--------SSIKST---S-SNNYNKLELRSIFATFDKNNDGYITKQEL
NsyNtaC3   PP--LVEQKI------------MKRS---T-SNSHNKVELRSIFATFDKNNDGYITKQEL
NicToC3L   PP--MAEQKI------------MRRS---T-SNSHNKVELRSIFATFDKNNDGYITKQEL
JugReC3L   PP--------------------TSHK---E-RSPHNKAELKKIFATFDKNGDGFITKQEM
NelNuC3L1  PPASVTVMA-------------SDKK---K-ESAHDRAELRNIFATFDKNSDGFINKEEL
NelNuC3L2  PA---------------------TTT---T-TTSSDKAELRNVFATFDKNSDGIITEEEL
CucMeC7L   PP---------------------PPP---P-PPPPSAMELKKVFGTFDKNDDGFITKKEL
CucSaC3L   PS---------------------PSP---S-PPPPSAMEMKKVFGTFDKNDDGFITKKEL
DenCaC3L   PD--LTKER-------------RANR---S-ESLADSLNLKTLFSTFDADGDGYISTAEL
AraThC24   KN---------------------GVV---R-SCLGSMDDIKKVFQRFDKNGDGKISVDEL


RapSaC3L2  SDSLENLGIYIPDKDLVQMIEKIDLNGDGYVDIEEFGGLYQSIM----------E-----
EucGrC3L2  SDSLENLGIYIPDKELAEMIEKIDVNGDGCVDIDEFGALYRSIM----------E-----
ZizJuC3L2  NDSLENLGIFIPDKELTQMIEKIDVNGDGCVDMDEFGELYQSIM----------D-----
LotJaC7L   NDSLENLGIFIPDKELTQMIERIDVNGDGCVDIDEFGELYQSIM----------D-----
VigAnC3L1  SDSLDNLGIFIPDKELTVMIERIDVNGDGCVDIDEFGELYQTIM----------D-----
VigRaC3L1  SDSLDNLGIFIPDKELTVMIERIDVNGDGCVDIDEFGELYQTIM----------D-----
PhaVuC3L1  NDSLENLGIFIPDKELTLMIERIDVNGDGCVDIDEFGELYQHIM----------D-----
GlyMaC3L1  NDSLENLGIFIPDKELGQMIERIDVNGDGCVDIDEFGELYQTIM----------D-----
CajCaC3L1  SDSLENLGIFIPDKELSLMIEKIDVNGDGCVDIDEFGELYQTIM----------D-----
PruMuC3L2  NDSLENLGIFIPDKELFNMIQKIDVDGDGCVDIDEFGELYQSIM----------D-----
PruPeC3L2  NDSLENLGIFIPDKELFNMIQKIDVNGDGCVDIDEFGELYQSIM----------D-----
PruAvC3L   NDSLENLGIFIPDKELFNMIQKIDVNGDGCVDIDEFGELYQSIM----------D-----
MalPyC3L   NDSLENLGIYIPDKELFNMIEKIDVNGDGCVDIDEFGELYQSIM----------D-----
PopEuC3L2  NDSLENLGIFIPDKELTQMIETIDVNGDGCVDIDEFGELYQSLM----------D-----
PopTrC3L1  NDSLENLGIFIPDKELTQMIETIDVDGDGCVDIDEFGELYQSLM----------D-----
PopEuC3L3  NDSLENIGIFIPDKELTQMIENIDANGDGCVDIDEFGELYRSLM----------D-----
PopEuC3L4  NDSLENIGIFIPDKELTQMIENIDANGDGCVDIDEFGELYRSLM----------D-----
PopTrC3L3  NDSLENIGIFIPDKELTQMIEKIDVNGDGCVDIDEFGELYQSLM----------D-----
```

```
CarPaC3L   NDSLENLGIFIPDKELAQMIEKIDVNGDGCVDIDEFGSLYKSIM----------D-----
JatCuC3L2  SDSLENLGIFIPDSELTQMIDNIDVNGDGCVDIEEFGVLYQSIM----------D-----
HevBraC3L  NDSLENLGIFIPDLELTQMIQNIDVNGDGCVDIDEFGALYQSIM----------D-----
VitViC3L2  NDSLENLGIYIPDKDLAQMIEKIDVNGDGCVDIDEFRALYESIM----------E-----
CicArC7L   NDSLENLGIFIPDKELSQMIEKIDVNRDGCVDIEEFRELYESIM----------N---GR
MedTrC7L   NDSLENLGIFIPDKELSQMIEKIDVNRDGCVDIEEFRELYESIM----------S-----
CiCl2CiSi2 NDSLENLGIYIPDVELTQMIERIDVNGDGCVDIDEFGALYKSIM----------E-----
ElaGuC3L1  SDSLENLGIYIPEGDLEAMIEKIDANGDGCVDVEEFGALYQNIM----------D-----
ElaGuC3L2  SDSLENLGIYIPEGDLESMIGKIDVNGDGCVDIEEFGALYQTIM----------D-----
PhoDaC3L   GDSLENLGIHIPEGDLESMIGKIDANGDGCVDIEEFGALYQTIM----------D-----
MacCoC3L   SDSLDNLGIFIPDKDLTQMIEKIDVNGDGCVDIDEFGALYQTIM----------D-----
EryGuC3L   SDSLENMGIFIPDKELSQMIDKIDVNGDGCVDIEEFGNLYQNIM----------D-----
SesInC3L   SDSLHNMGISIPDEELTQMIDKVDINGDGCVDIDEFGTLYQTIM----------D-----
RicCoC3L   NGSLENLGIFIPDKELSQMMETIDVNGDGGVDIEEFGALYQSIM----------D-----
GosArC7L   NDSLENMGICIPDPELTQMIEKIDVNGDKCIDIDEFSELYRSIM----------D-----
GosRaC7L   NDSLENMGICIPDPELTQMIEKIDVNGDKCIDIDEFSELYRSIM----------D-----
TheCaC3L2  NDSLENLGIFIPDGELTHMIEKIDVNGDNCVDIDEFGELYHSIM----------D-----
CorOlC3L   NDSLENLGIFIPDGELTQMIEKIDVNGDNCVDIDEFGELYQSIM----------D-----
CorCaC3L   NDSLENLGIFIPDGELTQMIEKIDVNGDNCVDIDEFGELYQSIM----------D-----
PunGrC3L   ADSLENLGIFIPDKELEDMIRRIDANGDGCVDIEEFEALYRSIM----------D-----
SolLyC3L1  NSSLENMGIFIPDPELIQMIEKIDVNGDGCVDIDEFGSLYQTIM----------D-----
SolTuC3L1  NDSLENMGIFIPDPELIEMIEKIDVNGDGCVDIDEFGSLYQTIM----------D-----
ADu2AIp2   TVSLENLGIFIPDKELAQMIDKIDANGDGFVDVEEFGELYESIM----------V-----
MusAcC3L4  SDSLENLGIYIPEAELASMIEKIDVNGDGCVDMDEFGALYRSIM----------D-----
AraLyC4L   NDSLENLGIFMPDKDLVQMIQKMDANGDGIVDIKEFESLYGSIV----------E-----
AraThC4    NDSLENLGIFMPDKDLIQMIQKMDANGDGCVDINEFESLYGSIV----------E-----
CamSaC4L1  NDSLENLGIFMPDKDLIQMIQKMDANGDGCVDINEFESLYGSIV----------E-----
CamSaC4L2  NDSLENLGIFMPDKDLIQMIQKMDANGDGCVDINEFESLYGSIV----------E-----
CapRuC4L   NDSLENLGIFMPDKDLIQMIQKMDANGDGCVDINEFESLYGSIV----------E-----
BraNaC4L1  NDSLENLGIFMPDKDLIQMIRKMDANGDGCVDINEFESLYGSIV----------E-----
BraRaC4L1  NDSLENLGIFMPDKDLIQMIRKMDANGDGCVDINEFESLYGSIV----------E-----
BraOlC4L2  NDSLENLGIFMPDKDLIQMIQKMDANGDGCVDINEFESLYGSIV----------E-----
RapSaC4L2  NDSLENLGIFMPDKDLIQMIQKMDANGDGCVDINEFESLYGSIV----------E-----
BraNaC4L2  NDSLENLGIFMPDKDLIQMIHKMDANGDGCVDIHEFESLYGSIV----------E-----
BraOlC4L1  NDSLENLGIFMPDKDLIQMIHKMDANGDGCVDIHEFESLYGSIV----------E-----
BNa3BRa2   NDSLENLGIFMPDKDLIQMIHKMDANGDGCVDIHEFESLYGSIV----------V-----
RapSaC4L1  NDSLENLGIFMPDKDLIQMIKNIDANGDGCVDIQEFESLYGSIV----------Q-----
EutSaC4L   NDSLENLGIFMPEKDLIQMIQKMDANGDGCVDIHEFESLYSSIV----------E-----
TarHaC4_5L NDSLENLGLFLPDRELAQMIQKIDANGDGCVDMDEFESLYKSIV----------D-----
AraLyC5L   NDSLENLGIYIPDKDLTQMIHKIDANGDGCVDIDEFESLYSSIV----------D-----
AraThC5    NDSLENLGIYIPDKDLTQMIHKIDANGDGCVDIDEFESLYSSIV----------D-----
```

```
CamSaC5L1   NDSLENLGIYIPDKDLTQMIHKIDANGDGCVDIDEFESLYSSIV----------D-----
CamSaC5L3   NDSLENLGIYIPDKDLTQMIHKIDANGDGCVDKDEFESLYSSIV----------D-----
CamSaC5L2   NDSLENLGIYIPDKDLTQMIHKIDANGDGCVDIDEFESLYSSIV----------D-----
EutSaC5L    NDSLENLGIYIPDKDLTQMIHKIDANGDGCVDIDEFESLYSSIV----------D-----
CapRuC5L    NDSLENLGIYIPDQDLTQMIHKIDANGDGCVDIDEFESLYGSIV----------D-----
BNa1BOl2    NDSLENLGIYIPDKDLTQMIHNIDANGDGCVDIDEFESLYSSIV----------D-----
BraNaC5L2   NDSLENLGIYIPDQELTQMIHNIDANGDGCVDIDEFESLYSSIV----------D-----
BraRaC5L1   NDSLENLGIYIPDKELTQMIHNIDANGDGCVDIDEFESLYSSIV----------D-----
BN53BO51    KDSLENLGIYIPDKDLTQMIHNIDTNHDGCVDIDEFESLYKSIV----------D-----
BraRaC5L2   KDSLENLGIYIPDKDLTQMIHNIDTNHDGCVDIDEFESLYRSIV----------N-----
RapSaC5L1   NNSLENLGIYIPDKDLTQMIHNIDKNHDGCVDIDEFESLYRSIV----------D-----
MusAcC3L5   SDSLRNLGMRVPEAELASMIERIDANGDGYVDSDEFATLYRSIM----------E-----
DauCaC3L2   NESLEKMGIFIPDQELTQMIEKIDVNNDGCVDIDEFGDLYQNIM----------N-----
CepFoC3L    NESLEKLGMFIPDKELTRMIEKIDVDGDGCVDIDEFGALYRSLM-DHEVDD---D-----
HelAnC3L    NESLENMKIFISDEDLVRMIDKVDINNDGCVDLDEFGVLYKEIM----------D-----
VigAnC3L2   SDSLDNLGIFIPDKELTVMIERIDVNGDGCVDIDEFGELYQTIM----------D-----
ElaGuC6L    EESFKRLGLFSTRNEIVSMMKRVDANGDGLIDLEEFGELYDSLG--RGRGGGDGD----E
CapAnC3L    KLSLKNIGIFMEDKDIVEMVEKVDSNKDGLIDLDEFCDLCHTYL-GIEEV----S----N
NicAtC3L    KLSLKNIGIFIEDKDIIDMVEKVDSNKDGLIDIDEFYQLCHTFL-GIEAV----------
NsyNtaC3    KQSLNNIGIYMEDRDIVEMVEKVDSNKDGLIDLDEFYELCHSFL-GIQGVIGSQE----N
NicToC3L    KQSLKNIGIYMEDIDIVEMVEKVDSNKDGLIDLDEFYELCHSFL-GIEGIIGSQE----N
JugReC3L    RESLKNIKMVVTDKEVEEMVVKVDANGDGLIEFDEFCVLCESMV-SEERAAGNYDEGDGA
NelNuC3L1   TESLKNIGISTTDAEVKDMIERLDANKDGLIDLDEFCKLYDSVG--KPQDRGRKD---GE
NelNuC3L2   RESLKNIGFSITDTDLVHMVEKLDSNRDGLIDLEEFSKLYESVGISRSKQRGGRD---GE
CucMeC7L    MESLKSMRMMITEKDAEEMLKEVDENGDGLIDFEEFCVLGEKLLMGFEE-----N-----
CucSaC3L    MESLKSMRMMITEKDAEEMLKGVDENGDGLIDFEEFCVLGGKLMMGFEE-----N-----
DenCaC3L    NDSLRRLGLHATGDDLTNMMERVDANGDGLIDLNEFKELCASLG----------S-----
AraThC24    KEVIRALSPTASPEETVTMMKQFDLDGNGFIDLDEFVALFQIGI-GGGG-----N-----


RapSaC3L2   ---------DR-D-----EEEDIREAFNVFDQNRDGFITVEELRSVLSSLGLKQGRTLED
EucGrC3L2   ---------ER-D-----EEEDMREAFNVFDQNGDGFITVDELRSVLASLGLKQGRTLED
ZizJuC3L2   ---------EK-D-----EEEDMREAFNVFDQNGDGFITVDELRSVLASLGLKQGRTVED
LotJaC7L    ---------ER-D-----EEEDMREAFNVFDQNGDGFITVEELRTVLASLGIKQGRTVED
VigAnC3L1   ---------ER-D-----EEDDMREAFNVFDQNGDGFITVEELRTVLSSLGLKQGRTVED
VigRaC3L1   ---------ER-D-----EEDDMREAFNVFDQNGDGFITVEELRTVLSSLGLKQGRTVED
PhaVuC3L1   ---------DR-D-----EDEDMREAFNVFDQNGDGFITVEELRTVLSSLGLKQGRTVED
GlyMaC3L1   ---------ER-D-----EEEDMREAFNVFDQNADGFITVDELRTVLSSLGLKQGRTVQD
CajCaC3L1   ---------ER-D-----EEEDMREAFNVFDQNGDGFITVDELRTVLSSLGLKQGRTVED
PruMuC3L2   ---------ER-D-----EDEDMKEAFNVFDQNGDGFITVDELRSVLSSLGLKQGRTIED
PruPeC3L2   ---------ER-D-----EDEDMKEAFNVFDQNGDGFITVDELRSVLSSLGLKQGRTIED
```

```
PruAvC3L   ---------ER-D-----EDEDMKEAFNVFDQNGDGFITVDELRSVLSSLGLKQGRTIED
MalPyC3L   ---------ER-D-----EEEDMKEAFNVFDQNGDGFITVDELRSVLSSLGLKQGRTIED
PopEuC3L2  ---------EK-D-----EEEDMREAFKVFDQNGDGFITVDELRSVLASLGLKQGRTLED
PopTrC3L1  ---------DK-D-----EEEDMREAFKVFDQNGDGFITVDELRSVLASLGLKQGRTLED
PopEuC3L3  ---------EK-D-----EEEDMREAFNVFDQNGDGFITVEELRSVLASLGLKQGRTFED
PopEuC3L4  ---------EK-D-----EEEDMREAFNVFDQNGDGFITVDELRSVLASLGLKQGRTFED
PopTrC3L3  ---------EK-D-----EEEDMREAFNVFDQNGDGFITVDELRSVLASLGLKQGRTFED
CarPaC3L   ---------EH-D-----EEEDMREAFNVFDQNGDGFITVDELKSVLASLGLKQGKTVED
JatCuC3L2  ---------ER-D-----EEEDMREAFNVFDRNGDGYITVDELRSVLASLGLKQGKAVED
HevBraC3L  ---------ER-D-----EEEDMKEAFNVFDQNGDGYITVDELRSVLAALGLKQGRTLED
VitViC3L2  ---------EK-D-----EDEDMKEAFNVFDQNGDGFITVDELKSVLGSLGLRHGRTVED
CicArC7L   ---------EE-E-----EEEDMREAFNVFDQNGDGFISVEELRSVLVTLGLKQGRTVED
MedTrC7L   ---------ER-D---EEEEEDMREAFNVFDQNGDGFISVDELRSVLVSLGLKQGRTVED
CiCl2CiSi2 ---------EK-D-----EEEDMKEAFNVFDQNGDGFITFDELKSVLGSLGLKQGRTVED
ElaGuC3L1  ---------ER-D-----EEEDMREAFNVFDQNGDGFITVEELRSVLASLGLKQGRTVED
ElaGuC3L2  ---------ER-D-----EEEDMREAFNVFDQNGDGFITVEELRSVLASLGLKQGRTVED
PhoDaC3L   ---------ER-D-----EEEDMREAFNVFDQNGDGFITVEELRSVLASLGLKQGRTVED
MacCoC3L   ---------EK-D-----EEEDMREAFNVFDQNGDGFITVEELRSVLSSLGLKQGRTVED
EryGuC3L   ---------ER-D-----EEEDMREAFNVFDQNGDGFITVDELKAVLASLGLKQGRAVED
SesInC3L   ---------ER-D-----EEEDMKEAFNVFDQNGDGFISVDELKSVLVSLGLKQGKAAED
RicCoC3L   ---------EK-D-----EDEDMREAFNVFDQNGDGYITGDELRSVLASLGLKQGRTAED
GosArC7L   ---------NK-D-----EEEDMKEAFNVFDQNGDGYISVEELRSVLESLGLKQGKGIED
GosRaC7L   ---------NK-D-----EEEDMKEAFNVFDQNGDGYISVEELRSVLESLGIKQGKGIED
TheCaC3L2  ---------DK-D-----EEEDMKEAFNVFDQNGDGYISVDELRSVLVSLGLKQGKTIED
CorOlC3L   ---------GK-D-----EEEDMKDAFNVFDQNGDGFISVDELRSVLVSLGLKQGKTIED
CorCaC3L   ---------GK-D-----EEEDMKDAFNVFDQNGDGFISVDELRSVLISLGLKQGKTIED
PunGrC3L   ---------ER-D-----EEEDMKEAFNVFDQNGDGFITVDELRSVLASLGLKQGRTIED
SolLyC3L1  ---------ER-D-----EEEDMREAFNVFDQNGDGFICVEELKSVLASLGLKQGRTVED
SolTuC3L1  ---------ER-D-----EEEDMREAFNVFDQNGDGFICVDELKSVLASLGLKQGRTVED
ADu2AIp2   ---------ERGD-----EEEDMKEAFNVFDQNGDGFISVEELRAVLSSLGLKQGRTDED
MusAcC3L4  ---------ER-D-----EEEDMREAFNVFDQNGDGYISVEELRSVLVSLGVKQGRTAED
AraLyC4L   ---------EK-------EEEDMRDAFNVFDQDGDGFITVEELKSVMASLGLKQGKTLEC
AraThC4    ---------EK-------EEGDMRDAFNVFDQDGDGFITVEELNSVMTSLGLKQGKTLEC
CamSaC4L1  ---------EK-------EEEDMRDAFNVFDQDGDGFITVKELKSVMASLGLKQGRTLKC
CamSaC4L2  ---------EK-------EEEDMRDAFNVFDQDGDGFITVKELKSVMASLGLKQGRTLKC
CapRuC4L   ---------EK-------EEEDMRDAFNVFDQDGDGFISVEELKSVMASLGLKQGKTLKC
BraNaC4L1  ---------EK-------EEEDMRDAFNVFDQDGDGFISVEELKSVMASLGLKQGKTLKC
BraRaC4L1  ---------EK-------EEEDMRDAFNVFDQDGDGFISVEELKSVMASLGLKQGKTLKC
BraOlC4L2  ---------EK-------EEEDMRDAFNVFDQDGDGFISVEELKSVMASLGLKQGKTLKC
RapSaC4L2  ---------EK-------EEEDMRDAFNVFDQDGDGFISVEELKSVMASLGLKQGKTLKC
BraNaC4L2  ---------EK-------EEEDMRDAFNVFDQDGDGFISVEELKSVMASLGLKQGKTLEC
```

```
BraOlC4L1  ---------EK-------EEEDMRDAFHVFDQDGDGFISVEELKSVMASLGLKQGKTLEC
BNa3BRa2   ---------EK-------EEEDMRDAFNVFDQDGDGFISVEELKSVMASLGLKQGKTLEC
RapSaC4L1  ---------EK-------EEEDMRDAFNVFDQDGDGFISVEELKSVMSSLGLKQVKTLEC
EutSaC4L   ---------EK-------VDEDMRDAFNVFDQDGDGYITVEELKSVMASLGLKQGKTLEC
TarHaC4_5L ---------QS-D-----KDDDMRDAFDVFDQDGDGFITVEELKSVMGSLGLKQGKTLED
AraLyC5L   ---------EH-HNDGETEEEDMKDAFNVFDQDGDGFITVDELKSVMASLGLKQGKTLDG
AraThC5    ---------EH-HNDGETEEEDMKDAFNVFDQDGDGFITVEELKSVMASLGLKQGKTLDG
CamSaC5L1  ---------EH-QNDGETEEEDMKDAFNVFDQDGDGFITVEELKSVMASLGLKQGKTLDG
CamSaC5L3  ---------EH-QKDGETEEEDMKDAFNVFDQDGDGFITVEELKSVMASLGLKQGKTLDG
CamSaC5L2  ---------EH-QNDGETEEENMKDAFNVFDQDGDGFITVEELKSVMASLGLKQGKTLDG
EutSaC5L   ---------EH-HNDGETEEEDMKDAFNVFDQDGDGFITVEELKSVMASLGLKQGKTLDG
CapRuC5L   ---------EH-HNDGGTEEEDMKDAFNVFDQDGDGFITVEELKSVMASLGLKQGKTLDG
BNa1BOl2   ---------EH-RKDGETEEDDMKDAFNVFDQDGDGFITVEELKSVMGSLGLKQGKTLEG
BraNaC5L2  ---------EH-RKDGETEEEDMKDAFNVFDQDGDGFITVEELKSVMGSLGLKQGKTLEG
BraRaC5L1  ---------EH-RKDGETEEEDMKDAFNVFDQDGDGFITVEELKSVMGSLGLKQGKTLEG
BN53BO51   ---------EH-HNDGETEEEDMKEAFNVFDQDGDGFITVEELKSVMGSLGLKQGKTQEG
BraRaC5L2  ---------EH-HNDGETKEEDMKEAFNVFDQDGDGFITVEELKSVMSSLGLKQGKTLEG
RapSaC5L1  ---------EH-HNDGETEEEDMKEAFNVFDQDGDGFITVEELKSVLASLGLKQGKTLEG
MusAcC3L5  ---------ER-D----EEEEDMREAFNVFDRNGDGFITVEELRSVLASLGLKQGRTAED
DauCaC3L2  ---------TR-E-----EEEDMKEAFSVFDQNGDGFITVDELKSVLASLGLKQGRTEED
CepFoC3L   ---------EE-E-----EEDMMKEAFNVFDSNGDGFISVDELRSVFVSLGVKQGRTIED
HelAnC3L   ---------NQ-E-----NEEDMMEAFNVFDQNRDGFIAVEELRSVLESLGLKQGKVVDD
VigAnC3L2  ---------ER-D-----EEDDMREAFN------DIYIYILYLDILITKI-YKIYSPLHS
ElaGuC6L   -RGERGKEEEE-E-----GEVELREAFDVFDENGDGLITVEELGLVLASLGLKRGATVED
CapAnC3L   -ESEMNEEEVA-N-----REKDLKDAFDVFDHDKDGLISKEELSKILSTLGMKEGKKLDY
NicAtC3L   -----NEEEES-N-----REKDLKDAFDVFDYDKDGLISVEELSKILSSLGLRQGKKLDY
NsyNtaC3   -SGEMNQEEEA-N-----RERDLKDAFDVFDYDKDGLISEEELSKVLSSLGLNQGKKLED
NicToC3L   -SGEMNQEEEA-N-----RERDLKDAFDVFDYDKDGLISEEELSKVLSSLGLNQGKKLED
JugReC3L   -KGVESSEGTG-D-----EEDDLKEAFDVFDKDRDGLITVEELGLVLCSLGLKEGKKKED
NelNuC3L1  EGSTEEEDGGV-D-----QEMELKEAFDVFDGNKDGLITVEELSLVLESLGLKQGWKSED
NelNuC3L2  -LLDCREEEEV-D-----EERDLKEAFDVFDGNRDGLITVEELSLVLSSLGLKQGLRSED
CucMeC7L   -----KKTSVG-D-----DEEGLKDAFGVFDKDSDGLISVEELSLVLCSLGMNEGKIVEN
CucSaC3L   -----KKTSVE-D-----EEDELKDAFGVFDKDSDGLISVEELSLVLCSLGMNEGKIVEN
DenCaC3L   -----EGEGEA-D-----EDRELREAFEVFDDNGDGLITVEELSLVLKSLGLRQGDRAEA
AraThC24   ---------NR-N-----DVSDLKEAFELYDLDGNGRISAKELHSVMKNLGEKC--SVQD


RapSaC3L2  CKRMISKVDVDGDGMVNFKEFKQMMK--GGGFAALESSL-
EucGrC3L2  CKRMIMKVDVDGDGMVDFKEFKQMMK--GGGFSALS----
ZizJuC3L2  CKRMIMKVDVDGDGMVNYKEFKQMMK--GGGFSALS----
LotJaC7L   CKKMIMKVDVDGDGMVDYKEFKQMMK--GGGFSALT----
```

```
VigAnC3L1  CKKMIMKVDVDGDGMVDYKEFKQMMK--GGGFSALT----
VigRaC3L1  CKKMIMKVDVDGDGMVDYKEFKQMMK--GGGFSALT----
PhaVuC3L1  CKKMIMKVDVDGDGMVDYKEFKQMMK--GGGFSALT----
GlyMaC3L1  CKNMISKVDVDGDGMVDFKEFKQMMK--GGGFSALT----
CajCaC3L1  CKNMIMKVDVDGDGMVDFKEFKHMMK--GGGFNALT----
PruMuC3L2  CKRMIMKVDVDGDGRVNYKEFKQMMK--GGGFSALS----
PruPeC3L2  CKRMIMKVDVDGDGRVNYKEFKQMMK--GGGFSALS----
PruAvC3L   CKRMIMKVDVDGDGRVNYKEFKQMMK--GGGFSALS----
MalPyC3L   CKRMIMKVDVDGDGRVNYKEFRQMMK--GGGFSALS----
PopEuC3L2  CKRMIMKVDVDGDGMVDYKEFKKMMK--GGGFSALG----
PopTrC3L1  CKRMIMKVDVDGDGMVDYKEFKKMMK--GGGFSALG----
PopEuC3L3  CKRMIMKVDVDGDGMVDYREFQKMMK--GGGFSAVG----
PopEuC3L4  CKRMIMKVDVDGDGMVDYREFQKMMK--GGGFSAVG----
PopTrC3L3  CKRMIMKVDVDGDGMVDYREFKKMMK--GGGFSAVG----
CarPaC3L   CKKMIMQVDEDGDGMVNYKEFRQMMK--GGGFSALS----
JatCuC3L2  CKRMIMRVDVDGDGMVNFMEFKQMMK--GGGFSALS----
HevBraC3L  CKTMIMKVDVDGDGMVNFKEFKQMMK--GGGFSALG----
VitViC3L2  CKRMIMKVDEDGDGKVDLKEFKQMMR--GGGFSALS----
CicArC7L   CKKMIGKVDVDGDGLVDYKEFVQMMK--GGGFTALS----
MedTrC7L   CKKMIGTVDVDGNGLVDYKEFKQMMK--GGGFTALS----
CiCl2CiSi2 CKRMIMKVDVDGDGMVDYKEFKQMMK--GGGFSALT----
ElaGuC3L1  CRRMISKVDADGDGMVNFKEFKQMMR--GGGFAALS----
ElaGuC3L2  CRRMISKVDVDGDGMVNFKEFKQMMR--GGGFAALG----
PhoDaC3L   CRKMITKVDVDGDGMVDFKEFKQMMR--GGGFAALS----
MacCoC3L   CRRMIRKVDVDGDGMVNFKEFKQMMR--GGGFAALS----
EryGuC3L   CKKMIMRVDADGDGMVNFTEFKQMMR--GGGFAALGN---
SesInC3L   CRQMIMRVDVDGDGMVNFSEFKQMMR--GGGFAALTN---
RicCoC3L   CKKIIMKVDVDGDGMVDFKEFKQMMK--GGVFTALSSCN-
GosArC7L   CKRMITKVDVDGDGRVNFMEFKQMMK--GGGFTAMA----
GosRaC7L   CKRMITKVDVDGDGRVNFMEFKQMMK--GGGFTAMA----
TheCaC3L2  CKRMIMKVDVDGDGRVNFKEFKQMMK--GGGFSALT----
CorOlC3L   CKRMIMKVDADGDGRVNFKEFKQMMK--GGGFSALT----
CorCaC3L   CKRMIMKVDADGDGRVNFKEFKQMMK--GGGFSALT----
PunGrC3L   CKRMIMKVDVDGDGRVNYKEFKQMMK--GGGFSALS----
SolLyC3L1  CKQMINKVDIDGDGMVNYDEFKQMMR--GGGDM-------
SolTuC3L1  CKQMINKVDIDGDGMVNFAEFKQMMR--GGGFAALS----
ADu2AIp2   CKKMIMKVDADGDGMVNYGEFKQMMK--GGGFSALS----
MusAcC3L4  CRMMINKVDVDGDGRVDFKEFKQMMK--GGGFAALS----
AraLyC4L   CKEMIKQVDEDGDGRVNYMEFLQMMK--SGDFSNRS----
AraThC4    CKEMIMQVDEDGDGRVNYKEFLQMMK--SGDFSNRS----
CamSaC4L1  CKEMIMQVDEDGDGRVNYKEFLQMMK--SVGFSNRS----
```

```
CamSaC4L2  CKEMIMQVDEDGDGRVNYKEFLQMMK--SVGFSNRS----
CapRuC4L   CKEMIMQVDEDGDGRVDYKEFLQMMK--SGGFSNRA----
BraNaC4L1  CKEMITQVDEDGDGRVNYKEFLQMMK--SGGFSNRSS---
BraRaC4L1  CKAMITQVDEDGDGRVNYKEFLQMMK--SGGFSNRSS---
BraOlC4L2  CKEMITQVDEDGDGRVNYKEFLQMMK--SGGFSNSSSSD-
RapSaC4L2  CKEMITQVDEDGDGRVNYNEFLQMMK--SGGFSNRS----
BraNaC4L2  CKEMIMQVDEDGDGRVNYKEFLQMMK--TGGFNNRSSSSN
BraOlC4L1  CKEMIMQVDEDGDGRVNYKEFLQMMK--TGGFNNRSSSSN
BNa3BRa2   CKEMIMQVDEDGDGRVNYKEFLQMMK--TGGFSNTSSSN-
RapSaC4L1  CKEMIMQVDEDGDGRVNYKEFLQMMK--TGGVSNTSSSS-
EutSaC4L   CKDMITQVDEDGDGRVNYKEFLQMMK--SGGFSNNRSSSN
TarHaC4_5L CKKMIMQVDVDGDGRVNYKEFLQMMK--SGDL--------
AraLyC5L   CKKMIMQVDADGDGRVNYKEFLQMMK--GGGFSSSN----
AraThC5    CKKMIMQVDADGDGRVNYKEFLQMMK--GGGFSSSN----
CamSaC5L1  CKKMIMQVDADGDGRVNYKEFLQMMK--GGGFSSSN----
CamSaC5L3  CKKMIMQVDADGDGRVNYKEFLQMMK--GGGFSSSN----
CamSaC5L2  CKKMIMQVDADGDGRVNYKEFLQMMK--GGGFSSSN----
EutSaC5L   CKKMIMQVDADGDGRVNYKEFLQMMK--GGGFSSSN----
CapRuC5L   CKKMIMQVDADGDGRVNYKEFLQMMK--GGGFSSSSN---
BNa1BOl2   CKKMIMQVDGDGDGRVNYKEFLQMMR--GGGFSCSNN---
BraNaC5L2  CKKMIMQVDGDGDGRVNYKEFLQMMK--GGGFSCSN----
BraRaC5L1  CKKMIMQVDGDGDGRVNYKEFLQMMK--GGGFSCSN----
BN53BO51   CKKMIMQVDVDGDGRVNYKEFLQMMK--GDGFSSRS----
BraRaC5L2  CKKMIMQVDVDGDGRVNYKEFLQMMK--GDGFSRSS----
RapSaC5L1  CKKMIMQVDSDGDGRVNYKEFLQMMK--GGGFSSSG----
MusAcC3L5  CKTMINTVDVDGDGMVDFKEFRQMMN--GGGFAASS----
DauCaC3L2  CKTMIMKVDVDGDGRVNFNEFKAMMR--GGGFAALN----
CepFoC3L   CKKMIMKVDVDGDGKVDYEEFKQMMKGGGGGFSSLS----
HelAnC3L   CRRMIMKVDVDGDGRVSFNEFKEMMK--SGGFVNLAQS--
VigAnC3L2  FKKHFIKV---------WSLY-------------------
ElaGuC6L   CRDMIRKVDLDGDGMVDFGEFKKMMV--EGVKLF------
CapAnC3L   CKEMIKKVDVDGDGMVNFDEFKKMMK--ACGTLIPFS---
NicAtC3L   CKEMISKVDVDGDGMVNFDEFKKMIK--GCGTLVPIS---
NsyNtaC3   CKEMIRKIDVDGDGMVNFDEFKKMMK--LGGRLIPIS---
NicToC3L   CKEMIRKIDVDGDGMVNFDEFKKMMK--VGGRLIPIS---
JugReC3L   CKEMIRNVDMDGDGMVNFDEFKKMMK--GGGRLLLAS---
NelNuC3L1  CKEMIRSVDMDGDGMVNFEEFKKMMM--KAGGCLVSLS--
NelNuC3L2  CREMIKSVDMDGDGMVNFEEFKKMMM--KAGGSCVGIS--
CucMeC7L   CKEMIRKVDLDGDGMVNFDEFKKMMR--NGVSILTSS---
CucSaC3L   CKEMIRKVDLDGDGMVNFDEFKKMMR--NGVTILTSS---
DenCaC3L   CRDMINRVDLDGDGMVNFEEFKRMMVVDGGGSFF------
```

```
AraThC24   CKKMISKVDIDGDGCVNFDEFKKMMS--NGGGA-------
```

Appendix V. License and official OUP permission for Figure 16

AgtDef

Dear Henning Ruge,

RE: Figure 1. An update of the Angiosperm Phylogeny Group classification for the orders and families of flowering plants: APG IV. *Botanical Journal of the Linnean Society* (2016) 181 (1): 1-20

Oxford University Press controls the copyright of the article in *Botanical Journal of the Linnean Society* on behalf of The Linnean Society of London.

Further to your Rightslink License #4221440271927, dated 03.11.17, we hereby acknowledge that you wish to adapt the above material for 'Functional and phylogenetic analysis of the endosomal targeted proteins CML4 and CML5 in Arabidopsis thaliana' in your thesis/dissertation. We therefore grant Mr. Henning Ruge the non-exclusive right to use the above material in this way, subject to payment of the fee (if applicable) and adherence to the terms and conditions as specified in your license.

Kind regards,

Aaron Edwards | Permissions Assistant|Rights Department

Academic and Journals Divisions|Global Business Development

Oxford University Press | Great Clarendon Street | Oxford | OX2 6DP

OXFORD UNIVERSITY PRESS LICENSE
TERMS AND CONDITIONS

Nov 03, 2017

This Agreement between Mr. Henning Ruge ("You") and Oxford University Press ("Oxford University Press") consists of your license details and the terms and conditions provided by Oxford University Press and Copyright Clearance Center.

License Number	4221440271927
License date	Nov 03, 2017
Licensed content publisher	Oxford University Press
Licensed content publication	Botanical Journal of the Linnean Sociey
Licensed content title	An update of the Angiosperm Phylogeny Group classification for the orders and families of flowering plants: APG IV
Licensed content author	Chase, M. W.
Licensed content date	Apr 6, 2016
Type of Use	Thesis/Dissertation
Institution name	
Title of your work	Functional and phylogenetic analysis of the endosomal targeted proteins CML4 and CML5 in Arabidopsis thaliana
Publisher of your work	n/a
Expected publication date	Dec 2017
Permissions cost	0.00 EUR
Value added tax	0.00 EUR
Total	0.00 EUR
	Mr. Henning Ruge
Requestor Location	
	Germany Attn: Mr. Henning Ruge
Publisher Tax ID	GB125506730
Billing Type	Invoice
Billing Address	Mr. Henning Ruge

	Attn: Mr. Henning Ruge
Total	0.00 EUR